

Potential and limitations of biomarkers and stable isotopes for  
chemotaxonomy and (paleo-)climate research in the Bale  
Mountains, Ethiopia

**Dissertation**

zur Erlangung des akademischen  
Doktorgrades der Naturwissenschaften (Dr. rer. nat.)

der

Naturwissenschaftlichen Fakultät III  
Agrar- und Ernährungswissenschaften,  
Geowissenschaften und Informatik

der

Martin-Luther-Universität Halle-Wittenberg

vorgelegt von

**M.Sc. Herrn Bruk Lemma Debebe**

geboren am 07 Oktober 1987 in Addis Ababa, Äthiopien

Halle (Saale), 19 Juli 2021

Vollständiger Abdruck der von der Fakultät für Agrar- und Ernährungswissenschaften, Geowissenschaften und Informatik der Martin-Luther-Universität Halle-Wittenberg genehmigten Dissertation zur Erlangung des Grades eines Doktors der Naturwissenschaftlichen (Dr. rer. nat.).

Die Arbeiten zur vorliegenden Dissertation wurden im Zeitraum von August 2017 bis July 2021 am Abteilungen für Bodenbiogeochemie (unter Leitung von Prof. Dr. Bruno Glaser) der Martin-Luther-Universität Halle-Wittenberg und an der Institut für Geographie, Heisenberg-Professur Für Physische Geographie mit Schwerpunkt Paläoumweltforschung (unter Betreuung von Prof. Dr. Michael Zech) der Technische Universität Dresden durchgeführt.

Dissertation eingereicht am: 12 November 2020

Tag der Verteidigung: 19 Juli 2021

Erstgutachter: Prof. Dr. Bruno Glaser

Zweitgutachter: Prof. Dr. Michael Zech

Prüfungsausschuss:

- Prof. Dr. Robert Mikutta (Vorsitz)
- Prof. Dr. Bruno Glaser (Gutachter)
- Prof. Dr. Michael Zech (Gutachter)
- Prof. Dr. Eva Lehdorff (Gutachter)
- Prof. Dr. Christopher Conrad
- apl. Prof. Dr. Wolfgang Gossel
- Prof. Dr. Edgar Peiter
- Prof. Dr. Hans-Jörg Vogel

**Dedicated to my parents and my wife**

**“Research is to see what everybody else has  
seen and think what nobody has thought”**

**Albert Szent-Györgyi**



## Table of Contents

<b>Contents</b>	<b>Page</b>
Table of Contents .....	i
Abbreviations.....	v
List of Tables.....	viii
List of Figures .....	viii
Summary .....	xiv
Zusammenfassung.....	xvii
<b>I. Extended Summary .....</b>	<b>1</b>
<b>1. Introduction.....</b>	<b>2</b>
<b>1.1 Background .....</b>	<b>2</b>
<b>1.2 Study Objectives .....</b>	<b>5</b>
<b>2. Study area.....</b>	<b>6</b>
<b>3. Analytical methods.....</b>	<b>10</b>
<b>3.1 Sample collection and preparation .....</b>	<b>10</b>
<b>3.2 Lignin phenols analyses.....</b>	<b>10</b>
<b>3.3 Lipid analyses.....</b>	<b>10</b>
<b>3.4 Stable isotope measurements.....</b>	<b>11</b>
<b>4. Results and discussion .....</b>	<b>11</b>
<b>4.1 Biomarkers .....</b>	<b>11</b>
<b>4.1.1 Lignin phenols in leaves and topsoils (Study [MS]–1).....</b>	<b>11</b>
<b>4.1.2 <i>n</i>-Alkanes in leaves and topsoils (Study [MS]–1).....</b>	<b>14</b>
<b>4.1.3 Phenolic compounds in the keystone plant species (Study [MS]–2).....</b>	<b>16</b>
<b>4.2 Stable Isotopes.....</b>	<b>18</b>
<b>4.2.1 Stable isotopes in precipitation (Study [MS]–3).....</b>	<b>18</b>
<b>4.2.2 Coupling <math>\delta^{18}\text{O}_{\text{sugar}}</math> and <math>\delta^2\text{H}_{n\text{-alkane}}</math> biomarkers (Study [MS]–4).....</b>	<b>21</b>
<b>5. Conclusions.....</b>	<b>26</b>
<b>6. References.....</b>	<b>28</b>
<b>7. Authors' contributions to the included manuscripts.....</b>	<b>39</b>
<b>II. Publications and manuscripts .....</b>	<b>41</b>
<b>Study 1:.....</b>	<b>42</b>
<b>Chemotaxonomic patterns of vegetation and soils along altitudinal transects of the Bale Mountains, Ethiopia and implications for paleovegetation reconstructions II: Lignin– derived phenols and leaf wax-derived <i>n</i>-alkanes .....</b>	<b>42</b>
<b>Abstract.....</b>	<b>43</b>

---

<b>1. Introduction</b> .....	45
<b>2. Material and Methods</b> .....	47
<b>2.1 Study area and sample description</b> .....	47
<b>2.2 Analysis of lignin-derived phenol and leaf wax-derived <i>n</i>-alkane biomarkers</b> .	49
<b>3. Results and Discussion</b> .....	50
<b>3.1 Lignin phenol concentration and patterns of contemporary vegetation</b> .....	50
<b>3.2 Lignin phenol patterns of O-layers and A<sub>h</sub>-horizons</b> .....	53
<b>3.3 <i>n</i>-Alkane concentrations and patterns of contemporary plants</b> .....	54
<b>3.4 <i>n</i>-Alkane concentration and patterns of O-layers and A<sub>h</sub>-horizons</b> .....	56
<b>4 Conclusions and implications for paleovegetation reconstructions in the Bale Mountains</b> .....	57
<b>Acknowledgments</b> .....	58
<b>References</b> .....	59
<b>Study 2:</b> .....	65
<b>Phenolic Compounds as Unambiguous Chemical Markers for the Identification of Keystone Plant Species in the Bale Mountains, Ethiopia</b> .....	65
<b>Abstract:</b> .....	66
<b>1. Introduction</b> .....	67
<b>2. Material and Methods</b> .....	69
<b>2.1 Study Area</b> .....	69
<b>2.1.1 Geomorphological Setting</b> .....	70
<b>2.1.2 Climate and Biota</b> .....	71
<b>2.2 Sample Collection</b> .....	72
<b>2.3 Analysis of Phenolic Compounds Released after Alkaline CuO Oxidation</b> .....	72
<b>2.4 Data Analysis</b> .....	73
<b>2.4.1 Hierarchical Clustering and PCA</b> .....	73
<b>2.4.2 Machine Learning</b> .....	74
<b>3. Results and Discussion</b> .....	74
<b>3.1 Distribution and Diversity of Phenols</b> .....	74
<b>3.2 Cluster Analysis of Phenolic Compounds</b> .....	78
<b>3.3 Biomarker Identification</b> .....	79
<b>4. Conclusions</b> .....	81
<b>Acknowledgments</b> .....	82
<b>References</b> .....	83
<b>Study 3:</b> .....	88

<b>Spatial and temporal <math>^2\text{H}</math> and <math>^{18}\text{O}</math> isotope variation of contemporary precipitation in the Bale Mountains, Ethiopia</b> .....	88
<b>Abstract</b> .....	89
<b>1. Introduction</b> .....	90
<b>2. Material and Methods</b> .....	91
<b>2.1 Study area description</b> .....	91
<b>2.2 Climate</b> .....	92
<b>2.3 Sampling design</b> .....	93
<b>2.4 Laboratory analysis</b> .....	94
<b>2.5 Backward trajectories</b> .....	94
<b>3. Results and discussion</b> .....	95
<b>3.1 <math>\delta^2\text{H}/\delta^{18}\text{O}</math> variation of precipitation and meteoric water line</b> .....	95
<b>3.2 Spatial patterns of <math>\delta^2\text{H}_{\text{prec}}</math> and <math>\delta^{18}\text{O}_{\text{prec}}</math> in the Bale Mountains</b> .....	96
<b>3.3 Temporal patterns of <math>\delta^2\text{H}_{\text{prec}}</math> and <math>\delta^{18}\text{O}_{\text{prec}}</math> in the Bale Mountains and <i>d</i>-excess</b> .....	98
<b>3.4 Backward trajectories and moisture source areas</b> .....	100
<b>4. Conclusions</b> .....	101
<b>Acknowledgments</b> .....	102
<b>References</b> .....	103
<b>Study 4:</b> .....	108
<b><math>\delta^2\text{H}_{n\text{-alkane}}</math> and <math>\delta^{18}\text{O}_{\text{sugar}}</math> biomarker proxies from leaves and topsoils of the Bale Mountains, Ethiopia, and implication for paleoclimate reconstruction</b> .....	108
<b>Abstract</b> .....	109
<b>1. Introduction</b> .....	110
<b>2. Material and Methods</b> .....	111
<b>2.1 Geography of the Bale Mountains</b> .....	111
<b>2.2 (Paleo)-climate</b> .....	113
<b>2.3 Sampling</b> .....	114
<b>2.4 Compound-specific <math>\delta^2\text{H}_{n\text{-alkane}}</math> and <math>\delta^{18}\text{O}_{\text{sugar}}</math> analyses</b> .....	114
<b>2.5 Conceptual framework for interpreting the coupled <math>\delta^2\text{H}_{n\text{-alkane}}</math>-<math>\delta^{18}\text{O}_{\text{sugar}}</math> approach: reconstruction of leaf water, source water, <i>d</i>-excess, and relative humidity</b> ..	116
.....	116
<b>3. Results and Discussion</b> .....	119
<b>3.1 Comparison of <math>\delta^2\text{H}_{n\text{-alkane}}</math> and <math>\delta^{18}\text{O}_{\text{sugar}}</math> results from leaves, O-layers, and <math>\text{A}_\text{h}</math>- horizons</b> .....	119
<b>3.2 Comparison of <math>\delta^2\text{H}_{n\text{-alkane}}</math> and <math>\delta^{18}\text{O}_{\text{sugar}}</math> results with <math>\delta^2\text{H}_{\text{prec}}</math> or <math>\delta^{18}\text{O}_{\text{prec}}</math> results</b> .....	121
<b>3.3 Interspecies comparison of <math>\delta^2\text{H}_{n\text{-alkane}}</math> and <math>\delta^{18}\text{O}_{\text{sugar}}</math> results from keystone plant species in the Bale Mountains</b> .....	123



---

<b>3.4</b>	<b>Coupled <math>\delta^2\text{H}_{n\text{-alkane}}</math> and <math>\delta^{18}\text{O}_{\text{sugar}}</math> biomarker results</b> .....	125
<b>3.4.1</b>	<b>Reconstructed <math>\delta^2\text{H}_{\text{leaf water}}</math> and <math>\delta^{18}\text{O}_{\text{leaf water}}</math> as well as <math>\delta^2\text{H}_{\text{source water}}</math> and <math>\delta^{18}\text{O}_{\text{source water}}</math></b> .....	125
<b>3.4.2</b>	<b>Deuterium excess, reconstructed relative humidity and its paleoclimate implication</b> .....	128
<b>4.</b>	<b>Conclusions</b> .....	130
	<b>Acknowledgments</b> .....	130
	<b>Declarations</b> .....	131
	<b>References</b> .....	131
	<b>List of Publications</b> .....	140
	<b>Acknowledgements</b> .....	142
	<b>Curriculum Vitae/Lebenslauf</b> .....	144
	<b>Eidesstattliche Erklärung / Declaration under Oath</b> .....	147
	<b>Erklärung über bestehende Vorstrafen und anhängige Ermittlungsverfahren / Declaration concerning Criminal Record and Pending Investigations</b> .....	148

**Abbreviations**

$\Sigma$ VSC	Sum of Vanillyl, Syringyl and Cinnamyl
Ac	Acid
ACL	Average Chain Length
AHC	Agglomerative Hierarchical Cluster
A <sub>h</sub> -horizon	Humus-rich mineral topsoil horizon
Al	Aldehydes
BSTFA	N, O-bis(trimethylsilyl)trifluoroaceticacetamide
C	Cinnamyl
C3	Photosynthetic pathway of trees and moss grasses
C4	Photosynthetic pathway of many savannah grasses
CAM	Crassulacean Acid Metabolism
CPI	Carbon Preference Index
CuO	Cupric oxide
DCM	Dichloromethane
DFG	German Research Foundation
EL	Evaporative line
$\epsilon_{app\ 18O}$	Apparent oxygen fractionation
$\epsilon_{app\ 2H}$	Apparent hydrogen fractionation
FID	Flame Ionization Detector
GC	Gas Chromatography
GC-MS	Gas Chromatography – Mass Spectrometry
GDAS	Global Data Assimilation System
GMWL	Global meteoric water line
HYSPLIT	Hybrid Single Particle Lagrangian Integrated Trajectory

---

IAEA	International Atomic Energy Agency
IRMS	Isotope Ratio Mass Spectrometry
IS	Internal Standard
ITCZ	Inter-Tropical Convergence Zone
LMWL	Local meteoric water line
MeOH	Methanol
<i>n</i> -Alkane	Unbranched hydrocarbon
OEP	Odd-over-Even predominance
O-layers	Strongly humified plant residue
OM	Organic Matter
PAA	Phenylacetic acid
PCA	Principal Component Analysis
RF	Random Forest
RH	Relative humidity
RP	Recursive Partitioning
S	Syringyl
SOM	Soil Organic Matter
SVM	Support Vector Machine
TAC	Total <i>n</i> -Alkane Concentration
TLEs	Total Lipid Extraction
TN	Total Nitrogen
TOC	Total Organic Carbon
V	Vanillyl
$\tilde{x}$	Median
$\delta^{18}\text{O}$	Stable Oxygen Isotope

$\delta^2\text{H}$

Stable Hydrogen Isotope

## List of Tables

**Table 1-1:** Summary of the relative abundance of individual phenols profiled in each dominant plant species. Key: ↑ (higher) and ↓ (lower)

**Table 1-2:** Phenol Diversity Index

## List of Figures

### Extended Summary

**Fig. I:** Map showing the location of Ethiopia in Africa, location of the Bale Mountains National Park (BMNP) in Ethiopia, and location of sampling points and weather stations in the BMNP.

**Fig. II:** Dendrogram differentiating the dominant plant species of the Bale Mountains based on the concentrations of vanillyl, syringyl and cinnamyl lignin phenols ( $\text{mg g}^{-1}$  sample). The dotted vertical line represents the distance or dissimilarity between clusters.

**Fig. III:** Box plot for the relative abundance of cinnamyl phenols (expressed as  $C/(V+S+C)$  in %) in plants, O-layers and  $A_h$ -horizons. The box plots indicate the median (solid line between the boxes) and interquartile range (IQR), with upper (75%) and lower (25%) quartiles and possible outliers (empty circles). The notches display the confidence interval around the median within  $\pm 1.57 \cdot \text{IQR}/\text{sqrt}$ . Note that small sample sizes result in unidentifiable boxes.

**Fig. IV:** Ternary diagram for the relative abundances (%) of vanillyl, syringyl and cinnamyl lignin phenols of the dominant vegetation. The blue line separates samples with more (right) versus less (left) than 40% cinnamyl.

**Fig. V:** Notched box plot for the ratio  $C_{31}/C_{29}$  in plant samples, organic layers and  $A_h$ -horizons. The box plots indicate the median (solid line between the boxes) and interquartile range (IQR), with upper (75%) and lower (25%) quartiles and possible outliers (empty circles). The notches display the confidence interval around the median within  $\pm 1.57 \cdot \text{IQR}/\text{sqrt}$ . Note that small sample sizes result in unidentifiable boxes.

**Fig. VI:** Two-dimensional plot of the relative contribution of the sum of coumaryl phenols (*p*-coumaric acid + ferulic acid) and benzoic acids (benzoic acid + salicylic acid + phthalic acid) in the dominant plant species under study.

- Fig. VII:** Representative decision tree of Random Forest (RF) model using relative phenols contribution. 32 training sample sets and 10,000 number of trees were used to compute the model.
- Fig. VIII:** Hydrogen ( $\delta^2\text{H}$ ) and oxygen ( $\delta^{18}\text{O}$ ) isotopic composition of meteoric water in the Bale Mountains, Ethiopia. LMWL = local meteoric water line ( $\delta^2\text{H} = 5.3 \pm 0.2 * \delta^{18}\text{O} + 14.6 \pm 0.9$ , dashed line) and GMWL = global meteoric water line ( $\delta^2\text{H} = 8.0 * \delta^{18}\text{O} + 10$ , solid line).
- Fig. IX:** Inner-annual variation of  $\delta^2\text{H}_{\text{prec}}$  (solid line), *d*-excess (dotted line and yellow circle) and precipitation amount (blue bars) of the representative sampling site Dinsho Head Quarter.
- Fig. X:** Map of Hybrid Single Particle Lagrangian Integrated Trajectory (HYSPPLIT) model based on meteorological data (Global Data Assimilation System, 1-degree resolution) for 168 h. Yellow, light blue and dark blue trajectories indicate the synoptic moisture source area of precipitation to the study site during dry and wet seasons. Dark blue refers to long distance traveling trajectories (LDT) and the white triangle indicates the sampling area or ending point of the water vapour. For the interpretation of the reference to color in this figure legend, the readers are referred to the online version of this dissertation.
- Fig. XI:** Altitudinal  $\delta^2\text{H}$  (left) and  $\delta^{18}\text{O}$  (right) gradients of *n*-alkanes (weighted mean of C<sub>29</sub> and C<sub>31</sub>) and sugar biomarkers (weighted mean of arabinose and xylose), respectively, reconstructed leaf water (squares) and precipitation (triangles).
- Fig. XII:** Comparison of  $\delta^2\text{H}_{n\text{-alkane}}$  (a) and  $\delta^{18}\text{O}_{\text{sugar}}$  (b) among leaves, O-layers and A<sub>h</sub>- horizons. The notched box plots indicate the median (solid lines between the boxes), interquartile range (IQR) with upper (75%) and lower (25%) quartiles. The notches display the confidence interval around the median within  $\pm 1.57 * \text{IQR} / \sqrt{n}$ .
- Fig. XIII:** Variations of  $\delta^2\text{H}_{n\text{-alkane}}$  (a) and  $\delta^{18}\text{O}_{\text{sugar}}$  (b) between keystone plant species. The notched box plots indicate the median (solid lines between the boxes), interquartile range (IQR) with upper (75%), and lower (25%) quartiles and outliers (empty circle). The notches display the confidence interval around the median within  $\pm 1.57 * \text{IQR} / \sqrt{n}$ .
- Fig. XIV:**  $\delta^{18}\text{O}$  versus  $\delta^2\text{H}$  diagram illustrating the conceptual framework of the coupled (paleo-) hygrometer approach after Zech et al., (2013b). Data are plotted for measured source water/precipitation (blue solid triangle), measured  $\delta^2\text{H}_{n\text{-alkane}}$ , and  $\delta^{18}\text{O}_{\text{sugar}}$  (black solid circle), reconstructed leaf water (green solid rectangle), measured Garba Guracha lake water (brown solid triangle).

## Manuscript 1

**Fig. 1–1:** Map of the Bale Mountains for the vegetation zones and study sites along the northeastern and the southwestern transect (modified following Miede and Miede, 1994). Dominant vegetation types sampled that comprise the Ericaceous and Afro-alpine belt.

**Fig. 1–2:** Sum of lignin phenol concentrations ( $\Sigma$ VSC) of contemporary plants, O-layers and  $A_h$ -horizons. Error bars illustrate standard deviations.

**Fig. 1–3:** Dendrogram differentiating the dominant plant species of the Bale Mountains based on the concentrations of vanillyl, syringyl and cinnamyl lignin phenols ( $\text{mg g}^{-1}$  sample). The dotted vertical line represents the distance or dissimilarity between clusters.

**Fig. 1–4:** Ternary diagram for the relative abundances (%) of vanillyl, syringyl and cinnamyl lignin phenols of the dominant vegetation. The blue line separates samples with more (right) versus less (left) than 40% cinnamyl.

**Fig. 1–5:** Box plot for the relative abundance of cinnamyl phenols (expressed as  $C/(V+S+C)$  in %) in plants, O-layers and  $A_h$ -horizons. The box plots indicate the median (solid line between the boxes) and interquartile range (IQR), with upper (75%) and lower (25%) quartiles and possible outliers (empty circles). The notches display the confidence interval around the median within  $\pm 1.57 \cdot \text{IQR}/\text{sqrt}$ . Note that small sample sizes result in unidentifiable boxes.

**Fig. 1–6:** Total long-chain *n*-alkane concentrations (TACs) of plants, O-layers and  $A_h$ -horizons. Error bars illustrate standard deviations.

**Fig. 1–7:** Ternary diagram illustrating the relative abundance (%) of the *n*-alkanes  $C_{27}$ ,  $C_{29}$  and  $C_{31}$  in the investigated plant samples.

**Fig. 1–8:** Box plot for the ratio  $C_{31}/C_{29}$  in plant samples, organic layers and  $A_h$ -horizons. The box plots indicate the median (solid line between the boxes) and interquartile range (IQR), with upper (75%) and lower (25%) quartiles and possible outliers (empty circles). The notches display the confidence interval around the median within  $\pm 1.57 \cdot \text{IQR}/\text{sqrt}$ . Note that small sample sizes result in unidentifiable boxes.

## Manuscript 2

**Fig. 2–1:** Map of the Bale Mountains showing the vegetation zones and study sites along the Northeast and Southwestern transect (modified after Miede and Miede, 1994). Leaves of the dominant vegetation within the Ericaceous and Afro-alpine belts were sampled during the dry season in February 2015 and 2017.

- Fig. 2–2:** Typical gas chromatogram of phenolic compounds released after alkaline CuO oxidation of *Lobelia rhynchopetalum*.
- Fig. 2–3:** Notched box plots illustrating the abundance of coumaryl phenols in the dominant plant species of the Bale Mountains. The box plots indicate the median (solid line between the boxes), interquartile range (IQR) with upper (75%) and lower (25%) quartiles and possible outlier (empty circles). The notches display the confidence interval around the median within  $\pm 1.57 \cdot \text{IQR} / \sqrt{n}$ .
- Fig. 2–4:** Notched box plots show the relative abundance of *p*-hydroxy phenols in the dominant plant species of the Bale Mountains. The box plots indicate the median (solid line between the boxes), interquartile range (IQR) with upper (75%) and lower (25%) quartiles and possible outlier (empty circles). The notches display the confidence interval around the median within  $\pm 1.57 \cdot \text{IQR} / \sqrt{n}$ .
- Fig. 2–5:** Agglomerated Hierarchical Cluster analysis of the dominant plant species of the Bale Mountains based on the abundance of phenolic compounds ( $\text{g kg}^{-1}$  TOC). Euclidean measurement of distances and Ward method for linkage calculation applied to cluster a normalized dataset (Z-score normalization,  $Z = (X - \text{mean}(X)) / \text{sd}(X)$ ).
- Fig. 2–6:** Two-dimensional plot illustrating the ratios of syringyl vs. vanillyl (S/V) and coumaryl vs. vanillyl (C/V) phenols of the dominant plant species under study.
- Fig. 2–7:** Two-dimensional plot of the relative contribution of the sum of coumaryl phenols (*p*-coumaric acid + ferulic acid) and benzoic acids (benzoic acid + salicylic acid + phthalic acid) in the dominant plant species under study.
- Fig. 2–8:** Set of relative phenols variables used for chemotaxonomy ordered by their importance as estimated by the Random Forest model. 32 training sample sets and 10,000 number of trees were used to compute the model.
- Fig. 2–9:** Representative decision tree of Random Forest (RF) model using relative phenols contribution. 32 training sample sets and 10,000 number of trees were used to compute the model.

### Manuscript 3

- Fig. 3–1:** Location of the Bale Mountains in Ethiopia and location of the precipitation collection sites in the Bale Mountains. The weather stations cover the Sanetti Plateau and its northern and southern escarpments.
- Fig. 3–2:** Hydrogen ( $\delta^2\text{H}$ ) and oxygen ( $\delta^{18}\text{O}$ ) isotopic composition of meteoric water in the Bale Mountains, Ethiopia. LMWL = local meteoric water line ( $\delta^2\text{H} = 5.3 \pm 0.2 \cdot \delta^{18}\text{O}$ )



+  $14.6 \pm 0.9$ , dashed line) and GMWL = global meteoric water line ( $\delta^2\text{H} = 8.0 * \delta^{18}\text{O} + 10$ , solid line).

**Fig. 3–3:** Annual and seasonal altitude effect describing the weighted  $\delta^{18}\text{O}_{\text{prec}}$  values in the Bale Mountains. Circles + solid line = annual, triangles + dotted line = spring, rectangles + short dash line = summer and stars + long dash line = winter.

**Fig. 3–4:** Inner-annual variation of  $\delta^2\text{H}_{\text{prec}}$  (solid line), *d*-excess (dotted line and yellow circle) and precipitation amount (blue bars) of the representative sampling site Dinsho Head Quarter.

**Fig. 3–5:** Correlation of  $\delta^{18}\text{O}_{\text{prec}}$  values with precipitation amount (mm) shown exemplarily for the stations Angesso and Dinsho.

**Fig. 3–6:** Map of Hybrid Single Particle Lagrangian Integrated Trajectory (HYSPLIT) model based on meteorological data (Global Data Assimilation System, 1-degree resolution) for 168 h. Yellow, light blue and dark blue trajectories indicate the synoptic moisture source area of precipitation to the study site during dry and wet seasons. Dark blue refers to long distance traveling trajectories (LDT) and the white triangle indicates the sampling area or ending point of the water vapour. For the interpretation of the reference to color in this figure legend, the readers are referred to the online version of this dissertation.

## Manuscript 4

**Fig. 4–1:** Map of vegetation zones and sample sites (red dots) along the southwest and northeast transect in the Bale Mountains (modified after Mieke and Mieke, 1994 and published in Lemma et al., 2019a; 2019b and Mekonnen et al., 2019).

**Fig. 4–2:** Altitudinal  $\delta^2\text{H}$  (left) and  $\delta^{18}\text{O}$  (right) gradients of *n*-alkanes (weighted mean of  $\text{C}_{29}$  and  $\text{C}_{31}$ ) and sugar biomarkers (weighted mean of arabinose and xylose), respectively, reconstructed leaf water (squares) and precipitation (triangles).

**Fig. 4–3:** Comparison of  $\delta^2\text{H}_{n\text{-alkane}}$  (a) and  $\delta^{18}\text{O}_{\text{sugar}}$  (b) among leaves, O-layers and  $\text{A}_h$ -horizons. The notched box plots indicate the median (solid lines between the boxes), interquartile range (IQR) with upper (75%) and lower (25%) quartiles. The notches display the confidence interval around the median within  $\pm 1.57 * \text{IQR} / \sqrt{n}$ .

**Fig. 4–4:** Conceptual model demonstrating the hydrogen-isotope and oxygen-isotope relationships, between precipitation, leaf water, and leaf wax-derived *n*-alkanes as well as hemicellulose-derived sugars (after Strobel et al., 2020).  $\epsilon_{\text{app } 2\text{H}}$  = apparent hydrogen-isotope fractionation;  $\epsilon_{\text{app } 18\text{O}}$  = apparent oxygen-isotope fractionation;  $\epsilon^{18}_{\text{bio}}$  =

biosynthetic oxygen-isotope fractionation;  $\varepsilon_{\text{bio}}^2$  = biosynthetic hydrogen-isotope fractionation.

**Fig. 4–5:** Variations of  $\delta^2\text{H}_{n\text{-alkane}}$  (a) and  $\delta^{18}\text{O}_{\text{sugar}}$  (b) between keystone plant species. The notched box plots indicate the median (solid lines between the boxes), interquartile range (IQR) with upper (75%), and lower (25%) quartiles and outliers (empty circle). The notches display the confidence interval around the median within  $\pm 1.57 \cdot \text{IQR} / \sqrt{n}$ .

**Fig. 4–6:**  $\delta^{18}\text{O}$  versus  $\delta^2\text{H}$  diagram illustrating the conceptual framework of the coupled (paleo-) hygrometer approach after Zech et al., (2013b). Data are plotted for measured source water/precipitation (blue solid triangle), measured  $\delta^2\text{H}_{n\text{-alkane}}$ , and  $\delta^{18}\text{O}_{\text{sugar}}$  (black solid circle), reconstructed leaf water (green solid rectangle), measured Garba Guracha lake water (brown solid triangle).

**Fig. 4–7:** The scatter plots to the left show the correlations between  $\delta^{18}\text{O}_{\text{source water}}$  and  $\delta^{18}\text{O}_{\text{prec}}$  as well as  $\delta^2\text{H}_{\text{source water}}$  and  $\delta^2\text{H}_{\text{prec}}$ , respectively. The linear regression lines (black line), correlation coefficients ( $r$ ), 95% confidence intervals (grey area) and significance values ( $p$ ) as well as the 1:1 regression lines (grey lines) are provided for each diagram. The box plots to the right illustrate the offset of  $\delta^{18}\text{O}_{\text{source water}}$  to  $\delta^{18}\text{O}_{\text{prec}}$  and  $\delta^2\text{H}_{\text{source water}}$  to  $\delta^2\text{H}_{\text{prec}}$ , respectively, for keystone plant species. The plots indicate the median (solid line between the boxes), interquartile range (IQR) with upper (75%) and lower (25%) quartiles and outliers (empty circles).

**Fig. 4–8:** The scatter plot to the left shows the correlation between reconstructed RH and actual RH. The linear regression line (black line), correlation coefficient ( $r$ ), 95% confidence interval (grey area), and significance value ( $p$ ) as well as the 1:1 regression line (grey line) are provided. The box plot to the right illustrates the offset of reconstructed RH to actual RH for key stone plant species. The plots indicate the median (solid line between the boxes), interquartile range (IQR) with upper (75%) and lower (25%) quartiles.

## Summary

Over the past decades, biomarkers (e.g. lignin, lipids) and stable isotopes (e.g.  $^2\text{H}$  and  $^{18}\text{O}$ ) were increasingly used to reconstruct vegetation and climate changes. Hitherto, factors affecting the abundance and distribution of biomarkers and their stable isotope composition are not similar worldwide and regional calibration studies are, therefore, highly recommended. The main aim of this Ph.D. dissertation is to evaluate the potential and limitations of biomarkers and their stable isotope composition for chemotaxonomic characterization of the keystone plant species in the Bale Mountains, Ethiopia, and its implication for paleovegetation and paleoclimate reconstruction. More specifically, I focused on lignin-derived phenols, leaf wax-derived *n*-alkanes, stable isotopes in precipitation ( $\delta^2\text{H}_{\text{prec}}$  and  $\delta^{18}\text{O}_{\text{prec}}$ ), and compound-specific stable isotopes ( $\delta^2\text{H}_{n\text{-alkane}}$  and  $\delta^{18}\text{O}_{\text{sugar}}$ ). Mild alkaline cupric oxide (CuO) oxidation method was used to extract phenolic compounds. Leaf wax-derived *n*-alkanes have been Soxhlet-extracted and purified using aminopropyl columns from leaves and topsoils (O-layers as well as  $\text{A}_\text{h}$ -horizons). Individual phenols and *n*-alkanes were separated by gas chromatography (GC) and detected by mass spectrometry (MS) and flame ionization detector (FID), respectively. The  $\delta^2\text{H}_{\text{prec}}$  and  $\delta^{18}\text{O}_{\text{prec}}$  values were measured using a Thermo Conversion Unit coupled with a ConFlo IV interface to an isotope ratio mass spectrometry (IRMS). Compound-specific  $\delta^2\text{H}_{n\text{-alkane}}$  and  $\delta^{18}\text{O}_{\text{sugar}}$  values were measured using gas chromatography - thermal conversion - isotope ratio mass spectrometry (GC-TC-IRMS).

While conventional phenol ratios such as syringyl vs. vanillyl (S/V) and cinnamyl vs. vanillyl (C/V) phenols failed for unambiguous *Erica* identification, using machine-learning approaches, we found that the relative abundance of coumaryl phenols ( $> 0.2$ ) and benzoic acids (0.05–0.12) can be used as a proxy to distinguish *Erica* from other keystone plant species. *Erica* in particular is characterized by relatively high cinnamyl contributions of  $> 40\%$ . However, litter degradation strongly decreases the lignin phenol content and changes the lignin phenol pattern. The relative cinnamyl contribution in the soils under *Erica* were  $< 40\%$ , while soils that developed under *Festuca abyssinica* exhibited relative cinnamyl contributions of  $> 40\%$ .

Similarly, long-chain *n*-alkanes extracted from the leaf waxes allowed a differentiation between *Erica* versus *Festuca abyssinica* and *Alchemilla haumannii*, based on a lower  $\text{C}_{31}/\text{C}_{29}$  ratio ( $\bar{x} = 1.7$ ) in *Erica*. Nevertheless, this characteristic plant pattern was also lost due to degradation in the respective O-layers and  $\text{A}_\text{h}$ -horizons.

At the first hand, the isotope composition of precipitation in the Bale Mountains shows values for  $\delta^2\text{H}_{\text{prec}}$  and  $\delta^{18}\text{O}_{\text{prec}}$  in the range of  $-38$  to  $+29\text{‰}$  and  $-8.7$  to  $+3.7\text{‰}$ , respectively. The local

meteoric water line (LMWL,  $\delta^2\text{H} = 5.3 * \delta^{18}\text{O} + 14.9$ ) is characterized by a lower slope and higher intercept compared to the global meteoric water line (GMWL,  $\delta^2\text{H} = 8 * \delta^{18}\text{O} + 10$ ). Furthermore, our isotope data correlate significantly with altitude and amount of precipitation. At the same time,  $\delta^{18}\text{O}_{\text{prec}}$  and  $\delta^2\text{H}_{\text{prec}}$  values exhibited seasonal pattern reflecting rainy versus dry season. Thus, shortly after the end of the dry season, isotope values were enriched, while more depleted isotope values coincided with high precipitation amounts recorded in May, August, and September. The Hybrid Single Particle Lagrangian Integrated Trajectory (HYSPPLIT) model revealed that during the dry season water vapour originates primarily from the Arabian Sea, whereas during the wet season it originates primarily from the Southern Indian Ocean.

On the other hand, the weighted mean  $\delta^2\text{H}_{n\text{-alkane}}$  and  $\delta^{18}\text{O}_{\text{sugar}}$  values ranged from  $-186$  to  $-89\text{‰}$  and from  $+27$  to  $+46\text{‰}$ , respectively and exhibited a much wider range than  $\delta^{18}\text{O}_{\text{prec}}$  and  $\delta^2\text{H}_{\text{prec}}$ . The  $\delta^2\text{H}_{n\text{-alkane}}$  and  $\delta^{18}\text{O}_{\text{sugar}}$  values of leaves, O-layers, and A<sub>h</sub>-horizons are statistically not significantly different from each other. Hence, in contrast to the biomarker contents and patterns, our dataset provides no evidence for degradation and/or root input affecting the isotope composition of the biomarkers of topsoils. The keystone plant species in the Bale Mountains are characterized by variable values of  $\delta^2\text{H}_{n\text{-alkane}}$  as well as apparent isotope fractionation ( $\epsilon_{\text{app}}$ );  $\delta^{18}\text{O}_{\text{sugar}}$  yielded the same species-dependent trends. When considering a systematic biosynthetic fractionation offset of  $-160\text{‰}$  and  $+27\text{‰}$  for  $\delta^2\text{H}_{n\text{-alkane}}$  and  $\delta^{18}\text{O}_{\text{sugar}}$ , respectively, leaf water of *Erica arborea* and *Erica trimera* is  $^2\text{H}$ - and  $^{18}\text{O}$ -enriched by  $+55 \pm 5$  and  $+9 \pm 1\text{‰}$ , respectively, compared to precipitation. By contrast, *Festuca abyssinica* reveals the most depleted  $\delta^2\text{H}_{n\text{-alkane}}$  and  $\delta^{18}\text{O}_{\text{sugar}}$  values. This can be attributed to “signal-dampening” caused by basal grass leaf growth. The intermediate values for *Alchemilla haumannii* and *Helichrysum splendidum* can be explained by plant physiological or microclimatic conditions affecting relative humidity (RH) and thus leaf water enrichment. Once the isotope composition of leaf water calculated, it is possible to reconstruct the isotope composition of source water, deuterium excess and RH using coupled  $\delta^2\text{H}_{n\text{-alkane}}\text{-}\delta^{18}\text{O}_{\text{sugar}}$  approach. While the actual RH values range from 69 to 82% ( $\bar{x} = 80 \pm 3.4\%$ ), the reconstructed relative humidity, based on a recently suggested coupled  $\delta^2\text{H}_{n\text{-alkane}}\text{-}\delta^{18}\text{O}_{\text{sugar}}$  (paleo-) hygrometer approach yielded a mean of  $78 \pm 21\%$ .

In conclusion, chemotaxonomic differentiation of modern-day plants (leaves) is possible using phenols and *n*-alkanes but soil degradation processes and root input seem to render the proxies unusable for the reconstruction of the past extent of *Erica* in the Bale Mountains. Similarly,

vegetation changes, particularly in terms of grass versus non-grassy vegetation, need to be considered in paleoclimate studies based on  $\delta^2\text{H}_{n\text{-alkane}}$  and  $\delta^{18}\text{O}_{\text{sugar}}$  records. Furthermore, our  $\delta^2\text{H}_{\text{prec}}$  and  $\delta^{18}\text{O}_{\text{prec}}$  results challenge the traditional amount effect interpretation of paleoclimate isotope records from Eastern Africa and rather pinpointed to a previously underestimated source effect. And, the coupled  $\delta^2\text{H}_{n\text{-alkane}}\text{-}\delta^{18}\text{O}_{\text{sugar}}$  (paleo-) hygrometer approach holds great potential for deriving additional paleoclimatic information compared to single isotope approaches.

## Zusammenfassung

Innerhalb der letzten Jahrzehnte kommen Biomarker (z.B. Lignin, Lipide) und Stabilisotope (z.B.  $^2\text{H}$  and  $^{18}\text{O}$ ) immer mehr zur Rekonstruktion von Vegetation- und Klimawandel zum Einsatz. Bisher sind die Faktoren, welche Häufigkeit und Verteilung dieser Proxies beeinflussen, wenig bekannt und weltweit nicht vergleichbar, daher werden regionale Kalibrierungen benötigt. Das Hauptziel dieser Promotion ist die Identifizierung des Potenzials von Biomarkern und stabiler Isotope im Hinblick auf 1. die chemotaxonomische Charakterisierung der dominierenden Pflanzenarten in den Bale Bergen Äthiopiens und 2. bezüglich der Rekonstruktion von Paläoklima und Paläovegetation. Der Fokus liegt auf Ligninbürtigen Phenolen, Blattwachsürtigen *n*-Alkanen, Stabilisotopen im Niederschlag ( $\delta^2\text{H}_{\text{prec}}$  and  $\delta^{18}\text{O}_{\text{prec}}$ ) und substanzspezifischen Stabilisotopen ( $\delta^2\text{H}_{n\text{-alkane}}$  and  $\delta^{18}\text{O}_{\text{sugar}}$ ) in Pflanzen und Oberböden. Mit einem milden alkalischen Kupferoxid-(CuO)-Oxidationsverfahren wurden Phenolverbindungen extrahiert. Blattwachsürtige *n*-Alkane wurden unter Verwendung von Soxhlet- und Aminopropylsäulen aus Blättern und Oberböden (O-Lagen sowie  $A_h$ -Horizonte) extrahiert und aufgereinigt. Einzelne Phenole und *n*-Alkane wurden mittels Gaschromatographie (GC) getrennt und durch Massenspektrometrie (MS) bzw. Flammenionisationsdetektion (FID) nachgewiesen. Die Werte für  $\delta^2\text{H}_{\text{prec}}$  und  $\delta^{18}\text{O}_{\text{prec}}$  wurden unter Verwendung einer Thermokonversionseinheit gemessen, die mit einer ConFlo IV-Schnittstelle an ein Isotopenverhältnis-Massenspektrometer (IRMS) gekoppelt war. Die substanzspezifischen  $\delta^2\text{H}_{n\text{-alkane}}$  and  $\delta^{18}\text{O}_{\text{sugar}}$ -Werte wurden unter Verwendung einer Gaschromatographie–Pyrolyse–Isotopenverhältnis–Massenspektrometrie (GC-TC-IRMS) gemessen.

Während herkömmliche Phenolverhältnisse wie Syringyl- zu Vanillyl-Phenole (S/V) und Cinnamyl- zu Vanillyl-Phenole (C/V) bei der eindeutigen Identifizierung von *Erica* versagten, fanden wir, dass die relativen Beiträge von Vanillyl-, Syringyl- und Cinnamylphenolen eine chemotaxonomische Unterscheidung rezenter Pflanzenarten der Bale Berge ermöglichen. Die relative Häufigkeit von Coumarylphenolen ( $> 0,2$ ) und Benzoesäuren ( $0,05\text{--}0,12$ ) kann als Proxy verwendet werden, um *Erica* von anderen Schlüsselpflanzenarten zu unterscheiden. Insbesondere *Erica* zeichnet sich durch relativ hohe Cinnamylbeiträge von  $> 40\%$  aus. Der Streuabbau verringert jedoch die Ligninphenolgehalte stark und verändert die Ligninphenolmuster. Die relativen Cinnamylbeiträge in den Böden unter *Erica* betragen  $< 40\%$ , während Böden, die sich unter *Festuca abyssinica* entwickelten, relative Cinnamylbeiträge von  $> 40\%$  aufwiesen.

In ähnlicher Weise ermöglichten langkettige *n*-Alkane, die aus den Blattwachsen extrahiert wurden, basierend auf niedrigeren C<sub>31</sub>/C<sub>29</sub>-Verhältnissen ( $\bar{x} = 1.7$ ) in *Erica* die Unterscheidung zwischen *Erica* und *Festuca abyssinica* sowie *Alchemilla haumannii*. Dieses charakteristische Pflanzenmuster ging jedoch auch durch Abbau in den jeweiligen O- und A<sub>h</sub>-Horizonten verloren.

Die Isotopenzusammensetzung des Niederschlags in den Bale Bergen zeigte Werte für  $\delta^2\text{H}_{\text{prec}}$  und  $\delta^{18}\text{O}_{\text{prec}}$  von  $-38$  bis  $+29\%$  bzw.  $-8,7$  bis  $+3,7\%$ . Die lokale meteorische Wasserlinie (LMWL,  $\delta^2\text{H} = 5.3 * \delta^{18}\text{O} + 14.9$ ) ist im Vergleich zur globalen meteorischen Wasserlinie (GMWL,  $\delta^2\text{H} = 8 * \delta^{18}\text{O} + 10$ ) durch eine geringere Steigung und einen höheren Achsenabschnitt gekennzeichnet. Darüber hinaus korrelieren unsere Isotopendaten signifikant mit der Höhe ü. NN und der Niederschlagsmenge. Gleichzeitig zeigen  $\delta^{18}\text{O}_{\text{prec}}$  und  $\delta^2\text{H}_{\text{prec}}$  ein saisonales Muster in Abhängigkeit von Regen- oder Trockenzeit. So zeigten sich kurz nach dem Ende der Trockenzeit angereicherte Isotopenwerte, während abgereicherte Isotopenwerte mit hohen Niederschlagsmengen zusammenfielen, die im Mai, August und September aufgezeichnet wurden. Das HYSPLIT-Modell (Hybrid Single Particle Lagrangian Integrated Trajectory) zeigt, dass Wasserdampf während der Trockenzeit hauptsächlich aus dem Arabischen Meer stammt und während der Regenzeit hauptsächlich aus dem südlichen Indischen Ozean.

Andererseits schwanken die gewichteten mittleren  $\delta^2\text{H}_{n\text{-alkane}}$  and  $\delta^{18}\text{O}_{\text{sugar}}$ -Werte von  $-186$  bis  $-89\%$  bzw. von  $+27$  bis  $+46\%$  und zeigen somit einen viel breiteren Bereich als  $\delta^{18}\text{O}_{\text{prec}}$  und  $\delta^2\text{H}_{\text{prec}}$ . Die  $\delta^2\text{H}_{n\text{-alkane}}$  und  $\delta^{18}\text{O}_{\text{sugar}}$ -Werte von Blättern, O- und A<sub>h</sub>-Horizonten unterscheiden sich statistisch nicht signifikant. Im Gegensatz zu den Biomarkergehalten und -mustern, liefert unser Datensatz daher keine Hinweise, dass Humusabbau und/oder Wurzelzufuhr die Isotopenzusammensetzung der Biomarker in Oberböden beeinflusst. Die dominierenden Pflanzen der Bale Berge zeigen unterschiedliche  $\delta^2\text{H}_{n\text{-alkane}}$ -Werte, sowie eine offensichtliche Isotopenfraktionierung ( $\epsilon_{\text{app}}$ );  $\delta^{18}\text{O}_{\text{sugar}}$  zeigt die gleichen speziesabhängigen Trends. Unter Berücksichtigung einer systematischen Biosynthesefraktionierung von  $-160\%$  und  $+27\%$  für  $\delta^2\text{H}_{n\text{-alkane}}$  bzw.  $\delta^{18}\text{O}_{\text{sugar}}$  ist das Blattwasser von *Erica arborea* und *Erica trimera* im Vergleich zum Niederschlag mit  $+55 \pm 5\%$  bzw.  $+9 \pm 1\%$  <sup>2</sup>H- und <sup>18</sup>O-angereichert. Im Gegensatz dazu zeigt *Festuca abyssinica* die am stärksten abgereicherten  $\delta^2\text{H}_{n\text{-alkane}}$  and  $\delta^{18}\text{O}_{\text{sugar}}$ -Werte. Dies ist auf eine Signaldämpfung zurückzuführen, die durch das Wachstum der basalen Grasblätter verursacht wird. Die mittleren  $\delta^2\text{H}_{n\text{-alkane}}$  and  $\delta^{18}\text{O}_{\text{sugar}}$ -Werte für *Alchemilla haumannii* und *Helichrysum splendidum* lassen sich möglicherweise mit pflanzenphysiologischen oder

mikroklimatischen Bedingungen erklären, die die relative Luftfeuchtigkeit und damit die Blattwasseranreicherung beeinflussen. Sobald die Isotopenzusammensetzung des Blattwassers berechnet ist, ist es möglich, die Isotopenzusammensetzung von Niederschlagswasser, Deuteriumüberschuss und relativer Luftfeuchtigkeit unter Verwendung eines gekoppelten  $\delta^2\text{H}_{n\text{-alkane}}\text{-}\delta^{18}\text{O}_{\text{sugar}}$ -Ansatzes zu rekonstruieren. Während die gemessenen relativen Luftfeuchtigkeitswerte zwischen 69 und 82% liegen ( $\bar{x} = 80 \pm 3,4\%$ ), ergaben die rekonstruierten Werte der relativen Luftfeuchtigkeit, basierend auf einem kürzlich vorgeschlagenen gekoppelten  $\delta^2\text{H}_{n\text{-alkane}}\text{-}\delta^{18}\text{O}_{\text{sugar}}$ -(Paläo-)Hygrometer-Ansatz, einen Mittelwert von  $78 \pm 21\%$ .

Zusammenfassend lässt sich sagen, dass eine chemotaxonomische Differenzierung rezenter Pflanzen (Blätter) unter Verwendung von Phenolen und *n*-Alkanen möglich ist. Bodenabbauprozesse und Wurzeleinträge verändern jedoch die Proxies, so dass sie für die Rekonstruktion des früheren Ausmaßes des *Erica*-Bestände in den Bale Berge nicht geeignet sind. Folglich müssen Vegetationsänderungen, insbesondere in Bezug auf Gras im Vergleich zu nicht grasartiger Vegetation, in Paläoklima-Studien, basierend auf  $\delta^2\text{H}_{n\text{-alkane}}$  und  $\delta^{18}\text{O}_{\text{sugar}}$ -Analysen, berücksichtigt werden. Darüber hinaus stellen unsere  $\delta^2\text{H}_{\text{prec}}$ - und  $\delta^{18}\text{O}_{\text{prec}}$ -Ergebnisse die traditionelle Interpretation des Mengeneffekts von Paläoklima-Isotopenaufzeichnungen aus Ostafrika in Frage und weisen eher auf einen zuvor unterschätzten Quelleneffekt hin. Der gekoppelte  $\delta^2\text{H}_{n\text{-alkane}}\text{-}\delta^{18}\text{O}_{\text{sugar}}$ -(Paläo-)Hygrometer-Ansatz bietet im Vergleich zu Einzelisotopansätzen ein großes Potenzial für die Ableitung zusätzlicher paläoklimatischer Informationen.



## **I. Extended Summary**

## 1. Introduction

### 1.1 Background

The present extent of the vegetation cover in the Bale Mountains (Mts) is the result of subsequent historical and ecological processes mainly influenced by climate change and/or human-induced driving factors such as fire and grazing (Heiri et al., 2006; Miede and Miede, 1994; Umer et al., 2007). This globally important ecosystem is still increasingly under threat of climate changes and human impacts (Kidane et al., 2012). To better realise how different ecosystems will react to accelerating global warming (IPCC, 2001) and population growth/human occupation (Ossendorf et al., 2019), it is vital to understand their past dynamics. However, natural versus human impact on vegetation dynamics at high altitudes is difficult to quantify and still speculative (Heiri et al., 2006; Jansen et al., 2010). To prove those speculations, a DFG project was developed to disentangle the Mountain Exile Hypothesis “How humans benefited from and re-shaped African high altitude ecosystems during Quaternary climate changes”. In this dissertation, I focused on identifying the potential and constraints of biomarkers and their stable isotopes regarding (a) the chemotaxonomic characterization of the dominant (keystone) plant species, (b) the spatial and temporal variation of stable isotopes in the contemporary precipitation, and (c) on the evaluation of how accurately and precisely the isotope composition of precipitation is imprinted in biomarkers, importantly to provide calibration studies for a semi-quantitative reconstruction of the Late Quaternary paleoclimate and paleovegetation history of the Bale Mts.

Although the vegetation pattern and history of the Bale Mts in Ethiopia were reconstructed using pollen records from lacustrine sediments and peat deposits (Bonnefille and Hamilton, 1986; Bonnefille and Mohammed, 1994; Hamilton, 1982; Umer et al., 2007), little has been known about the former extent of *Erica* shrub across the Sanetti Plateau. Umer et al. (2007) described a sediment core retrieved from Garba Guracha, glacial lake at 3950 m a.s.l and found that just after the start of the Holocene, *Ericaceous* vegetation extended across the Sanetti plateau, in response to increased moisture and temperature. Subsequently, after 6 cal kyr BP *Erica* shrub and trees retreated in area and altitude in response to aridity. Since 4.5 cal kyr BP, the Afro-alpine vegetation expanded across the Sanetti plateau being dominated by dwarf shrubs (e.g. *Helichrysum splendidum*, *Alchemilla haumannii*, *Lobelia rhynchopetalum*) and grasses (e.g. *Festuca abyssinica*).

One of the main problems of pollen-based vegetation reconstruction is pollen preservation can be biased by the dispersal potential of pollinators (Hicks, 2006; Jansen et al., 2010; Ortu et al.,

2006). To overcome such a drawback, we tested the applicability and chemotaxonomic roles of sixteen lignin-derived phenolic compounds and leaf wax-derived *n*-alkane biomarkers in locally dominant plant species of the Sanetti plateau, Bale Mts. We argue that biomarkers are organic compounds with a known origin, which are not influenced by the dispersal of parent materials and can be extracted from nearly all types of (paleo-)environmental archives and reflect more of the standing vegetation (Eganhouse, 1997; Glaser and Zech, 2005). Therefore, they offer the potential to complement pollen-based vegetation reconstructions and detect vegetation change at a higher temporal and spatial resolution.

Polyphenols are the most widespread class of secondary metabolites, and ubiquitous in their distribution (Singh, 2016). Phenolic compounds are a major component of terrestrial vascular plants (Ertel and Hedges, 1984) and may show lignin and non-lignin-derived biochemical structures. Phenols in general and lignin, in particular, are essential for the survival of vascular plant and provide strength and rigidity to the plant, important for cell wall formation, defense against pathogens, and environmental stress (Akula and Ravishankar, 2011; Míka et al., 2005; Thevenot et al., 2010). Phenolic compounds exhibited significant qualitative and quantitative variation among plant kingdoms and have been used extensively in botanical chemotaxonomic studies (Hakulinen et al., 1995; Míka et al., 2005; Nichols-Orians et al., 1993; Witzell et al., 2003).

Lignin-derived phenols of the vanillyl (V), syringyl (S), and cinnamyl (C) types are used to differentiate sources of organic matter in soils and provide information about the state of degradation of vascular plant materials in the terrestrial and aquatic sediments (Castañeda et al., 2009; Hedges et al., 1988; Tareq et al., 2006, 2004; Ziegler et al., 1986). For instance, low ratios of S/V  $\sim 0$  were considered as a proxy of gymnosperms and high values of S/V ratios were found to be indicative for the presence of angiosperms (Tareq et al., 2004). Likewise, the C/V-ratios are proposed to indicate the abundance of woody (C/V < 0.1) and non-woody (C/V > 0.1) vegetation in soils and sediments (Tareq et al., 2011). Moreover, the ratios of acid to aldehyde forms of vanillyl (Ac/Al)<sub>V</sub> and syringyl units (Ac/Al)<sub>S</sub> were suggested as proxies for quantifying the degree of lignin degradation (Amelung et al., 2002; Hedges and Ertel, 1982; Möller et al., 2002).

*n*-Alkanes are important constituents of epicuticular plant leaf waxes (Kolattukudy, 1970), where they serve to protect the plants against excessive evaporation, fungal and insect attacks (Eglinton and Hamilton, 1967; Koch et al., 2009). Due to their recalcitrant nature, *n*-alkanes are well preserved in sedimentary archives; that's why they received increasing scientific attention

during the last decades as molecular markers to trace the origin of organic matter and as proxies for paleoclimate studies (Asia et al., 2009; Eglinton and Eglinton, 2008; Glaser and Zech, 2005; Zech et al., 2011c). The potential of *n*-alkanes for chemotaxonomic studies has been suggested based on the finding that the homologues C<sub>27</sub> and C<sub>29</sub> are sourced predominately from trees and shrubs, whereas homologues C<sub>31</sub> and C<sub>33</sub> are sourced predominately from grasses and herbs (Maffei, 1996; Maffei et al., 2004; Rommerskirchen et al., 2006; Schäfer et al., 2016; Zech et al., 2009). Moreover, long-chain *n*-alkanes (C<sub>27</sub> and C<sub>33</sub>) with a strong odd-over-even predominance (OEP) are an important constituent of terrestrial plant leaf-waxes (Kolattukudy, 1970; Zech et al., 2009), whereas short-chain (C<sub>15</sub> to C<sub>19</sub>) and middle-chain *n*-alkanes (C<sub>20</sub> to C<sub>25</sub>) are mostly found in aquatic organisms (Ficken et al., 1998; Zhang et al., 2004). However, the potential pitfalls when applying *n*-alkanes in paleovegetation studies should not be overlooked. For instance, caution has to be given against the chemotaxonomic application of *n*-alkanes because of high *n*-alkanes pattern variability within graminoids and woody plants (Bush and McInerney, 2013) as well as for the effect of degradation (Zech et al., 2011b, 2013a). Therefore, Schäfer et al. (2016) emphasised the need for establishing regional *n*-alkanes calibration studies.

Stable isotopes in precipitation (<sup>2</sup>H, <sup>17</sup>O, and <sup>18</sup>O) and compound-specific stable isotopes ( $\delta^2\text{H}_{n\text{-alkane}}$  and  $\delta^{18}\text{O}_{\text{sugar}}$ ) are useful proxies to understand the modern-day atmospheric circulation patterns (Araguás-Araguás et al., 2000; Rozanski et al., 1996) and valuable proxies for paleoclimate and paleoenvironmental studies (Eglinton and Eglinton, 2008; Zech et al., 2014; Zech and Glaser, 2009). The variation of  $\delta^2\text{H}_{\text{prec}}$  and  $\delta^{18}\text{O}_{\text{prec}}$  results from isotope fractionation that occurs during evaporation and condensation along the hydrological cycle (Araguás-Araguás et al., 2000; Dansgaard, 1964). Apart from this, other sites and climatic factors such as latitude, altitude, distance to the coast, temperature, relative humidity, wind, cloud, rain size, rain type, size and type of convection as well as source and amount of precipitation are factors influencing the isotope composition of precipitation (Aggarwal et al., 2016; Araguas et al., 1996; Araguás-Araguás et al., 2000; Dansgaard, 1964; Kurita, 2013). The seasonal migration of the Inter-Tropical Convergence Zone (ITCZ) coincides with a marked seasonality effect in the isotope composition of precipitation (Araguás-Araguás et al., 2000; Mohamed et al., 2005; Nicholson, 1996). This variation of stable isotopes in precipitation is also reflected in the isotope composition of leaf wax-derived *n*-alkanes ( $\delta^2\text{H}$ ) and hemicellulose-derived sugar ( $\delta^{18}\text{O}$ ) (Hepp et al., 2017a; Tuthorn et al., 2015; Zech et al., 2013b) and can thus be used for paleoclimate studies.

## 1.2 Study Objectives

The present dissertation is part of the DFG research unit 2358 “The Mountain Exile Hypothesis - How humans benefited from and re-shaped African high altitude ecosystems during Quaternary climate change”, within Sub-project 5: Paleoclimatology aims at contributing to a semi-quantitative reconstruction of the Late Quaternary paleoclimate history of the Bale Mts in Ethiopia. My dissertation focusses on identifying the potential and limitations of biomarkers and stable isotopes for chemotaxonomy and paleoclimate reconstruction in the Bale Mts, Ethiopia. More specifically, it aims to answer the following research questions:

- I. Do plant-derived phenols and *n*-alkanes allow a chemotaxonomic differentiation of the contemporary keystone plant species of the Bale Mts? (MS 1 and 2)
- II. Are the biomarker patterns of the plants reflected by and incorporated into the respective topsoils? (MS 1)
- III. Which implications have to be drawn from those results for the planned paleoclimate and paleovegetation reconstruction mainly concerning the reconstruction of the former extent of *Erica* shrubs? (MS 1 and 2)
- IV. Are there any characteristic altitude and amount effects discernible in the  $^2\text{H}/^{18}\text{O}$  isotope patterns of precipitation in the Bale Mts? (MS 3)
- V. Is there a characteristic seasonal  $^2\text{H}/^{18}\text{O}$  isotope pattern of precipitation in the Bale Mts? (MS 3)
- VI. Is it possible to trace the moisture sources for the Bale Mts and thus to contribute to a better understanding of the modern-day atmospheric circulation patterns? (MS 3)
- VII. Are there systematic  $\delta^2\text{H}_{n\text{-alkane}}$  and  $\delta^{18}\text{O}_{\text{sugar}}$  differences between leaves, O-layers, and  $A_h$ -horizons? (MS 4)
- VIII. Do the  $^2\text{H}/^{18}\text{O}$  isotope patterns of *n*-alkane and sugar biomarkers in leaves and topsoils reflect the isotope signature of the precipitation? (MS 4)
- IX. Are there any systematic  $\delta^2\text{H}_{n\text{-alkane}}$  and  $\delta^{18}\text{O}_{\text{sugar}}$  differences among the keystone plant species? (MS 4)
- X. Does the application of the coupled  $\delta^2\text{H}_{n\text{-alkane}}\text{-}\delta^{18}\text{O}_{\text{sugar}}$  (paleo-) hygrometer approach provide any additional paleoclimate information compared to the single isotope approaches? (MS 4)

## 2. Study area

### 2.1 Geomorphological Setting

The Bale Mts belong to the Bale-Arsi mountain massif located 400 km southeast of Addis Ababa, capital of Ethiopia (Fig. I). It is geographically situated between 39°03' to 40°00' longitude (E) and between 6°29' to 7°10' latitude (N) with an elevation ranging from 1400–4377 m a.s.l. (Hillman, 1986). The Bale Mts comprise an area of 2,600 km<sup>2</sup>, which forms one of the most extensive high altitude plateaus called Sanetti (above 3000 m a.s.l.) in Africa (Hillman, 1988; Kidane et al., 2012; Tiercelin et al., 2008). The lava outpouring around 40 million years ago resulted in the formation of the mountains and ridges up to 4377 m a.s.l. (Mohr, 1961). Since the crust of the Bale Mts is of volcanic origin, the soils which are developed from the basaltic, rhyolitic, and trachytic parent rock, can be generally characterized as silty loams of reddish-brown to black colour (Woldu et al., 1989). Nevertheless, the areas higher than ~3500 m a.s.l were substantially flattened and influenced by repeated glaciations (between ~50 – 30 and around 20 – 12 cal kyr BP) as documented by moraines, solifluction covers and kettles (Groos et al., 2020; Ossendorf et al., 2019). The soils developed from glacial deposits are usually shallow and stony (Hedberg, 1964; Osmaston et al., 2005). Andosols are the most ubiquitous soil types but also Cambisols and Leptosols are prevalent in some parts of the Bale Mts. In the wetlands and sedimentary basins Gleysols and Histosols (Billi, 2015; Yimer et al., 2006), and in the rock shelters Anthrosols (Ossendorf et al., 2019) are also a common soil type.

The Bale Mts are topographically divided into three major parts: The Northern slopes (3000–3800 m. a.s.l.), the Sanetti plateau (3800–4377 m a.s.l), and the Southern Harena escarpment (1400–3800 m. a.s.l.). The Sanetti Plateau is placed in the center, on which the second highest peak of the country Mt. Tulu Dimtu (4377 m a.s.l.), is located. The northern slope of the mountains is dissected by the Togona Valley, which descends towards the extensive Arsi Plateau and further down to the central Ethiopian Rift Valley lowlands, which divide the country into two parts. The Southern slope includes the steep Harena escarpment and goes down to the surrounding lowland at about 1400 m a.s.l. (Hillman, 1988; Tiercelin et al., 2008).

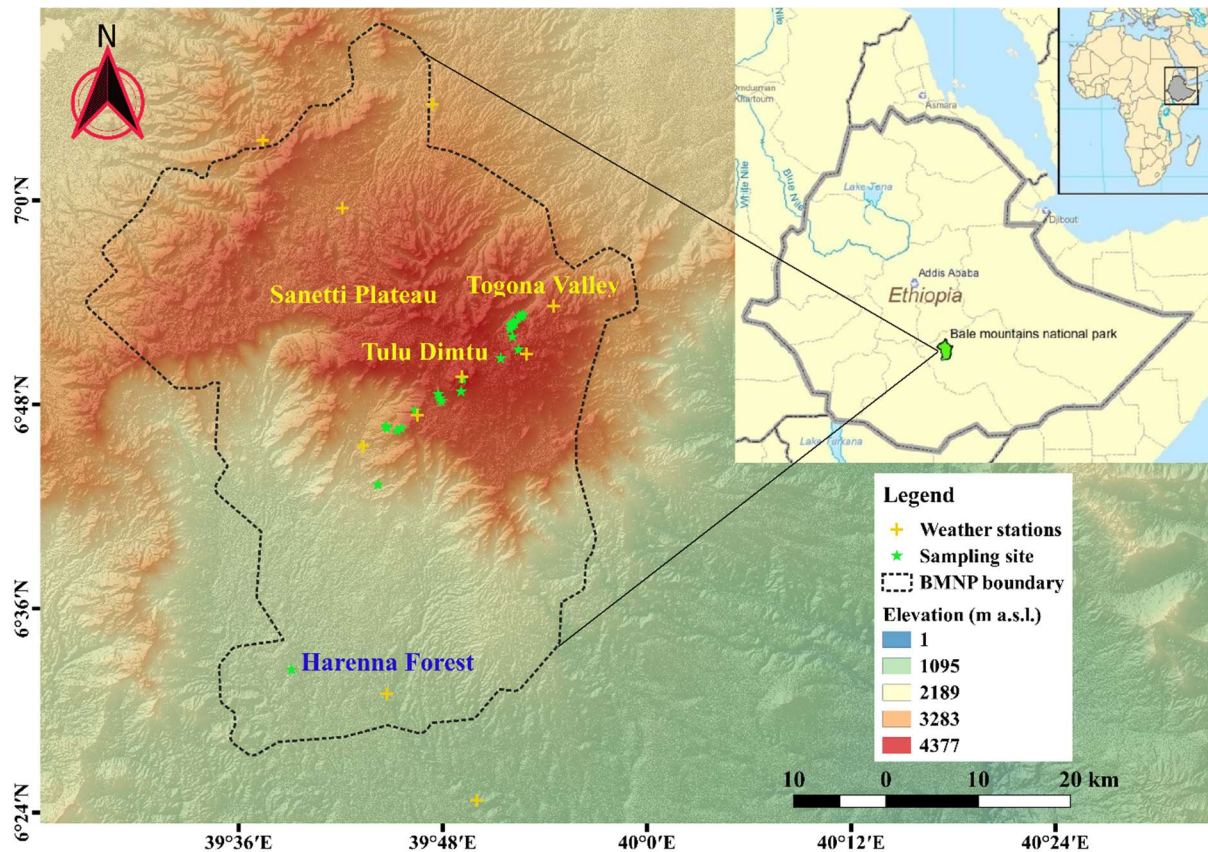


**Fig. I:** Map showing the location of Ethiopia in Africa, location of the Bale Mountains National Park (BMNP) in Ethiopia, and location of sampling points and weather stations in the BMNP.

## 2.2 Climate

The Bale Mts are a historically vulnerable ecosystem influenced by extreme climate changes over the past geological time. This is mainly reflected in vegetation changes, moisture and temperature fluctuations (Osmaston et al., 2005; Umer et al., 2007). The climatic conditions of the Bale Mts mainly depend on orography. Such orographic and topographical differences result in a wide range of temperature and rainfall distribution in the northern, central, and southern aspects (Kidane et al., 2012; Tiercelin et al., 2008). Albeit there is a wider variability of climate in the Bale Mts, only a few records were reported. In this dissertation, I also report some recent records gathered from ten newly installed weather stations across the Bale Mts. The highest mean annual temperatures range between 6 to 12 °C in the mountain peaks. At Dinsho (Bale Mountains National Park Headquarter, 3170 m a.s.l.) the mean annual temperature (MAT) is 11.8 °C. The lowest MAT range from 0.6 to 10 °C, with frequent frost occurring on the high plateau areas during the winter season (November to January) (Hillman, 1986; Miehe and Miehe, 1994; Tiercelin et al., 2008). The Afro-alpine region of the Bale Mts

(mainly Sanetti Plateau) is characterized by high diurnal temperature differences with a range of 40 °C (−15 °C to + 26 °C), that resemble summer in the day and winter in the night (Hillman, 1988, 1986). The lowest temperatures are recorded during the dry season, whereas during the wet season nights are warmer and days are cooler (Bonnefille, 1983; Hillman, 1988).

Precipitation of the Bale Mts originates from different sources, mainly from equatorial westerlies, the Mediterranean Sea, and the Indian Ocean (Miehe and Miehe, 1994; Viste and Sorteberg, 2013). Seasonal migration of the ITCZ results in a long rainy season (March to October) and a short dry season (November to February) (Admasu et al., 2004; Kidane et al., 2012). The wet season is characterized by a slightly bimodal rainfall pattern, which is associated with the convergence of the southwest and northeast airstreams (Bonnefille, 1983). In summer (June to September), the ITCZ is located north of Ethiopia and the northwest and central part of the country receives precipitation via south-westerly and southerly monsoon airflows. Between October and March, the ITCZ is located south of Ethiopia and induces southward airflow originating from the Arabian Sea and the Northern Indian Ocean bringing moisture up to southeastern plateau and producing rainfall during October (Tiercelin et al., 2008). The highest precipitation occurs in the southern part of the mountains with 1000–1500 mm year<sup>-1</sup>, whereas the northern part of the mountains receives annual rainfall ranging between 800–1000 mm year<sup>-1</sup> (Bonnefille, 1983; Tiercelin et al., 2008; Woldu et al., 1989).

Since the beginning of 2017, ten newly installed weather stations enabled us to record the contemporary weather data across the Bale Mts. Accordingly, the southern escarpment is warmer than the northern declivities with a MAT of 22 °C at Delo Mena station (1304 m a.s.l.). The Sanetti Plateau is the coldest region of the Bale Mts with a MAT of 2 °C at Tulu Dimtu station (4375 m a.s.l.). The present MAT record at Dinsho station is 11 °C, which supports previously reported records in literature (Hillman, 1986; Miehe and Miehe, 1994; Tiercelin et al., 2008). Mean annual relative humidity at 2 meters above the ground ranges from 67 to 87%. 1228 mm year<sup>-1</sup> was the highest mean annual precipitation over the last three years and recorded at Magnete station (1580 m a.s.l.).

### **2.3 Biota**

The Bale Mts are part of the Eastern Afromontane biodiversity hotspot area and a habitat for more than 1300 vascular flowering plants, of which 163 are endemic to Ethiopia and 27 of them are restricted to the Bale floristic region (Dullo et al., 2015; Williams et al., 2004). The distribution and abundance of the contemporary vegetation in the Bale Mts are shaped partly by human intervention, long distance dispersal events (migrations) and often emphasize the



landforms and paleoclimate (Assefa et al., 2007; Kebede et al., 2007; Osmaston et al., 2005). Diverse topographic variations in the Bale Mts form an altitudinal zonation's of the vegetation, which are dependent on slope, aspect, soils, and climate (Hillman, 1988). In broad terms, floristically the mountains, particularly within the National Park, are divided into three topographic regions. The southern escarpment (1400–3800 m a.s.l.) is delineated by the moist Afromontane Haremma forest, Ericaceous belt, and Afro-alpine vegetation, whereas the central Sanetti plateau (3800–4377 m a.s.l.) is dominated by a sparse Afro-alpine vegetation and the northern slope (3000–3800 m a.s.l.) encompasses dry Afromontane forest, Gaysay grassland, Ericaceous belt, and Afro-alpine zones (Friis, 1986; Hillman, 1988; Miehe and Miehe, 1994).

The Afro-alpine regions of the Sanetti Plateau are characterized by tussock grassland, cushion-forming plants and dwarf shrubs and herbaceous plants (e.g., *Festuca abyssinica*, *Helichrysum citrispinum*, *Helichrysum splendidum*, *Alchemilla haumannii*, and *Lobelia rhynchopetalum*) (Hedberg and Hedberg, 1979). The Ericaceous belt (3300–3800 m a.s.l.) comprises forests, thickets, and scrublands of *Erica trimeria* and *Erica arborea* with mosses and grasses dominating in the ground layer. The Haremma forest (1500–3300) is a natural remnant of a moist Afromontane forest dominated by broadleaved evergreen trees and clustered floristically into two different classes. Around 1500–2300 m a.s.l. the forest is dominated by *Podocarpus falcatus* associated with *Croton macrostachyus*, *Pouteria adolfi-friederici*, *Syzygium guineense*, *Warburgia ugandensis*, and worth noting is also *Coffea arabica*. Between 2300–3200 m a.s.l., *Oldeania alpina*, *Hagenia abyssinica*, *Hypericum revolutum*, *Erythrina brucei*, *Prunus africana*, and *Schefflera volkensii* are the dominant plants (Friis, 1986; Hillman, 1988, 1986; Miehe and Miehe, 1994; Woldu et al., 1989). The northern slopes are dominated by scattered *Juniperus procera*, *Hagenia abyssinica*, and *Hypericum revolutum* woodlands and Gaysay grasslands rich in *Artemisia afra*, *Ferula communis*, and *Kniphofia foliosa*, with the *Erica* belt above the treeline (3400 m a.s.l.).

Furthermore, over 50 wild mammal species (20% endemic), more than 180 wild bird species, of which 15 are endemic to Ethiopia, and 14 amphibian species are inhabiting the Bale Mts. This all makes the Bale Mts a centre for faunal diversity and holds the highest rate of animal endemism for a terrestrial habitat anywhere in the world (Hillman, 1988). The Bale Mts are known mainly by its flagship mammals like Mountain Nyala (*Tragelaphus buxtoni*), Ethiopian Wolf (*Canis simensis*), Giant mole rat (*Tachyoryctes macrocephalus*), Menelik's bushbuck (*Tragelaphus scriptus menelik*), and Rock hyrax (*Procavia capensis capillosa Brauer*) (Hillman, 1988; Williams et al., 2004).

### 3. Analytical methods

#### 3.1 Sample collection and preparation

Leaves ( $n = 47$ ), organic surface layers (O-layers, litter,  $n = 15$ ), and mineral topsoils ( $A_h$ -horizons,  $n = 22$ ) were sampled, then air-dried, homogenized, sieved using a mesh size of 2 mm, finely ground and finally subjected to biogeochemical analyses (study 1, 2 and 4). 164 precipitation samples (study 3) were collected biweekly since February 2017 using custom-built rain gauges from ten weather stations established along an altitudinal transect ranging from 1304 to 4375 m a.s.l.

#### 3.2 Lignin phenols analyses

Sixteen phenolic compounds were extracted from 35, 50, and 500 mg of leaf/twig, O-layer, and  $A_h$ -horizon soil samples, respectively, using cupric oxide (CuO) oxidation method developed by Hedges and Ertel (1982) and modified by Goñi and Hedges (1992). Briefly, the samples were transferred into Teflon digestion tubes together with 100 mg of  $(NH_4)_2Fe(SO_4)_2 \cdot 6H_2O$ , 500 mg of CuO, 50 mg of  $C_6H_{12}O_6$ , 1 mL of ethylvanillin solution ( $100 \text{ mg L}^{-1}$ ) as first internal standard and 15 mL of 2M NaOH and digested at  $170 \text{ }^\circ\text{C}$  for two hours under elevated pressure. Reaction products were cooled overnight and transferred into centrifuge tubes. Then the phenolic compounds were purified by adsorption on C18 columns and desorbed by ethylacetate and concentrated under a stream of nitrogen gas for 30 min. Afterward the residue was re-dissolved in 1 mL of a solution containing the second internal standard, phenylacetic acid (PAA), in methanol ( $25 \text{ } \mu\text{g ml}^{-1}$ ) to determine the recovery of ethylvanillin before derivatization (Amelung et al., 2002; Möller et al., 2002). Finally, the samples were derivatized using 200  $\mu\text{L}$  of N, O-Bis(trimethylsilyl) trifluoroacetamide (BSTFA) and 100  $\mu\text{L}$  of pyridine. Oxidation products of phenolic compounds were quantified using a SHIMADZU QP 2010 Gas Chromatography (GC) instrument coupled with a Mass Spectrometry (MS), (GCMS-QP2010, Kyoto, Japan).

#### 3.3 Lipid analyses

Leaf wax-derived  $n$ -alkanes were extracted from 0.5 to 1 g of homogenised leaf, O-layer, and  $A_h$ -horizon soil samples using Soxhlet extraction by adding 150 ml of dichloromethane (DCM) and methanol (MeOH) as solvents (9:1 ratio) for 24 h following a method modified after Zech and Glaser (2008). In brief, 50  $\mu\text{l}$  of  $5\alpha$ -androstane were added to the total lipid extracts as an internal standard. Total lipid extracts were concentrated using rotary evaporation and transferred to aminopropyl pipette columns (Supelco, 45  $\mu\text{m}$ ). Three lipid fractions containing

the *n*-alkanes, alcohols, and fatty acids, respectively, were eluted successively by using 3 ml of hexane, DCM/MeOH (1:1), and diethyl ether and acetic acid (95:5) as eluent. The *n*-alkanes were separated using a gas chromatography (GC) and detected by a flame ionization detector (FID), whereas the other two lipid fractions (alcohols and fatty acids) were archived.

### 3.4 Stable isotope measurements

The  $\delta^2\text{H}_{\text{prec}}$  and  $\delta^{18}\text{O}_{\text{prec}}$  isotope values were measured using a Thermo Conversion Unit (HTO HEKAtech Wegberg, Germany) coupled with a ConFlo IV interface to an Isotope Ratio Mass Spectrometry (IRMS, Thermo Fisher Scientific, Bremen, Germany) in Bayreuth Center of Ecology and Environmental Research (BayCEER), University of Bayreuth, Germany. Laboratory calibration was made against Vienna Standard Mean Ocean Water (V-SMOW) by co-analysing standards every ten samples resulting in a precision of  $\pm 0.6\text{‰}$  for  $\delta^{18}\text{O}_{\text{prec}}$  and  $\pm 3\text{‰}$  for  $\delta^2\text{H}_{\text{prec}}$ .

The  $\delta^2\text{H}_{n\text{-alkane}}$  and  $\delta^{18}\text{O}_{\text{sugar}}$  values were determined using a gas chromatography-thermal conversion-isotope ratio mass spectrometry (GC-TC-IRMS, Delta V, Thermo Fisher Scientific, Bremen, Germany) in the laboratory of the Soil Biogeochemistry, Martin Luther University of Halle–Wittenberg, Germany. Each sample was analyzed in triplicate and measurements of known standards at various concentrations were embedded in-between the sample batches. The measured  $\delta^2\text{H}_{n\text{-alkane}}$  and  $\delta^{18}\text{O}_{\text{sugar}}$  values were corrected for drift and amount-dependence, according to Zech and Glaser (2009). The mean standard error for triplicate measurements of the samples was 0.8‰, 0.9‰, 3.1‰, 2.3‰ for arabinose, xylose, C<sub>29</sub>, and C<sub>31</sub>, respectively. The standard error for the sugars and *n*-alkanes standards was 2‰ (n = 22) and 5‰ (n = 28), respectively. The  $\delta^2\text{H}_{n\text{-alkane}}$  values refer to weighted mean values of C<sub>29</sub> and C<sub>31</sub> alkanes and  $\delta^{18}\text{O}_{\text{sugar}}$  values refer to weighted mean values of arabinose and xylose. All  $\delta^2\text{H}_{\text{prec}}$  and  $\delta^{18}\text{O}_{\text{prec}}$ , as well as  $\delta^2\text{H}_{n\text{-alkane}}$  and  $\delta^{18}\text{O}_{\text{sugar}}$ , values are reported in per mil (‰) according to the usual  $\delta$ -notation relative to V-SMOW given in the following equation.

$$\delta = (R_{\text{sample}}/R_{\text{standard}} - 1) \times 10^3$$

where R refers to the ratio of  $^{18}\text{O}/^{16}\text{O}$  and  $^2\text{H}/^1\text{H}$  for the sample or standard (V-SMOW) materials.

## 4. Results and discussion

### 4.1 Biomarkers

#### 4.1.1 Lignin phenols in leaves and topsoils (Study [MS]–1)

The sum of lignin phenols, vanillyl, syringyl, and cinnamyl ( $\Sigma\text{VSC}$ ) of the investigated plants ranges from 1.8 to 41.8 mg g<sup>-1</sup><sub>sample</sub> with *Festuca* yielding the highest (33 mg g<sup>-1</sup><sub>sample</sub>). This is

within the range reported in the literature (Belanger et al., 2015; Hedges et al., 1986). The Agglomerative Hierarchical Cluster analyses (AHC) allow to chemotaxonomically differentiate keystone plant species of the Bale Mts using the total abundance of lignin phenols (Fig. II). The abundance of individual lignin phenols is specific to the individual or restricted groups of plant and/or tissues applied to cluster different taxa (Belanger et al., 2015; Castañeda et al., 2009; Goñi and Hedges, 1992; Hedges and Mann, 1979; Tareq et al., 2006, 2004).

However, it is not clear to us so far which lignin phenols are the most decisive character for which plants and which lignin proxies might have the potential for paleovegetation reconstruction. Thus, to find out the most determining proxies, we draw a notched box plot (Fig. III). Figure III corroborates that *Erica arborea* and *Erica trimera* are characterized by cinnamyl percentages of > 40%, whereas, except for two *Festuca* samples, all other plants are characterized by cinnamyl percentages of < 40%. Despite a relatively large scattering and a partial overlapping, our results suggest that the ratio  $C/(V+S+C)$  might be used as a proxy for distinguishing the contemporary *Erica spp.* from another vegetation type of the Bale Mts, with values > 0.40 being generally characteristic for *Erica spp* (Fig. III).

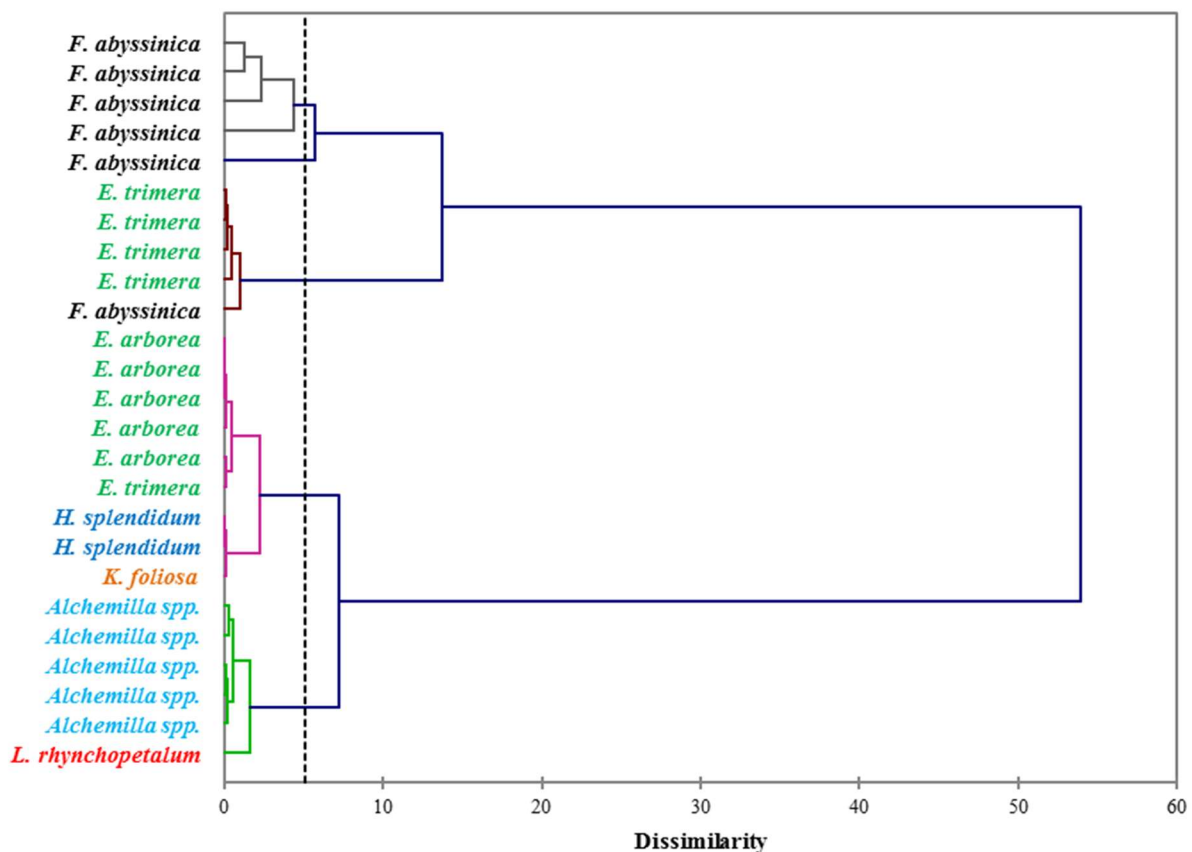


**Fig. II:** Dendrogram differentiating the dominant plant species of the Bale Mountains based on the concentrations of vanillyl, syringyl, and cinnamyl lignin phenols ( $\text{mg g}^{-1}$  sample). The dotted vertical line represents the distance or dissimilarity between clusters.

The  $\sum\text{VSC}$  strongly decreases from plants over O-layers to  $A_h$ -horizons except for *Helichrysum*. This descending trend reflects a degradation of plant-derived lignin phenols during organic matter decomposition (Amelung et al., 1997; Thevenot et al., 2010; Belanger et al., 2015). At the same time, the input of root-derived lignin is very likely (Abiven et al., 2011; Baumann et al., 2013; Thomas et al., 2014). As a result of both processes, i.e., degradation and lignin input by roots, the large and chemotaxonomically characteristic contribution of C in *Erica* species ( $\geq 40\%$ ) is lost in the O-layers ( $C < 27\%$ ), whereas the two investigated O-layers under *Festuca* yielded relative C contributions  $> 40\%$ . Indeed, the composition of lignin phenols is characteristic for contemporary plants, but preferential degradation of S and C phenols compared to V phenols can affect the value of source parameters calculated for soils (Otto and Simpson, 2006; Thevenot et al., 2010; and references therein) and roots had C phenols higher than stems and leaves, and contribute more to the total soil lignin content than the shoot parts (Abiven et al., 2011). This finding does not *ad hoc* preclude the above proposed lignin phenol proxy  $C/(V+S+C)$  for reconstructing vegetation history, but it challenges its application. Therefore, degradation and lignin input by roots need to be considered when interpreting lignin phenol proxies from sedimentary archives.

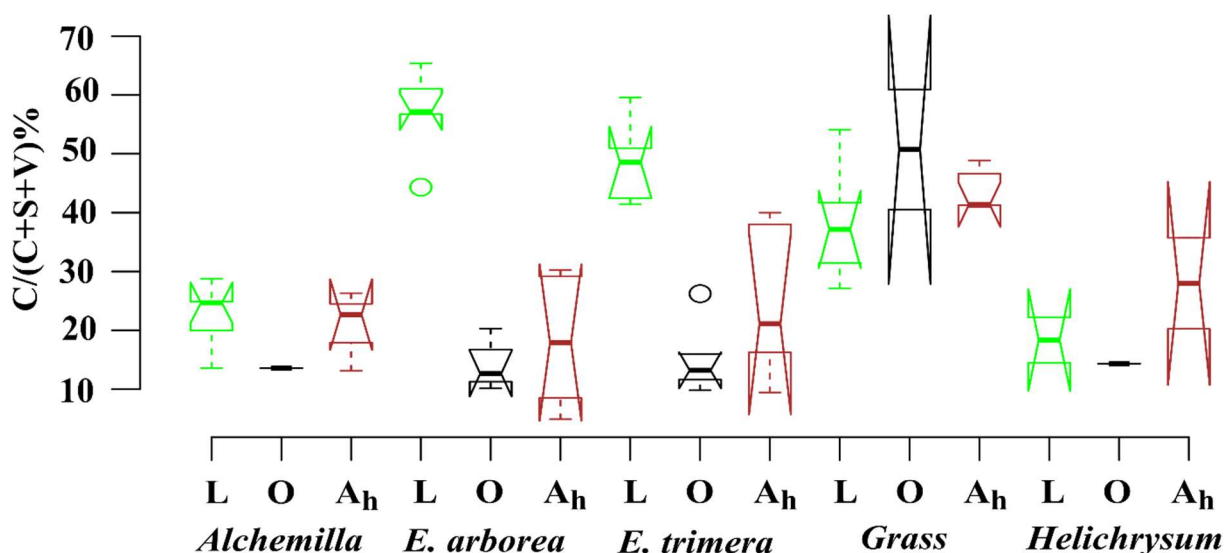


**Fig. III:** Box plot for the relative abundance of cinnamyl phenols (expressed as  $C/(V+S+C)$  in %) in plants, O-layers and  $A_h$ -horizons. The box plots indicate the median (solid line between the boxes) and interquartile range (IQR), with upper (75%) and lower (25%)

quartiles and possible outliers (empty circles). The notches display the confidence interval around the median within  $\pm 1.57 \cdot \text{IQR} / \sqrt{n}$ . Note that small sample sizes result in unidentifiable boxes.

#### 4.1.2 *n*-Alkanes in leaves and topsoils (Study [MS]–1)

Most of the investigated plant species depicted total *n*-alkane contents (TAC, C<sub>25</sub>–C<sub>35</sub>) above 800  $\mu\text{g g}^{-1}$ . Only *Lobelia* and *Festuca* exhibited TAC values below 800  $\mu\text{g g}^{-1}$ . Such *n*-alkanes abundance is considered as characteristic of epicuticular leaf waxes, being typical for higher plants (Eglinton and Hamilton, 1967; Hoffmann et al., 2013). Also, the average chain length (ACL) of leaves and topsoils ranged between 28 to 32 and 29 to 31, respectively. The ACL of *Erica arborea* (30.5) and *Erica trimera* (30.5) are identical, which could be explained by the monophyletic origin of the species (Guo et al., 2014). The grass samples (*Festuca abyssinica*) revealed a clear predominance of C<sub>31</sub> (Fig. IV), which was reported before by different authors (Schäfer et al., 2016; Zech et al., 2009). Most other investigated plant species revealed a predominance of either C<sub>29</sub> or C<sub>31</sub>. Only *Kniphofia foliosa* is characterized by a high relative abundance of C<sub>27</sub> and C<sub>29</sub>, while C<sub>31</sub> is almost absent (Fig. IV).

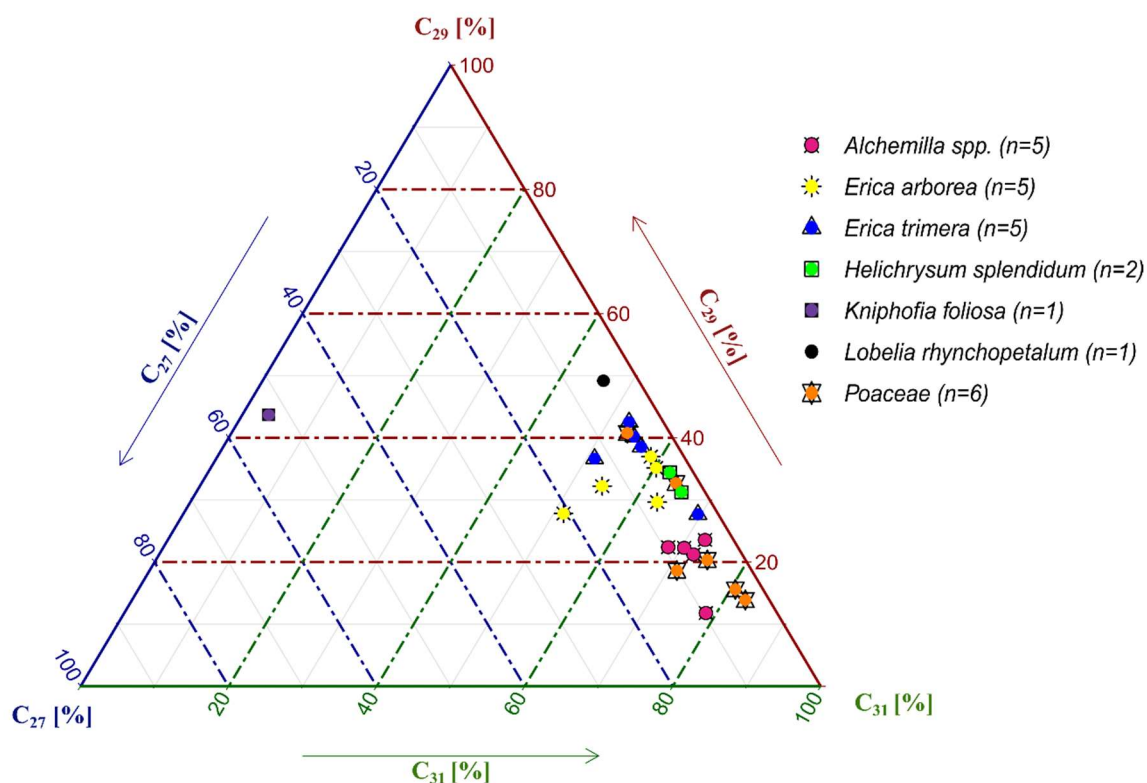


**Fig. IV:** Ternary diagram illustrating the relative abundance of the  $n$ -alkanes  $C_{27}$ ,  $C_{29}$ , and  $C_{31}$  in the investigated plant samples.

Contrary to plant-derived lignin phenols, hierarchical cluster analysis of individual  $n$ -alkanes did not allow unambiguous differentiation between *Erica* and non-*Erica* species. Therefore, the  $n$ -alkane patterns do not support developing a proxy for identifying *Erica*, at least in the Bale Mts. Nevertheless, apart from the individual  $n$ -alkanes, lower ratio of  $C_{31}/C_{29}$  ( $\bar{x} = 1.7$ ) depicts *Erica* litter is significantly ( $p = 0.05$ ) distinguishable from the other species except for *Helichrysum splendidum* (Fig. V).

The odd over even predominance (OEP) and TAC values decrease in the order plants > O-layers >  $A_h$ -horizons. Decreasing OEP values towards O-layers and  $A_h$ -horizons are often observed and can be explained with organic matter degradation (Schäfer et al., 2016; Zech et al., 2011a). Importantly,  $n$ -alkane degradation does not only affect the OEP values but also  $n$ -alkane ratios such as the above presented ratio  $C_{31}/C_{29}$  that allows to distinguish *Erica* from non-*Erica* vegetation. As a result, this ratio is not feasible to chemotaxonomically distinguish between soils having developed under *Erica* versus *Alchemilla* and grass. The effort towards finding unambiguous *Erica* markers using lignin-derived phenols and leaf wax-derived  $n$ -alkanes was unusable.

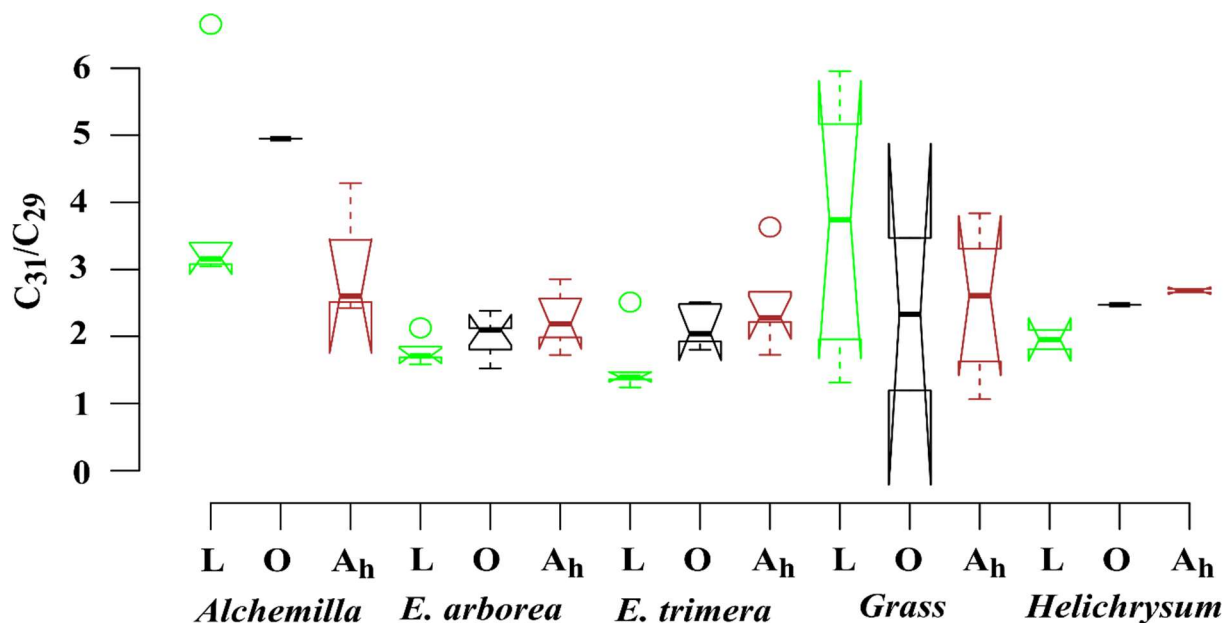


**Fig. V:** Notched box plot for the ratio  $C_{31}/C_{29}$  in plant samples, organic layers, and  $A_h$ -horizons.

The box plots indicate the median (solid line between the boxes) and interquartile range (IQR), with upper (75%) and lower (25%) quartiles and possible outliers (empty circles). The notches display the confidence interval around the median within  $\pm 1.57 \cdot IQR / \sqrt{n}$ . Note that small sample sizes result in unidentifiable boxes.

### 4.1.3 Phenolic compounds in the keystone plant species (Study [MS]–2)

In order to clearly define the extent of the *Erica* species along the Sanetti Plateau in the Bale Mts, the potential and limitations of phenols and *n*-alkanes were evaluated that had previously been applied by several researchers in various (paleo-)environmental archives (Glaser and Zech, 2005, Tareq et al., 2006, Zech et al., 2011a, 2013a). Thus, each of the keystone plant species in the Bale Mts showed a different phenolic compound pattern (Table 1-1). The sum of mean weighted phenolic compound contents of *Alchemilla haumannii*, *Erica* spp., *Helichrysum splendidum*, *Kniphofia foliosa*, *Lobelia rhynchopetalum*, and *Festuca abyssinica* are 18, 16, 22, 6, 22 and 51 g kg<sup>-1</sup> TOC, respectively. The widespread occurrence of secondary metabolites, like phenols in the plant kingdom, enables us to conduct lower taxonomic level chemotaxonomic studies (Mika et al., 2005; Singh, 2016)

A high abundance of coumaryl (*p*-coumaric acid, ferulic acid) and syringyl (syringic acid, 3,5-Dimethoxy-4-hydroxyacetophenone) phenols and low abundance of vanillyl phenols and benzoic acids characterize *Festuca abyssinica*. The same genus of different species, *Festuca vallesiaca*, could be also ascribed by high coumaryl phenols (*p*-coumaric acid, ferulic acid) and low benzoic acid derivatives (Djurdjevic et al., 2005). Generally, in the grass taxon, most of phenol-related information was provided by coumaryl phenols due to ample presence of the enzyme phenyl (tyrosine) ammonia-lyase and it is known for its high biological activity (Chesson et al., 1982; Djurdjevic et al., 2005; Mika et al., 2005). Likewise, Hedges and Mann (1979) stated that non-woody vascular angiosperm plants have characteristic products of coumaryl phenols and account for approximately one-third of the total phenolic compounds.

The sum of *p*-hydroxy phenols unambiguously identifies *Helichrysum splendidum* from the other locally dominant plant species of the Bale Mts. On the other hand, *Erica* species are characterized by high coumaryl and low *p*-hydroxy phenols. The genus *Erica* (family: *Ericaceae*) is characterized by having polyphenols (*p*-coumaric acid derivate, vanillic acid, cinnamic acid derivate, and caffeic acid) and flavonoids (Guendouze-Bouchefa et al., 2015). Among the flavonoids, dihydromyricetin 3-O- $\alpha$ -L-rhamnopyranoside is the most important chemotaxonomic marker of *Erica* (Nazemiyeh et al., 2008).

We here evaluated phenolic compounds through the classical approach such as hierarchal clustering, 2D plots analysis using source proxies (S/V and C/V) to chemotaxonomically characterize locally dominant plant species. Both approaches failed to explicitly characterize the locally dominant plant species. However, we found that *Erica* species in the Bale Mts can



be identified using the relative contribution of coumaryl phenols ( $> 0.2$ ) and benzoic acids ( $0.05\text{--}0.12$ ; Fig. VI). Furthermore, three different machine-learning algorithms namely Support Vector Machine (SVM), Random Forest (RF), and Recursive Partitioning (RP) were tested to unambiguously identify *Erica* species based on our phenolic compounds dataset. Among the tested machine learning approaches, RF performed best. The proposed algorithm has been shown to be better in terms of various performance indicators like accuracy and F1-score. In the experiment using the relative phenols dataset, the key variables for the chemotaxonomic classification of the contemporary species in the Bale Mts is depicted in Fig. VII. Among them, benzoic acids ( $> 0.06$ ) and coumaryl phenols ( $> 0.21$ ) were the most decisive variables to identify *Erica* from the other species, which has been corroborated in Fig. VI.

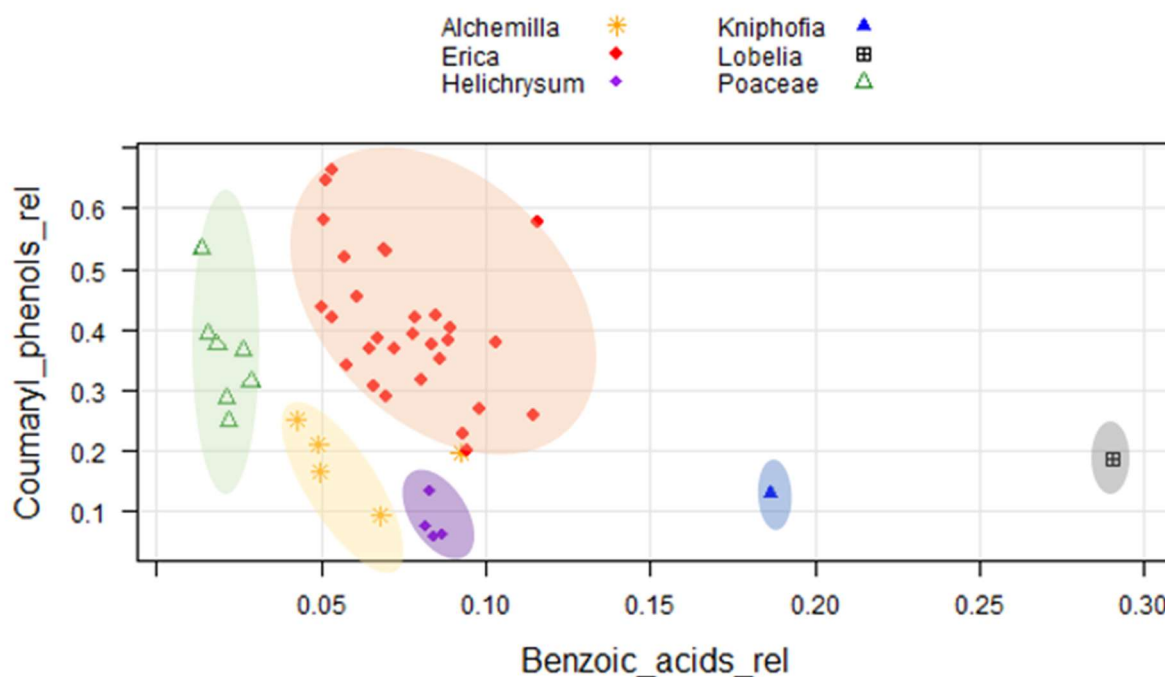


**Fig. VI:** Two-dimensional plot of the relative contribution of the sum of coumaryl phenols (*p*-coumaric acid + ferulic acid) and benzoic acids (benzoic acid + salicylic acid + phthalic acid) in the dominant plant species under study.

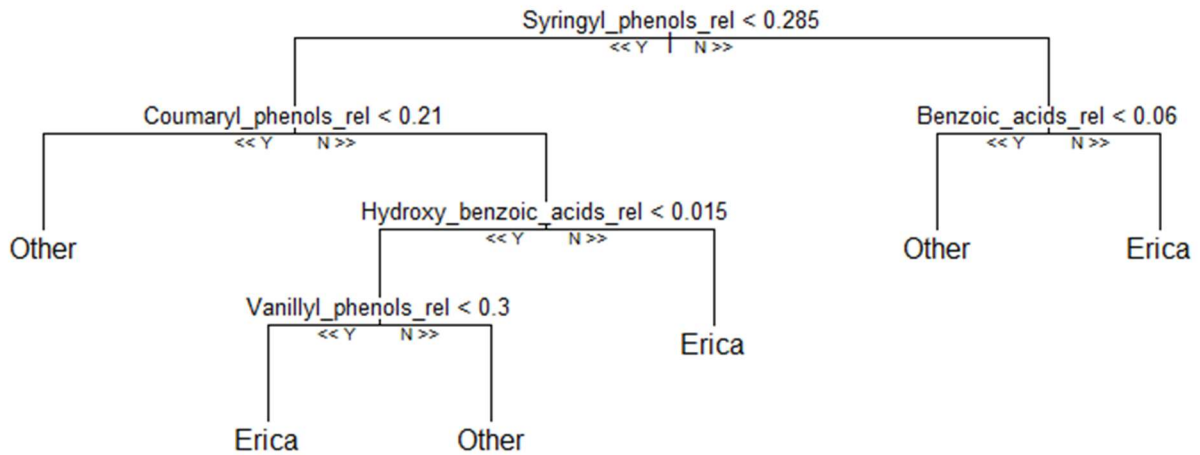


**Fig. VII:** Representative decision tree of Random Forest (RF) model using relative phenols contribution. 32 training sample sets and 10,000 number of decision trees were used to compute the model.

## 4.2 Stable Isotopes

### 4.2.1 Stable isotopes in precipitation (Study [MS]–3)

The relationship between  $\delta^2\text{H}_{\text{prec}}$  and  $\delta^{18}\text{O}_{\text{prec}}$  at a certain site is known as the Local Meteoric Water Line (LMWL, Crawford et al., 2014; Hughes and Crawford, 2012). The LMWL ( $\delta^2\text{H} = 5.3 * \delta^{18}\text{O} + 14.6$ ) for the Bale Mts is characterised by a lower slope and a higher intercept (Fig. VIII) compared to the Global Meteoric Water Line, GMWL (Craig, 1961) and the LMWL of the Addis Ababa station (Rozanski et al., 1996). This can be explained by the local climate in the Bale Mts modified by orographic process, i.e. altitude induced climatic condition and multiple moisture sources.

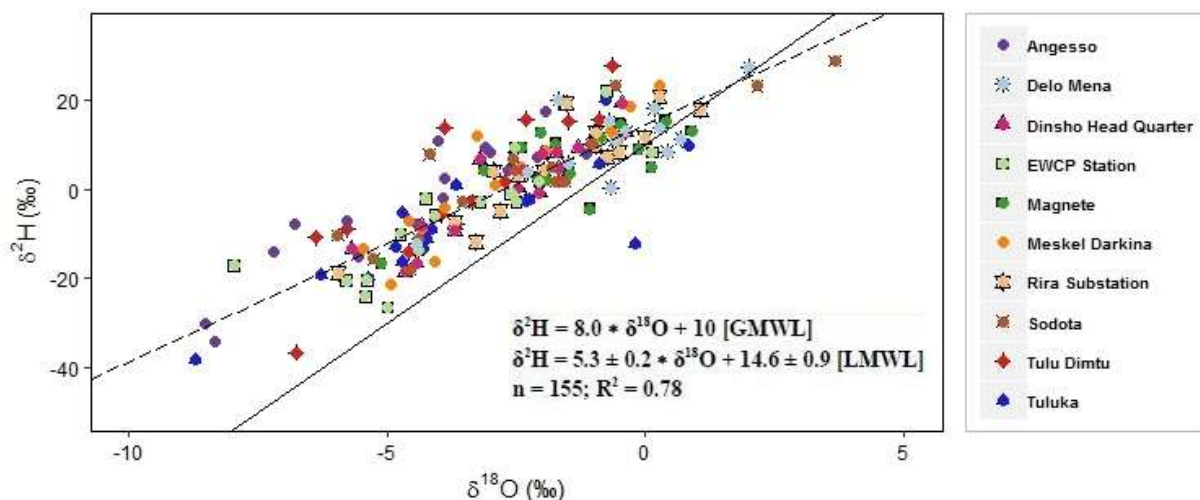


**Fig. VIII:** Hydrogen ( $\delta^2\text{H}$ ) and oxygen ( $\delta^{18}\text{O}$ ) isotopic composition of meteoric water in the Bale Mountains, Ethiopia. LMWL = local meteoric water line ( $\delta^2\text{H} = 5.3 * \delta^{18}\text{O} + 14.6$ , dashed line) and GMWL = global meteoric water line ( $\delta^2\text{H} = 8.0 * \delta^{18}\text{O} + 10$ , solid line).

The mean annual weighted isotope composition of precipitation ( $\delta^2\text{H}_{\text{prec}}$  and  $\delta^{18}\text{O}_{\text{prec}}$ ) exhibit a significant negative correlation with elevation. This result is well known as the altitude effect (Dansgaard, 1964; Poage and Chamberlain, 2001; Tekleab et al., 2014; Zech et al., 2015). The altitude effect is expressed as isotope lapse rate (Poage and Chamberlain, 2001). The isotopic lapse rate for the Bale Mts is  $-0.11\text{‰} * 100 \text{ m}^{-1}$  ( $R^2 = 0.73$ ,  $P = 0.002$ ) and  $-0.52\text{‰} * 100 \text{ m}^{-1}$  ( $R^2 = 0.60$ ,  $P = 0.01$ ) for  $\delta^{18}\text{O}_{\text{prec}}$  and  $\delta^2\text{H}_{\text{prec}}$ , respectively. Similarly, the altitude effect in the Upper Blue Nile basin, Ethiopia, accounts for a lapse rate of  $\delta^{18}\text{O}_{\text{prec}}$  ( $-0.12\text{‰} * 100 \text{ m}^{-1}$ ) and  $\delta^2\text{H}_{\text{prec}}$  ( $-0.58\text{‰} * 100 \text{ m}^{-1}$ ) (Kebede and Travi, 2012; Tekleab et al., 2014). The  $\delta^{18}\text{O}_{\text{prec}}$  lapse rate in the present study is also in agreement with findings from transect studies of other tropical mountains (Gonfiantini et al., 2001; Otte et al., 2017; Sánchez-Murillo and Birkel, 2016; Zech et al., 2015). However, it is less pronounced than the global isotopic lapse rate ( $-0.28 \text{‰} * 100 \text{ m}^{-1}$ ) (Poage and Chamberlain, 2001).

The  $\delta^2\text{H}_{\text{prec}}$ ,  $\delta^{18}\text{O}_{\text{prec}}$ , and  $d$ -excess of the Bale Mts are characterised by a systematic seasonal variability (Fig. IX). The isotopes in precipitation data from Addis Ababa, the Main Ethiopian Rift Valley regions, and the northwestern plateau of Ethiopia also revealed seasonal variations of  $\delta^2\text{H}_{\text{prec}}$ ,  $\delta^{18}\text{O}_{\text{prec}}$ , and  $d$ -excess (Kebede, 2004; Kebede and Travi, 2012; Tekleab et al., 2014). The most positive  $\delta^2\text{H}_{\text{prec}}$  and  $\delta^{18}\text{O}_{\text{prec}}$  values were recorded shortly after the end of the dry season, which may reflect various moisture sources, low precipitation amounts, and high air temperatures. The seasonal patterns (Fig. IX) reveal the most negative  $\delta^2\text{H}_{\text{prec}}$  and  $\delta^{18}\text{O}_{\text{prec}}$  values during May, August, and September. In May, August, and September, precipitation was highest for most of our weather stations. This finding is in accordance with the well-known amount effect described for tropical regions (Araguás-Araguás et al., 2000; Rozanski et al., 1996, 1993; Tekleab et al., 2014). However, there is a weak amount effect on the northwestern Ethiopian plateau and the Addis Ababa IAEA station (Kebede, 2004; Kebede and Travi, 2012). Overall, many of our weather stations located at higher elevations tend to reveal a stronger amount effect compared to stations at a lower elevation such as Rira and Delo Mena. A strong correlation between  $\delta^{18}\text{O}_{\text{prec}}$  and precipitation amount at higher elevation is illustrated by decreasing air temperature, rainout of heavier isotopes, and the Rayleigh fractionation process (Gonfiantini et al., 2001; Rozanski et al., 1993). Furthermore,  $d$ -excess reveals a strong correlation ( $R^2 = 0.6$ ) with elevation. This elevation dependence of  $d$ -excess partly contributes

to the low slope of the LMWL (Fig. VIII). High values of  $d$ -excess ( $>10\%$ ) recorded in the present study reflect recycled vapor evaporated from the Hareenna Forest or direct rainfall from vapor source regions.

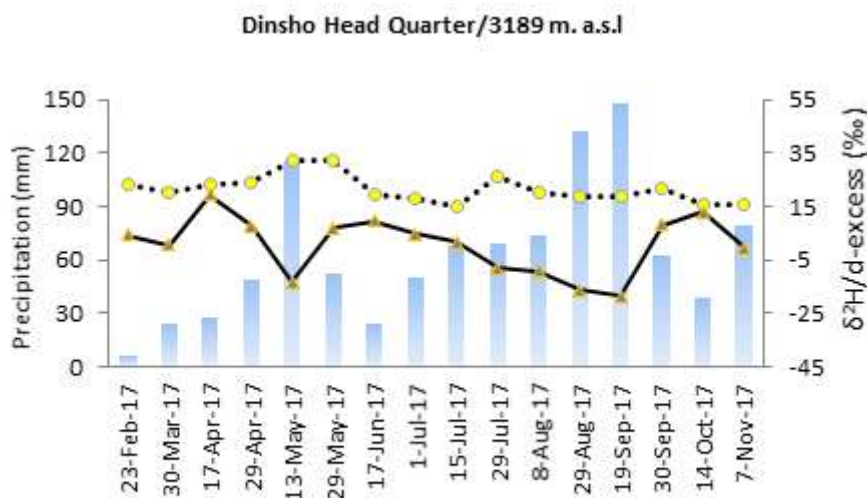


**Fig. IX:** Inner-annual variation of  $\delta^2\text{H}_{\text{prec}}$  (solid line),  $d$ -excess (dotted line and yellow circle), and precipitation amount (blue bars) of the representative sampling site Dinsho Head Quarter.

The HYSPLIT backward trajectories (Fig. X) show that air masses in our study area originate from different regions depending on the season. During the dry season, moisture is coming from the Gulf of Aden and the Arabian Sea. Moisture from those areas is responsible for generating little precipitation in the study area. By contrast, during the wet season precipitation originates mainly from the Southern Indian Ocean. Our results are in agreement with earlier studies of Kebede and Travi (2012). Nevertheless, for northern Ethiopia, backward trajectory studies of Costa et al. (2014) having previously confirmed the Sudd and the Congo Basin, as well as the Mediterranean Sea, as a potential moisture source. Based on our backward trajectories, we found no evidence that these regions have been moisture sources at least for the Bale Mts in 2017. According to other climate simulation studies, the Ethiopian highlands receive moisture mainly from two branches. One from the northeast direction across the Red Sea and the Arabian Peninsula over the Mediterranean Sea and the Indian Ocean and the second from southwest direction across the Gulf of Guinea and Central Africa over the Atlantic Ocean (Diro et al., 2011; Mohamed et al., 2005; Segele et al., 2009; Viste and Sorteberg, 2013).

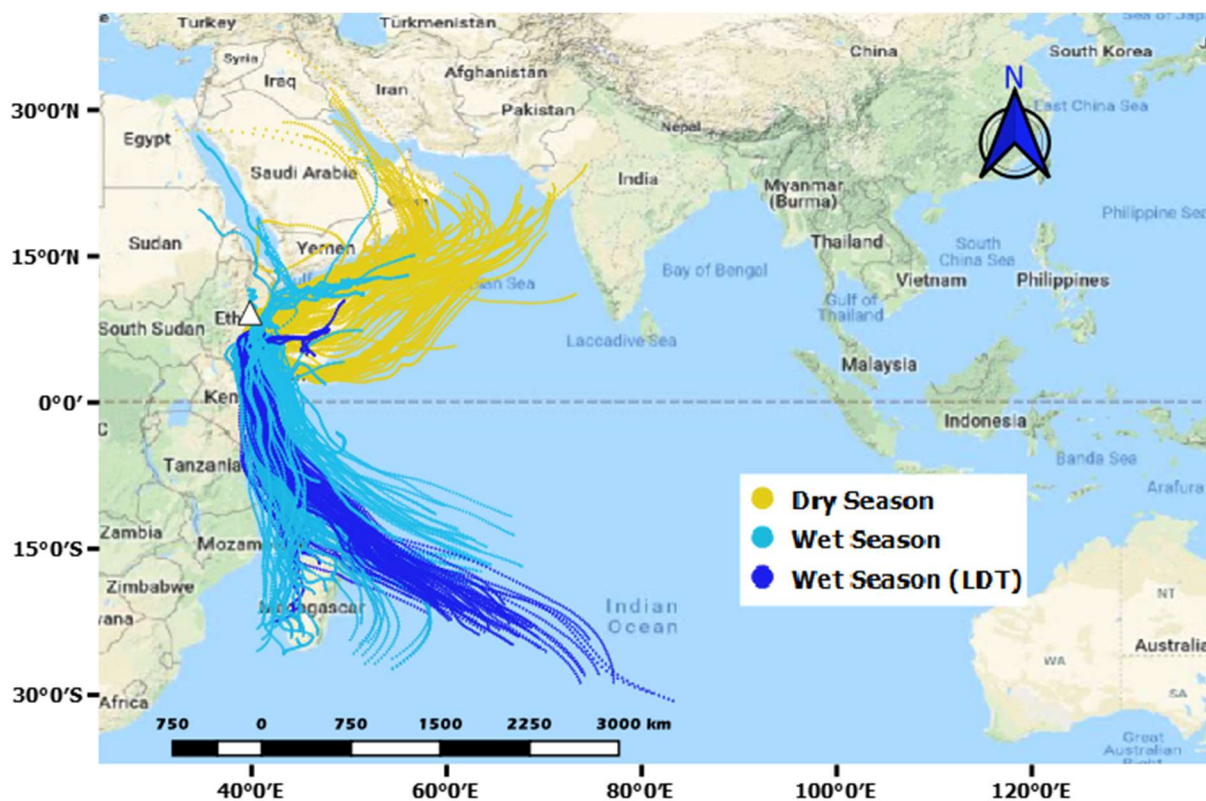


**Fig. X:** Map of Hybrid Single Particle Lagrangian Integrated Trajectory (HYSPPLIT) model based on meteorological data (Global Data Assimilation System, 1-degree resolution) for 168 h. Yellow, light blue, and dark blue trajectories indicate the synoptic moisture source area of precipitation to the study site during dry and wet seasons. Dark blue refers to long distance traveling trajectories (LDT) and the white triangle indicates the sampling area or ending point of the water vapour. For the interpretation of the reference to color in this figure legend, the readers are referred to the online version of this dissertation.

#### 4.2.2 Coupling $\delta^{18}\text{O}_{\text{sugar}}$ and $\delta^2\text{H}_{n\text{-alkane}}$ biomarkers (Study [MS]–4)

The weighted mean  $\delta^2\text{H}_{n\text{-alkane}}$  (weighted mean values of  $\text{C}_{29}$  and  $\text{C}_{31}$  alkanes) and  $\delta^{18}\text{O}_{\text{sugar}}$  (weighted mean values of arabinose and xylose) values range from  $-186$  to  $-89\text{‰}$  and from  $+27$  to  $+46\text{‰}$ , respectively (Fig. XI). Particularly, the topsoil (O-layer as well as  $\text{A}_h$ -horizon) samples in the Bale Mts yielded a  $\delta^2\text{H}_{n\text{-alkane}}$  values range between  $-157$  to  $-113\text{‰}$  ( $\bar{x} = -136\text{‰}$ ), which is in good agreement with findings from the highest Eastern African Mt. Kilimanjaro (Hepp et al., 2017; Peterse et al., 2009; Zech et al., 2015).

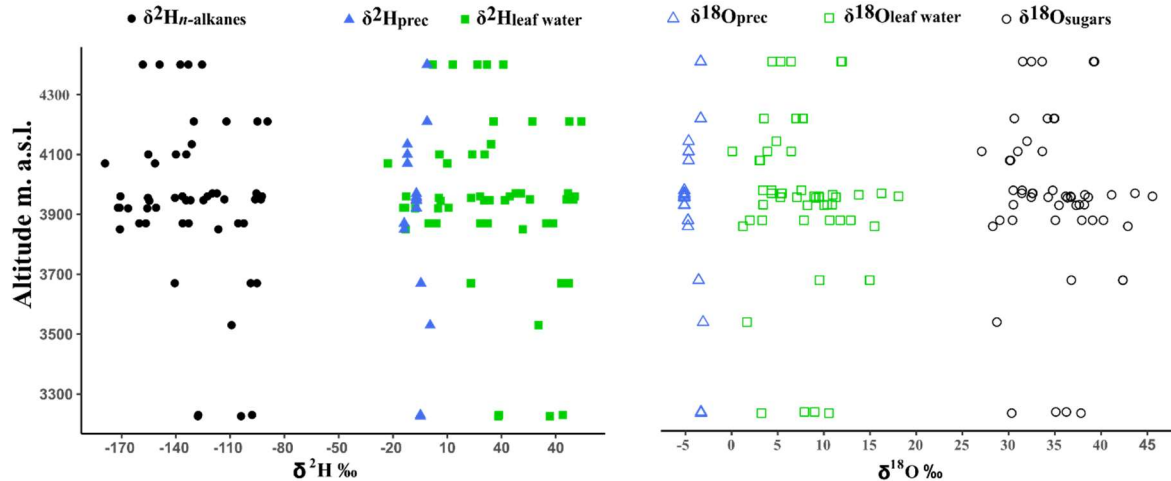


**Fig. XI:** Altitudinal  $\delta^2\text{H}$  (left) and  $\delta^{18}\text{O}$  (right) gradients of  $n$ -alkanes (weighted mean of  $\text{C}_{29}$  and  $\text{C}_{31}$ ) and sugar biomarkers (weighted mean of arabinose and xylose), respectively, reconstructed leaf water (squares) and precipitation (triangles).

The  $\delta^2\text{H}_{n\text{-alkane}}$  and  $\delta^{18}\text{O}_{\text{sugar}}$  values of leaves, O-layers, and  $\text{A}_h$ -horizons do not differ statistically significant ( $p = 0.7$  and  $p = 0.4$ , respectively) from each other (Fig. XII). Hence, our data provide no evidence for degradation effects and/or root input affecting the isotope composition of the biomarkers in topsoils. This is noteworthy because our previous chemotaxonomy studies (cf. study 1) reveal that the characteristic plant biomarker patterns of long-chain  $n$ -alkanes (Lemma et al., 2019) and sugars (Mekonnen et al., 2019) are strongly altered in the respective O-layers and  $\text{A}_h$ -horizons due to degradation and roots inputs.

The  $\delta^2\text{H}_{n\text{-alkane}}$  values correlate significantly with the weighted mean annual isotope composition of local meteoric water,  $\delta^2\text{H}_{\text{prec}}$  ( $r = 0.3$ ,  $p = 0.04$ ,  $n = 53$ ). However, it does not correlate in a 1:1 relationship ( $\delta^2\text{H}_{\text{prec}} = 0.05 * \delta^2\text{H}_{n\text{-alkane}} - 1.03$ ) and this is the first important indication that  $n$ -alkanes do not directly reflect  $\delta^2\text{H}_{\text{prec}}$ . Instead,  $\delta^2\text{H}_{n\text{-alkane}}$  reflects the isotope signal of local precipitation modified by leaf water enrichment as emphasized by Zech et al. (2015). By contrast, there is no statistically significant correlation between  $\delta^{18}\text{O}_{\text{sugar}}$  and  $\delta^{18}\text{O}_{\text{prec}}$ . This might indicate that the isotope signal of  $\delta^{18}\text{O}_{\text{prec}}$  is strongly altered prior to the biosynthesis of the sugar biomarkers. We argue that soil water evaporation, leaf water evapo(transpi)ration and seasonality effects are the most likely responsible factors.

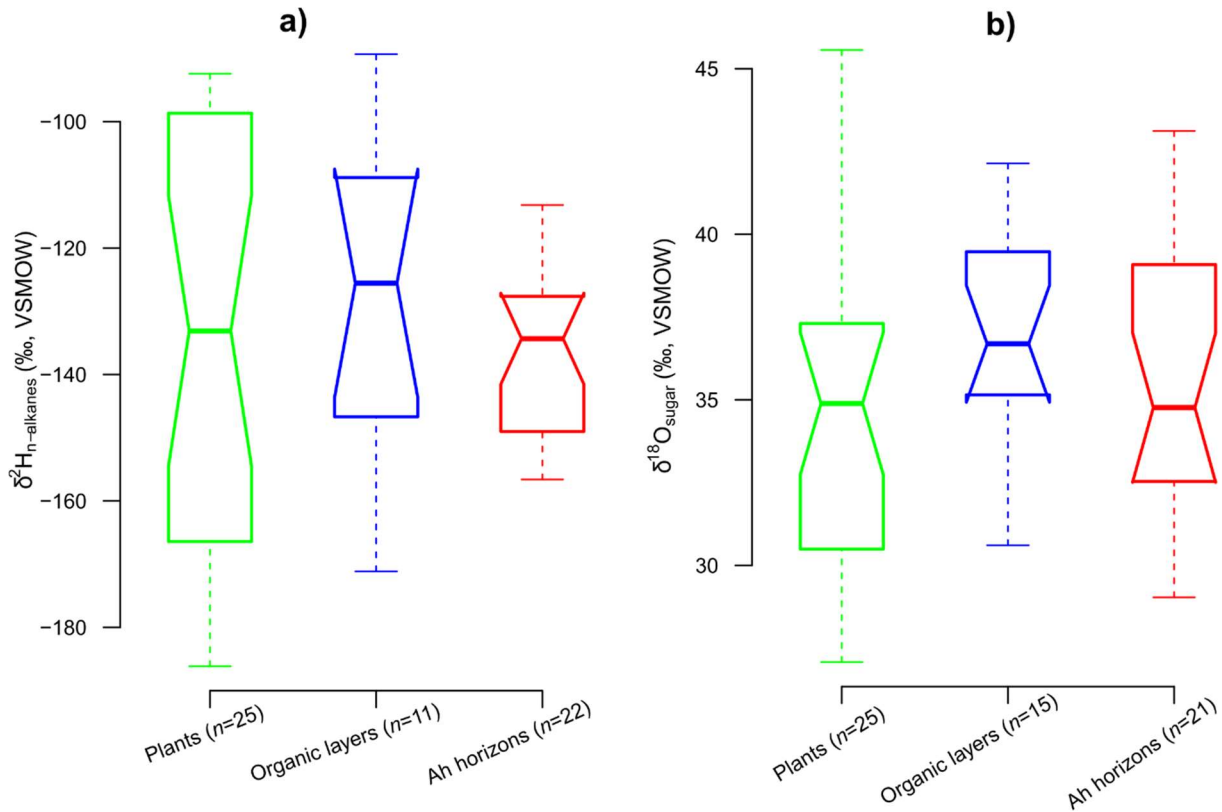


**Fig. XII:** Comparison of  $\delta^2\text{H}_{n\text{-alkane}}$  (a) and  $\delta^{18}\text{O}_{\text{sugar}}$  (b) among leaves, O-layers, and  $\text{A}_h$ -horizons. The notched box plots indicate the median (solid lines between the boxes), interquartile range (IQR) with upper (75%) and lower (25%) quartiles. The notches display the confidence interval around the median within  $\pm 1.57 \cdot \text{IQR} / \sqrt{n}$ .

A recent publication by Strobel et al. (2020) indicated that plant-related and/or environmental factors strongly bias the  $\delta^{18}\text{O}_{\text{sugar}}$  signal compared to  $\delta^{18}\text{O}_{\text{prec}}$  and points especially to the significant impact of evapo(transpi)rative soil and leaf water enrichment. Similarly, a climate transect study revealed that  $\delta^{18}\text{O}_{\text{hemicellulose}}$  does not reflect  $\delta^{18}\text{O}_{\text{prec}}$  along an Argentinian transect (Tuthorn et al., 2014). Overall it can be summarized that our  $\delta^2\text{H}_{n\text{-alkane}}$  and  $\delta^{18}\text{O}_{\text{sugar}}$  values do not directly reflect the isotope composition of precipitation in the Bale Mts.

The keystone plant species in the Bale Mts are characterized by statistically significant species-dependent  $\delta^2\text{H}_{n\text{-alkane}}$  (Fig. XIIIa).  $\delta^{18}\text{O}_{\text{sugar}}$  (Fig. XIIIb) yielded the same species-dependent trends. On the one hand the median  $\delta^2\text{H}_{n\text{-alkane}}$  and  $\delta^{18}\text{O}_{\text{sugar}}$  values of *F. abyssinica* are the lowest of all investigated plant species (Fig. XIII). This can be attributed to physiological and biochemical differences and the fact that *F. abyssinica* (grass) is a monocot, whereas the other plant species are dicots. The leaves of monocots and dicots differ in structure, location, and timing of lipid synthesis (Sachse et al., 2012). The growth of grasses is associated with intercalary meristems. They occur at the base of the grass leaf blade, where leaf water is not

fully  $^2\text{H}$ - and  $^{18}\text{O}$ -enriched, which is called  $^2\text{H}_{n\text{-alkane}}$  and  $^{18}\text{O}_{\text{sugar}}$  “dampening effect” (Hepp et al., 2020, 2019). But, on the other hand the median  $\delta^2\text{H}_{n\text{-alkane}}$  and  $\delta^{18}\text{O}_{\text{sugar}}$  values of *E. arborea* and *E. trimera* are the highest of all the investigated species and show strong leaf water enrichment. Intermediate  $\delta^2\text{H}_{n\text{-alkane}}$  and  $\delta^{18}\text{O}_{\text{sugar}}$  values for *A. haumannii* and *H. splendidum* might be attributed to plant physiological or microclimatic conditions affecting relative humidity and thus leaf water enrichment as compared to *Erica* and *F. abyssinica*. Therefore, caution must be given in terms of vegetation change when interpreting  $\delta^2\text{H}_{n\text{-alkane}}$  for paleoclimate reconstruction. The mean  $\delta^2\text{H}_{n\text{-alkane}}$  and  $\delta^{18}\text{O}_{\text{sugar}}$  values of *E. arborea* and *E. trimera* are  $-114$  and  $-109\text{‰}$ , and  $+37$  and  $+36\text{‰}$ , respectively. These very close mean  $\delta^2\text{H}_{n\text{-alkane}}$  and  $\delta^{18}\text{O}_{\text{sugar}}$  values of the two *Erica* species likely reflect the monophyletic nature (Guo et al., 2014).

Furthermore, there is a significant difference in apparent isotope fractionation of hydrogen ( $\epsilon_{\text{app } 2\text{H}}$ ) between the keystone plant species. Unlike other species, *E. arborea* ( $-94\text{‰}$ ) and *E. trimera* ( $-92\text{‰}$ ) have the least negative and *F. abyssinica* ( $-161\text{‰}$ ) has the most negative  $\epsilon_{\text{app } 2\text{H}}$ . It is identified that C3 graminoid (Sachse et al., 2012) and C3 grasses (Gamarra et al., 2016) exhibited the most negative  $\epsilon_{\text{app } 2\text{H}}$  compared to shrubs and trees.

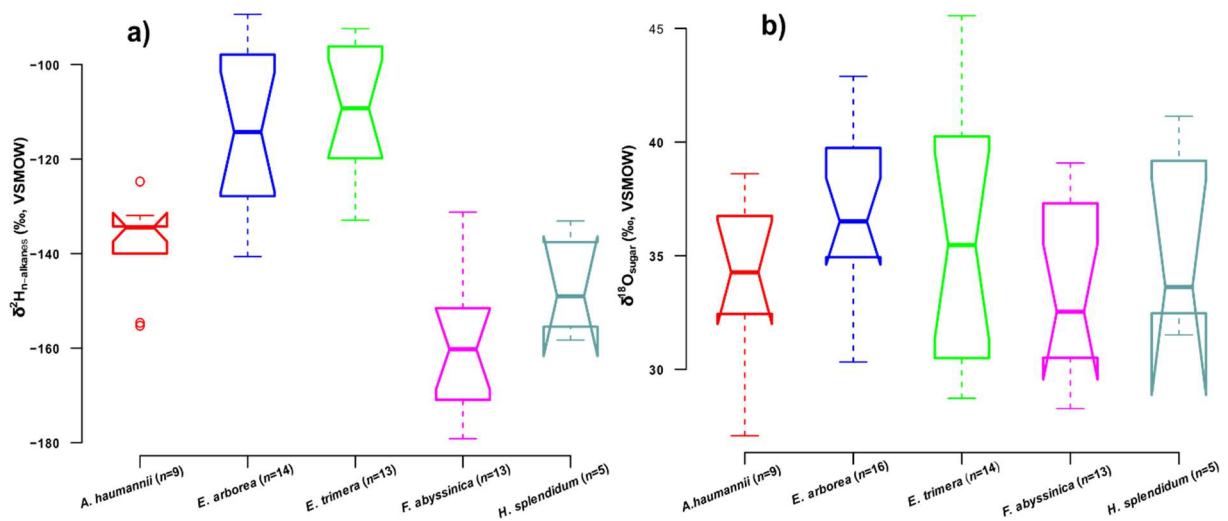


**Fig. XIII:** Variations of  $\delta^2\text{H}_{n\text{-alkane}}$  (a) and  $\delta^{18}\text{O}_{\text{sugar}}$  (b) between keystone plant species. The notched box plots indicate the median (solid lines between the boxes), interquartile range (IQR) with upper (75%), and lower (25%) quartiles and outliers (empty circle). The notches display the confidence interval around the median within  $\pm 1.57 \cdot \text{IQR} / \sqrt{n}$ .

Most of the reconstructed leaf water data plot below the GMWL (Fig. XIV). The reconstructed leaf water data plotting below the GMWL are a typical feature of evaporation loss. By applying a biosynthetic fractionation factor of  $-160\text{‰}$ , the reconstructed  $\delta^2\text{H}_{\text{leaf water}}$  values highlight that



the  $n$ -alkanes of *F. abyssinica* (Fig. XIIIa) reflect quite accurately and precisely the weighted mean annual  $\delta^2\text{H}_{\text{prec}}$  ( $-2.7 \pm 2\text{‰}$ ) of the Bale Mts (Lemma et al., 2020). However, it is known that the effect of evaporative leaf water isotope enrichment of grasses is negligible (Helliker and Ehleringer, 2002). By contrast, the reconstructed  $\delta^2\text{H}_{\text{leaf water}}$  values of *E. arborea* and *E. trimera* (Fig. XIIIa) do not reflect accurately and precisely the weighted mean annual  $\delta^2\text{H}_{\text{prec}}$  and the reconstructed  $\delta^2\text{H}_{\text{leaf water}}$  is enriched compared to  $\delta^2\text{H}_{\text{prec}}$  by up to  $55 \pm 5\text{‰}$ . One well known and widely accepted factor responsible for this finding is leaf water enrichment. For instance, Zech et al. (2015) emphasized that  $\delta^2\text{H}_{n\text{-alkane}}$  data from a climate transect along the southern slopes of Mt. Kilimanjaro do not reflect  $\delta^2\text{H}_{\text{prec}}$  either and explained this with a strongly variable degree of leaf water enrichment along the altitudinal transect.

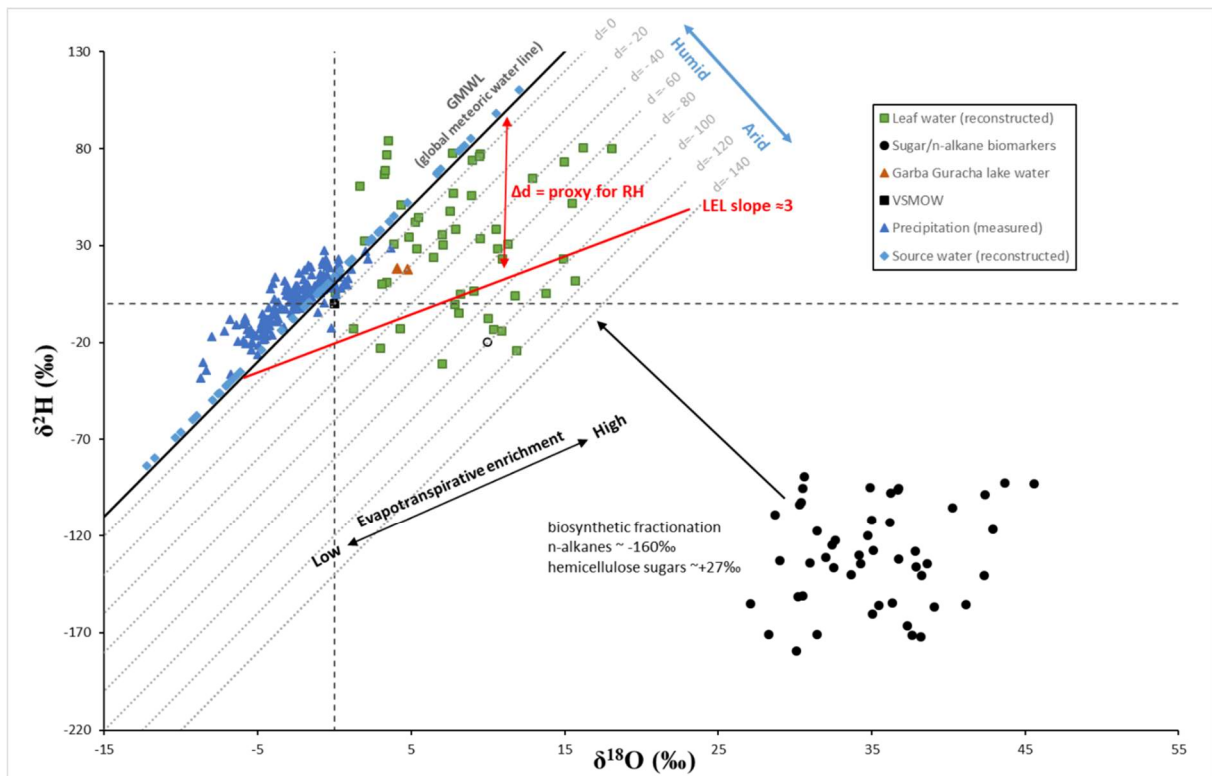


**Fig. XIV:**  $\delta^{18}\text{O}$  versus  $\delta^2\text{H}$  diagram illustrating the conceptual framework of the coupled (paleo-) hygrometer approach after Zech et al., (2013b). Data are plotted for measured source water/precipitation (blue solid triangle), measured  $\delta^2\text{H}_{n\text{-alkane}}$ , and  $\delta^{18}\text{O}_{\text{sugar}}$  (black solid circle), reconstructed leaf water (green solid rectangle), measured Garba Guracha lake water (brown solid triangle).

Similarly, considering a biosynthetic fractionation factor of  $+27\text{‰}$  (Cernusak et al., 2003), the reconstructed  $\delta^{18}\text{O}_{\text{leaf water}}$  values of all investigated plant species (Fig. XIIIb) do not reflect the isotope composition of precipitation. More specifically, the reconstructed  $\delta^{18}\text{O}_{\text{leaf water}}$  values of *E. arborea* and *E. trimera* are enriched compared to  $\delta^{18}\text{O}_{\text{prec}}$  by up to  $+9 \pm 1\text{‰}$ . Tree ring

research has shown that cellulose does not reflect the full leaf water  $\delta^{18}\text{O}$  enrichment signal (Gessler et al., 2013). Results from climate chamber experiments indicate that  $\delta^{18}\text{O}_{\text{leaf water}}$  values, reconstructed from sugar biomarkers, are enriched compared to plant source water by up to +25‰ (Zech et al., 2014a).

The reconstructed  $\delta^2\text{H}_{\text{source water}}$  and  $\delta^{18}\text{O}_{\text{source water}}$  values range from -84 to +110‰ ( $\bar{x} = 8.6 \pm 7\text{‰}$ ) and -12 to +12‰ ( $\bar{x} = -0.7 \pm 0.8\text{‰}$ ), respectively. The mean reconstructed  $\delta^2\text{H}_{\text{source water}}$  and  $\delta^{18}\text{O}_{\text{source water}}$  values reveal slight isotope enrichment as compared with the modern-day isotope composition of  $\delta^2\text{H}_{\text{prec}}$  ( $-2.7 \pm 2\text{‰}$ ) and  $\delta^{18}\text{O}_{\text{prec}}$  ( $-3.3 \pm 0.4\text{‰}$ ) in the Bale Mts, respectively (Lemma et al., 2020). Despite the large scattering of the reconstructed source water values, this finding demonstrates that the coupled  $\delta^2\text{H}_{n\text{-alkane}}\text{-}\delta^{18}\text{O}_{\text{sugar}}$  approach allows to reconstruct the isotope composition of source water quite accurately.

While the actual RH values range from 69 to 82% ( $\bar{x} = 80 \pm 3.4\%$ ), the reconstructed RH values, based on a recently suggested coupled  $\delta^2\text{H}_{n\text{-alkane}}\text{-}\delta^{18}\text{O}_{\text{sugar}}$  (paleo-) hygrometer approach yielded a mean of  $78 \pm 21\%$ . The coupled approach enables us to reconstruct RH with an offset of  $\Delta\text{RH} = +2 \pm 18\%$ . The difference between actual and reconstructed RH might be analytical errors associated with the individual  $\delta^2\text{H}_{n\text{-alkane}}$  and  $\delta^{18}\text{O}_{\text{sugar}}$  measurement, uncertainties of the  $\varepsilon_{\text{bio}}$ , and leaf-air temperature differences (Hepp et al., 2017; Zech et al., 2013b).

## 5. Conclusions

In this Ph.D. dissertation, the potential and limitations of different biomarker proxies were tested for unambiguous identification of locally dominant plant species with the objective to reconstruct the former extent of *Erica* species in the Bale Mts. Furthermore, the contemporary stable isotope in precipitation and moisture source regions of the Bale Mts were studied to better understand the current atmospheric circulation patterns. Similarly, stable isotopes in biomarkers were evaluated to check the imprint of rainfall-isotopes in leaves and topsoils with the implication of paleoclimate reconstruction.

The relative contribution of coumaryl phenols ( $> 0.2$ ) and benzoic acid (0.05–0.12) are promising and allowed the chemotaxonomic differentiation of *Erica* and non-*Erica* vegetation. However, this characteristic pattern of phenols is not reflected in the O-layers and  $A_{\text{h}}$ -horizons under *Erica*. The loss of cinnamyl dominance is likely caused by preferential degradation and lignin input by roots.

Individual leaf wax-derived *n*-alkanes have not allowed us to chemotaxonomically differentiate *Erica* from non-*Erica*. But *Erica* can be distinguished from *Alchemilla* and grass significantly

( $p = 0.05$ ) by lower  $C_{31}/C_{29}$  ratios ( $\bar{x} = 1.7$ ). However, like lignin-derived phenol proxies, the  $n$ -alkane patterns are changing due to degradation from plant material over O-layers to  $A_h$ -horizons, thus inhibiting their application for an unambiguous chemotaxonomic identification of *Erica* in soils and sediments. Therefore, future work is planned to focus on alternative molecular markers such as tannin-derived phenols and terpenes for unambiguous identification of *Erica* along the Sanetti Plateau in the Bale Mts.

The isotope composition of precipitation in the Bale Mts is isotopically heavier compared to other Eastern African stations. Precipitation in the Bale Mts exhibits a highly significant altitude effect ( $\delta^{18}O_{\text{prec}}$  lapse rate of  $-0.11\text{‰} * 100 \text{ m}^{-1}$ ). Furthermore, our data corroborate the existence of a seasonal amount effect with more positive  $\delta^2H_{\text{prec}}$  and  $\delta^{18}O_{\text{prec}}$  values prevailing shortly after the end of the dry season and more negative  $\delta^2H_{\text{prec}}$  and  $\delta^{18}O_{\text{prec}}$  values prevailing during May, August, and September when precipitation amount is highest. Similarly, the values of  $\delta^2H_{\text{prec}}$  and  $\delta^{18}O_{\text{prec}}$  are clearly associated with the moisture sources. Thus, HYPLIT backward trajectories assign the Gulf of Aden and the Arabian Sea as the primary moisture source during the dry season, whereas the Southern Indian Ocean is the primary moisture source for the Bale Mts during the rainy season.

There are no systematic  $\delta^2H_{n\text{-alkane}}$  and  $\delta^{18}O_{\text{sugar}}$  trends and significant differences between leaves, O-layers, and  $A_h$ -horizons. Hence, there is no evidence from our dataset for degradation and underground roots input affecting  $\delta^2H_{n\text{-alkane}}$  and  $\delta^{18}O_{\text{sugar}}$  values of topsoils. The keystone plant species in the Bale Mts are characterized by variable amounts of  $\delta^2H_{n\text{-alkane}}$  and also  $\delta^{18}O_{\text{sugar}}$  yielded the same species-dependent trends. While  $\delta^2H_{n\text{-alkane}}$  and  $\delta^{18}O_{\text{sugar}}$  of *E. arborea* and *E. trimera* shows the full leaf water enrichment signal, *F. abyssinica* reveals the most negative values due to “signal dampening” caused by basal grass leaf growth. Intermediate values for *A. haumannii* and *H. splendidum* might be attributed to plant physiological or microclimatic conditions affecting RH and thus leaf water enrichment as compared to *Erica* and *F. abyssinica*. Substantial species-specific apparent isotope fractionation highlights the importance of investigating apparent as well as biosynthetic isotope fractionation factor of the representative flora at a given geographical region. Thus, vegetation shifts should be considered before applying  $\delta^2H_{n\text{-alkane}}$  and  $\delta^{18}O_{\text{sugar}}$  records for the paleoenvironmental applications. The coupled approach enables us to reconstruct RH with an offset of  $\Delta\text{RH} = +2 \pm 18\%$ . Although several simplified assumptions challenge our interpretation, the coupled  $\delta^2H_{n\text{-alkane}}\text{-}\delta^{18}O_{\text{sugar}}$  (paleo-) hygrometer approach holds great potential for deriving additional paleoclimatic information compared to single isotope approaches.

## 6. References

- Abiven, S., Heim, A., Schmidt, M.W., 2011. Lignin content and chemical characteristics in maize and wheat vary between plant organs and growth stages: consequences for assessing lignin dynamics in soil. *Plant and Soil* 343, 369–378.
- Admasu, E., Thirgood, S.J., Bekele, A., Karen Laurenson, M., 2004. Spatial ecology of golden jackal in farmland in the Ethiopian Highlands. *African Journal of Ecology* 42, 144–152.
- Aggarwal, P.K., Romatschke, U., Araguas-Araguas, L., Belachew, D., Longstaffe, F.J., Berg, P., Schumacher, C., Funk, A., 2016. Proportions of convective and stratiform precipitation revealed in water isotope ratios. *Nature Geoscience* 9, 624–629.
- Akula, R., Ravishankar, G.A., 2011. Influence of abiotic stress signals on secondary metabolites in plants. *Plant signaling & behavior* 6, 1720–1731.
- Amelung, W., Martius, C., Bandeira, A.G., Garcia, M.V., Zech, W., 2002. Lignin characteristics and density fractions of termite nests in an Amazonian rain forest—indicators of termite feeding guilds? *Soil Biology and Biochemistry* 34, 367–372.
- Amelung, W., Zech, W., Flach, K.W., 1997. Climatic effects on soil organic matter composition in the Great Plains. *Soil Science Society of America Journal* 61, 115–123.
- Araguas, L.A., Danesi, P., Froehlich, K., Rozanski, K., 1996. Global monitoring of the isotopic composition of precipitation. *Journal of radioanalytical and nuclear chemistry* 205, 189–200.
- Araguás-Araguás, L., Froehlich, K., Rozanski, K., 2000. Deuterium and oxygen-18 isotope composition of precipitation and atmospheric moisture. *Hydrological processes* 14, 1341–1355.
- Asia, L., Mazouz, S., Guiliano, M., Doumenq, P., Mille, G., 2009. Occurrence and distribution of hydrocarbons in surface sediments from Marseille Bay (France). *Marine Pollution Bulletin* 58, 443.
- Assefa, A., Ehrich, D., Taberlet, P., Nemomissa, S., Brochmann, C., 2007. Pleistocene colonization of afro-alpine ‘sky islands’ by the arctic-alpine *Arabis alpina*. *Heredity* 99, 133–142.
- Baumann, K., Sanaullah, M., Chabbi, A., Dignac, M.-F., Bardoux, G., Steffens, M., Kögel-Knabner, I., Rumpel, C., 2013. Changes in litter chemistry and soil lignin signature during decomposition and stabilisation of <sup>13</sup>C labelled wheat roots in three subsoil horizons. *Soil Biology and Biochemistry* 67, 55–61.

- Belanger, E., Lucotte, M., Gregoire, B., Moingt, M., Paquet, S., Davidson, R., Mertens, F., Passos, C.J.S., Romana, C., 2015. Lignin signatures of vegetation and soils in tropical environments. *Advances in environmental research* 4, 247–262.
- Billi, P., 2015. Geomorphological landscapes of Ethiopia, in: *Landscapes and Landforms of Ethiopia*. Springer, pp. 3–32.
- Bonnefille, R., 1983. Evidence for a cooler and drier climate in the Ethiopian uplands towards 2.5 Myr ago. *Nature* 303, 487–491.
- Bonnefille, R., Hamilton, A., 1986. Quaternary and late Tertiary history of Ethiopian vegetation. *Symb. Bot. Ups* 26, 48–63.
- Bonnefille, R., Mohammed, U., 1994. Pollen-inferred climatic fluctuations in Ethiopia during the last 3000 years. *Palaeogeography, Palaeoclimatology, Palaeoecology* 109, 331–343.
- Bush, R.T., McInerney, F.A., 2013. Leaf wax n-alkane distributions in and across modern plants: implications for paleoecology and chemotaxonomy. *Geochimica et Cosmochimica Acta* 117, 161–179.
- Castañeda, I.S., Werne, J.P., Johnson, T.C., Filley, T.R., 2009. Late Quaternary vegetation history of southeast Africa: the molecular isotopic record from Lake Malawi. *Palaeogeography, Palaeoclimatology, Palaeoecology* 275, 100–112.
- Cernusak, L.A., Wong, S.C., Farquhar, G.D., 2003. Oxygen isotope composition of phloem sap in relation to leaf water in *Ricinus communis*. *Functional Plant Biology* 30, 1059–1070.
- Chesson, A., Stewart, C.S., Wallace, R.J., 1982. Influence of plant phenolic acids on growth and cellulolytic activity of rumen bacteria. *Appl. Environ. Microbiol.* 44, 597–603.
- Costa, K., Russell, J., Konecky, B., Lamb, H., 2014. Isotopic reconstruction of the African Humid Period and Congo air boundary migration at Lake Tana, Ethiopia. *Quaternary Science Reviews* 83, 58–67.
- Craig, H., 1961. Isotopic variations in meteoric waters. *Science* 133, 1702–1703.
- Crawford, J., Hughes, C.E., Lykoudis, S., 2014. Alternative least squares methods for determining the meteoric water line, demonstrated using GNIP data. *Journal of Hydrology* 519, 2331–2340.
- Dansgaard, W., 1964. Stable isotopes in precipitation. *Tellus* 16, 436–468.
- Diro, G.T., Toniazzo, T., Shaffrey, L., 2011. Ethiopian rainfall in climate models, in: *African Climate and Climate Change*. Springer, pp. 51–69.
- Djurdjevic, L., Mitrovic, M., Pavlovic, P., Perisic, S., Macukanovic-Jocic, M., 2005. Total phenolics and phenolic acids content in low (*Chrysopogon gryllus*) and mediocre

- quality (*Festuca vallesiaca*) forage grasses of Deliblato Sands meadow-pasture communities in Serbia. *Czech J. Anim. Sci* 50, 54–59.
- Dullo, B.W., Grootjans, A.P., Roelofs, J.G.M., Senbeta, A.F., Fritz, C., 2015. Fen mires with cushion plants in Bale Mountains, Ethiopia. *Mires Peat* 15, 1–10.
- Eganhouse, R.P., 1997. Molecular Markers and Environmental Organic Geochemistry: An Overview, in: *Molecular Markers in Environmental Geochemistry*. ACS Publications, p. 1-20.
- Eglinton, G., Hamilton, R.J., 1967. Leaf epicuticular waxes. *Science* 156, 1322–1335.
- Eglinton, T.I., Eglinton, G., 2008. Molecular proxies for paleoclimatology. *Earth and Planetary Science Letters* 275, 1–16.
- Ertel, J.R., Hedges, J.I., 1984. The lignin component of humic substances: distribution among soil and sedimentary humic, fulvic, and base-insoluble fractions. *Geochimica et Cosmochimica Acta* 48, 2065–2074.
- Ficken, K.J., Barber, K.E., Eglinton, G., 1998. Lipid biomarker,  $\delta^{13}\text{C}$  and plant macrofossil stratigraphy of a Scottish montane peat bog over the last two millennia. *Organic Geochemistry* 28, 217–237.
- Friis, I., 1986. Zonation of Forest Vegetation on the South Slope of Bale Mountains, South Ethiopia. *SINET- An Ethiopian Journal of Science* 9, 29–44.
- Gamarra, B., Sachse, D., Kahmen, A., 2016. Effects of leaf water evaporative  $^2\text{H}$ -enrichment and biosynthetic fractionation on leaf wax n-alkane  $\delta^2\text{H}$  values in C3 and C4 grasses. *Plant, cell & environment* 39, 2390–2403.
- Gessler, A., Brandes, E., Keitel, C., Boda, S., Kayler, Z.E., Granier, A., Barbour, M., Farquhar, G.D., Treydte, K., 2013. The oxygen isotope enrichment of leaf-exported assimilates—does it always reflect lamina leaf water enrichment? *New Phytologist* 200, 144–157.
- Glaser, B., Zech, W., 2005. Reconstruction of climate and landscape changes in a high mountain lake catchment in the Gorkha Himal, Nepal during the Late Glacial and Holocene as deduced from radiocarbon and compound-specific stable isotope analysis of terrestrial, aquatic and microbial biomarkers. *Organic Geochemistry* 36, 1086–1098.
- Gonfiantini, R., Roche, M.-A., Olivry, J.-C., Fontes, J.-C., Zuppi, G.M., 2001. The altitude effect on the isotopic composition of tropical rains. *Chemical Geology* 181, 147–167.
- Goñi, M.A., Hedges, J.I., 1992. Lignin dimers: Structures, distribution, and potential geochemical applications. *Geochimica et Cosmochimica Acta* 56, 4025–4043.
- Griepentrog, M., De Wispelaere, L., Bauters, M., Bodé, S., Hemp, A., Verschuren, D., Boeckx, P., 2019. Influence of plant growth form, habitat and season on leaf-wax n-alkane

- hydrogen-isotopic signatures in equatorial East Africa. *Geochimica et Cosmochimica Acta* 263, 122–139.
- Groos, A.R., Niederhauser, J., Wraase, L., Hänsel, F., Nauss, T., Akçar, N., Veit, H., 2020. Implications of present ground temperatures and relict stone stripes in the Ethiopian Highlands for the palaeoclimate of the tropics. *Earth Surface Dynamics Discussions* 1–37.
- Guendouze-Bouchefa, N., Madani, K., Chibane, M., Boulekbache-Makhlouf, L., Hauchard, D., Kiendrebeogo, M., Stevigny, C., Okusa, P.N., Duez, P., 2015. Phenolic compounds, antioxidant and antibacterial activities of three Ericaceae from Algeria. *Industrial crops and products* 70, 459–466.
- Guo, N., Gao, J., He, Y., Zhang, Z., Guo, Y., 2014. Variations in leaf epicuticular n-alkanes in some *Broussonetia*, *Ficus* and *Humulus* species. *Biochemical systematics and ecology* 54, 150–156.
- Hamilton, A.C., 1982. *Environmental history of East Africa: a study of the Quaternary*. Academic press London.
- Hedberg, I., Hedberg, O., 1979. Tropical-alpine life-forms of vascular plants. *Oikos* 297–307.
- Hedberg, O., 1964. *Features of afroalpine plant ecology*. Uppsala: Svenska växtgeografiska Sällskapet. *Acta Phytogeographica Suecica*; 49.
- Hedges, J.I., Blanchette, R.A., Weliky, K., Devol, A.H., 1988. Effects of fungal degradation on the CuO oxidation products of lignin: a controlled laboratory study. *Geochimica et Cosmochimica Acta* 52, 2717–2726.
- Hedges, J.I., Clark, W.A., Quay, P.D., Richey, J.E., Devol, A.H., Santos, M., 1986. Compositions and fluxes of particulate organic material in the Amazon River 1. *Limnology and Oceanography* 31, 717–738.
- Hedges, J.I., Ertel, J.R., 1982. Characterization of lignin by gas capillary chromatography of cupric oxide oxidation products. *Analytical Chemistry* 54, 174–178.
- Hedges, J.I., Mann, D.C., 1979. The characterization of plant tissues by their lignin oxidation products. *Geochimica et Cosmochimica Acta* 43, 1803–1807.
- Heiri, C., Bugmann, H., Tinner, W., Heiri, O., Lischke, H., 2006. A model-based reconstruction of Holocene treeline dynamics in the Central Swiss Alps. *Journal of Ecology* 94, 206–216.
- Helliker, B.R., Ehleringer, J.R., 2002. Grass blades as tree rings: environmentally induced changes in the oxygen isotope ratio of cellulose along the length of grass blades. *New Phytologist* 155, 417–424.

- Hepp, J., Tuthorn, M., Zech, R., Mügler, I., Schlütz, F., Zech, W., Zech, M., 2015. Reconstructing lake evaporation history and the isotopic composition of precipitation by a coupled  $\delta^{18}\text{O}$ – $\delta^2\text{H}$  biomarker approach. *Journal of hydrology* 529, 622–631.
- Hepp, J., Zech, R., Rozanski, K., Tuthorn, M., Glaser, B., Greule, M., Keppler, F., Huang, Y., Zech, W., Zech, M., 2017a. Late Quaternary relative humidity changes from Mt. Kilimanjaro, based on a coupled  $^2\text{H}$ – $^{18}\text{O}$  biomarker paleohygrometer approach. *Quaternary International* 438, 116–130.
- Hepp, J., Zech, R., Rozanski, K., Tuthorn, M., Glaser, B., Greule, M., Keppler, F., Huang, Y., Zech, W., Zech, M., 2017b. Late Quaternary relative humidity changes from Mt. Kilimanjaro, based on a coupled  $^2\text{H}$ – $^{18}\text{O}$  biomarker paleohygrometer approach. *Quaternary International* 438, 116–130.
- Hicks, S., 2006. When no pollen does not mean no trees. *Vegetation History and Archaeobotany* 15, 253–261.
- Hillman, J.C., 1988. The Bale Mountains National Park area, southeast Ethiopia, and its management. *Mountain Research and Development* 8, 253–258.
- Hillman, J.C., 1986. Conservation in Bale mountains national park, Ethiopia. *Oryx* 20, 89–94.
- Hoffmann, B., Kahmen, A., Cernusak, L.A., Arndt, S.K., Sachse, D., 2013. Abundance and distribution of leaf wax n-alkanes in leaves of *Acacia* and *Eucalyptus* trees along a strong humidity gradient in northern Australia. *Organic Geochemistry* 62, 62–67.
- Hughes, C.E., Crawford, J., 2012. A new precipitation weighted method for determining the meteoric water line for hydrological applications demonstrated using Australian and global GNIP data. *Journal of Hydrology* 464, 344–351.
- IPCC, C.C., 2001. The Scientific Basis. Contribution of Working Group I to the Third Assessment Report of the Intergovernmental Panel on Climate Change. Cambridge University Press: Cambridge, United Kingdom 881.
- Jansen, B., van Loon, E.E., Hooghiemstra, H., Verstraten, J.M., 2010. Improved reconstruction of palaeo-environments through unravelling of preserved vegetation biomarker patterns. *Palaeogeography, Palaeoclimatology, Palaeoecology* 285, 119–130.
- Kebede, M., Ehrlich, D., Taberlet, P., Nemomissa, S., Brochmann, C., 2007. Phylogeography and conservation genetics of a giant lobelia (*Lobelia giberroa*) in Ethiopian and Tropical East African mountains. *Molecular Ecology* 16, 1233–1243.
- Kebede, S., 2004. Environmental isotopes and geochemistry in investigating groundwater and lake hydrology: cases from the Blue Nile basin & the Ethiopian Rift. These de Doctorat, Universite d'Avignon, France, 176pp.



- Kebede, S., Travi, Y., 2012. Origin of the  $\delta^{18}\text{O}$  and  $\delta^2\text{H}$  composition of meteoric waters in Ethiopia. *Quaternary International* 257, 4–12.
- Kidane, Y., Stahlmann, R., Beierkuhnlein, C., 2012. Vegetation dynamics, and land use and land cover change in the Bale Mountains, Ethiopia. *Environmental monitoring and assessment* 184, 7473–7489.
- Koch, K., Bhushan, B., Barthlott, W., 2009. Multifunctional surface structures of plants: an inspiration for biomimetics. *Progress in Materials science* 54, 137–178.
- Kolattukudy, P.E., 1970. Plant waxes. *Lipids* 5, 259–275.
- Kurita, N., 2013. Water isotopic variability in response to mesoscale convective system over the tropical ocean. *Journal of Geophysical Research: Atmospheres* 118, 10–376.
- Lemma, B., Kebede Gurmessa, S., Nemomissa, S., Otte, I., Glaser, B., Zech, M., 2020. Spatial and temporal  $^2\text{H}$  and  $^{18}\text{O}$  isotope variation of contemporary precipitation in the Bale Mountains, Ethiopia. *Isotopes in Environmental and Health Studies* 1–14.
- Lemma, B., Mekonnen, B., Glaser, B., Zech, W., Nemomissa, S., Bekele, T., Bittner, L., Zech, M., 2019. Chemotaxonomic patterns of vegetation and soils along altitudinal transects of the Bale Mountains, Ethiopia, and implications for paleovegetation reconstructions—Part II: lignin-derived phenols and leaf-wax-derived n-alkanes. *E&G Quaternary Science Journal* 68, 189–200.
- Maffei, M., 1996. Chemotaxonomic significance of leaf wax alkanes in the Gramineae. *Biochemical systematics and ecology* 24, 53–64.
- Maffei, M., Badino, S., Bossi, S., 2004. Chemotaxonomic significance of leaf wax n-alkanes in the Pinales (*Coniferales*). *Journal of Biological Research* 1, 3–19.
- Mekonnen, B., Zech, W., Glaser, B., Lemma, B., Bromm, T., Nemomissa, S., Bekele, T., Zech, M., 2019. Chemotaxonomic patterns of vegetation and soils along altitudinal transects of the Bale Mountains, Ethiopia, and implications for paleovegetation reconstructions—Part 1: stable isotopes and sugar biomarkers. *E&G Quaternary Science Journal* 68, 177–188.
- Miehe, S., Miehe, G., 1994. Ericaceous forests and heathlands in the Bale Mountains of South Ethiopia. *Ecology and man's impact*. Warnke.
- Mika, V., Kuban, V., Klejdus, B., Odstroilova, V., Nerusil, P., 2005. Phenolic compounds as chemical markers of low taxonomic levels in the family Poaceae. *Plant Soil and Environment* 51, 506-512.

- Mohamed, Y.A., Van den Hurk, B., Savenije, H.H.G., Bastiaanssen, W.G.M., 2005. Hydroclimatology of the Nile: results from a regional climate model. *Hydrology and Earth System Sciences* 9, 263-278.
- Mohr, P.A., 1961. The geology of Ethiopia. Addis Ababa University Press. Addis Ababa.
- Möller, A., Kaiser, K., Zech, W., 2002. Lignin, carbohydrate, and amino sugar distribution and transformation in the tropical highland soils of northern Thailand under cabbage cultivation, Pinus reforestation, secondary forest, and primary forest. *Soil Research* 40, 977–998.
- Nazemiyeh, H., Bahadori, F., Delazar, A., Ay, M., Topçu, G., Nahar, L., Majinda, R.R., Sarker, S.D., 2008. Antioxidant phenolic compounds from the leaves of *Erica arborea* (Ericaceae). *Natural Product Research* 22, 1385–1392.
- Nicholson, S.E., 1996. A review of climate dynamics and climate variability in Eastern Africa. The limnology, climatology and paleoclimatology of the East African lakes 25–56.
- Ortu, E., Brewer, S., Peyron, O., 2006. Pollen-inferred palaeoclimate reconstructions in mountain areas: problems and perspectives. *Journal of Quaternary Science* 21, 615–627.
- Osmaston, H.A., Mitchell, W.A., Osmaston, J.N., 2005. Quaternary glaciation of the Bale Mountains, Ethiopia. *Journal of Quaternary Science* 20, 593–606.
- Ossendorf, G., Groos, A.R., Bromm, T., Tekelemariam, M.G., Glaser, B., Lesur, J., Schmidt, J., Akçar, N., Bekele, T., Beldados, A., 2019. Middle Stone Age foragers resided in high elevations of the glaciated Bale Mountains, Ethiopia. *Science* 365, 583–587.
- Otte, I., Detsch, F., Gütlein, A., Scholl, M., Kiese, R., Appelhans, T., Nauss, T., 2017. Seasonality of stable isotope composition of atmospheric water input at the southern slopes of Mt. Kilimanjaro, Tanzania. *Hydrological Processes* 31, 3932–3947.
- Otto, A., Simpson, M.J., 2006. Evaluation of CuO oxidation parameters for determining the source and stage of lignin degradation in soil. *Biogeochemistry* 80, 121–142.
- Peterse, F., van Der Meer, M.T.J., Schouten, S., Jia, G., Ossebaar, J., Blokker, J., Sinninghe Damsté, J.S., 2009. Assessment of soil n-alkane  $\delta D$  and branched tetraether membrane lipid distributions as tools for paleoelevation reconstruction. *Biogeosciences* 6, 2799–2807.
- Poage, M.A., Chamberlain, C.P., 2001. Empirical relationships between elevation and the stable isotope composition of precipitation and surface waters: considerations for studies of paleoelevation change. *American Journal of Science* 301, 1–15.
- Rommerskirchen, F., Plader, A., Eglinton, G., Chikaraishi, Y., Rullkötter, J., 2006. Chemotaxonomic significance of distribution and stable carbon isotopic composition of

- long-chain alkanes and alkan-1-ols in C<sub>4</sub> grass waxes. *Organic Geochemistry* 37, 1303–1332.
- Rozanski, K., Araguas-Araguas, L., Gonfiantini, R., 1996. Isotope patterns of precipitation in the East African region, in: *The limnology, climatology and paleoclimatology of the East African Lakes*. CRC Press, p. 79–93.
- Rozanski, K., Araguás-Araguás, L., Gonfiantini, R., 1993. Isotopic patterns in modern global precipitation. *Climate change in continental isotopic records* 78, 1–36.
- Sachse, D., Billault, I., Bowen, G.J., Chikaraishi, Y., Dawson, T.E., Feakins, S.J., Freeman, K.H., Magill, C.R., McInerney, F.A., Van Der Meer, M.T., 2012. Molecular paleohydrology: interpreting the hydrogen-isotopic composition of lipid biomarkers from photosynthesizing organisms. *Annual Review of Earth and Planetary Sciences* 40, 221–249.
- Sánchez-Murillo, R., Birkel, C., 2016. Groundwater recharge mechanisms inferred from isoscapes in a complex tropical mountainous region. *Geophysical Research Letters* 43, 5060–5069.
- Sauer, P.E., Eglinton, T.I., Hayes, J.M., Schimmelmann, A., Sessions, A.L., 2001. Compound-specific D/H ratios of lipid biomarkers from sediments as a proxy for environmental and climatic conditions. *Geochimica et Cosmochimica Acta* 65, 213–222.
- Schäfer, I.K., Lanny, V., Franke, J., Eglinton, T.I., Zech, M., Vysloužilová, B., Zech, R., 2016. Leaf waxes in litter and topsoils along a European transect. *Soil* 2, 551–564.
- Segele, Z.T., Lamb, P.J., Leslie, L.M., 2009. Large-scale atmospheric circulation and global sea surface temperature associations with Horn of Africa June–September rainfall. *International Journal of Climatology: A Journal of the Royal Meteorological Society* 29, 1075–1100.
- Sessions, A.L., Burgoyne, T.W., Schimmelmann, A., Hayes, J.M., 1999. Fractionation of hydrogen isotopes in lipid biosynthesis. *Organic Geochemistry* 30, 1193–1200.
- Singh, R., 2016. Chemotaxonomy: a tool for plant classification. *Journal of Medicinal Plants* 4, 90–93.
- Strobel, P., Haberzettl, T., Bliedtner, M., Struck, J., Glaser, B., Zech, M., Zech, R., 2020. The potential of  $\delta^2\text{H}_{\text{n-alkanes}}$  and  $\delta^{18}\text{O}_{\text{sugar}}$  for paleoclimate reconstruction—A regional calibration study for South Africa. *Science of The Total Environment* 716, 137045.
- Tareq, S.M., Handa, N., Tanoue, E., 2006. A lignin phenol proxy record of mid Holocene paleovegetation changes at Lake DaBuSu, northeast China. *Journal of Geochemical Exploration* 88, 445–449.

- Tareq, S.M., Kitagawa, H., Ohta, K., 2011. Lignin biomarker and isotopic records of paleovegetation and climate changes from Lake Erhai, southwest China, since 18.5 ka BP. *Quaternary International* 229, 47–56.
- Tareq, S.M., Tanaka, N., Ohta, K., 2004. Biomarker signature in tropical wetland: lignin phenol vegetation index (LPVI) and its implications for reconstructing the paleoenvironment. *Science of the Total Environment* 324, 91–103.
- Tekleab, S., Wenninger, J., Uhlenbrook, S., 2014. Characterisation of stable isotopes to identify residence times and runoff components in two meso-scale catchments in the Abay/Upper Blue Nile basin, Ethiopia. *Hydrology and Earth System Sciences* 18, 2415–2431.
- Thevenot, M., Dignac, M.-F., Rumpel, C., 2010. Fate of lignins in soils: a review. *Soil Biology and Biochemistry* 42, 1200–1211.
- Thomas, F.M., Molitor, F., Werner, W., 2014. Lignin and cellulose concentrations in roots of Douglas fir and European beech of different diameter classes and soil depths. *Trees* 28, 309–315.
- Tiercelin, J.-J., Gibert, E., Umer, M., Bonnefille, R., Disnar, J.-R., Lézine, A.-M., Hureau-Mazaudier, D., Travi, Y., Kéravis, D., Lamb, H.F., 2008. High-resolution sedimentary record of the last deglaciation from a high-altitude lake in Ethiopia. *Quaternary Science Reviews* 27, 449–467.
- Tuthorn, M., Zech, M., Ruppenthal, M., Oelmann, Y., Kahmen, A., del Valle, H.F., Wilcke, W., Glaser, B., 2014. Oxygen isotope ratios ( $^{18}\text{O}/^{16}\text{O}$ ) of hemicellulose-derived sugar biomarkers in plants, soils and sediments as paleoclimate proxy II: Insight from a climate transect study. *Geochimica et cosmochimica acta* 126, 624–634.
- Tuthorn, M., Zech, R., Ruppenthal, M., Oelmann, Y., Kahmen, A., del Valle, H.F., Eglinton, T., Rozanski, K., Zech, M., 2015. Coupling  $\delta^2\text{H}$  and  $\delta^{18}\text{O}$  biomarker results yields information on relative humidity and isotopic composition of precipitation—a climate transect validation study. *Biogeosciences* 12, 3913–3924.
- Umer, M., Lamb, H.F., Bonnefille, R., Lézine, A.-M., Tiercelin, J.-J., Gibert, E., Cazet, J.-P., Watrin, J., 2007. Late pleistocene and holocene vegetation history of the bale mountains, Ethiopia. *Quaternary Science Reviews* 26, 2229–2246.
- Viste, E., Sorteberg, A., 2013. Moisture transport into the Ethiopian highlands. *International journal of climatology* 33, 249–263.

- Williams, S., Vivero Pol, J.L., Spawls, S., Shimelis, A., Kelbessa, E., 2004. Ethiopian highlands. in: *Hotspots Revisited: Earths Biologically Richest and Most Endangered Eco-regions*. CEMEX, Mexico City, p. 262-273.
- Woldu, Z., Feoli, E., Nigatu, L., 1989. Partitioning an elevation gradient of vegetation from southeastern Ethiopia by probabilistic methods, in: *Numerical Syntaxonomy*. Springer, pp. 189–198.
- Yimer, F., Ledin, S., Abdelkadir, A., 2006. Soil organic carbon and total nitrogen stocks as affected by topographic aspect and vegetation in the Bale Mountains, Ethiopia. *Geoderma* 135, 335–344.
- Zech, M., Buggle, B., Leiber, K., Markovic, S., Glaser, B., Hambach, U., Huwe, B., Stevens, T., Sümegi, P., Wiesenberg, G.L., 2009. Reconstructing Quaternary vegetation history in the Carpathian Basin, SE Europe, using n-alkane biomarkers as molecular fossils: problems and possible solutions, potential and limitations. *E&G: Quaternary Science Journal* 58, 148–155.
- Zech, M., Glaser, B., 2009. Compound-specific  $\delta^{18}\text{O}$  analyses of neutral sugars in soils using gas chromatography–pyrolysis–isotope ratio mass spectrometry: problems, possible solutions and a first application. *Rapid Communications in Mass Spectrometry: An International Journal Devoted to the Rapid Dissemination of Up-to-the-Minute Research in Mass Spectrometry* 23, 3522–3532.
- Zech, M., Glaser, B., 2008. Improved compound-specific  $\delta^{13}\text{C}$  analysis of n-alkanes for application in palaeoenvironmental studies. *Rapid Communications in Mass Spectrometry: An International Journal Devoted to the Rapid Dissemination of Up-to-the-Minute Research in Mass Spectrometry* 22, 135–142.
- Zech, M., Krause, T., Meszner, S., Faust, D., 2013a. Incorrect when uncorrected: reconstructing vegetation history using n-alkane biomarkers in loess-paleosol sequences—a case study from the Saxonian loess region, Germany. *Quaternary International* 296, 108–116.
- Zech, M., Leiber, K., Zech, W., Poetsch, T., Hemp, A., 2011a. Late Quaternary soil genesis and vegetation history on the northern slopes of Mt. Kilimanjaro, East Africa. *Quaternary international* 243, 327–336.
- Zech, M., Mayr, C., Tuthorn, M., Leiber-Sauheitl, K., Glaser, B., 2014. Oxygen isotope ratios ( $^{18}\text{O}/^{16}\text{O}$ ) of hemicellulose-derived sugar biomarkers in plants, soils and sediments as paleoclimate proxy I: Insight from a climate chamber experiment. *Geochimica et Cosmochimica Acta* 126, 614–623.

- Zech, M., Pedentchouk, N., Buggle, B., Leiber, K., Kalbitz, K., Marković, S.B., Glaser, B., 2011b. Effect of leaf litter degradation and seasonality on D/H isotope ratios of n-alkane biomarkers. *Geochimica et Cosmochimica Acta* 75, 4917–4928.
- Zech, M., Tuthorn, M., Detsch, F., Rozanski, K., Zech, R., Zöller, L., Zech, W., Glaser, B., 2013b. A 220 ka terrestrial  $\delta^{18}\text{O}$  and deuterium excess biomarker record from an eolian permafrost paleosol sequence, NE-Siberia. *Chemical Geology* 360, 220–230.
- Zech, M., Zech, R., Buggle, B., Zöller, L., 2011c. Novel methodological approaches in loess research—interrogating biomarkers and compound-specific stable isotopes. *Eiszeitalter & Gegenwart—Quaternary Science Journal* 60, 170–187.
- Zech, M., Zech, R., Rozanski, K., Gleixner, G., Zech, W., 2015. Do n-alkane biomarkers in soils/sediments reflect the  $\delta^2\text{H}$  isotopic composition of precipitation? A case study from Mt. Kilimanjaro and implications for paleoaltimetry and paleoclimate research. *Isotopes in environmental and health studies* 51, 508–524.
- Zhang, Z., Zhao, M., Yang, X., Wang, S., Jiang, X., Oldfield, F., Eglinton, G., 2004. A hydrocarbon biomarker record for the last 40 kyr of plant input to Lake Heqing, southwestern China. *Organic Geochemistry* 35, 595–613.
- Ziegler, F., Kögel, I., Zech, W., 1986. Alteration of gymnosperm and angiosperm lignin during decomposition in forest humus layers. *Zeitschrift für Pflanzenernährung und Bodenkunde* 149, 323–331.

## 7. Authors' contributions to the included manuscripts

In the present cumulative Ph.D. dissertation, four manuscripts are included. All of the manuscripts were prepared by myself as a first author and in collaboration with other co-authors. All peer-reviewed publications published during my Ph.D. period and related to the topic of my dissertation are listed in the section "List of Publications", the estimated contribution of authors in all four different manuscripts is given as follow:

### **Study 1: Chemotaxonomic patterns of vegetation and soils along altitudinal transects of the Bale Mountains, Ethiopia and implications for paleovegetation reconstructions II: Lignin-derived phenols and leaf wax-derived *n*-alkanes**

<https://doi.org/10.5194/egqsj-68-189-2019>

B. Lemma:	45% (field and laboratory work, data evaluation, discussion of results, manuscript preparation)
B. Mekonnen:	7% (field work and comments to improve the manuscript)
B. Glaser:	7% (data evaluation and comments to improve the manuscript)
W. Zech	7% (field work, discussion of results and comments to improve the manuscript)
S. Nemomissa:	5% (comments to improve the manuscript)
T. Bekele:	5% (comments to improve the manuscript)
L. Bittner:	4% (laboratory support during <i>n</i> -alkanes extraction, and data evaluation)
M. Zech:	20% (conceptualization, discussion of results and comments to improve the manuscript)

### **Study 2: Phenolic Compounds as Unambiguous Chemical Markers for the Identification of Keystone Plant Species in the Bale Mountains, Ethiopia**

<https://doi.org/10.3390/plants8070228>

B. Lemma:	40% (field and laboratory work, data evaluation, discussion of results, manuscript preparation)
C. Grehl:	10% (statistical data evaluation and comments to improve the manuscript)
M. Zech:	6% (discussion of results and comments to improve the manuscript)
B. Mekonnen:	5% (field work and comments to improve the manuscript)
W. Zech	6% (field work, discussion of results and comments to improve the manuscript)

S. Nemomissa: 4% (comments to improve the manuscript)  
 T. Bekele: 4% (comments to improve the manuscript)  
 B. Glaser: 25% (conceptualization, data evaluation and comments to improve the manuscript)

**Study 3: Spatial and temporal  $^2\text{H}$  and  $^{18}\text{O}$  isotope variation of contemporary precipitation in the Bale Mountains, Ethiopia**

*<https://doi.org/10.1080/10256016.2020.1717487>*

B. Lemma: 45% (field work, data evaluation, discussion of results, manuscript preparation)  
 S. Kebede: 10% (data evaluation and comments to improve the manuscript)  
 S. Nemomissa: 5% (comments to improve the manuscript)  
 I. Otte: 5% (comments to improve the manuscript)  
 B. Glaser: 10% (comments to improve the manuscript)  
 M. Zech: 25% (conceptualization, discussion of results and comments to improve the manuscript)

**Study 4:  $\delta^2\text{H}_{n\text{-alkane}}$  and  $\delta^{18}\text{O}_{\text{sugar}}$  biomarker proxies from leaves and topsoils of the Bale Mountains, Ethiopia, and implication for paleoclimate reconstruction**

*Submitted to Biogeochemistry-BIOG-D-20-00226*

B. Lemma: 40% (field work, data evaluation, discussion of results, manuscript preparation)  
 L. Bittner: 8% (data evaluation and comments to improve the manuscript)  
 B. Glaser: 12% (comments to improve the manuscript)  
 S. Kebede: 5% (comments to improve the manuscript)  
 S. Nemomissa: 5% (comments to improve the manuscript)  
 W. Zech: 5% (comments to improve the manuscript)  
 M. Zech: 25% (conceptualization, data evaluation, discussion of results and comments to improve the manuscript)



## **II. Publications and manuscripts**

## Study 1:

### **Chemotaxonomic patterns of vegetation and soils along altitudinal transects of the Bale Mountains, Ethiopia and implications for paleovegetation reconstructions II: Lignin-derived phenols and leaf wax-derived *n*-alkanes**

Bruk Lemma<sup>1,2\*</sup>, Betelhem Mekonnen<sup>1,3</sup>, Bruno Glaser<sup>1</sup>, Wolfgang Zech<sup>4</sup>, Sileshi Nemomissa<sup>5</sup>, Tamrat Bekele<sup>5</sup>, Lucas Bittner<sup>1</sup>, Michael Zech<sup>1,6</sup>

<sup>1</sup> Institute of Agronomy and Nutritional Sciences, Soil Biogeochemistry, Martin Luther University Halle–Wittenberg, Von–Seckendorff–Platz 3, D–06120, Halle, Germany,

<sup>2</sup> Ethiopian Biodiversity Institute, Forest and Rangeland Directorate, P.O. Box 30726, Addis Ababa, Ethiopia,

<sup>3</sup> Department of Urban Agriculture, Misrak Polytechnic College, P.O. Box 785, Addis Ababa, Ethiopia.

<sup>4</sup> Institute of Soil Science and Soil Geography, University of Bayreuth, Universitätsstrasse 30, D–95440, Bayreuth, Germany,

<sup>5</sup> Department of Plant Biology and Biodiversity Management, Addis Ababa University, P.O. Box 3434, Addis Ababa, Ethiopia,

<sup>6</sup> Institute of Geography, Technical University of Dresden, Helmholtzstrasse 10, D–01062, Dresden, Germany,

**\*Corresponding author: Bruk Lemma ([bruklemma@gmail.com](mailto:bruklemma@gmail.com))**

**Published in**

**E&G Quaternary Science Journal, 2019, 68: 189-200;**

**<https://doi.org/10.5194/egqsj-68-189-2019>**

## Abstract

*Erica* is a dominant vegetation type in many sub-afroalpine ecosystems such as the Bale Mountains in Ethiopia. However, the past extent of *Erica* is not well known and climate versus anthropogenic influence on altitudinal shifts are difficult to assign unambiguously especially during the Holocene. The main objective of the present study is to chemotaxonomically characterize the dominant plant species occurring in the Bale Mountains using lignin phenols and *n*-alkane biomarkers and to examine the potential of those biomarkers for reconstructing vegetation history. Fresh plant material, organic layer and mineral topsoil samples were collected along a northeastern and a southwestern altitudinal transect (4134–3870 and 4377–2550 m a.s.l., respectively). Lignin-derived vanillyl, syringyl and cinnamyl phenols were analyzed using the cupric oxide oxidation method. Leaf wax-derived *n*-alkanes were extracted and purified using Soxhlet and aminopropyl columns. Individual lignin phenols and *n*-alkanes were separated by gas-chromatography and detected by mass spectrometry and flame ionization detector, respectively.

We found that the relative contribution of vanillyl, syringyl, and cinnamyl phenols allow us to chemotaxonomically distinguish contemporary plant species of the Bale Mountains. *Erica* in particular is characterized by relatively high cinnamyl contributions of > 40%. However, litter degradation strongly decreases the lignin phenol concentrations and completely changes the lignin phenol patterns. Relative cinnamyl contributions in soils under *Erica* were < 40%, while soils that developed under *Poaceae* (*Festuca abyssinica*) exhibited relative cinnamyl contributions of > 40%.

Similarly, long-chain *n*-alkanes extracted from the leaf-waxes allowed for differentiation between *Erica* versus *Festuca abyssinica* and *Alchemilla*, based on lower C<sub>31</sub>/C<sub>29</sub> ratios in *Erica*. However, this characteristic plant pattern was also lost due to degradation in the respective O-layers and A<sub>h</sub>-horizons. In conclusion, although in modern-day plant samples a chemotaxonomic differentiation is possible, soil degradation processes seem to render the proxies unusable for the reconstruction of the past extent of *Erica* on the Sanetti Plateau, Bale Mountains, Ethiopia. This finding is of high relevance beyond our case study.

**Key Words:** Chemotaxonomy, biomarkers, molecular proxies, humification, soil organic matter, pedogenesis, Sanetti Plateau, *Erica* and *Festuca abyssinica*

## Zusammenfassung

*Erica* prägt als dominante Pflanzengattung viele Sub-afroalpine Ökosysteme, so auch die Bale Berge in Äthiopien. Das Ausmaß der flächenhaften Ausdehnung von *Erica* in der Vergangenheit ist jedoch unklar, genauso wie die klimatische versus menschliche Verursachung solcher Vegetationsänderungen insbesondere im Holozän. Das Ziel dieser Studie war es herauszufinden (i) ob sich die dominante Vegetation in den Bale Bergen anhand von ligninbürtigen Phenolen und blattwachsbürtigen *n*-Alkanbiomarkern chemotaxonomisch unterscheiden lässt und (ii) ob diese Biomarker das Potential haben zur Vegetationsrekonstruktion im Untersuchungsgebiet beizutragen. Untersucht wurden Pflanzenproben, O-Lagen und A<sub>h</sub>-Horizonte entlang eines Nord- und eines Südwest-Höhentransektes (3870–4134 m bzw. 2550–4377 m ü. NN). Die ligninbürtigen Phenoleinheiten Vanillyl, Syringyl und Cinnamyl wurden mittels der Kupferoxidationsmethode gewonnen; die *n*-Alkane wurden mittels Soxhlet extrahiert und über Aminopropylsäulen aufgereinigt. Die Quantifizierung der Ligninphenole und *n*-Alkane erfolgte mittels Gaschromatographie – Massenspektrometrie bzw. Gaschromatographie – Flammenionisationsdetektion.

Die Ergebnisse zeigen, dass sich die dominanten Pflanzenarten in den Bale Bergen anhand ihrer Vanillyl, Syringyl und Cinnamyl Einheiten chemotaxonomisch unterscheiden lassen. So weist insbesondere *Erica* charakteristischerweise relativ hohe Cinnamyl-Anteile von >40% auf. Vermutlich degradationsbedingt nimmt jedoch in der Reihe Pflanze – O-Lage – A<sub>h</sub>-Horizont nicht nur die Ligninkonzentration stark ab, sondern auch die Ligninmuster ändern sich völlig. Dadurch weisen Böden unter *Erica* Cinnamyl-Anteile < 40% auf, während Böden die sich unter der dominanten Grasart *Festuca abyssinica* entwickelt haben Cinnamyl-Anteile von >40% aufweisen. Auch anhand der Alkanbiomarker ist eine chemotaxonomische Unterscheidung zumindest zwischen *Erica* versus *Festuca abyssinica* und *Alchemilla* möglich. Als Proxy dient hier das Verhältnis von C<sub>31</sub> zu C<sub>29</sub>. Allerdings führt auch hier Degradation in der Reihe Pflanze – O-Lage – A<sub>h</sub>-Horizont zum Verlust des charakteristischen Alkanmusters. Obwohl sich rezentes Pflanzenmaterial chemotaxonomisch unterscheiden lässt, zwingt dies zur Schlussfolgerung, dass Degradationseffekte bei der Rekonstruktion von *Erica* im Untersuchungsgebiet der Bale Berge in Äthiopien anhand von ligninbürtigen Phenolen und blattwachsbürtigen Alkanbiomarkern nicht unberücksichtigt bleiben dürfen. Dieser Befund ist über unsere Fallstudie hinaus von hoher Relevanz.

**Schlagerworte:** Chemotaxonomie, Biomarker, molekulare Proxies, Humifizierung, organische Bodensubstanz, Pedogenese, *Erica*, *Festuca abyssinica*

## 1. Introduction

The Bale Mountains are an eastern afro-montane biodiversity hotspot area with 27 endemic species of flowering plants (Hillman, 1988). Like in many other afro-montane ecosystems, an altitudinal zonation of the vegetation is well established with an Ericaceous belt forming a prominent feature. Ericaceous vegetation dominates above 3300 m a.s.l., shows different stages of post-fire succession and remains continuous up to 3800 m a.s.l. However, it becomes patchy on the Sanetti Plateau (Miehe and Miehe, 1994). The Bale Mountains National Park is increasingly under threat from climate change and anthropogenic impacts (Kidane et al., 2012). Ascertaining the past environmental and vegetation history of the area will support conservation efforts and may help to disentangle the influence of climate versus human impact on the present biodiversity.

Until now, the vegetation history of the Bale Mountains was studied using pollen records from lacustrine sediments and peat deposits (Bonnefille and Hamilton, 1986; Bonnefille and Mohammed, 1994; Hamilton, 1982; Umer et al., 2007). The results suggest the extension of the Ericaceous belt towards higher altitudes during the early and middle Holocene. As potential drawbacks, such pollen studies depend on pollen preservation and can be biased by variable pollination rates as well as middle- and long-distance pollen transport (Hicks, 2006; Jansen et al., 2010; Ortu et al., 2006). By contrast, stable isotopes and biomarkers can be applied to more degraded sedimentary archives and soils and are assumed to reflect the standing vegetation more (Glaser and Zech, 2005). Thus, they offer the potential to complement pollen-based vegetation reconstructions and to reconstruct vegetation at a higher temporal and spatial resolution. For instance, the stable carbon isotopic composition ( $\delta^{13}\text{C}$ ) of lacustrine sediments suggests an expansion of alpine C4 grasses on Mt. Kenya especially during glacial times (Street-Perrott et al., 2004), whereas  $\delta^{13}\text{C}$  results from (paleo-)soils provide no evidence for C4 grass expansion close to Mt. Kilimanjaro during late Pleistocene glacial periods (Zech, 2006; Zech et al., 2011b). We focus here on lignin-derived phenols and leaf wax-derived *n*-alkanes as biomarkers, while stable isotopes and sugar biomarkers and their chemotaxonomic potential for reconstructions of the Bale Mountains vegetation are addressed in a companion paper by Mekonnen et al., (2019).

Lignin has a polyphenolic biochemical structure produced by terrestrial vascular plants (Ertel and Hedges, 1984) providing strength and rigidity to the plants (Thevenot et al., 2010). The lignin-derived phenols vanillyl (V), syringyl (S) and cinnamyl (C) as products of cupric oxide (CuO) oxidation are used to differentiate sources of organic matter and provide information

about the diagenetic state (degree of degradation) of vascular plant material in terrestrial and aquatic sediments (Castañeda et al., 2009; Hedges et al., 1988; Tareq et al., 2004, 2006; Ziegler et al., 1986). For instance, low ratios of S/V  $\sim 0$  were suggested as proxy for the relative contribution of gymnosperms and elevated S/V ratios were found to be indicative for the presence of angiosperms (Tareq et al., 2004). Likewise, the C/V ratio was proposed to indicate the relative contribution of woody (C/V < 0.1) and non-woody (C/V > 0.1) plants to the soil and sediment organic matter (Tareq et al., 2011). Moreover, the ratios of acid to aldehyde forms of vanillyl and syringyl units (Ac/Al)<sub>v,s</sub> were suggested as proxies for quantifying the degree of lignin degradation (Amelung et al., 2002; Hedges and Ertel, 1982; Möller et al., 2002).

*n*-Alkanes are important constituents of plant leaf waxes (Kolattukudy, 1970), where they serve to protect plants against water loss by evaporation as well as from fungal and insect attacks (Eglinton and Hamilton, 1967; Koch et al., 2009). Due to their recalcitrant nature, they are often well preserved in sedimentary archives and used as biomarkers (also called molecular fossils) in paleoclimate and environmental studies (Eglinton and Eglinton, 2008; Glaser and Zech, 2005; Zech et al., 2011c). The potential of *n*-alkanes for chemotaxonomic studies has been suggested based on the finding that the homologues C<sub>27</sub> and C<sub>29</sub> are sourced predominantly from trees and shrubs, whereas the homologues C<sub>31</sub> and C<sub>33</sub> are sourced predominantly from grasses and herbs (Maffei, 1996; Maffei et al., 2004; Rommerskirchen et al., 2006; Schäfer et al., 2016; Zech, 2009). Potential pitfalls when applying *n*-alkane proxies in paleovegetation studies should not be overlooked. For instance, (Bush and McInerney, 2013) caution against the chemotaxonomic application of *n*-alkanes because of high *n*-alkane pattern variability within graminoids and woody plants (Schäfer et al., 2016) emphasized the need for establishing regional calibration studies and Zech et al., (2011a, 2013) point to degradation affecting *n*-alkane proxies.

While the overall aim of our research is to contribute to the reconstruction of the paleoclimate and environmental history of the Bale Mountains, this study focuses more specifically on the following questions: (i) do lignin phenols and *n*-alkane biomarkers allow a chemotaxonomic differentiation of the dominant plant types of the Bale Mountains? (ii) Are the biomarker patterns of the plants reflected by and incorporated into the respective soils? (iii) Which implications have to be drawn from those results for planned paleovegetation reconstructions in the study area, e.g., concerning the reconstruction of the former extent of *Erica*? Finally, improved knowledge of the vegetation history of the Bale Mountains may help to support the

biodiversity conservation program of the park in the face of future climate change and increasing human pressure.

## 2. Material and Methods

### 2.1 Study area and sample description

The Bale Mountains are located 400 km southeast of Addis Ababa, the capital of Ethiopia (Hillman, 1986). Geographically, they belong to the Bale–Arsi massif, which forms the western section of the southeastern Ethiopian highlands (Hillman, 1988; Mieke and Mieke, 1994; Tiercelin et al., 2008). The Bale Mountains National Park (BMNP) is situated at 39°28' to 39°57' longitude (E) and 6°29' to 7°10' latitude (N) (Hillman, 1988; Mieke and Mieke, 1994; Umer et al., 2007) with elevation ranging from 1400 to 4377 m a.s.l. The highest part forms the Sanetti Plateau, on which the second highest peak of the country, Mount Tulu Dimtu at 4377 m a.s.l. is also located (Hillman, 1988). The plateau is limited by the steep Hareenna escarpment in the south and the southeast. The northeastern part is encompassed by high ridges and broad valleys that gradually descend towards the extensive Arsi–Bale plateaus and further into the Central Rift Valley lowlands (Hillman, 1988; Tiercelin et al., 2008). The topography of the Bale Mountains results in climatic gradients with respect to spatial and temporal distribution of rainfall as well as temperature (Tiercelin et al., 2008). Mean maximum temperature (MMT) on the mountain peaks ranges between 6–12 °C. At Dinsho (headquarter, 3170 m a.s.l.) the MMT is 11.8 °C. Mean minimum temperature ranges from 0.6–10 °C with frequent frost occurring in the high peak areas during the winter season (Tiercelin et al., 2008). The highest annual rain fall and humidity occurs in the southwest part of the mountain with 1000–1500 mm year<sup>-1</sup> and the northern part of the mountains exhibits annual rainfall ranging between 800 and 1000 mm year<sup>-1</sup> (Woldu et al., 1989). The vegetation shows an altitudinal zonation comprised of the afro-montane forest (1450–2000 m a.s.l.), the upper montane forests dominated by *Hagenia* – *Hypericum* species (2000–3200 m a.s.l.), the Ericaceous belt (3200–3800 m a.s.l.); and the Afro-alpine zone (3800–4377 m a.s.l.) dominated by dwarf shrubs such as *Helichrysum*, *Alchemilla*, herbs and grasses (mostly *Festuca*; Fig. 1–1) (Friis, 1986; Mieke and Mieke, 1994). Geologically, the Bale Mountains consist of a highly elevated volcanic plateau dominated by alkali basalt, tuffs and rhyolite rocks. During the last glacial maximum (LGM), it is understood that the regions of the high peak summits were glaciated and later flattened by repeated glaciations (Kidane et al., 2012; Osmaston et al., 2005; Umer et al., 2004). The soils having developed on the basaltic and trachyte rocks can be generally characterized as silt loam having reddish brown to black color (Woldu et al., 1989). They are usually shallow, gravelly and are

assumed to have developed since the glacial retreat (Hedberg, 1964). Andosols are the most ubiquitous soil types. Nevertheless, Cambisols and Leptosols are also prevalent soil types in some parts of the Bale Mountains. In wetland and sedimentary basins, Gleysols and Histosols are also common (Billi, 2015; Yimer et al., 2006).

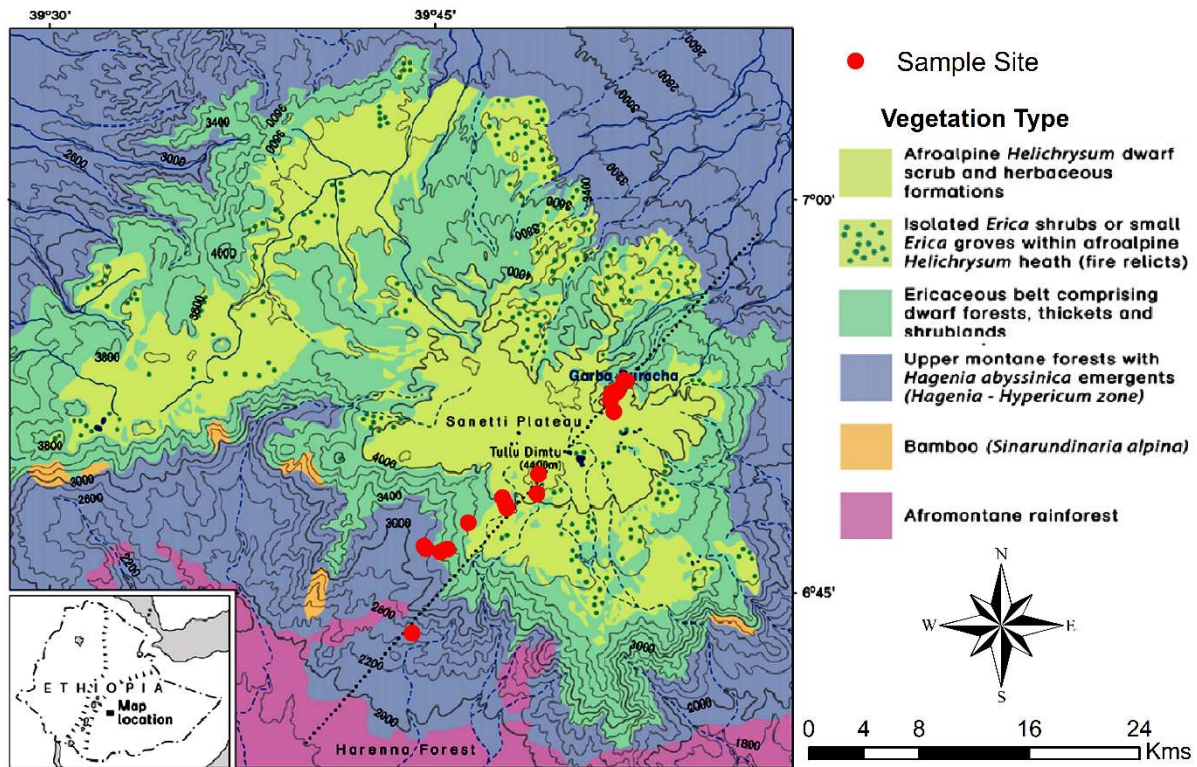


**Fig. 1–1:** Map of the Bale Mountains for the vegetation zones and study sites along the northeastern and the southwestern transect (modified following Mieke and Mieke, 1994). Dominant vegetation types sampled that comprise the Ericaceous and Afro-alpine belt.

In February 2015, 25 leaf and twig samples of locally dominant plant species were collected (Fig. 1–1) along a southwestern and a northeastern transect (ranging from 2550 to 4377 m a.s.l. and 3870 to 4134 m a.s.l., respectively). Samples comprised of *Erica trimera* (Engl.) Beentje (n=5), *Erica arborea* L. (n=5), *Alchemilla haumannii* Rothm (n=5), *Festuca abyssinica* Hochst. ex A. Rich. (n=6), *Helichrysum splendidum* (Thunb.) Less. (n=2), *Kniphofia foliosa* Hochst. (n=1) and *Lobelia rhynchopetalum* Hemsl. (n=1). Additionally, 15 organic surface layers (= O-layers, strongly humified plant residues) and 22 mineral topsoils (= A<sub>h</sub>-horizons) that developed under the above listed locally dominant vegetation were collected from 27 sampling sites, resulting in 62 samples in total. For photos illustrating the investigated plant species and typical study sites, the reader is referred to Fig. 2 of our companion paper by Mekonnen et al., (2019). All samples were air-dried in the Soil Store Laboratory of the National Herbarium,



Department of Plant Biology and Biodiversity Management, Addis Ababa University. In the laboratories of the Soil Biogeochemistry Group, Martin Luther University of Halle–Wittenberg, soil samples were sieved using a mesh size of 2 mm, finely ground, homogenized and subjected to further biogeochemical analysis.

## 2.2 Analysis of lignin-derived phenol and leaf wax-derived *n*-alkane biomarkers

Lignin phenols were extracted from 35, 50, and 500 mg of plant, O-layer and A<sub>h</sub>-horizon soil samples, respectively. The analytical procedure followed the cupric oxide (CuO) oxidation method developed by Hedges and Ertel, (1982) as modified later on by Goñi and Hedges, (1992). Briefly, the samples were transferred into Teflon digestion tubes together with 100 mg of (NH<sub>4</sub>)<sub>2</sub>Fe(SO<sub>4</sub>)<sub>2</sub>·6H<sub>2</sub>O, 500 mg of CuO, 50 mg of C<sub>6</sub>H<sub>12</sub>O<sub>6</sub>, 1 mL of ethylvanillin solution (100ppm) as internal standard 1 (IS1) and 15 mL of 2M NaOH and digested at 170 °C for two hours under pressure. Reaction products were cooled overnight and transferred into centrifuge tubes. Then the phenolic compounds were purified by adsorption on C18 columns and desorbed by ethylacetate and concentrated under a stream of nitrogen gas for 30 min. Residue was dissolved in 1 mL phenylacetic acid (PAA), a working internal standard stock solution to determine the recovery of ethylvanillin before derivatization (Amelung et al., 2002; Möller et al., 2002). Finally, the samples were derivatized using 200 µL of N, O-bis(trimethylsilyl) trifluoroacetamide (BSTFA) and 100 µL of pyridine. Oxidation products of lignin phenols were quantified using a SHIMADZU QP 2010 Gas Chromatography (GC) instrument coupled with a Mass Spectrometry (MS), (GCMS–QP2010, Kyoto, Japan).

After recovery correction, the concentration of each lignin phenol (in mg g<sup>-1</sup>) was calculated from two or three CuO oxidation products according to the Eqs. (1), (2) and (3), respectively.

$$\text{Vanillyl (V)} = \text{vanillin} + \text{acetovanillone} + \text{vanillic acid} \quad (1)$$

$$\text{Syringyl (S)} = \text{syringaldehyde} + \text{acetosyringone} + \text{syringic acid} \quad (2)$$

$$\text{Cinnamyl (C)} = p\text{-coumaric acid} + \text{ferulic acid} \quad (3)$$

For data evaluation, additionally the sum of V, S and C ( $\Sigma$ VSC); the ratios of S/V, and C/V; and the ratios of acids to aldehydes (Ac/Al) for the syringyl and vanillyl units were additionally calculated.

Leaf wax-derived *n*-alkanes were extracted from 0.5 to 1 g of plant, O-layer and A<sub>h</sub>-horizon soil samples using Soxhlet extraction by adding 150 ml of dichloromethane (DCM) and methanol (MeOH) as solvents (9:1 ratio) for 24 h following a method modified following Zech

and Glaser, (2008). In brief, 50  $\mu\text{l}$  of 5 $\alpha$ -androstane were added to the total lipid extracts (TLEs) as internal standard. TLEs were concentrated using rotary evaporation and transferred to aminopropyl columns. Three lipid fractions containing the *n*-alkanes, alcohols and fatty acids, respectively, were eluted successively by using 3 ml of hexane, DCM/MeOH (1:1) and diethyl ether and acetic acid (95:5) as eluent. The *n*-alkanes were separated on a gas chromatography (GC) and detected by a flame ionization detector (FID), whereas the other two lipid fractions (alcohols and fatty acids) were archived. The GC instrument (GC-2010 SHMADZU) was equipped with a SPB-5 columns (28.8 m length, 0.25 mm inner diameter, 0.25  $\mu\text{m}$  film thickness). The injector and detector temperature were 300 and 330  $^{\circ}\text{C}$ , respectively. The initial oven temperature was 90  $^{\circ}\text{C}$ . It is then raised in three ramps to 250  $^{\circ}\text{C}$  at 20  $^{\circ}\text{C}/\text{min}$ , further to 300  $^{\circ}\text{C}$  at 2  $^{\circ}\text{C}/\text{min}$  and finally to 320  $^{\circ}\text{C}$  at 4  $^{\circ}\text{C}/\text{min}$ , resulting in a total oven runtime of 50 minutes. Helium (He) was used as carrier gas and *n*-alkane mixture (C8–C40) was used as external standard for peak identification and quantification.

The total *n*-alkane concentration (TAC), the average chain length (ACLs, following Poynter et al., (1989) and the odd over even predominance (OEP, following Hoefs et al., (2002), the latter being very similar to the carbon preference index (CPI), were calculated according to the Eqs. (4), (5) and (6), respectively.

$$\text{TAC} = \sum C_n, \text{ with } n \text{ ranging from } 25 \text{ to } 35, \quad (4)$$

$$\text{ACL} = \frac{\sum (C_n * n)}{\sum C_n}, \quad (5)$$

Where *n* refers to the odd numbered *n*-alkanes ranging from 27 to 33

$$\text{OEP} = \frac{(C_{27}+C_{29}+C_{31}+C_{33})}{(C_{26}+C_{28}+C_{30}+C_{32})}. \quad (6)$$

All calibrated datasets of the analytical results were subjected to simple correlation test and agglomerative hierarchical clustering (AHC) using XLSTAT (2014) statistical software. R software version 3.4.2 was also used to demonstrate taxonomic differences and effect of biodegradation on the sample materials via ternary diagrams and notched box plots.

### 3. Results and Discussion

#### 3.1 Lignin phenol concentration and patterns of contemporary vegetation

The  $\sum\text{VSC}$  of modern plants investigated from the two transects of the Bale Mountains ranges from 1.8 to 41.8  $\text{mg g}^{-1}$ , the sample with *Festuca* yielding the highest average contribution to TOC with up to 33  $\text{mg g}^{-1}$  sample (Fig. 1–2). This is within the range reported in the literature (Belanger et al., 2015; Hedges et al., 1986). Note that lignin phenol concentrations of grasses

are higher compared to other vegetation of the Bale Mountains, although it is known that grasses contain only low amounts of lignin when compared to trees.

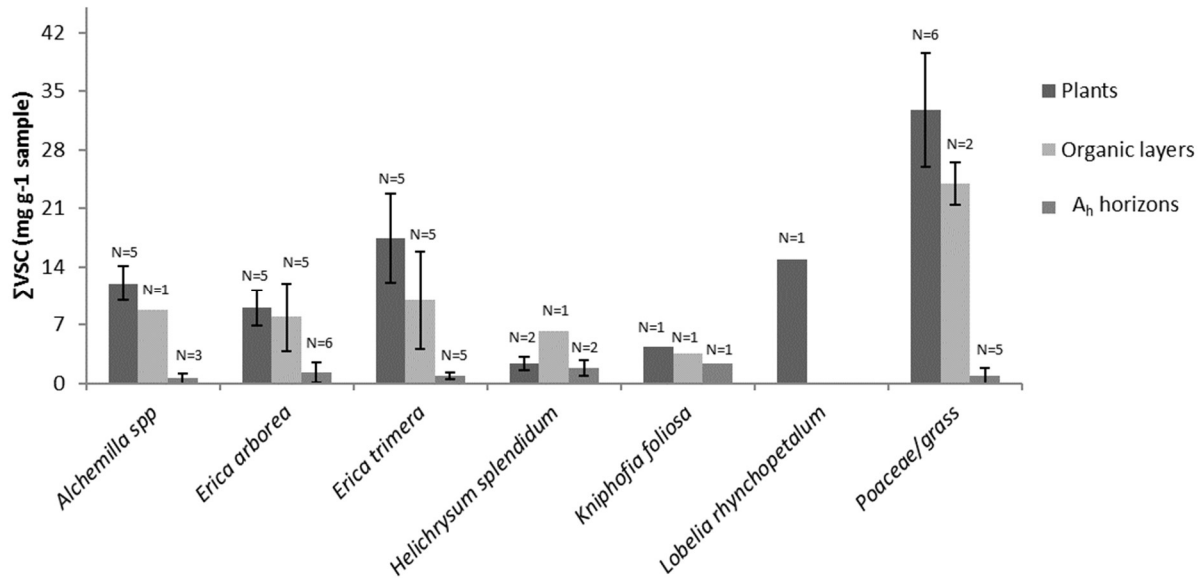


**Fig. 1–2:** Sum of lignin phenol concentrations ( $\Sigma$ VSC) of contemporary plants, O-layers and A<sub>h</sub>-horizons. Error bars illustrate standard deviations.

The concentrations of individual lignin phenols (vanillyl, syringyl, and cinnamyl) allow us to chemotaxonomically differentiate the contemporary dominant plant species of the Bale Mountains. This is illustrated in Fig. 1–3, based on an Agglomerative Hierarchical Cluster analyses (AHC). The abundance of individual lignin phenols (V, S, and C) was specific to individual or restricted groups of plant and/or tissues applied to cluster different taxa (Belanger et al., 2015; Castañeda et al., 2009; Goñi and Hedges, 1992; Hedges and Mann, 1979; Tareq et al., 2004, 2006).

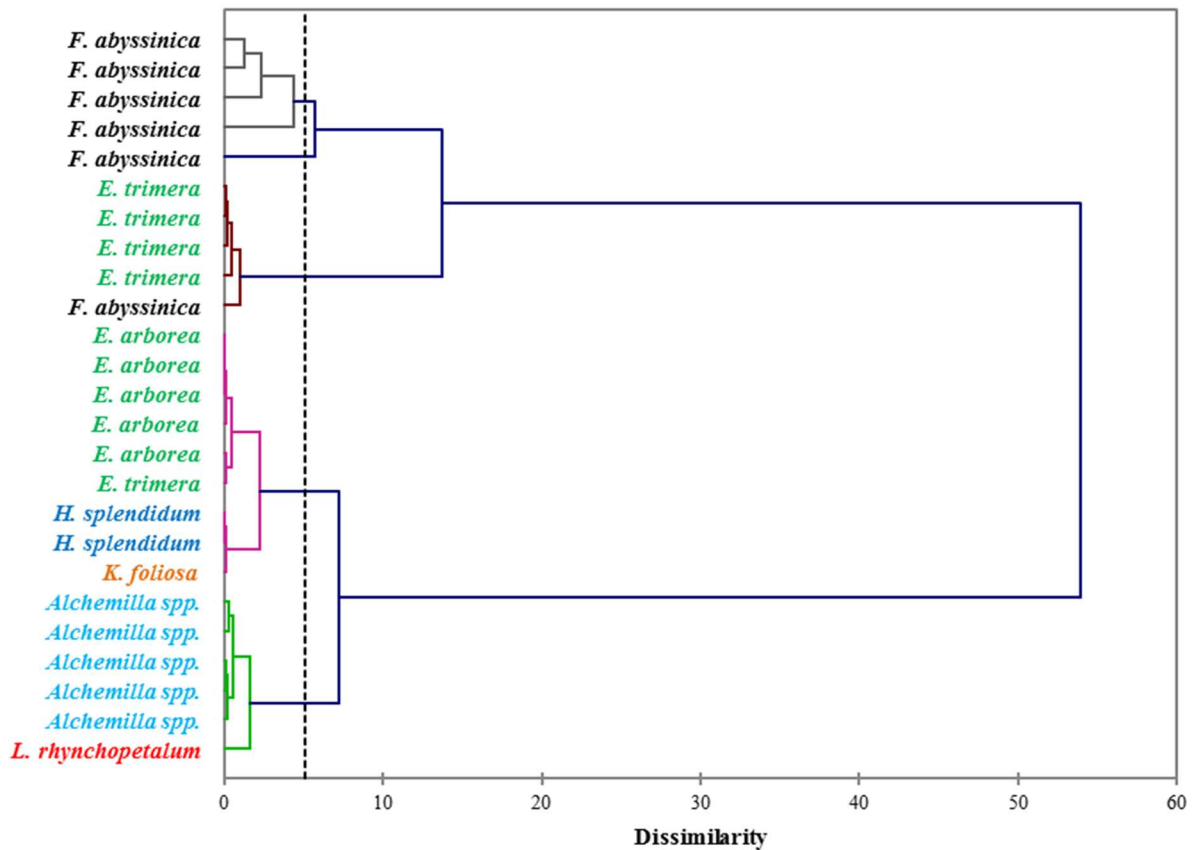


**Fig. 1–3:** Dendrogram differentiating the dominant plant species of the Bale Mountains based on the concentrations of vanillyl, syringyl and cinnamyl lignin phenols ( $\text{mg g}^{-1}$  sample). The dotted vertical line represents the distance or dissimilarity between clusters.

While Fig. 1–3 highlights the potential for chemotaxonomic differentiation of the investigated plants, it does not yet become clear from this hierarchical cluster analyses result which lignin phenols are characteristic for which plants and which lignin proxy might have potential in paleovegetation reconstructions. Therefore, Fig. 1–4 shows the relative abundance of V, S and C for all investigated plant species in a ternary diagram. Accordingly, *Erica arborea* and *Erica trimera* are characterized by cinnamyl percentages of  $> 40\%$ , whereas, except for two *Festuca* samples, all other plants are characterized by cinnamyl percentages of  $< 40\%$ . Our results from fresh plant material are hence not in agreement with the finding of Hedges and Mann (1979) and Hedges et al. (1988) that high contributions of cinnamyl phenols are characteristic of non-woody grass and fern. Despite a relatively large scattering and a partial overlapping, our results suggest that the ratio  $C/(V+S+C)$  might be used as a proxy for distinguishing *Erica spp.* from other vegetation types of the Bale Mountains, with values  $> 0.40$  being generally characteristic for *Erica spp.*

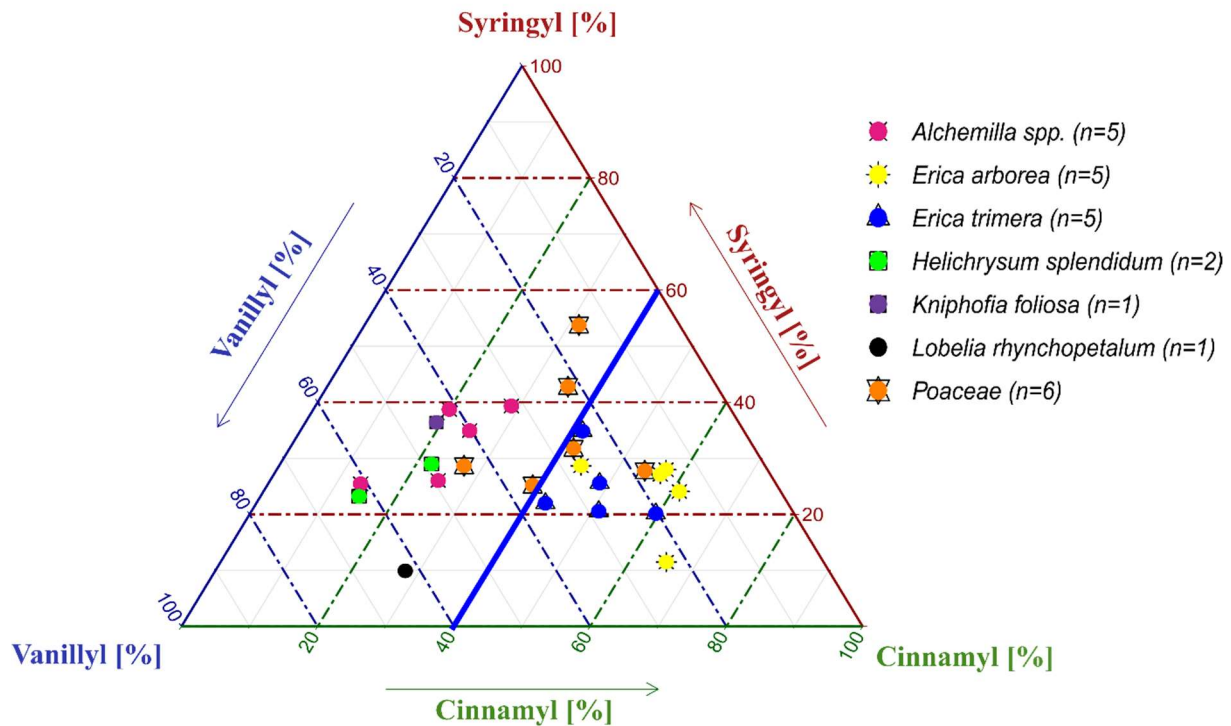


**Fig. 1–4:** Ternary diagram for the relative abundances (%) of vanillyl, syringyl and cinnamyl lignin phenols of the dominant vegetation. The blue line separates samples with more (right) versus less (left) than 40% cinnamyl.

### 3.2 Lignin phenol patterns of O-layers and A<sub>h</sub>-horizons

The  $\sum$ VSC strongly decreases from plants over O-layers to A<sub>h</sub>-horizons, except for *Helichrysum*, which yielded the lowest  $\sum$ VSC values of all plants (Fig. 1–2). This descending trend is in agreement with literature (Amelung et al., 1997; Belanger et al., 2015) and reflects the preferential degradation of the plant-derived lignin phenols compared to other soil organic matter constituents. At the same time, the input of root-derived lignin is very likely. As a result of both processes, i.e., degradation and lignin input by roots and the large and chemotaxonomically characteristic contribution of C in *Erica* plant material ( $\geq 41.5\%$ ) is lost in the O-layers ( $C < 27\%$ ), whereas the two investigated O-layers under *Festuca* yielded relative C contributions  $> 40\%$ . Similarly, A<sub>h</sub>-horizons under *Festuca* are characterized by C contributions  $> 40\%$ , while all A<sub>h</sub>-horizons that developed under other vegetation types are characterized by C contributions  $< 40\%$ . This finding does not *ad hoc* preclude the above proposed lignin phenol proxy  $C/(V+S+C)$  for reconstructing vegetation history, but it definitely challenges its application. Degradation and lignin input by roots need to be considered when interpreting phenol proxies. This is relevant beyond our case study concerning *Erica* versus

*Festuca* and *Helichrysum* (Fig. 1–5) and is likely more relevant in paleosols than in sedimentary archives.

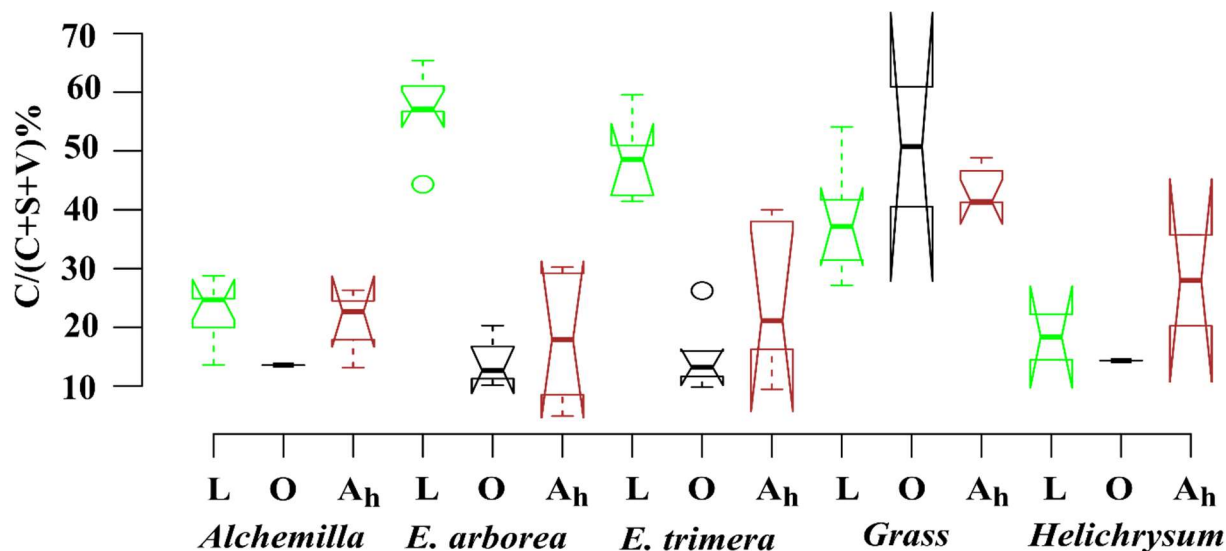


**Fig. 1–5:** Box plot for the relative abundance of cinnamyl phenols (expressed as  $C/(V+S+C)$  in %) in plants, O-layers and  $A_h$ -horizons. The box plots indicate the median (solid line between the boxes) and interquartile range (IQR), with upper (75%) and lower (25%) quartiles and possible outliers (empty circles). The notches display the confidence interval around the median within  $\pm 1.57 \cdot \text{IQR}/\text{sqrt}$ . Note that small sample sizes result in unidentifiable boxes.

In our study, we found no consistent increase and systematic relationship between  $Ac/Al$  ratios of V and S, which are used as degradation proxies in some studies (Amelung et al., 2002; Hedges and Ertel, 1982; Möller et al., 2002; Tareq et al., 2011), and source proxy (S/V). This is in agreement with other studies (Belanger et al., 2015) and we, therefore, suggest that caution needs to be taken when using  $Ac/Al$  ratios as degradation proxies.

### 3.3 *n*-Alkane concentrations and patterns of contemporary plants

To characterize the dominant plant species chemotaxonomically, *n*-alkanes with a chain length of 21–37 C atoms were considered as characteristic for epicuticular leaf waxes, typical for higher plants (Eglinton and Hamilton, 1967; Hoffmann et al., 2013). Most of the investigated plant species showed total *n*-alkane concentrations (TAC,  $C_{25-35}$ ) above  $800 \mu\text{g g}^{-1}$ . Only *Lobelia* and *Festuca* exhibited total *n*-alkane concentrations below  $800 \mu\text{g g}^{-1}$  (Fig. 1–6). The TAC values of the O-layers were only slightly lower when compared to contemporary plants. By contrast, the TAC values of the  $A_h$ -horizons were significantly lower compared to contemporary plants (Fig. 1–6). The *n*-alkane concentrations in this study are in agreement with

research findings for fresh plant materials (Bush and McInerney, 2013; Feakins et al., 2016) and soils (Schäfer et al., 2016).

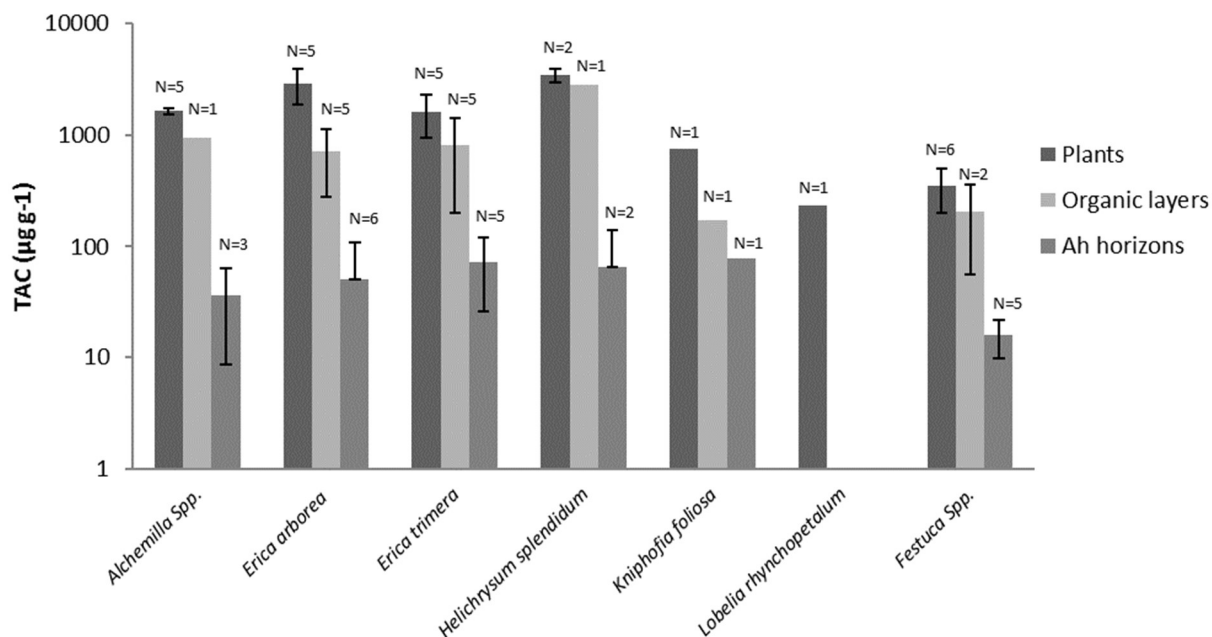


**Fig. 1–6:** Total long-chain *n*-alkane concentrations (TACs) of plants, O-layers and A<sub>h</sub>-horizons. Error bars illustrate standard deviations.

Contrary to lignin phenols, hierarchical cluster analysis of individual *n*-alkanes did not allow for unambiguous differentiation between *Erica* and non-*Erica* species. Therefore, the *n*-alkane patterns do not allow for developing a proxy for identifying *Erica*, at least in the Bale Mountains. Average chain length values (ACLs) of plant and soil *n*-alkanes range between 28 to 32 and 29 to 31, respectively. The ACLs of *Erica arborea* (30.5) and *Erica trimera* (30.5) are identical, which could be explained by the monophyletic origin of the species (Guo et al., 2014). The grass samples (*Festuca abyssinica*) exhibited a clear predominance of C<sub>31</sub> (Fig. 1–7), which was reported before by different authors (Schäfer et al., 2016; Zech, 2009). Most other investigated plant species revealed a predominance of either C<sub>29</sub> or C<sub>31</sub>. Only *Kniphofia foliosa* is characterized by high relative abundance of C<sub>27</sub> and C<sub>29</sub>, while C<sub>31</sub> is almost absent (Fig. 1–7). Apart from individual *n*-alkanes, the ratio of C<sub>31</sub>/C<sub>29</sub> depicts *Erica* litter is significantly distinguishable from the other species, except for *Helichrysum splendidum* (Fig. 1–8).

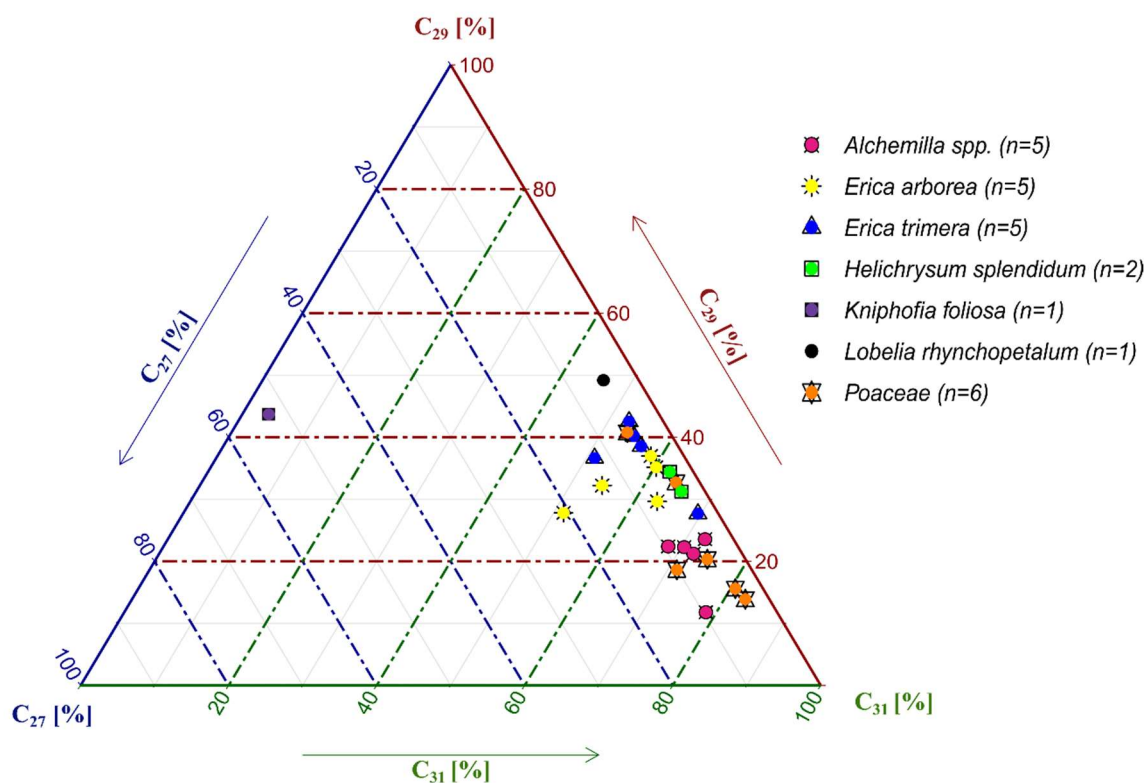


**Fig. 1–7:** Ternary diagram illustrating the relative abundance (%) of the  $n$ -alkanes  $C_{27}$ ,  $C_{29}$  and  $C_{31}$  in the investigated plant samples.

### 3.4 $n$ -Alkane concentration and patterns of O-layers and $A_h$ -horizons

The TAC values decrease in the order: plants > O-layers >  $A_h$ -horizon (Fig.2–6). The odd over even predominance values (OEPs) of the plants, O-layers and  $A_h$ -horizons range from 5 to 90 ( $\bar{x} = 21$ ), 4 to 42 ( $\bar{x} = 15$ ) and 2 to 37 ( $\bar{x} = 16$ ), respectively. The OEP values of the plants (which are almost identical to the CPI values) are therefore well within the range reported (Diefendorf et al., 2011) for angiosperms. Decreasing OEP values towards O-layers and  $A_h$ -horizons are often observed and can be explained with organic matter degradation (Schäfer et al., 2016; Zech et al., 2011b). The still relatively high OEP values ( $\bar{x} = 16$ ) obtained for the topsoils of our study area indicate that the  $n$ -alkanes are not strongly degraded. Importantly,  $n$ -alkane degradation affects not only the OEP values but also  $n$ -alkane ratios, such as the above presented ratio  $C_{31}/C_{29}$  that allows distinguishing *Erica* from non-*Erica* vegetation. As a result, this ratio in particular no longer allows for chemotaxonomically distinguishing between soils that have developed under *Erica* versus *Alchemilla* and grass (Fig. 1–8). Unlike with lignin phenols, a noteworthy influence from root-derived  $n$ -alkanes on O-layers and  $A_h$ -horizons can be excluded. This is based on the notion that roots contain lower  $n$ -alkane concentrations by



several magnitudes than above-ground plant material and results from studies using  $^{14}\text{C}$  dating of *n*-alkanes in loess-paleosol sequences (Haeggi et al., 2014; Zech et al., 2017).

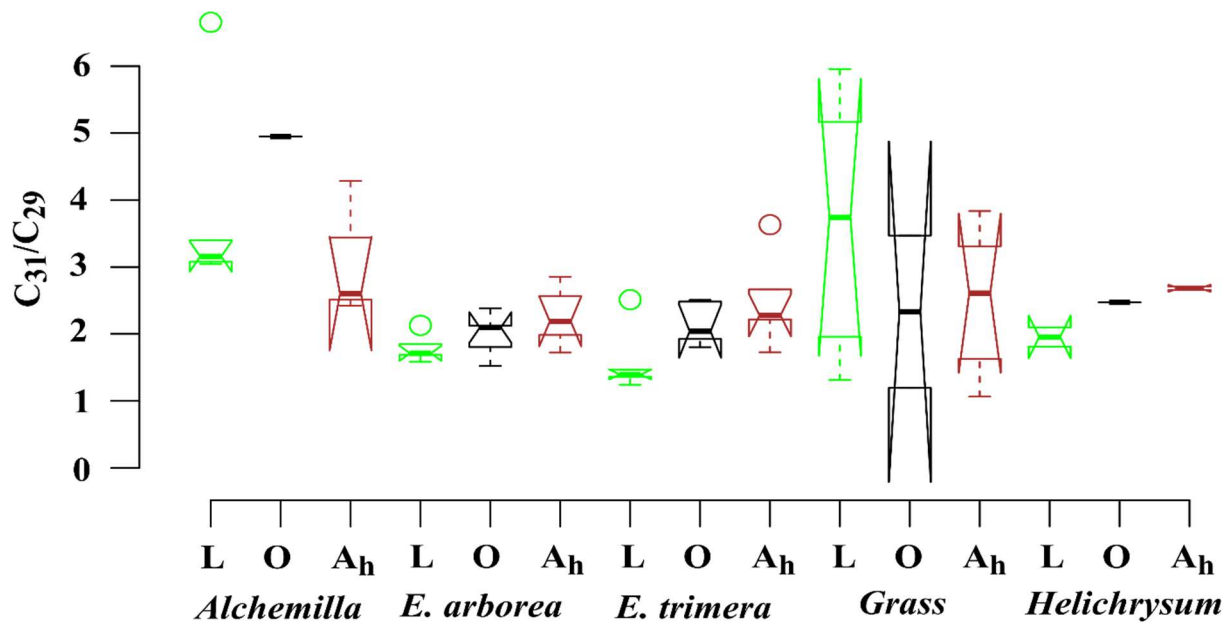


**Fig. 1–8:** Box plot for the ratio  $C_{31}/C_{29}$  in plant samples, organic layers and  $A_h$ -horizons. The box plots indicate the median (solid line between the boxes) and interquartile range (IQR), with upper (75%) and lower (25%) quartiles and possible outliers (empty circles). The notches display the confidence interval around the median within  $\pm 1.57 \cdot \text{IQR}/\text{sqrt}$ . Note that small sample sizes result in unidentifiable boxes.

#### 4 Conclusions and implications for paleovegetation reconstructions in the Bale Mountains

One of the premises within the Mountain Exile Hypothesis project (DFG-FOR 2358) is to reconstruct the dynamics of *Erica* vegetation on the Sanetti Plateau in the Bale Mountains National Park, Ethiopia. While our companion paper by Mekonnen et al., (2019) focused on stable carbon and nitrogen isotopes and hemicellulose-derived sugar biomarkers, we tested in this regional calibration study the potential of cupric oxide lignin phenols and leaf-wax-derived *n*-alkanes to serve as unambiguous proxies for differentiating between *Erica* versus non-*Erica* vegetation.

A hierarchical cluster analysis of individual lignin phenols was promising and allowed the chemotaxonomic differentiation of *Erica* from non-*Erica* vegetation based on relatively high relative contribution of cinnamyl ( $\geq 40\%$ ) phenols. However, this characteristic pattern is not reflected in the O-layers and  $A_h$ -horizons. In all likelihood, the loss of the cinnamyl dominance

is caused by preferential degradation. Unlike expected, we found no overall evidence for increasing (Ac/Al)<sub>v+s</sub> ratios as proxy for degradation from plant material over O-layers to A<sub>h</sub>-horizons.

*Erica* could not be differentiated chemotaxonomically from all other investigated plant species using *n*-alkanes in a hierarchical cluster analysis. Nevertheless, *Erica* was still characterized in our dataset by significantly lower C<sub>31</sub>/C<sub>29</sub> ratios compared to *Alchemilla* and grasses. However, like lignin-derived phenol proxies, the *n*-alkane patterns are changing due to degradation from plant material over O-layers to A<sub>h</sub>-horizons, thus inhibiting their application for an unambiguous chemotaxonomic identification of *Erica* in soils and sediments. Therefore, future work is planned focusing on alternative molecular markers such as tannin-derived phenols and terpenoids.

**Data availability:** The underlying datasets used in this study are accessible via <https://doi.org/10.5281/zenodo.3372104>.

**Authors contributions:** BG, WZ and MZ developed the project idea in collaboration with SN and TB. WZ, BL and BM designed and handled field research work. BL and LB performed the laboratory work. The manuscript was prepared by BL with the support of MZ and the other co-authors.

**Competing interests:** The authors declare that they have no conflict of interest.

## Acknowledgments

We are grateful to the Ethiopian Biodiversity Institute, Ethiopian Wildlife Conservation Authority, Bale Mountains National Park and Addis Ababa University for providing us with access to the plant genetic resources, access to the Bale Mountains National Park and for their scientific collaboration, respectively. We acknowledge the financial support within the funding program Open Access Publishing by the German Research Foundation (DFG). Bruk Lemma expresses his gratitude to the Catholic Academic Exchange Services (KAAD, Germany) for the Ph.D. scholarship and his sincere thanks to Heike Maennicke for kind assistance during the laboratory work. We kindly thank three anonymous reviewers for their constructive comments and suggestions that helped us to improve the quality of this paper.

**Financial support:** This research has been supported by the DFG within Research Unit “The Mountain Exile Hypothesis” (grant nos. GL 327/18-1, ZE 844/10-1 and ZE 154/70-1).

## References

- Amelung, W., Zech, W. and Flach, K. W., 1997. Climatic effects on soil organic matter composition in the Great Plains. *Soil Science Society of America Journal*, 61(1), 115–123.
- Amelung, W., Martius, C., Bandeira, A. G., Garcia, M. V. and Zech, W., 2002. Lignin characteristics and density fractions of termite nests in an Amazonian rain forest—indicators of termite feeding guilds? *Soil Biology and Biochemistry*, 34(3), 367–372.
- Belanger, E., Lucotte, M., Gregoire, B., Moingt, M., Paquet, S., Davidson, R., Mertens, F., Passos, C. J. S. and Romana, C., 2015. Lignin signatures of vegetation and soils in tropical environments. *Advances in environmental research*, 4(4), 247–262.
- Billi, P., 2015 Geomorphological landscapes of Ethiopia, in *Landscapes and landforms of Ethiopia*, pp. 3–32, Springer: Dordrecht, The Netherlands, pp. 3–32.
- Bonnefille, R. and Hamilton, A., 1986. Quaternary and late Tertiary history of Ethiopian vegetation. *Symb. Bot. Ups*, 26(2), 48–63.
- Bonnefille, R. and Mohammed, U., 1994. Pollen-inferred climatic fluctuations in Ethiopia during the last 3000 years. *Palaeogeography, Palaeoclimatology, Palaeoecology*, 109(2–4), 331–343.
- Bush, R. T. and McInerney, F. A., 2013. Leaf wax n-alkane distributions in and across modern plants: implications for paleoecology and chemotaxonomy. *Geochimica et Cosmochimica Acta*, 117, 161–179.
- Castañeda, I. S., Werne, J. P., Johnson, T. C. and Filley, T. R., 2009. Late Quaternary vegetation history of southeast Africa: the molecular isotopic record from Lake Malawi. *Palaeogeography, Palaeoclimatology, Palaeoecology*, 275(1–4), 100–112.
- Diefendorf, A. F., Freeman, K. H., Wing, S. L. and Graham, H. V., 2011. Production of n-alkyl lipids in living plants and implications for the geologic past. *Geochimica et Cosmochimica Acta*, 75(23), 7472–7485.
- Eglinton, G. and Hamilton, R. J., 1967. Leaf epicuticular waxes. *Science*, 156(3780), 1322–1335.
- Eglinton, T. I. and Eglinton, G., 2008. Molecular proxies for paleoclimatology. *Earth and Planetary Science Letters*, 275(1–2), 1–16.
- Ertel, J. R. and Hedges, J. I., 1984. The lignin component of humic substances: distribution among soil and sedimentary humic, fulvic, and base-insoluble fractions. *Geochimica et Cosmochimica Acta*, 48(10), 2065–2074.

- Feakins, S. J., Peters, T., Wu, M. S., Shenkin, A., Salinas, N., Girardin, C. A., Bentley, L. P., Blonder, B., Enquist, B. J. and Martin, R. E., 2016. Production of leaf wax n-alkanes across a tropical forest elevation transect. *Organic geochemistry*, 100, 89–100.
- Friis, I., 1986. Zonation of Forest Vegetation on the South Slope of Bale Mountains, South Ethiopia. *Sinet-an Ethiopian Journal of Science*, 9: 29–44.
- Glaser, B. and Zech, W., 2005. Reconstruction of climate and landscape changes in a high mountain lake catchment in the Gorkha Himal, Nepal during the Late Glacial and Holocene as deduced from radiocarbon and compound-specific stable isotope analysis of terrestrial, aquatic and microbial biomarkers. *Organic Geochemistry*, 36(7), 1086–1098.
- Goñi, M. A. and Hedges, J. I., 1992. Lignin dimers: Structures, distribution, and potential geochemical applications. *Geochimica et Cosmochimica Acta*, 56(11), 4025–4043.
- Guo, N., Gao, J., He, Y., Zhang, Z. and Guo, Y., 2014. Variations in leaf epicuticular n-alkanes in some *Broussonetia*, *Ficus* and *Humulus* species. *Biochemical systematics and ecology*, 54, 150–156.
- Haeggi, C., Zech, R., McIntyre, C., Zech, M. and Eglinton, T. I., 2014. On the stratigraphic integrity of leaf-wax biomarkers in loess paleosols. *Biogeosciences*, 11(9), 2455–2463.
- Hamilton, A. C., 1982. *Environmental history of East Africa: a study of the Quaternary*, Academic press London, UK p. 328.
- Hedberg, O., 1964. *Features of afroalpine plant ecology*. Uppsala: Svenska växtgeografiska Sällskapet. *Acta Phytogeographica Suecica*; 49.
- Hedges, J. I. and Ertel, J. R., 1982. Characterization of lignin by gas capillary chromatography of cupric oxide oxidation products. *Analytical Chemistry*, 54(2), 174–178.
- Hedges, J. I. and Mann, D. C., 1979. The characterization of plant tissues by their lignin oxidation products. *Geochimica et Cosmochimica Acta*, 43(11), 1803–1807.
- Hedges, J. I., Clark, W. A., Quay, P. D., Richey, J. E., Devol, A. H. and Santos, M., 1986. Compositions and fluxes of particulate organic material in the Amazon River. *Limnology and Oceanography*, 31(4), 717–738.
- Hedges, J. I., Blanchette, R. A., Weliky, K. and Devol, A. H., 1988. Effects of fungal degradation on the CuO oxidation products of lignin: a controlled laboratory study. *Geochimica et Cosmochimica Acta*, 52(11), 2717–2726.
- Hicks, S., 2006. When no pollen does not mean no trees. *Vegetation History and Archaeobotany*, 15(4), 253–261.

- Hillman, J. C., 1986. Conservation in Bale mountains national park, Ethiopia. *Oryx*, 20(2), 89–94.
- Hillman, J. C., 1988. The Bale Mountains National Park area, southeast Ethiopia, and its management. *Mountain Research and Development*, 253–258.
- Hoefs, M. J., Rijpstra, W. I. C. and Damsté, J. S. S., 2002. The influence of oxic degradation on the sedimentary biomarker record I: Evidence from Madeira Abyssal Plain turbidites. *Geochimica et Cosmochimica Acta*, 66(15), 2719–2735.
- Hoffmann, B., Kahmen, A., Cernusak, L. A., Arndt, S. K. and Sachse, D., 2013. Abundance and distribution of leaf wax n-alkanes in leaves of *Acacia* and *Eucalyptus* trees along a strong humidity gradient in northern Australia. *Organic geochemistry*, 62, 62–67.
- Jansen, B., van Loon, E. E., Hooghiemstra, H. and Verstraten, J. M., 2010. Improved reconstruction of palaeo-environments through unravelling of preserved vegetation biomarker patterns. *Palaeogeography, Palaeoclimatology, Palaeoecology*, 285(1–2), 119–130.
- Kidane, Y., Stahlmann, R. and Beierkuhnlein, C., 2012. Vegetation dynamics, and land use and land cover change in the Bale Mountains, Ethiopia. *Environmental monitoring and assessment*, 184(12), 7473–7489.
- Koch, K., Bhushan, B. and Barthlott, W., 2009. Multifunctional surface structures of plants: an inspiration for biomimetics. *Progress in Materials science*, 54(2), 137–178.
- Kolattukudy, P. E., 1970. Plant waxes. *Lipids*, 5(2), 259–275.
- Maffei, M., 1996. Chemotaxonomic significance of leaf wax alkanes in the Gramineae. *Biochemical systematics and ecology*, 24(1), 53–64.
- Maffei, M., Badino, S. and Bossi, S., 2004. Chemotaxonomic significance of leaf wax n-alkanes in the Pinales (Coniferales). *Journal of Biological Research*, 1(1), 3–19.
- Mekonnen, B., Zech, W., Glaser, B., Lemma, B., Bromm, T., Nemomissa, S., Bekele, T. and Zech, M., 2019. Chemotaxonomic patterns of vegetation and soils along altitudinal transects of the Bale Mountains, Ethiopia, and implications for paleovegetation reconstructions—Part 1: stable isotopes and sugar biomarkers. *E&G Quaternary Science Journal*, 68(2), 177–188.
- Miehe, G., Miehe, S., 1994. Ericaceous forests and heathlands in the Bale Mountains of South Ethiopia: ecology and man's impact. T. Warnke, Hamburg, Germany, p. 206.
- Möller, A., Kaiser, K. and Zech, W., 2002. Lignin, carbohydrate, and amino sugar distribution and transformation in the tropical highland soils of northern Thailand under cabbage

- cultivation, *Pinus* reforestation, secondary forest, and primary forest. *Soil Research*, 40(6), 977–998.
- Ortu, E., Brewer, S. and Peyron, O., 2006. Pollen-inferred palaeoclimate reconstructions in mountain areas: problems and perspectives. *Journal of Quaternary Science*, 21, 615–627.
- Osmaston, H. A., Mitchell, W. A. and Osmaston, J. N., 2005. Quaternary glaciation of the Bale Mountains, Ethiopia. *Journal of Quaternary Science*, 20(6), 593–606.
- Poynter, J. G., Farrimond, P., Robinson, N. and Eglinton, G., 1989. Aeolian-derived higher plant lipids in the marine sedimentary record: Links with palaeoclimate, in *Paleoclimatology and paleometeorology: modern and past patterns of global atmospheric transport*. Springer, pp. 435–462.
- Rommerskirchen, F., Plader, A., Eglinton, G., Chikaraishi, Y. and Rullkötter, J., 2006. Chemotaxonomic significance of distribution and stable carbon isotopic composition of long-chain alkanes and alkan-1-ols in C<sub>4</sub> grass waxes. *Organic Geochemistry*, 37(10), 1303–1332.
- Schäfer, I. K., Lanny, V., Franke, J., Eglinton, T. I., Zech, M., Vysloužilová, B. and Zech, R., 2016. Leaf waxes in litter and topsoils along a European transect. *Soil*, 2(4), 551–564.
- Street-Perrott, F. A., Ficken, K. J., Huang, Y. and Eglinton, G., 2004. Late Quaternary changes in carbon cycling on Mt. Kenya, East Africa: an overview of the  $\delta^{13}\text{C}$  record in lacustrine organic matter. *Quaternary Science Reviews*, 23(7–8), 861–879.
- Tareq, S. M., Tanaka, N. and Ohta, K., 2004. Biomarker signature in tropical wetland: lignin phenol vegetation index (LPVI) and its implications for reconstructing the paleoenvironment. *Science of the Total Environment*, 324(1–3), 91–103.
- Tareq, S. M., Handa, N. and Tanoue, E., 2006. A lignin phenol proxy record of mid Holocene paleovegetation changes at Lake DaBuSu, northeast China. *Journal of Geochemical Exploration*, 88(1–3), 445–449.
- Tareq, S. M., Kitagawa, H. and Ohta, K., 2011. Lignin biomarker and isotopic records of paleovegetation and climate changes from Lake Erhai, southwest China, since 18.5 ka BP. *Quaternary International*, 229(1–2), 47–56.
- Thevenot, M., Dignac, M.-F. and Rumpel, C., 2010. Fate of lignins in soils: a review. *Soil Biology and Biochemistry*, 42(8), 1200–1211.
- Tiercelin, J.-J., Gibert, E., Umer, M., Bonnefille, R., Disnar, J.-R., Lézine, A.-M., Hureau-Mazaudier, D., Travi, Y., Kéravis, D. and Lamb, H. F., 2008. High-resolution

- sedimentary record of the last deglaciation from a high-altitude lake in Ethiopia. *Quaternary Science Reviews*, 27(5–6), 449–467.
- Umer, M., Kebede, S. and Osmaston, H., 2004. Quaternary glacial activity on the Ethiopian Mountains. *Developments in Quaternary Sciences*, 2, 171–174.
- Umer, M., Lamb, H. F., Bonnefille, R., Lézine, A.-M., Tiercelin, J.-J., Gibert, E., Cazet, J.-P. and Watrin, J., 2007. Late pleistocene and holocene vegetation history of the bale mountains, Ethiopia. *Quaternary Science Reviews*, 26(17–18), 2229–2246.
- Woldu, Z., Feoli, E., Nigatu, L., 1989. Partitioning an Elevation Gradient of Vegetation from Southeastern Ethiopia by Probabilistic Methods Stable by probabilistic methods from southeastern Ethiopia. *Plateau* 81, 189–198.
- Yimer, F., Ledin, S. and Abdelkadir, A., 2006. Soil organic carbon and total nitrogen stocks as affected by topographic aspect and vegetation in the Bale Mountains, Ethiopia. *Geoderma*, 135, 335–344.
- Zech, M., 2006. Evidence for Late Pleistocene climate changes from buried soils on the southern slopes of Mt. Kilimanjaro, Tanzania. *Palaeogeography, Palaeoclimatology, Palaeoecology*, 242(3–4), 303–312.
- Zech, M., 2009. Reconstructing Quaternary vegetation history in the Carpathian Basin, SE Europe, using n-alkane biomarkers as molecular fossils: problems and possible solutions, potential and limitations. *Quaternary International-Journal of the InternUnion for Quaternary Research*, 279, 555.
- Zech, M. and Glaser, B., 2008. Improved compound-specific  $\delta^{13}\text{C}$  analysis of n-alkanes for application in palaeoenvironmental studies. *Rapid Communications in Mass Spectrometry*, 22(2), 135–142.
- Zech, M., Pedentchouk, N., Buggle, B., Leiber, K., Kalbitz, K., Marković, S. B. and Glaser, B., 2011a. Effect of leaf litter degradation and seasonality on D/H isotope ratios of n-alkane biomarkers. *Geochimica et Cosmochimica Acta*, 75(17), 4917–4928.
- Zech, M., Leiber, K., Zech, W., Poetsch, T. and Hemp, A., 2011b. Late Quaternary soil genesis and vegetation history on the northern slopes of Mt. Kilimanjaro, East Africa. *Quaternary international*, 243(2), 327–336.
- Zech, M., Zech, R., Buggle, B. and Zöller, L., 2011c. Novel methodological approaches in loess research—interrogating biomarkers and compound-specific stable isotopes. *Eiszeitalter & Gegenwart—Quaternary Science Journal*, 60(1), 170–187.
- Zech, M., Krause, T., Meszner, S. and Faust, D., 2013. Incorrect when uncorrected: reconstructing vegetation history using n-alkane biomarkers in loess-paleosol

- sequences—a case study from the Saxonian loess region, Germany. *Quaternary international*, 296, 108–116.
- Zech, M., Kreuzer, S., Zech, R., Goslar, T., Meszner, S., McIntyre, C., Häggi, C., Eglinton, T., Faust, D. and Fuchs, M., 2017. Comparative  $^{14}\text{C}$  and OSL dating of loess-paleosol sequences to evaluate post-depositional contamination of n-alkane biomarkers. *Quaternary Research*, 87(1), 180–189.
- Ziegler, F., Kögel, I. and Zech, W., 1986. Alteration of gymnosperm and angiosperm lignin during decomposition in forest humus layers. *Zeitschrift für Pflanzenernährung und Bodenkunde*, 149(3), 323–331.



**Study 2:**

**Phenolic Compounds as Unambiguous Chemical Markers for the Identification of Keystone Plant Species in the Bale Mountains, Ethiopia**

**Bruk Lemma<sup>1,2\*</sup>, Claudius Grehl<sup>1,7</sup>, Michael Zech<sup>1,6</sup>, Betelhem Mekonnen<sup>1,4</sup>, Wolfgang Zech<sup>5</sup>, Sileshi Nemomissa<sup>3</sup>, Tamrat Bekele<sup>3</sup> and Bruno Glaser<sup>1</sup>**

<sup>1</sup> Institute of Agronomy and Nutritional Sciences, Soil Biogeochemistry, Martin Luther University Halle–Wittenberg, Von–Seckendorff–Platz 3, D–06120 Halle, Germany

<sup>2</sup> Ethiopian Biodiversity Institute, Forest and Rangeland Biodiversity Directorate, P.O. Box 30726 Addis Ababa, Ethiopia

<sup>3</sup> Department of Plant Biology and Biodiversity Management, Addis Ababa University, P.O. Box 3434 Addis Ababa, Ethiopia

<sup>4</sup> Department of Urban Agriculture, Misrak Polytechnic College, P.O. Box 785, Addis Ababa, Ethiopia,

<sup>5</sup> Institute of Soil Science and Soil Geography, University of Bayreuth, Universitätsstrasse 30, D–95440 Bayreuth, Germany

<sup>6</sup> Institute of Geography, Technical University of Dresden, Helmholtzstrasse 10, D–01062 Dresden, Germany

<sup>7</sup> Institute of Computer Science, Bioinformatics, Martin Luther University Halle–Wittenberg, Von Seckendorff-Platz 1, 06120 Halle (Saale), Germany

\* **Corresponding author: Bruk Lemma ([bruklemma@gmail.com](mailto:bruklemma@gmail.com))**

**Published in**

**Plants 2019, 8(7): 228;**

**<https://doi.org/10.3390/plants8070228>**

**Abstract:**

Despite the fact that the vegetation pattern and history of the Bale Mountains in Ethiopia were reconstructed using pollen, little is known about the former extent of *Erica* species. The main objective of the present study is to identify unambiguous chemical proxies from plant-derived phenolic compounds to characterize *Erica* and other keystone species. Mild alkaline CuO oxidation has been used to extract sixteen phenolic compounds. After removal of undesired impurities, individual phenols were separated by gas chromatography and were detected by mass spectrometry. While conventional phenol ratios such as syringyl vs. vanillyl and cinnamyl vs. vanillyl and hierarchical cluster analysis of phenols failed for unambiguous *Erica* identification, the relative abundance of coumaryl phenols ( $> 0.20$ ) and benzoic acids (0.05–0.12) can be used as a proxy to distinguish *Erica* from other plant species. Moreover, a Random Forest decision tree based on syringyl phenols, benzoic acids ( $> 0.06$ ), coumaryl phenols ( $< 0.21$ ), hydroxybenzoic acids, and vanillyl phenols ( $> 0.3$ ) could be established for unambiguous *Erica* identification. In conclusion, serious caution should be given before interpreting this calibration study in paleovegetation reconstruction in respect of degradation and underground inputs of soil organic matter.

**Keywords:** paleoclimate; pollen; paleovegetation; oxidation; phenols; *Erica*; biomarkers; machine learning

## 1. Introduction

The present vegetation cover in mountain ecosystems is the result of subsequent historical and ecological processes primarily influenced by climate and humans (Heiri et al., 2006; Umer et al., 2007). However, natural versus human impact on ecosystem dynamics at a higher elevation is difficult to quantify and is still speculative (Heiri et al., 2006; Jansen et al., 2010). To reconstruct and draw full pictures of environmental changes over the past centuries, Ethiopia is an ideal place for several reasons. Firstly, it is the origin of *Homo sapiens* and many other fauna and flora. Secondly, it comprises diverse geographical zones attributed to various climatic features (Terwilliger et al., 2008; Tiercelin et al., 2008). The Bale Mountains are one of the Eastern Afromontane Biodiversity Hotspots, which encompass many endemic and endangered species of Ethiopia (Hillman, 1988, 1986). Diverse topographical features of the Bale Mountains are marked by altitudinal vegetation zones. The ecosystem of the Bale Mountains is divided into three main regions and five distinct and unique habitats. The Southern declivity is demarcated by moist Afromontane Haremma forest and a prominent Ericaceous belt whereas, the central plateau is dominated by the Afro-alpine vegetation, and the Northern slopes encompass dry Afromontane forest, as well as Gaysay grassland (Friis, 1986; Hillman, 1986; Mieke and Mieke, 1994). The Afro-alpine regions of the Sanetti Plateau (3800–4377 m a.s.l.) are characterized by tussock grasses (mainly *Festuca* spp.), dwarf shrubs, and herbaceous plants (e.g. *Alchemilla haumannii*, *Helichrysum splendidum* and *Lobelia rhynchopetalum*) (Friis, 1986; Hedberg, 1964; Mieke and Mieke, 1994). The prominent Ericaceous belt dominant above 3300 m a.s.l shows different stages of post-fire succession and remains continuous up to 3800 m a.s.l. However, it becomes patchy on the Sanetti Plateau above 3800 m a.s.l. (Mieke and Mieke, 1994). The characteristic species of the Northern slopes are *Hagenia abyssinica*, *Hypericum revolutum*, *Juniperus procera*, and *Podocarpus falcatus* (Friis, 1986; Hillman, 1986).

In the Bale Mountains, the contemporary distribution of the *Erica* vegetation in specific and of the Afro-alpine biodiversity in general is the legacy of climate change (Umer et al., 2007) or human-induced driving factors like fire and grazing (Mieke and Mieke, 1994) or a combination of both. Hitherto, this globally important ecosystem is still increasingly under threat of climate change and human impacts (Kidane et al., 2012). The vegetation history of the Bale Mountains was investigated and reconstructed using pollen records from lacustrine sediments and peat deposits (Bonnefille, R and Hamilton, 1986; Bonnefille and Mohammed, 1994; Hamilton, 1982; Umer et al., 2007). The findings showed that *Erica* shrubs inhabited different altitudinal

zones during different time periods. During the early Holocene, *Erica* shrubs had extended up to the Sanetti plateau in response to increased moisture and temperature (Umer et al., 2007). *Erica* shrubs and forest had retreated to lower altitude in response to lower rainfall at about 6000 cal years BP and onwards (Umer et al., 2007). Presently, *Erica* forming an Ericaceous belt is located between 3300 to 3800 m. a.s.l. (Miehe and Miehe, 1994).

The biggest deterrent of pollen-based studies depends on pollen preservation and can be biased by the dispersal potential of pollinators (Hicks, 2006; Jansen et al., 2010; Ortu et al., 2006). To overcome such drawbacks, we tested, for the first time, the chemotaxonomic roles of phenol biomarkers in the dominant plant species of the Bale Mountains. Chemical biomarkers are not influenced by a dispersal of parent material and can be extracted from sedimentary archives and soils and reflect more of the standing vegetation (Glaser and Zech, 2005). Therefore, they offer the potential to complement pollen-based vegetation reconstructions and to detect vegetation at a higher temporal and spatial resolution.

Polyphenols are the most widespread class of secondary metabolites, and ubiquitous in their distribution (Ram Singh, 2016). Phenolic compounds are a major component of terrestrial vascular plants (Ertel and Hedges, 1984) and may have lignin and non-lignin-derived biochemical structures. Secondary metabolites, mainly phenolic compounds, are important for cell wall structural formation, defense against pathogen, and environmental stress as well as essential for survival of vascular plants (Míka et al., 2005; Ramakrishna and Ravishankar, 2011). Plant phenolic compounds also exhibited significant qualitative and quantitative variation at different genetic level between and within species and clones (Hakulinen et al., 1995; Nichols-Orians et al., 1993; Witzell et al., 2003). They are extensively used in botanical chemosystematic studies (Míka et al., 2005). The chemotaxonomic values of polyphenolic biomolecules such as tannins has been well recognized in the plant kingdom and the distribution of hydrolysable tannins used as chemotaxonomic markers in the family *Rosaceae* (Määttä-Riihinen et al., 2004; Okuda et al., 1992) and chestnut (family: *Fagaceae*) (Fernandez-Lorenzo et al., 1999). Stilbenoids, family of polyphenols, due to its limited but heterogeneous distribution in the plant kingdom also played a significant taxonomic role in the plant families such as *Vitaceae*, *Gnetaceae*, and *Fabaceae* (Rivière et al., 2012). Notably gossypetin (flavonol) are useful taxonomic marker for distinguishing Ericaceous species/genera (family: *Ericaceae*) (Harborne and Williams, 1973). The absence of leucoanthocyanidins, ellagic acid and phenyl-trihydroxylated characterized the genus *Pittosporum* (*Pittosporaceae*) (Jay, 1969). Even if there is a need to encourage phenols application in chemotaxonomic studies/plant

phylogeny, as more studies have been completed, some inconsistency has been revealed (Giannasi, 1978). For instance the polyphenolic compound differences among the various tribes of *Anacardiaceae* are not very pronounced (Umadevi et al., 1988).

Nevertheless, little has been done to chemotaxonomically characterize *Erica* and other keystone species specifically in the Bale Mountains and generally in other similar geographical regions using phenols as a tool for paleovegetation reconstruction. Apart from the chemotaxonomic significance of phenols, the antioxidant and antibacterial activities of phenolic compounds by Guendouze-Bouchefa et al. (Guendouze-Bouchefa et al., 2015), as well as the role of phenolic compounds as indicators of presence of metals in the leaves of different genera in the family *Ericaceae* by Marquez-Garcia et al. (Márquez-García et al., 2012, 2009) were described previously. The antioxidant strength of *Erica* species depend upon the total abundance of phenolic compounds (Márquez-García et al., 2009). The abundance of phenolic compounds in *Festuca vallesiaca* were also used as indicators of fodder quality. High contents of total phenolic in the grass species are unfavorable for digestion (Djurdjević et al., 2005). Polyphenols obtained from flowers of *Helichrysum* (family: *Asteraceae*) species are used by some folks as ethno-medicine (Albayrak et al., 2010; Babotă et al., 2018; Pljevljakušić et al., 2018; Sroka et al., 2004). The affinity bounds in plant systematic classification using profiles of phenolic compounds were computed and compared, commonly using hierarchical cluster analysis (HCA) and principal component analysis (PCA) (Cruz et al., 2008; Liu et al., 2013; Mika et al., 2005; Pan et al., 2016).

While the overall aim of our research is to understand how humans benefited from and re-shaped the African high altitude ecosystem during Quaternary climate changes, this study mainly focuses on identifying the potential of plant derived phenolic compounds as a proxy for unambiguous identification of *Erica* and other keystone species in the Bale Mountains. More specifically, this research attempts to address the following questions: (i) Do phenol biomarkers allow a chemotaxonomic differentiation of the contemporary dominant plant species of the Bale Mountains? (ii) Which implications have to be drawn from those results for planned paleovegetation reconstructions in the study area, e.g., concerning the reconstruction of the former extent of *Erica* stands?

## **2. Material and Methods**

### **2.1 Study Area**

### 2.1.1 Geomorphological Setting

The Bale Mountains belong to the Bale-Arsi mountain massif located 400 km Southeast of Addis Ababa, Ethiopia (Hillman, 1986). They are situated between 39°03' to 40°00' longitude (E) and between 6°29' to 7°10' latitude (N) (Figure 1-1). Lava mainly outpouring 40 million years ago resulted in the formation of mountains and ridges up to 4377 m a.s.l. (Mohr, 1963). The most extensive high altitude plateau (Sanetti Plateau) in Africa above 3000 m. a.s.l., comprised within the Bale Mountains National Park, extends to about 2,600 km<sup>2</sup> (Hillman, 1988; Kidane et al., 2012; Tiercelin et al., 2008; Umer et al., 2007). The Bale Mountains are topographically divided into three major declivities: The Northern slopes (3000–3800 m. a.s.l.), the central plateau (3800–4377 m a.s.l.), and the Southern Harenna escarpment (1400–3800 m. a.s.l.). The Sanetti Plateau is located in the center, on which the second highest peak of the country Mt. Tulu Dimtu (4377 m a.s.l.) rests. The northern slope of the mountains is dissected by the Togona Valley, which descends towards the extensive Arsi Plateau and further down to the Great Rift Valley lowlands, which divide the country into two parts. The Southern slope includes the steep Harenna escarpment and goes down to the surrounding lowland at about 1400 m a.s.l. (Hillman, 1988; Tiercelin et al., 2008). Repeated glaciations of the high altitudes created typical features of glaciated landscapes with moraines and glacial lake (Osmaston et al., 2005; Umer et al., 2007). Basalt and rhyolite are typical parent rocks (Billi, 2015) of the dominant Cambisols and Leptosol at the Sanetti Plateau (Hedberg, 1964; Miehe and Miehe, 1994; Woldu et al., 1989).

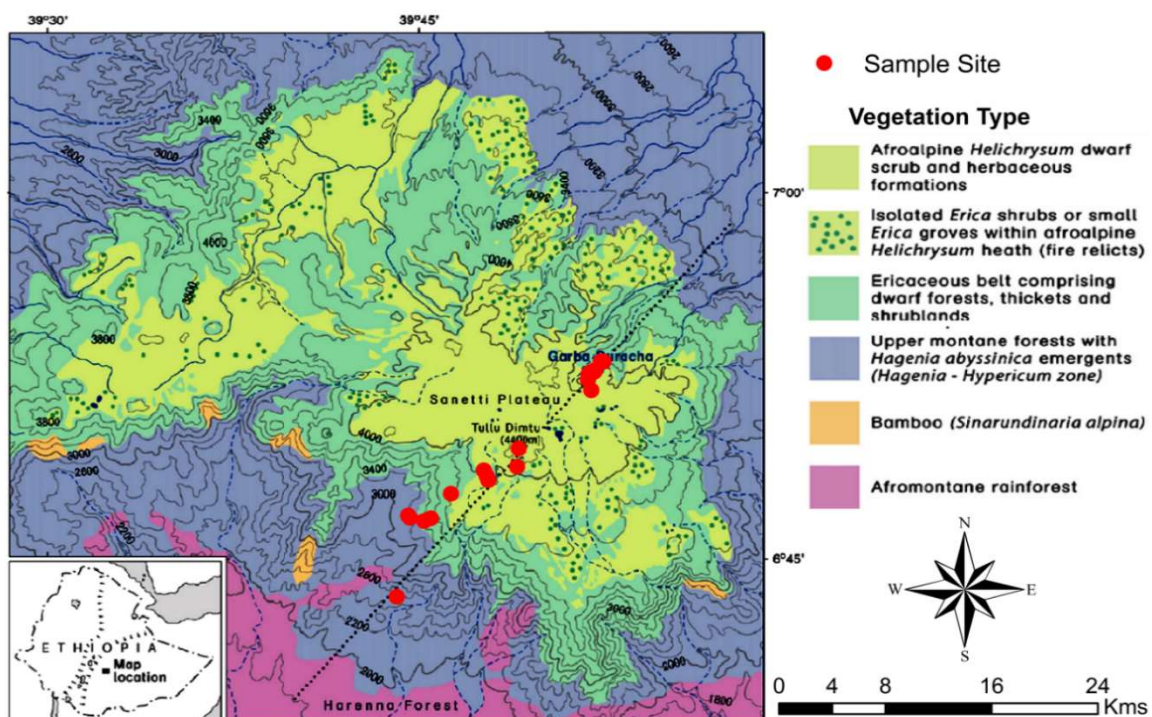


**Fig. 2–1:** Map of the Bale Mountains showing the vegetation zones and study sites along the Northeast and Southwestern transect (modified after Mieke and Mieke, 1994). Leaves of the dominant vegetation within the Ericaceous and Afro-alpine belts were sampled during the dry season in February 2015 and 2017.

### 2.1.2 Climate and Biota

The climatic conditions of the Bale Mountains depend on orography and are vulnerable to extreme climatic conditions over the past years (Umer et al., 2007). The mean annual minimum temperature in the mountainous region ranges between 0.6 to 10 °C with frequent frost during winter season and mean annual maximum temperature ranges between 6–12 °C. The mean annual temperature in Dinsho headquarter (3170 m a.s.l.) is 11.8 °C (Bonafille, 1983; Tiercelin et al., 2008). Precipitation in the Bale Mountains is influenced by the shift of the Inter Tropical Convergence Zone (ITCZ) resulting in long rainy (March–September) and short dry (October–February) seasons (Admasu et al., 2004). The Southern slopes of the Bale Mountains receive high annual rainfall (1000–1500 mm year<sup>-1</sup>) as compared to the Northern declivity (800–1000 mm year<sup>-1</sup>) (Bonafille, 1983; Tiercelin et al., 2008; Woldu et al., 1989). Moisture reaching the Bale Mountains originates from the Red Sea, the Mediterranean Sea, the Indian Ocean, and the Atlantic Ocean (Kebede and Travi, 2012; Mieke and Mieke, 1994; Segele et al., 2009).

The Bale Mountains National Park and its surrounding are home for more than 1300 vascular flowering plant species and 50 mammal species (Dullo et al., 2015; Hillman, 1988). The composition of enormous endemic and endangered fauna and flora labeled the Bale Mountains as one of the biodiversity hotspot areas of the world. The distribution and abundance of the contemporary vegetation in the Bale Mountains are shaped partly by human intervention and often emphasizes the landforms and paleoclimate (Osmaston et al., 2005). Diverse topographical variability in the Bale Mountains shows altitudinal zonation of vegetation. In broad terms, floristically the mountains are divided into three topographical regions. The southern declivity is delineated by moist Afromontane forest, Ericaceous belt and Afro-alpine vegetation, whereas the central plateau is dominated by the Afro-alpine vegetation and the northern slope encompasses dry Afromontane forest, Gaysay grassland, Ericaceous belt, and Afro-alpine zones (Friis, 1986; Hillman, 1986; Mieke and Mieke, 1994). The Afro-alpine regions of the Sanetti Plateau (3800–4377 m a.s.l.) are characterized by tussock grassland and dwarf shrubs and herbaceous (e.g., *Alchemilla haumannii*, *Helichrysum splendidum*, and *Lobelia rhynchopetalum*) plants. The Ericaceous belt (3300–3800 m a.s.l.) comprises forest, thickets, and scrublands of *Erica trimera* and *Erica arborea* with mosses and grasses

dominating in the ground layer. The Haremma forest (1500–3300 m a.s.l.) is a natural remnant of a moist Afromontane forest dominated by broadleaved evergreen trees and clustered floristically into two different classes. Around 1500–2300 m a.s.l., the forest is dominated by *Podocarpus falcatus* associated with *Croton macrostachyus*, *Pouteria adolfi-friederici*, *Syzygium guineense*, *Warburgia ugandensis*, and worth noting *Coffea arabica*. Between 2300–3200 m a.s.l. *Arundinaria alpina*, *Hagenia abyssinica*, *Hypericum revolutum*, *Erythrina brucei*, *Prunus africana*, and *Schefflera volkensii* are the dominant plants (Friis, 1986; Hillman, 1988; Miehe and Miehe, 1994; Umer et al., 2007; Woldu et al., 1989). Furthermore, the Bale Mountains are center for faunal diversity and holds the highest rate of animal endemism for a terrestrial habitat anywhere in the world (Hillman, 1988). The mountains are known by its flagship mammals like Mountain Nyala (*Tragelaphus buxtoni*), Ethiopian Wolf (*Canis simensis*) and Giant mole rat (*Tachyoryctes macrocephalus*). Also about 180 bird species and 14 amphibian species are inhabiting the Bale Mountains (Hillman, 1988, 1986).

## 2.2 Sample Collection

25 and 22 (total of 47) samples (leaves and twig) of locally dominant plant species were collected in February 2015 and 2017, respectively along a SW and a NE transect (ranging from 2550 to 4377 m a.s.l. and 3870 to 4134 m a.s.l., respectively) (Fig. 2–1). Samples comprise *Erica trimera* and *Erica arborea* ( $n = 29$ ), *Alchemilla haumannii* Rothm. ( $n = 5$ ), *Festuca abyssinica* Hochst. ex A. Rich. ( $n = 7$ ), *Helichrysum splendidum* (Thunb.) Less. ( $n = 4$ ), *Kniphofia foliosa* Hochst. ( $n = 1$ ) and *Lobelia rhynchopetalum* Hemsl. ( $n = 1$ ). All samples were air-dried in the Soil Store Laboratory of the National Herbarium, Department of Plant Biology and Biodiversity Management, Addis Ababa University. Samples were finely ground, homogenized, and subjected to further biogeochemical analysis at the laboratories of the Soil Biogeochemistry, Martin Luther University of Halle–Wittenberg.

## 2.3 Analysis of Phenolic Compounds Released after Alkaline CuO Oxidation

Phenolic compounds were extracted from 35 mg of dried plant leaf and twig samples using the mild alkaline cupric oxide (CuO) oxidation method developed by Hedges and Ertel (1982) as later modified by Goñi and Hedges (1992). Briefly, the samples were transferred into Teflon digestion tubes together with 100 mg of  $(\text{NH}_4)_2\text{Fe}(\text{SO}_4)_2 \cdot 6\text{H}_2\text{O}$ , 500 mg of CuO, 50 mg of  $\text{C}_6\text{H}_{12}\text{O}_6$ , 1 mL of ethylvanillin solution ( $100 \text{ mg L}^{-1}$ ) as internal standard 1 and 15 mL of 2M NaOH and digested at 170 °C for two hours under elevated pressure. Reaction products were cooled overnight and transferred into centrifuge tubes. Then the phenolic compounds were



purified by adsorption on C18 columns and desorbed by ethylacetate and concentrated under a stream of nitrogen gas for 30 min. Residue was dissolved in 1 mL phenylacetic acid (PAA), as internal standard 2 to determine the recovery of ethylvanillin before derivatization (Amelung et al., 2002; Möller et al., 2002). Finally, the samples were derivatized using 200  $\mu$ L of BSTFA and 100  $\mu$ L of pyridine. Oxidation products of phenolic compounds were quantified using a Gas Chromatography coupled to a Mass Spectrometry (SHIMADZU, GC-MS-QP2010, Kyoto, Japan).

## 2.4 Data Analysis

After recovery correction, the content of each of sixteen phenolic compounds (in  $\text{g kg}^{-1}$  TOC) was calculated and groups of phenolic derivative of mild alkaline CuO oxidation products were calculated according to Equations (1) – (6).

$$p\text{-hydroxy} = 4\text{-Hydroxybenzaldehyde} + 4\text{-Hydroxyacetophenone} + 4\text{-Hydroxybenzoic acid} \quad (1)$$

$$\text{Vanillyl (V)} = \text{vanillin} + 4\text{-hydroxy-3-methoxyacetophenone} + \text{vanillic acid} \quad (2)$$

$$\text{Syringyl (S)} = \text{syringaldehyde} + 3,5\text{-dimethoxy-4-hydroxyacetophenone} + \text{syringic acid} \quad (3)$$

$$\text{Coumaryl (C)} = p\text{-coumaric acid} + \text{ferulic acid} \quad (4)$$

$$\text{Benzoic acids} = \text{benzoic acid} + \text{salicylic acid} + \text{phthalic acid} \quad (5)$$

$$\text{Hydroxy-Benzoic-Acids} = 3\text{-hydroxybenzoic acid} + 4\text{-hydroxybenzoic acid} + 3,5\text{-dihydroxybenzoic acid} \quad (6)$$

### 2.4.1 Hierarchical Clustering and PCA

Calibrated and normalized data sets of the analytical results were subjected to Principal Component Analysis (PCA, Fig. S2) and hierarchical clustering (AHC) using Euclidean measurement of distances and Ward method for linkage calculation to examine taxonomic differences based on phenolic compounds. Z-score normalization method,  $Z = (X - \text{mean}(X)) / \text{sd}(X)$ , were used to standardize data. Furthermore, descriptive statistics (notched box plot and scatter plot) were performed to identify an unambiguous biomarker using R free software version 3.6.0.

## 2.4.2 Machine Learning

We examined three different machine learning algorithms (Random forest, Support Vector Machines, and Recursive Partitioning) regarding their accuracy (Fig. S1A) and F1 score (Fig. S1B) based on different proportions of training and prediction dataset with five replications. Due to the reliable performance of Random forest classification of *Erica* vs. non-*Erica* species, we looked for the most important features in a 2/3 to 1/3 training against prediction setting. To verify the reliability of the used model, cross-validation has been performed (Fig. S3).

## 3. Results and Discussion

### 3.1 Distribution and Diversity of Phenols

A typical gas chromatogram of phenolic compounds released after mild alkaline CuO oxidation illustrates the compositional complexity of a typical plant sample (*Lobelia rhynchopetalum*; Fig. 2–2). The mean weighted sum of phenols content of *Alchemilla haumannii*, *Erica* spp., *Helichrysum splendidum*, *Kniphofia foliosa*, *Lobelia rhynchopetalum*, and *Festuca abyssinica* were 18, 16, 22, 6, 22, and 51 g kg<sup>-1</sup> TOC, respectively (Table S1).

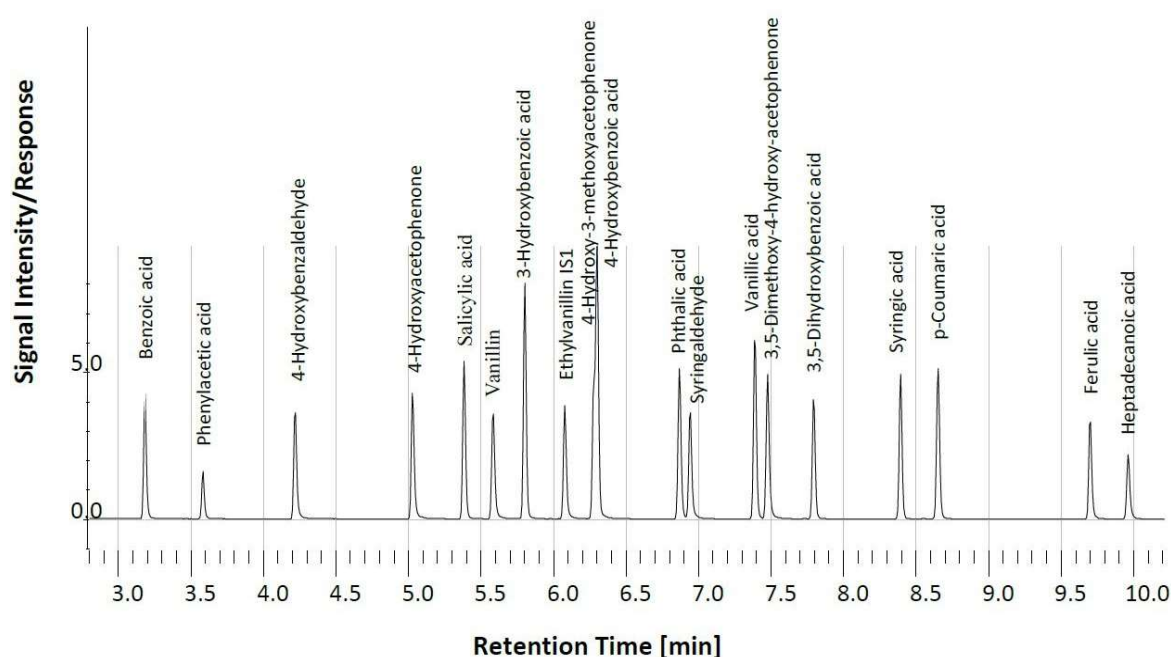


**Fig. 2–2:** Typical gas chromatogram of phenolic compounds released after alkaline CuO oxidation of *Lobelia rhynchopetalum*.

*Festuca abyssinica* (*Poaceae*) is characterized by high abundance of coumaryl phenols (*p*-coumaric acid, ferulic acid) and syringyl phenols (syringic acid, 3,5-Dimethoxy-4-hydroxyacetophenone; Fig. 2–3) and low abundance of vanillyl phenols and benzoic acids

(Table 1-1). Similarly, the phenolic compounds from *Festuca vallesiaca* species investigated in Serbia accounts for low benzoic acid derivatives and high coumaryl phenols (*p*-coumaric acid, ferulic acid). The total phenolics extracted from *Festuca vallesiaca* using Soxhlet extraction and later quantified by HPLC is 26.1 mg g<sup>-1</sup> (Djurdjević et al., 2005). In the grass taxon, most of phenol-related information was provided by coumaryl phenols (*p*-coumaric acid, ferulic acid) due to ample presence of the enzyme phenyl (thyrosine) ammonia-lyase and it is known for its high biological activity (Chesson et al., 1982; Djurdjević et al., 2005; Míka et al., 2005). The abundance of coumaryl phenols in our *Poaceae* samples holds one third of the total phenols. Likewise, Hedges and Mann (1979) stated that non woody vascular angiosperm plants have characteristic products of coumaryl phenols and it accounts for approximately one third of the total phenolic compounds. *Lobelia rhynchopetalum* and *Kniphofia foliosa* have high abundance of benzoic acid and 4-hydroxy-3-methoxyacetophenone (Table 1-1). The total phenolic contents of *Lobelia chinensis* measured by the Folin-Ciocalteu methods is 4.7 mg GAE g<sup>-1</sup> (Li et al., 2008).

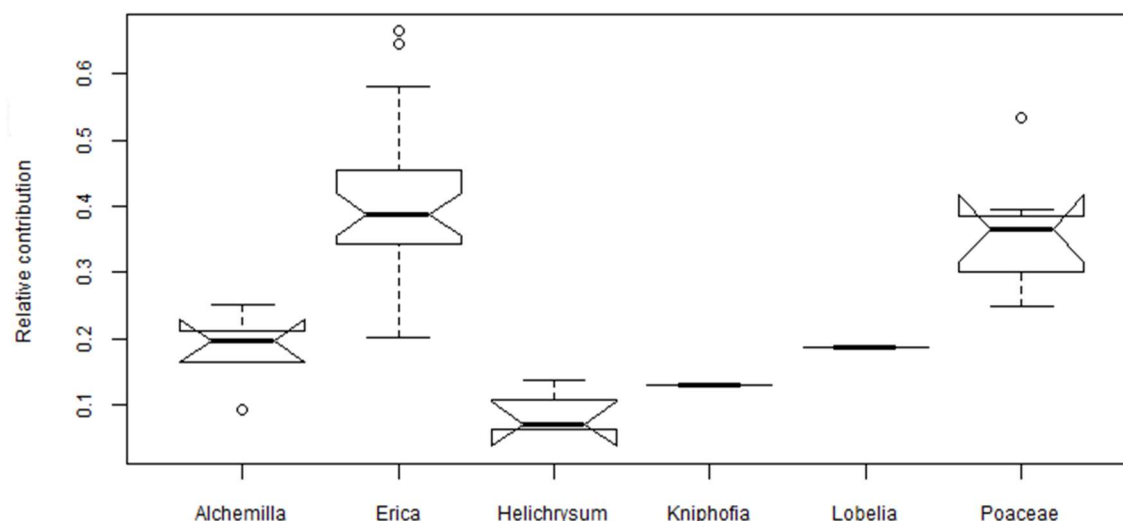


**Fig. 2–3:** Notched box plots illustrating the abundance of coumaryl phenols in the dominant plant species of the Bale Mountains. The box plots indicate the median (solid line between the boxes), interquartile range (IQR) with upper (75%) and lower (25%) quartiles and possible outlier (empty circles). The notches display the confidence interval around the median within  $\pm 1.57 \cdot \text{IQR} / \sqrt{n}$ .

The sum of *p*-hydroxy phenols in the leaves unambiguously identifies *Helichrysum splendidum* from the other dominant plant species of the Bale Mountains (Fig. 2–4). Qualitative analysis by thin layer chromatography (TLC) of the inflorescence of *Helichrysum* showed the presence of phenolic acids such as syringic, coumaric, and *p*-hydroxybenzoic (Sroka et al., 2004). The total

phenolic contents extracted from different species of *Helichrysum* in Eastern Anatolia, Turkey ranges between 72 to 146 mg GAE g<sup>-1</sup> (Albayrak et al., 2010). On the other hand, *Erica* species were characterized by high coumaryl (Fig. 1–3) and low *p*-hydroxy phenols (Fig. 2–4). The genus *Erica* (family: *Ericaceae*) is characterized by having polyphenols (*p*-coumaric acid derivate, vanillic acid, cinnamic acid derivate, and caffeic acid) and flavonoids (Guendouze-Bouchefa et al., 2015). The total phenolic compounds determined via Folin-Ciocalteu method and analysis by HPLC for *Erica arborea* and *Erica multiflora* are 71 and 68 mg GAE g<sup>-1</sup>, respectively (Guendouze-Bouchefa et al., 2015). In the genus *Erica* among the flavonoids, dihydromyricetin 3-O- $\alpha$ -L-rhamnopyranoside is the most important chemotaxonomic marker (Nazemiyeh et al., 2008). Each of the dominant plant species on the Bale Mountains is profiled by a different abundance of phenolic compounds (Table 1-1).

**Table 1-1:** Summary of the relative abundance of individual phenols profiled in each dominant plant species. Key: ↑ (higher) and ↓ (lower).

Relative Contribution	<i>Alchemilla</i>	<i>Erica</i>	<i>Helichrysum</i>	<i>Kniphofia</i>	<i>Lobelia</i>	<i>Poaceae</i>
Vanillyl phenols					↑	↓
Vanillin						
Vanillic_acid						
4_hydroxy_3_methoxyacetophenone						
Syringyl phenols	↑				↓	↑
Syringaldehyde						
Syringic_acid						
3_5_dimethoxy_4_acetophenone						
Coumaryl phenols		↑	↓			↑
p_coumaric_acid						
Ferulic_acid						
p_hydroxy_phenols		↓	↑			
4_hydroxybenzaldehyde						
4_hydroxybenzacetophenone						
Benzoic_acids				↑	↑	↓
Benzoic_acid						
Salicylic_acid						
Phthalic_acid						
Hydroxy_benzoic_acids	↑		↓			↑
3_hydroxybenzoic_acid						
4_hydroxybenzoic_acid						
3_5_Dihydroxy_benzoic_acid						

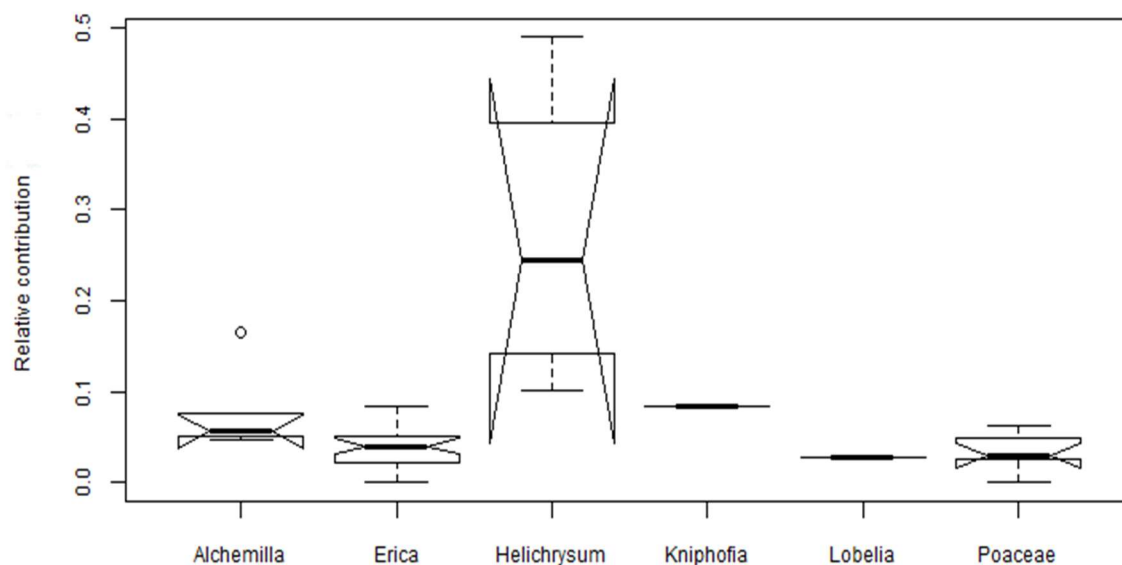


**Fig. 2–4:** Notched box plots show the relative abundance of *p*-hydroxy phenols in the dominant plant species of the Bale Mountains. The box plots indicate the median (solid line between the boxes), interquartile range (IQR) with upper (75%) and lower (25%) quartiles and possible outlier (empty circles). The notches display the confidence interval around the median within  $\pm 1.57 \cdot \text{IQR} / \sqrt{n}$ .

Even though *Kniphofia foliosa* has lower phenolic content, the quantitative values of Shannon-Wiener phenol diversity index ( $H = -\sum (p_i) [\ln(p_i)]$ ) indicated that *Kniphofia foliosa* has evenly distributed phenolic compounds. By contrast, *Helichrysum splendidum* has less evenly distributed phenolic compounds (Table 1-2). Innovative techniques and widespread occurrence of secondary metabolites like phenolic profiles in the plant diversity allow low taxonomic level chemosystematic studies (Mika et al., 2005; Ram Singh, 2016).

**Table 1-2:** Phenol Diversity Index.

Species	Diversity Index (H)
<i>Alchemilla haumannii</i>	2.28
<i>Erica</i> spp.	2.19
<i>Helichrysum splendidum</i>	1.63
<i>Kniphofia foliosa</i>	2.47
<i>Lobelia rhynchopetalum</i>	2.09
<i>Festuca abyssinica</i>	2.17

### 3.2 Cluster Analysis of Phenolic Compounds

The cluster analysis computed for 47 plant samples grouped the dominant plant species into six groups, as shown in Fig. 2–5. In the cluster, *Poaceae* and *Lobelia* species are grouped independently (there are two independent *Poaceae* groups), while the other dominant species *Erica*, *Kniphofia*, *Helichrysum*, and *Alchemilla* were clustered together into two different groups (Fig. 2–5). Therefore, no unambiguous identification of *Erica* is possible, but identify the former extent of the distribution of *Poaceae* in the Bale Mountains using alkaline CuO phenol products might be feasible (Fig. 2–5). Previously, some studies used phenolic compounds to systematically characterize grasses even at lower taxonomic level (Ram Singh, 20168). However, phenols are environmentally labile secondary metabolites. As a result, caution should be given before extraction and standardizing the growing condition and growth stage of the sample materials (Mika et al., 2005; Ramakrishna and Ravishankar, 2011; Stanković et al., 2017). Thus far, our cluster analysis did not justify which phenol type is the most determining characteristic for the identification of the dominant plant species, one from the other. The only obvious independent group is the *Lobelia*, and *Poaceae* is also somewhat distinct. Therefore, the ambiguity is less clear for all the rest.

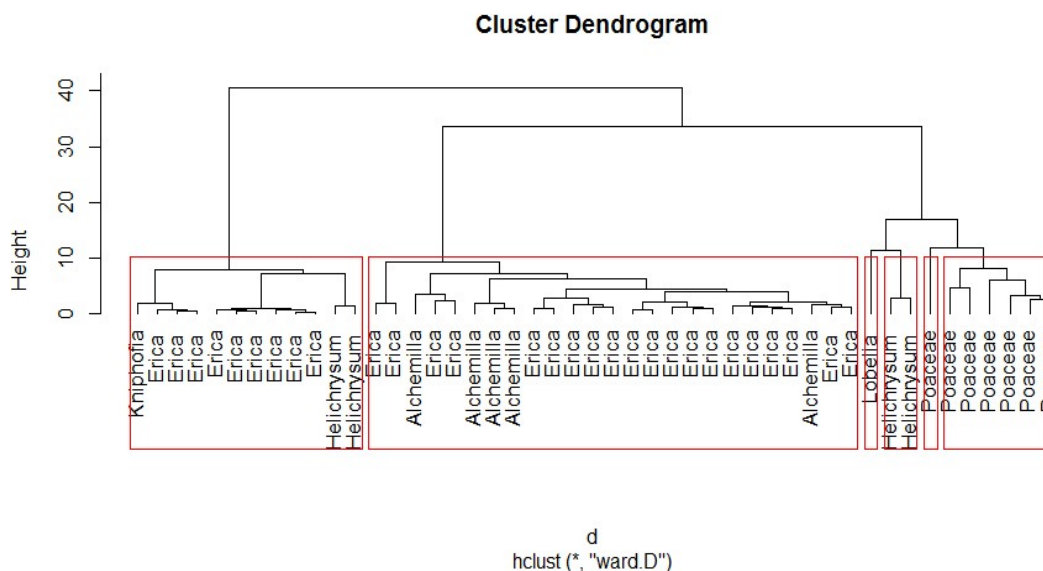


**Fig. 2–5:** Agglomerated Hierarchical Cluster analysis of the dominant plant species of the Bale Mountains based on the abundance of phenolic compounds ( $\text{g kg}^{-1}$  TOC). Euclidean measurement of distances and Ward method for linkage calculation applied to cluster a normalized dataset ( $Z$ -score normalization,  $Z = (X - \text{mean}(X)) / \text{sd}(X)$ ).

### 3.3 Biomarker Identification

The ratios of syringyl over vanillyl (S/V) and cinnamyl over vanillyl (C/V) phenols, which were used previously as a source proxy did not turn out to be useful in the present study to categorize the dominant plant species (Fig. 2–6). The ratios of S/V and C/V allowed us to distinguish organic matter sources in soil and sediments (Hedges and Mann, 1979). However, these ratios cannot provide profound results of plants belonging to the same taxon (Thevenot et al., 2010). The limitation of S/V and C/V ratios to pinpoint the source of organic matter in soils and sediments of the same taxon were described in detail by Thevenot et al. (2010). Here, we also proved that the ratios of S/V and C/V were unable to characterize modern plants of the same taxon at least in our study area (Fig. 2–6). The drawback of those ratios could be associated with the overlap between plant molecular signatures (Dümig et al., 2009; Thevenot et al., 2010). The sampled woody vegetation (e.g. *Erica*, *Helichrysum*) in the present study exhibited C/V ratios higher than zero. However, Hedges and Mann (1979) stated that woody gymnosperm and angiosperm plants are characterized by C/V ratio nearly equal to zero.

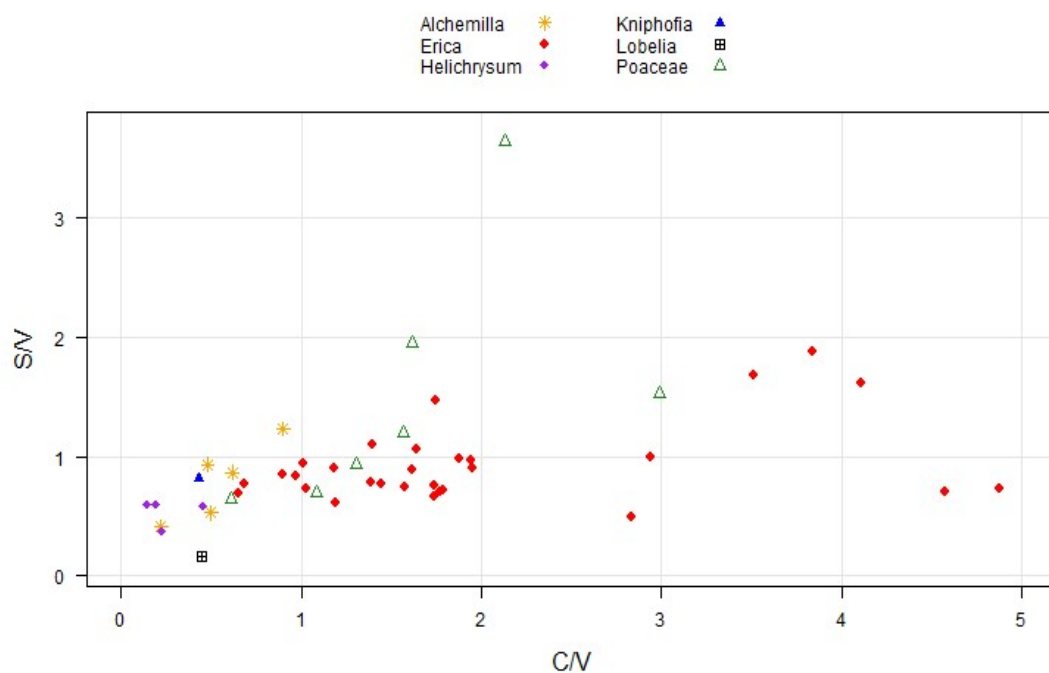


**Fig. 2–6:** Two-dimensional plot illustrating the ratios of syringyl vs. vanillyl (S/V) and coumaryl vs. vanillyl (C/V) phenols of the dominant plant species under study.

We here evaluated the phenolic compounds via the classical approach such as hierarchical clustering, 2D plots analysis using source proxies (S/V and C/V) to chemotaxonomically characterize locally dominant plant species in the Bale Mountains. Both approaches failed to

explicitly characterize the dominant plant species. However, we found that *Erica* vegetation in the Bale Mountains can be identified using the relative contribution of coumaryl phenols ( $> 0.2$ ) and benzoic acids (0.05–0.12; Fig. 2–7).

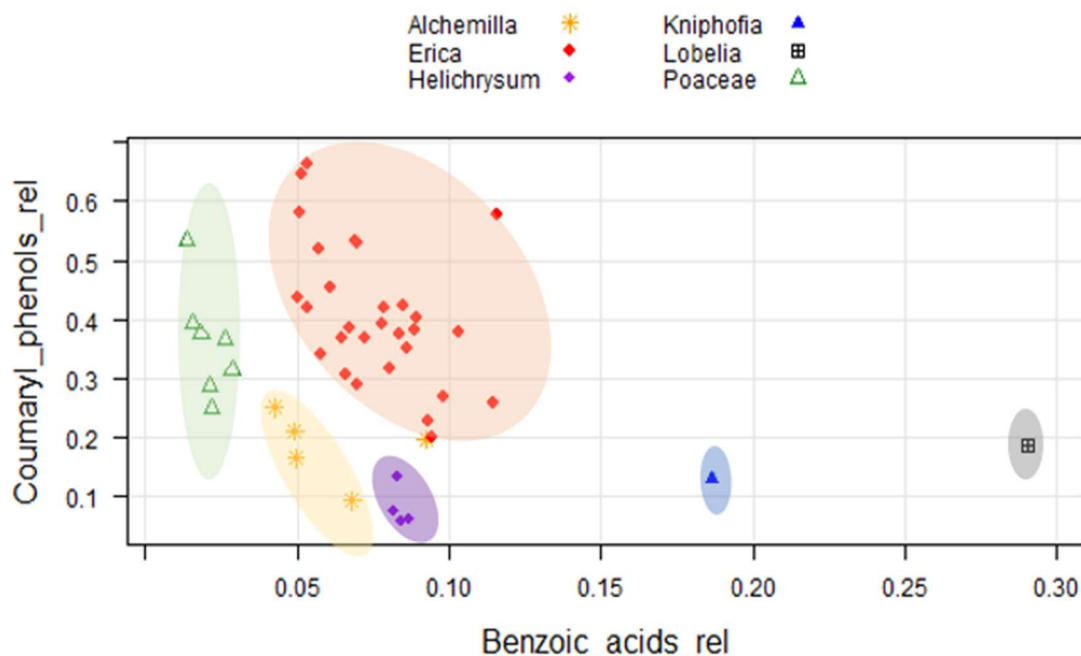


**Fig. 2–7:** Two-dimensional plot of the relative contribution of the sum of coumaryl phenols (*p*-coumaric acid + ferulic acid) and benzoic acids (benzoic acid + salicylic acid + phthalic acid) in the dominant plant species under study.

The three different machine-learning algorithms namely Support Vector Machine, Random Forest, and Recursive Partitioning were tested to unambiguously identify *Erica* vegetation based on our phenolic compounds dataset. Among the tested machine learning approaches, Random Forest performed best. The proposed algorithm has been shown to be better in terms of various performance indicators like accuracy (Fig. S1A) and F1-score (Fig. S1B). In the experiment using relative phenols dataset, the key variable for chemotaxonomic classification of the contemporary species in the Bale Mountains are given in Fig. 2–8. Among them, benzoic acids ( $< 0.06$ ) and coumaryl phenols (0.21) were the most decisive variables to identify *Erica* from the other species (Figs. 1–7 and 1–8). The cross-validation of the used model is shown in Fig. S3.



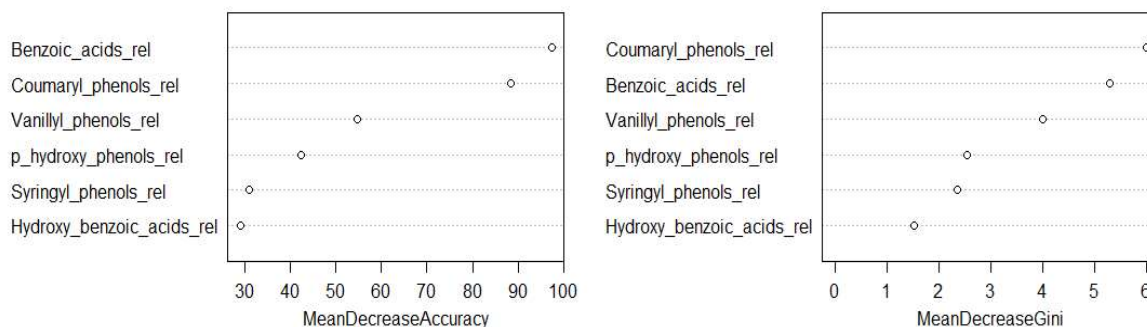


**Fig. 2–8:** Set of relative phenols variables used for chemotaxonomy ordered by their importance as estimated by the Random Forest model. 32 training sample sets and 10,000 number of trees were used to compute the model.

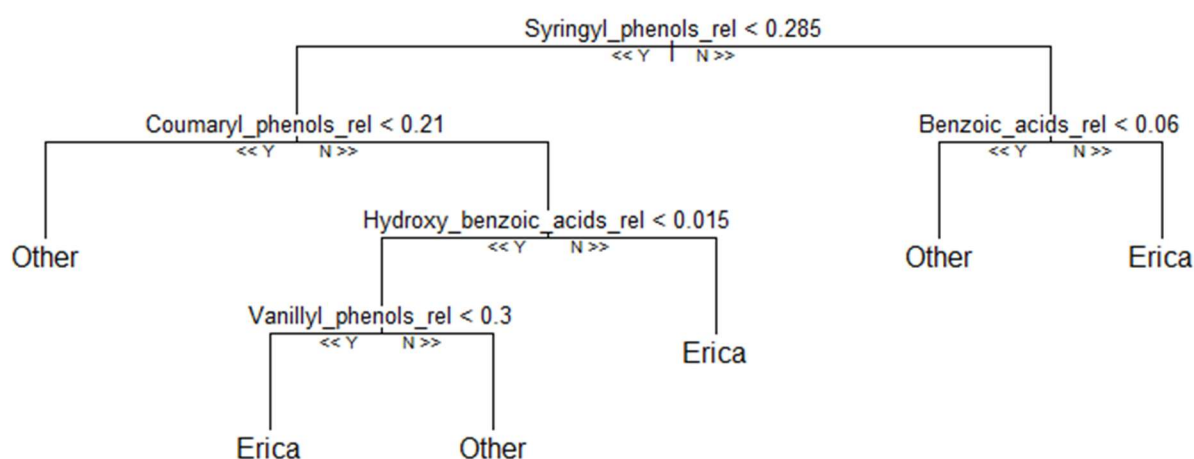


**Fig. 2–9:** Representative decision tree of Random Forest (RF) model using relative phenols contribution. 32 training sample sets and 10,000 number of trees were used to compute the model.

#### 4. Conclusions

Unambiguous identification of chemical proxies using mild alkaline CuO oxidation products of phenols were not simple to apply on plants of the same taxon growing along the SW and NE exposed transects in the Bale Mountains. Nonetheless, leaves and twigs of the woody *Erica* shrubs can be distinguished from leaves of the present day dominant herbaceous *Poaceae* and other lower plants by the relative abundance of coumaryl phenols and benzoic acids. However, as it is known that coumaryl phenols are preferentially degraded in soils, these proxies are not suitable for the evaluation of sites covered in former times by *Erica* (reconstruction of paleovegetation in soils and sediments). To avoid such ambiguities in future studies,

identification of other suitable proxies such as tannin-derived phenols and terpenoids are recommended.

**Supplementary Materials:** The following are available online at <http://www.mdpi.com/2223-7747/8/7/228/s1>, Figure S1: Comparison of Accuracy (A) and F1 Score (B) of Support Vector Machine (SVM, blue), Random Forest (RF, red) and Recursive Partitioning (RP, grey) algorithm based on the level of relative phenols, in relation to the ratio of tested/total number of samples ( $n = 47$ ) that has been split into test and training datasets, each model has been computed 5 times, the bars indicate the standard derivation between the prediction results of the models; Figure S2: Principal Component Analysis, PCA based on the relative phenol abundance in 47 leaf and twig samples from the Bale Mountains, shown are the first two principal components (PC1 and PC2). Dark red arrows indicate the direction of each vector of feature; Figure S3: Cross-validation of the model used; Table S1: Sum of weighted mean of phenolic compounds of each dominant plant species.

**Authors Contributions:** Conceptualization: B.G., W.Z., M.Z.; sample collection: B.M., W.Z., B.L.; Biochemical analysis: B.L.; Data analysis, B.G., C.G., M.Z., B.L.; writing—original draft preparation, B.L., B.G.; writing—review and editing, S.N., T.B., C.G., M.Z., B.M., W.Z.

**Funding:** This research work was funded by the German Research Foundation within the DFG Research Unit ‘The Mountain Exile Hypothesis’ (DFG GL327/18–1, ZE844/10–1). Bruk Lemma expresses his gratitude to the Catholic Academic Exchange Services (KAAD, Germany) for a Ph.D. fellowship. We acknowledge the financial support within the funding programme Open Access Publishing by the German Research Foundation (DFG).

## Acknowledgments

The authors are grateful for the scientific and technical support obtained from Addis Ababa University, Ethiopian Biodiversity Institute and Ethiopian Wildlife Conservation Authority. Bruk Lemma is extended his gratitude to Ms. Heike Maennicke for kind assistance during laboratory work. We appreciate the comments from the anonymous reviewers to improve this manuscript.

**Conflicts of Interest:** The authors declare no conflict of interest. And, the funder had no role in the design of the study; in the collection, analyses, or interpretation of data; in the writing of the manuscript, or in the decision to publish the results.

## References

- Admasu, E., Thirgood, S.J., Bekele, A., Karen Laurenson, M., 2004. Spatial ecology of golden jackal in farmland in the Ethiopian Highlands. *African Journal of Ecology* 42, 144–152.
- Albayrak, S., Aksoy, A., SAĞDIÇ, O., BUDAK, Ü., 2010. Phenolic compounds and antioxidant and antimicrobial properties of *Helichrysum* species collected from eastern Anatolia, Turkey. *Turkish Journal of Biology* 34, 463–473.
- Amelung, W., Martius, C., Bandeira, A.G., Garcia, M.V.B., Zech, W., 2002. Lignin characteristics and density fractions of termite nests in an Amazonian rain forest - Indicators of termite feeding guilds? *Soil Biology and Biochemistry* 34, 367–372.
- Babotă, M., Mocan, A., Vlase, L., Crişan, O., Ielciu, I., Gheldiu, A.-M., Vodnar, D., Crişan, G., Păltinean, R., 2018. Phytochemical analysis, antioxidant and antimicrobial activities of *Helichrysum arenarium* (L.) Moench. and *Antennaria dioica* (L.) Gaertn. flowers. *Molecules* 23, 409.
- Billi, P., 2015. Geomorphological landscapes of Ethiopia. In *Landscapes and Landforms of Ethiopia*; Springer: Dordrecht, The Netherlands, pp. 3–32.
- Bonnefille, R., 1983. Evidence for a cooler and drier climate in the Ethiopian uplands towards 2.5 Myr ago. *Nature* 303, 487–491.
- Bonnefille, R and Hamilton, A., 1986. Quaternary and Late Tertiary history of Ethiopian vegetation. *Symb. Bot. Ups.* 26, 48–63.
- Bonnefille, R., Mohammed, U., 1994. Pollen-inferred climatic fluctuations in Ethiopia during the last 3000 years. *Palaeogeography, Palaeoclimatology, Palaeoecology* 109, 331–343.
- Chesson, A., Stewart, C.S., Wallace, R.J., 1982. Influence of Plant Phenolic Acids on Growth and Cellulolytic Activity of Rumen Bacteria 44, 597–603.
- Cruz, A.V.M., Ferreira, M.J., Scotti, M.T., Kaplan, M.A., Emerenciano, V.P., 2008. Chemotaxonomic relationships in Celastraceae inferred from principal component analysis (PCA) and partial least squares (PLS). *Natural Product Communications* 3, 911–917.
- Djurdjević, L., Mitrović, M., Pavlović, P., Perišić, S., 2005. Total phenolics and phenolic acids content in low (*Chrysopogon gryllus*) and mediocre quality (*Festuca vallesiaca*) forage grasses of Deliblato Sands meadow-pasture communities in Serbia 2005, 54–59.
- Dullo, B.W., Grootjans, A.P., Roelofs, J.G.M., Senbeta, A.F., Fritz, C., 2015. Fen mires with cushion plants in Bale Mountains, Ethiopia. *Mires and Peat* 15, 1–10.
- Dümig, A., Knicker, H., Schad, P., Rumpel, C., Dignac, M.F., Kögel-Knabner, I., 2009. Changes in soil organic matter composition are associated with forest encroachment

- into grassland with long-term fire history. *European Journal of Soil Science* 60, 578–589.
- Ertel, J.R., Hedges, J.I., 1984. The lignin component of humic substances: Distribution among soil and sedimentary humic, fulvic, and base-insoluble fractions. *Geochimica et Cosmochimica Acta* 48, 2065–2074.
- Fernandez-Lorenzo, J.L., Rigueiro, A., Ballester, A., 1999. Polyphenols as potential markers to differentiate juvenile and mature chestnut shoot cultures. *Tree Physiology* 19, 461–466.
- Friis, I., 1986. Zonation of Forest Vegetation on the South Slope of Bale Mountains, South Ethiopia. *SINET- An Ethiopian Journal of Science* 9, 29–44.
- Giannasi, D.E., 1978. Systematic aspects of flavonoid biosynthesis and evolution. *The Botanical Review* 44, 399–429.
- Glaser, B., Zech, W., 2005. Reconstruction of climate and landscape changes in a high mountain lake catchment in the Gorkha Himal, Nepal during the Late Glacial and Holocene as deduced from radiocarbon and compound-specific stable isotope analysis of terrestrial, aquatic and microbi. *Organic Geochemistry* 36, 1086–1098.
- Goñi, M.A., Hedges, J.I., 1992. Lignin dimers: Structures, distribution, and potential geochemical applications. *Geochimica et Cosmochimica Acta* 56, 4025–4043.
- Guendouze-Bouchefa, N., Madani, K., Chibane, M., Boulekbache-Makhlouf, L., Hauchard, D., Kiendrebeogo, M., Stévigny, C., Okusa, P.N., Duez, P., 2015. Phenolic compounds, antioxidant and antibacterial activities of three Ericaceae from Algeria. *Industrial Crops and Products*. 70, 459–466.
- Hakulinen, J., Julkunen-Tiitto, R., Tahvanainen, J., 1995. Does nitrogen fertilization have an impact on the trade-off between willow growth and defensive secondary metabolism? *Trees* 9, 235–240.
- Hamilton, A.C., 1982. *Environmental History of East Africa: A Study of the Quaternary*; Academic Press: London, UK p. 328.
- Harborne, J.B., Williams, C.A., 1973. A chemotaxonomic survey of flavonoids and simple phenols in leaves of the Ericaceae. *Botanical journal of the Linnean Society* 66, 37–54.
- Hedberg, O., 1964. Features of afroalpine plant ecology. Uppsala: Svenska växtgeografiska Sällskapet. *Acta Phytogeographica Suecica*; 49.
- Hedges, J.I., Ertel, J.R., 1982. Characterization of Lignin. *Analytical Chemistry* 54, 174–178.
- Hedges, J.I., Mann, D.C., 1979. The characterization of plant tissues by their lignin oxidation products. *Geochimica et Cosmochimica Acta* 43, 1803–1807.

- Heiri, C., Bugmann, H., Tinner, W., Heiri, O., Lischke, H., 2006. A model-based reconstruction of Holocene treeline dynamics in the Central Swiss Alps. *Journal of Ecology* 94, 206–216.
- Hicks, S., 2006. When no pollen does not mean no trees. *Vegetation History and Archaeobotany* 15, 253–261.
- Hillman, J., 1988. The Bale Mountains National Park area, Southeast Ethiopia, and its management. *Mountain Research and Development* 8, 253–258.
- Hillman, J.C., 1986. Conservation in Bale Mountains National Park, Ethiopia. *Oryx* 20, 89–94.
- Jansen, B., van Loon, E.E., Hooghiemstra, H., Verstraten, J.M., 2010. Improved reconstruction of palaeo-environments through unravelling of preserved vegetation biomarker patterns. *Palaeogeography, Palaeoclimatology, Palaeoecology* 285, 119–130.
- Jay, M., 1969. Chemotaxonomic researches on vascular plants. XIX. Flavonoid distribution in the Pittosporaceae. *Botanical Journal of the Linnean Society* 62, 423–429.
- Kebede, S., Travi, Y., 2012. Origin of the  $\delta^{18}\text{O}$  and  $\delta^2\text{H}$  composition of meteoric waters in Ethiopia. *Quaternary International* 257, 4–12.
- Kidane, Y., Stahlmann, R., Beierkuhnlein, C., 2012. Vegetation dynamics, and land use and land cover change in the Bale Mountains, Ethiopia. *Environmental Monitoring and Assessment* 184, 7473–7489.
- Li, H.-B., Wong, C.-C., Cheng, K.-W., Chen, F., 2008. Antioxidant properties in vitro and total phenolic contents in methanol extracts from medicinal plants. *LWT-Food Science and Technology* 41, 385–390.
- Liu, Z., Liu, Y., Liu, C., Song, Z., Li, Q., Zha, Q., Lu, C., Wang, C., Ning, Z., Zhang, Y., 2013. The chemotaxonomic classification of *Rhodiola* plants and its correlation with morphological characteristics and genetic taxonomy. *Chemistry central journal* 7, 118.
- Määttä-Riihinen, K.R., Kamal-Eldin, A., Törrönen, A.R., 2004. Identification and quantification of phenolic compounds in berries of *Fragaria* and *Rubus* species (family Rosaceae). *Journal of Agricultural and Food Chemistry* 52, 6178–6187.
- Márquez-García, B., Fernández, M.Á., Córdoba, F., 2009. Phenolics composition in *Erica* sp. differentially exposed to metal pollution in the Iberian Southwestern Pyritic Belt. *Bioresource technology* 100, 446–451.
- Márquez-García, B., Fernández-Recamales, M., Córdoba, F., 2012. Effects of cadmium on phenolic composition and antioxidant activities of *Erica andevalensis*. *Journal of botany* 2012, 936950.

- Miehe, G., Miehe, S., 1994. Ericaceous forests and heathlands in the Bale Mountains of South Ethiopia: ecology and man's impact. T. Warnke, Hamburg, Germany, p. 206.
- Míka, V., Kubáň, V., Klejdus, B., Odstrčilová, V., Nerušil, P., 2005. Phenolic compounds as chemical markers of low taxonomic levels in the family Poaceae. *Plant, Soil and Environment* 51, 506–512.
- Mohr, P.A., 1963. *The Geology of Ethiopia*. Addis Ababa University Press, Addis Ababa.
- Möller, A., Kaiser, K., Zech, W., 2002. Lignin, carbohydrate, and amino sugar distribution and transformation in the tropical highland soils of northern Thailand under cabbage cultivation, Pinus reforestation, secondary forest, and primary forest. *Australian Journal of Soil Research* 40, 977–998.
- Nazemiyeh, H., Bahadori, F., Delazar, A., Ay, M., Topçu, G., Nahar, L., Majinda, R.R., Sarker, S.D., 2008. Antioxidant phenolic compounds from the leaves of *Erica arborea* (Ericaceae). *Natural Product Research* 22, 1385–1392.
- Nichols-Orians, C.M., Fritz, R.S., Clausen, T.P., 1993. The genetic basis for variation in the concentration of phenolic glycosides in *Salix sericea*: Clonal variation and sex-based differences. *Biochemical Systematics and Ecology* 21, 535–542.
- Okuda, T., Yoshida, T., Hatano, T., Iwasaki, M., Kubo, M., Orime, T., Yoshizaki, M., Naruhashi, N., 1992. Hydrolysable tannins as chemotaxonomic markers in the Rosaceae. *Phytochemistry* 31, 3091–3096.
- Ortu, E., Brewer, S., Peyron, O., 2006. Pollen-inferred palaeoclimate reconstructions in mountain areas: Problems and perspectives. *Journal of Quaternary Science* 21, 615–627.
- Osmaston, H.A., Mitchell, W.A., Osmaston, J.A.N., 2005. Quaternary glaciation of the Bale Mountains, Ethiopia. *Journal of Quaternary Science* 20, 593–606.
- Pan, Y., Zhang, J., Zhao, Y.-L., Wang, Y.-Z., Jin, H., 2016. Chemotaxonomic studies of nine Gentianaceae species from western China based on liquid chromatography tandem mass spectrometry and Fourier transform infrared spectroscopy. *Phytochemical Analysis* 27, 158–167.
- Pljevljakušić, D., Bigović, D., Janković, T., Jelačić, S., Šavikin, K., 2018. Sandy everlasting (*Helichrysum arenarium* (L.) Moench): botanical, chemical and biological properties. *Frontiers in plant science* 9, 1–12.
- Ram Singh, C., 2016. Chemotaxonomy: A Tool for Plant Classification. *Journal of Medicinal Plants Studies JMPS* 90, 90–93.

- Ramakrishna, A., Ravishankar, G.A., 2011. Influence of abiotic stress signals on secondary metabolites in plants. *Plant Signaling and Behavior* 6, 1720–1731.
- Rivière, C., Pawlus, A.D., Mérillon, J.-M., 2012. Natural stilbenoids: distribution in the plant kingdom and chemotaxonomic interest in Vitaceae. *Natural product reports* 29, 1317–1333.
- Segele, Z.T., Lamb, P.J., Leslie, L.M., 2009. Large-scale atmospheric circulation and global sea surface temperature associations with horn of Africa June-September rainfall. *International Journal of Climatology* 29, 1075–1100.
- Sroka, Z., Kuta, I., Cisowski, W., Dryś, A., 2004. Antiradical activity of hydrolyzed and non-hydrolyzed extracts from *Helichrysi inflorescentia* and its phenolic contents. *Zeitschrift für Naturforschung C* 59, 363–367.
- Stanković, M., Čurčić, S., Zlatić, N., Bojović, B., 2017. Ecological variability of the phenolic compounds of *Olea europaea* L. leaves from natural habitats and cultivated conditions. *Biotechnology and Biotechnological Equipment* 31, 499–504.
- Terwilliger, V.J., Eshetu, Z., Colman, A., Bekele, T., Gezahgne, A., Fogel, M.L., 2008. Reconstructing palaeoenvironment from  $\delta^{13}\text{C}$  and  $\delta^{15}\text{N}$  values of soil organic matter: A calibration from arid and wetter elevation transects in Ethiopia. *Geoderma* 147, 197–210.
- Thevenot, M., Dignac, M.F., Rumpel, C., 2010. Fate of lignins in soils: A review. *Soil Biology and Biochemistry* 42, 1200–1211.
- Tiercelin, J.J., Gibert, E., Umer, M., Bonnefille, R., Disnar, J.R., Lézine, A.M., Hureau-Mazaudier, D., Travi, Y., Keravis, D., Lamb, H.F., 2008. High-resolution sedimentary record of the last deglaciation from a high-altitude lake in Ethiopia. *Quaternary Science Reviews* 27, 449–467.
- Umadevi, I., Daniel, M., Sabnis, S.D., 1988. Chemotaxonomic studies on some members of Anacardiaceae. *Proceedings: Plant Sciences* 98, 205–208.
- Umer, M., Lamb, H.F., Bonnefille, R., Lézine, A.M., Tiercelin, J.J., Gibert, E., Cazet, J.P., Watrin, J., 2007. Late Pleistocene and Holocene vegetation history of the Bale Mountains, Ethiopia. *Quaternary Science Reviews* 26, 2229–2246.
- Witzell, J., Gref, R., Na, T., 2003. Plant-part specific and temporal variation in phenolic compounds of boreal bilberry (*Vaccinium myrtillus*) plants 31, 115–127.
- Woldu, Z., Feoli, E., Nigatu, L., 1989. Partitioning an Elevation Gradient of Vegetation from Southeastern Ethiopia by Probabilistic Methods Stable by probabilistic methods from southeastern Ethiopia. *Plateau* 81, 189–198.

### Study 3:

## Spatial and temporal $^2\text{H}$ and $^{18}\text{O}$ isotope variation of contemporary precipitation in the Bale Mountains, Ethiopia

Bruk Lemma<sup>a,b\*</sup>, Seifu Kebede<sup>c,d</sup>, Sileshi Nemomissa<sup>e</sup>, Insa Otte<sup>f</sup>, Bruno Glaser<sup>a</sup>, Michael Zech<sup>a,g</sup>

<sup>a)</sup> Institute of Agronomy and Nutritional Sciences, Soil Biogeochemistry, Martin Luther University Halle-Wittenberg, Halle, Germany,

<sup>b)</sup> Ethiopian Biodiversity Institute, Forest and Rangeland Biodiversity Directorate, Addis Ababa, Ethiopia;

<sup>c)</sup> Department of Earth Science, Addis Ababa University, Addis Ababa, Ethiopia;

<sup>d)</sup> Center for Water Resources Research, School of Agricultural, Earth and Environmental Sciences, University of KwaZulu Natal, South Africa;

<sup>e)</sup> Department of Plant Biology and Biodiversity Management, Addis Ababa University, Addis Ababa, Ethiopia;

<sup>f)</sup> Environmental informatics, Faculty of Geography, Philipps University of Marburg, Germany

<sup>g)</sup> Institute of Geography, Technical University of Dresden, Dresden, Germany

**\*Corresponding author: Bruk Lemma (e-mail: [bruklemma@gmail.com](mailto:bruklemma@gmail.com))**

**Published in**

**Isotopes in Environmental and Health Studies, 2020, 56(2): 122-135;**

**<https://doi.org/10.1080/10256016.2020.1717487>**



## Abstract

Eastern Africa is an underrepresented region in respect of monitoring the stable isotopic composition of precipitation ( $\delta^{18}\text{O}_{\text{prec}}$  and  $\delta^2\text{H}_{\text{prec}}$ ). In 2017, we collected precipitation samples from ten weather stations located along an altitudinal transect ranging from 1304 to 4375 m a.s.l. The  $\delta^{18}\text{O}_{\text{prec}}$  and  $\delta^2\text{H}_{\text{prec}}$  values varied from  $-8.7$  to  $+3.7\text{‰}$  and  $-38$  to  $+29\text{‰}$ , respectively. The local meteoric water line is characterised by a lower slope, a higher intercept and more positive *d*-excess values ( $\delta^2\text{H} = 5.3 \pm 0.2 * \delta^{18}\text{O} + 14.9 \pm 0.9$ ) compared to the global meteoric water line. Both altitude and amount of precipitation clearly correlate with our isotope data. However, the  $\delta^{18}\text{O}_{\text{prec}}$  and  $\delta^2\text{H}_{\text{prec}}$  values show at the same time a seasonal pattern reflecting rainy versus dry season. More enriched isotope values prevailed shortly after the end of the dry season; more negative isotope values coincided with high precipitation amounts recorded in May, August and September. Moreover, HYSPLIT trajectories reveal that during the dry season water vapor originates primarily from the Arabian Sea, whereas during the wet season it originates primarily from the Southern Indian Ocean. These findings challenge the traditional amount effect interpretation of paleoclimate isotope records from Eastern Africa and rather point to a previously underestimated source effect.

**Key Words:** Bale Mountains, East Africa,  $\delta^2\text{H}$ ,  $\delta^{18}\text{O}$ , amount effect, altitude effect, source effect, trajectories

## Study 4:

### **$\delta^2\text{H}_{n\text{-alkane}}$ and $\delta^{18}\text{O}_{\text{sugar}}$ biomarker proxies from leaves and topsoils of the Bale Mountains, Ethiopia, and implication for paleoclimate reconstruction**

Bruk Lemma<sup>1,2\*</sup>, Lucas Bittner<sup>3</sup>, Bruno Glaser<sup>1</sup>, Seifu Kebede<sup>4</sup>, Sileshi Nemomissa<sup>5</sup>, Wolfgang Zech<sup>6</sup>, and Michael Zech<sup>1,3</sup>

<sup>1)</sup> Institute of Agronomy and Nutritional Sciences, Soil Biogeochemistry, Martin Luther University Halle-Wittenberg, Von-Seckendorff-Platz 3, D-06120, Halle, Germany,

<sup>2)</sup> Forest and Rangeland Biodiversity Directorate, Ethiopian Biodiversity Institute, P.O. Box 30726, Addis Ababa, Ethiopia,

<sup>3)</sup> Institute of Geography, Technische Universität Dresden, Helmholtzstraße 10, D-01062, Dresden, Germany

<sup>4)</sup> Center for Water Resources Research, School of Agricultural, Earth and Environmental Sciences, University of KwaZulu-Natal, Pietermaritzburg 3021, South Africa,

<sup>5)</sup> Department of Plant Biology and Biodiversity Management, Addis Ababa University, P.O. Box 3434, Addis Ababa, Ethiopia,

<sup>6)</sup> Institute of Soil Science and Soil Geography, University of Bayreuth, Universitätsstraße 30, D-95440, Bayreuth, Germany

**\*Corresponding author: Bruk Lemma (e-mail: [bruklemma@gmail.com](mailto:bruklemma@gmail.com))**

**Submitted to**

**Biogeochemistry-BIOG-D-20-00226**

## Abstract

The hydrogen isotope composition of leaf wax-derived  $n$ -alkane ( $\delta^2\text{H}_{n\text{-alkane}}$ ) and oxygen isotope composition of hemicellulose-derived sugar ( $\delta^{18}\text{O}_{\text{sugar}}$ ) biomarkers are valuable proxies for paleoclimate reconstructions. Here, we present a calibration study along the Bale Mountains in Ethiopia to evaluate how accurately and precisely the isotope composition of precipitation is imprinted in these biomarkers.  $n$ -Alkanes and sugars were extracted from the plant and topsoil samples and compound-specific  $\delta^2\text{H}_{n\text{-alkane}}$  and  $\delta^{18}\text{O}_{\text{sugar}}$  values were measured using a gas chromatograph-thermal conversion-isotope ratio mass spectrometer (GC-TC-IRMS). The weighted mean  $\delta^2\text{H}_{n\text{-alkane}}$  and  $\delta^{18}\text{O}_{\text{sugar}}$  values range from  $-186$  to  $-89\text{‰}$  and from  $+27$  to  $+46\text{‰}$ , respectively. Our results provide no evidence for degradation and/or root input affecting the isotope composition of the biomarkers in topsoils. Yet, the  $\delta^2\text{H}_{n\text{-alkane}}$  values show a statistically significant species dependence and  $\delta^{18}\text{O}_{\text{sugar}}$  yielded the same species-dependent trends. The reconstructed leaf water of *Erica arborea* and *Erica trimera* is  $^2\text{H}$ - and  $^{18}\text{O}$ -enriched by  $+55 \pm 5$  and  $+9 \pm 1\text{‰}$ , respectively, compared to precipitation. By contrast, *Festuca abyssinica* reveals the most depleted  $\delta^2\text{H}_{n\text{-alkane}}$  and  $\delta^{18}\text{O}_{\text{sugar}}$  values. This can be attributed to “signal-dampening” caused by basal grass leaf growth. The intermediate values for *Alchemilla haumannii* and *Helichrysum splendidum* can be likely explained with plant physiological differences or microclimatic conditions affecting relative humidity (RH) and thus RH-dependent leaf water isotope enrichment. While the actual RH values range from 69 to 82% ( $\bar{x} = 80 \pm 3.4\%$ ), the reconstructed RH values based on a recently suggested coupled  $\delta^2\text{H}_{n\text{-alkane}}$ - $\delta^{18}\text{O}_{\text{sugar}}$  (paleo-) hygrometer approach yielded a mean of  $78 \pm 21\%$ . Our findings corroborate (i) that vegetation changes, particularly in terms of grass versus non-grassy vegetation, need to be considered in paleoclimate studies based on  $\delta^2\text{H}_{n\text{-alkane}}$  and  $\delta^{18}\text{O}_{\text{sugar}}$  records and (ii) that the coupled  $\delta^2\text{H}_{n\text{-alkane}}$ - $\delta^{18}\text{O}_{\text{sugar}}$  (paleo-) hygrometer approach holds great potential for deriving additional paleoclimatic information compared to single isotope approaches.

**Keywords:**  $n$ -alkane, hydrogen-2, sugar, oxygen-18, evapotranspirative enrichment, (paleo-) hygrometer

## 1. Introduction

The compound-specific hydrogen isotope composition of leaf wax-derived *n*-alkanes ( $\delta^2\text{H}_{n\text{-alkane}}$ ) and oxygen isotope composition of hemicellulose-derived sugars ( $\delta^{18}\text{O}_{\text{sugar}}$ ) serve as proxies in paleoclimate and -environmental studies (Hepp et al., 2017; Tuthorn et al., 2015; Zech et al., 2014a, 2013b). The above-mentioned biomarkers are preserved for a long period of time (Eglinton and Hamilton, 1967; Eglinton and Eglinton, 2008; Glaser and Zech, 2005; Zech et al., 2014a) and their application was tested in different paleoclimate archives; for instance lake sediments (Hepp et al., 2015; Sachse et al., 2004; Zech et al., 2014b), loess-paleosols (Buggle and Zech, 2015; Zech et al., 2013b), and tree rings (Gessler et al., 2009). The isotope composition of  $\delta^2\text{H}_{n\text{-alkane}}$  and  $\delta^{18}\text{O}_{\text{sugar}}$  from terrestrial vascular plants primarily reflects the isotope composition of precipitation. In turn, the isotope composition of  $\delta^2\text{H}_{\text{prec}}$  and  $\delta^{18}\text{O}_{\text{prec}}$  on the continents is mainly controlled by different site and climatic factors. Amongst others, these include latitude, altitude, distance to the coast, temperature, source and amount of precipitation, relative humidity, wind, cloud and rain type/size as well as size and type of convection (Araguás-Araguás et al., 2000; Craig, 1961; Dansgaard, 1964; Gonfiantini et al., 2001; Rozanski et al., 1993).

Some studies reveal the absence of isotope fractionation during decomposition (Zech et al., 2012b) and water uptake by the roots (Ehleringer et al., 1991; Feakins and Sessions, 2010; White et al., 1985). Nevertheless, caution must be given when using  $\delta^2\text{H}_{n\text{-alkane}}$  for paleoclimate reconstruction due to the effects of degradation and synthesis of leaf wax-derived *n*-alkanes by microorganisms (Brittingham et al., 2017; Zech et al., 2009, 2012a). Similarly, investigations on halophytic and xerophytic plants show evidence of hydrogen isotope fractionation during water uptake at the root-soil interface (Ellsworth and Williams, 2007; Ladd and Sachs, 2015). Apart from this, it is well known that leaf water is isotopically more enriched than plant source water due to evapotranspiration. This enrichment is primarily dependent on relative humidity (RH) and can challenge a robust  $\delta^2\text{H}_{\text{prec}}$  and  $\delta^{18}\text{O}_{\text{prec}}$  reconstruction (Zech et al., 2015). Moreover, the evaporative enrichment of leaf water affects the  $\delta^2\text{H}_{n\text{-alkane}}$  and  $\delta^{18}\text{O}_{\text{sugar}}$  values of monocot and dicot plants at different magnitudes. This latter effect is called “signal-dampening” and causes grasses to have generally depleted compound-specific stable hydrogen and oxygen isotope values than broad-leaf plant species (Hepp et al., 2020, 2019). Hence, the interpretation of the isotope composition of plant-derived biomarkers should consider (i) the isotope composition of precipitation, (ii) RH-dependent evapo(transpi)rative enrichment of leaf water, (iii) biosynthetic fractionation and signal-dampening (cf. section 2.5).

Some years ago, Zech et al. (2013b) proposed a coupled  $\delta^2\text{H}_{n\text{-alkane}}\text{-}\delta^{18}\text{O}_{\text{sugar}}$  approach. This coupled approach aims at providing additional information to reconstruct paleoclimate and allows the reconstruction of  $\delta^2\text{H}$  and  $\delta^{18}\text{O}$  source water ( $\delta^2\text{H}_{\text{source water}}$  and  $\delta^{18}\text{O}_{\text{source water}}$ ) and deuterium excess (*d*-excess, a proxy for RH). This approach was validated along a climate transect across Argentina (Tuthorn et al., 2015) as well as South Africa (Strobel et al., 2020) and yielded a highly significant correlation between actual and reconstructed RH and precipitation. The coupled approach was also successfully applied to eolian/loess-paleosol sediments and lacustrine sediments to reconstruct paleoclimate changes (Hepp et al., 2019, 2017; Zech et al., 2013b). The concept of using both  $\delta^2\text{H}$  and  $\delta^{18}\text{O}$  was independently developed for tree-ring cellulose to deduce RH (Voelker et al., 2014).

The main objective of the present study was to evaluate how accurately and precisely the isotope signature of contemporary precipitation and RH are imprinted on compound-specific stable isotopes of leaves and topsoils of the Bale Mountains. More specifically, we answer the following questions: (I) Are there systematic  $\delta^2\text{H}_{n\text{-alkane}}$  and  $\delta^{18}\text{O}_{\text{sugar}}$  differences between leaves, O-layers, and  $A_h$ -horizons? (II) Do *n*-alkane and sugar biomarkers in leaves and topsoils reflect  $\delta^2\text{H}_{\text{prec}}$  and  $\delta^{18}\text{O}_{\text{prec}}$ ? (III) Are there systematic  $\delta^2\text{H}_{n\text{-alkane}}$  and  $\delta^{18}\text{O}_{\text{sugar}}$  differences among the keystone plant species? (IV) Does the application of the coupled  $\delta^2\text{H}_{n\text{-alkane}}\text{-}\delta^{18}\text{O}_{\text{sugar}}$  (paleo-) hygrometer approach provide additional information compared to the single isotope approaches?

## 2. Material and Methods

### 2.1 Geography of the Bale Mountains

The Bale Mountains are located 400 km southeast of Addis Ababa, capital of Ethiopia, and belong to the Bale-Arsi Mountains massif (Fig. 4–1). The Bale Mountains National Park (BMNP) is situated between 39°28' to 39°57' longitude (E) and between 6°29' to 7°10' latitude (N), spanning a large altitudinal (1400 to 4377 m a.s.l.) gradient (Hillman, 1988, 1986; Mieke and Mieke, 1994; Tiercelin et al., 2008). The study area was described previously in detail by Lemma et al. (2020, 2019a, 2019b). Briefly, the Bale Mountains are topographically divided into three major parts: The northern slopes (3000–3800 m. a.s.l.), the central Sanetti Plateau (3800–4377 m a.s.l.), and the southern Harena escarpment (1400–3800 m. a.s.l.). The Sanetti Plateau is located in the center, on which the second highest peak of the country Mt. Tulu Dimtu (4377 m a.s.l.) perches (Friis, 1986; Hillman, 1986; Mieke and Mieke, 1994). The northern slopes of the mountains are dissected by the Togona Valley, which descends towards the extensive Arsi Plateau and further down to the Great Rift Valley lowlands, which divide the

country into two parts. The southern slope includes the steep Harena escarpment and goes down to the surrounding lowland at about 1400 m a.s.l. The vegetation shows an altitudinal zonation comprising the Afro-montane forest (1450–2000 m a.s.l.), the upper montane forest dominated by *Hagenia* – *Hypericum* species (2000–3200 m a.s.l.), the Ericaceous belt (3200–3800 m a.s.l.), and the Afro-alpine zone (3800–4377 m a.s.l.) being dominated by dwarf-shrubs (e.g., *Helichrysum*, *Alchemilla*), herbs, and grasses (mostly *Festuca*) (Hillman, 1988; Mieke and Mieke, 1994; Woldu et al., 1989).

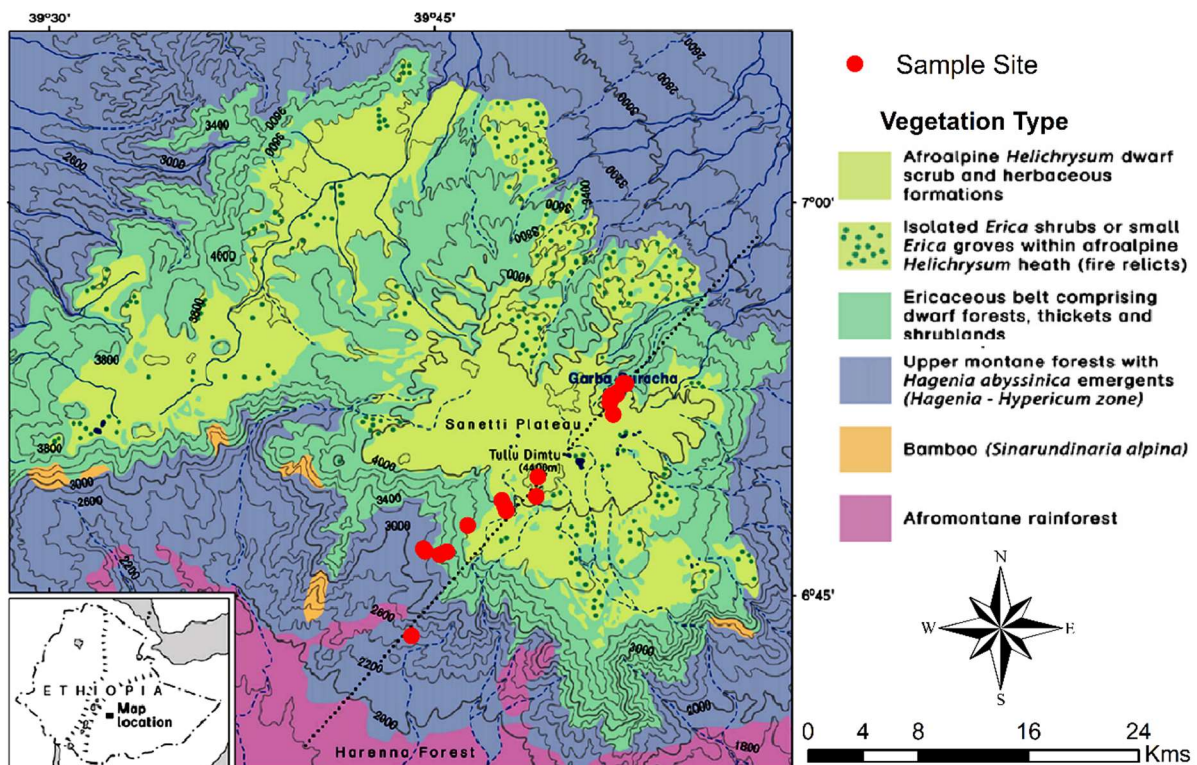


**Fig. 4–1:** Map of vegetation zones and sample sites (red dots) along the southwest and northeast transect in the Bale Mountains (modified after Mieke and Mieke, 1994 and published in Lemma et al., 2019a; 2019b and Mekonnen et al., 2019).

The crust of the Bale Mountains is of volcanic origin, the soils which are developed from the basaltic, rhyolitic, and trachytic parent rock, can be generally characterized as silty loams of reddish-brown to black colour (Woldu et al., 1989). Nevertheless, the mountain's summit higher than 3000 m a.s.l were substantially flattened by repeated glaciations (for example between 20 – 12 cal kyr BP), the soils developed from such glacial rocks are usually shallow and gravelly (Hedberg, 1964; Osmaston et al., 2005). Therefore, Andosols are the most ubiquitous soil type but also Cambisols and Leptosols are prevalent in some parts of the Bale Mountains. In the wetland and sedimentary basin, Gleysols and Histosols, and in rock shelters, Anthrosols are also a common soil type (Billi, 2015; Yimer et al., 2006).

## 2.2 (Paleo)-climate

The Bale Mountains are historically vulnerable to extreme climate changes that depict quaternary glacier cover with a spatial extent of about 180 km<sup>2</sup> (Osmaston et al., 2005; Umer et al., 2004) and anthropogenic impacts (Gil-Romera et al., 2019; Ossendorf et al., 2019). The chronology of lacustrine sediment from the lake Garba Guracha (a glacial lake at 3950 m a.s.l.) dated back to the Late Glacial (~ 16.5 cal kyr BP) illustrates the presence of regional climate events, the African Humid Period (AHP), that encompasses major dry fluctuations such as Younger Dryas (YD), 6.5 cal kyr BP and 4.2 cal kyr BP (Bittner et al., 2020; Umer et al., 2007). A pollen record from the lake sediment shows vegetation response to climate change. Around 13.4 cal kyr BP, indicators of arid climate vegetation like *Artemisia* and *Amaranthaceae* declined and *Cyperaceae* increased, suggesting a change to moister conditions. The marked change on organic lake sedimentation during the onset of Holocene reflects the expansion of woody vegetation like *Erica* across the Sanetti Plateau (Umer et al., 2007) and aquatic biomass production (Bittner et al., 2020) in response to increased moisture and temperature. Thus the biodiversity of the Bale Mountains is the legacy of natural Holocene vegetation change (Umer et al., 2007) and anthropogenically induced fire (Gil-Romera et al., 2019).

Currently, the climate of the Bale Mountains is characterized by four months (November to February) of dry season and eight months (March to October) of wet season (Kidane et al., 2012; Lemma et al., 2020). The seasonal migration of Intertropical Convergence Zone (ITCZ) determines the present climate and rainfall patterns of the Ethiopian Highlands (Tiercelin et al., 2008). The highest annual rainfall occurs in the southwestern part (1000–1500 mm per year) and the northern part of the mountains exhibits annual rainfall ranging between 800–1000 mm per year (Miehe and Miehe, 1994; Tiercelin et al., 2008). Moisture during the dry season originates primarily from the Arabian Sea, whereas during the wet season it originates primarily from the Southern Indian Ocean (Lemma et al., 2020). The Afro-alpine regions of the Bale Mountains are characterized by a large diurnal temperature range of 40 °C (–15 to + 26 °C) (Hedberg, 1964; Hillman, 1988). Even if there is a wider variability of climate in the Bale Mountains, only few records are reported. The highest mean annual temperatures in the mountains peaks range between 6–12 °C. At Dinsho (headquarter of the BMNP, 3170 m a.s.l.) the mean annual temperature is 11.8 °C. The lowest mean annual temperatures range from 0.6– 10 °C with frequent frost occurring in the high peak areas during the winter season (Tiercelin et al., 2008).

### 2.3 Sampling

For the present study, 25 leaf samples of locally dominant plant species were collected (Fig. 4– 1) along a southwestern and a northeastern transect (ranging from 2550 to 4377 m a.s.l. and 3870 to 4134 m a.s.l., respectively). Samples comprise *Erica trimera* (n=5), *Erica arborea* (n=5), *Alchemilla haumannii* (n=5), *Festuca abyssinica* (n=6), *Helichrysum splendidum* (n=2), *Kniphofia foliosa* (n=1) and *Lobelia rhynchopetalum* (n=1). Photos illustrating the investigated plant species were previously published by Mekonnen et al. (2019). Additionally, 15 organic surface layers (= O-layers, strongly humified plant residues) and 22 mineral topsoils (= A<sub>n</sub>-horizons, 0-10 cm soil depth) that developed under the above-listed locally dominant vegetation were collected, resulting in 62 samples in total. All samples were air-dried in the Soil Store Laboratory of the National Herbarium, Department of Plant Biology and Biodiversity Management, Addis Ababa University. In the laboratory of the Soil Biogeochemistry Group, Martin Luther University of Halle–Wittenberg, the samples were sieved using a mesh size of 2 mm, finely ground, homogenized, and subjected to further biogeochemical analysis.

Additionally, from ten newly established weather stations, we recorded RH, temperature, and a total of 164 precipitation samples were collected along an altitudinal transect ranging from 1304 to 4375 m a.s.l. The  $\delta^2\text{H}_{\text{prec}}$  and  $\delta^{18}\text{O}_{\text{prec}}$  as well as RH and temperature records above 2550 m a.s.l. were used for the present study. For more details, information regarding the spatial and temporal  $^2\text{H}$  and  $^{18}\text{O}$  isotope variation of the contemporary precipitation in the Bale Mountains, the readers are referred to (Lemma et al., 2020).

### 2.4 Compound-specific $\delta^2\text{H}_{n\text{-alkane}}$ and $\delta^{18}\text{O}_{\text{sugar}}$ analyses

Leaf wax-derived *n*-alkanes were extracted from 0.5 to 1 g of leaves, O-layers and A<sub>n</sub>-horizons using Soxhlet extraction by adding 150 ml of dichloromethane (DCM) and methanol (MeOH) as solvents (9:1 ratio) for 24 h following a method modified after Zech and Glaser (2008). 50  $\mu\text{l}$  of 5 $\alpha$ -androstane were added to the total lipid extracts as an internal standard. Total lipid extracts were separated over aminopropyl pipette columns (Supelco, 45  $\mu\text{m}$ ). Three lipid fractions containing the *n*-alkanes, alcohols, and fatty acids were eluted successively by using 3 ml of hexane, DCM/MeOH (1:1), and diethyl ether and acetic acid (95:5), respectively.

The compound-specific stable hydrogen isotope analyses of the most abundant *n*-alkanes (C<sub>29</sub> and C<sub>31</sub>) were determined using Trace GC 2000 coupled to a Delta V Advantage IRMS via a thermal conversion reactor (GC IsoLink) and a ConFlo IV interface (GC-TC-IRMS, Delta V, Thermo Fisher Scientific, Bremen, Germany) operating in pyrolysis mode with reactor



temperature of 1420 °C. The GC was equipped with a split/splitless injector and an Rtx-5 Sil MS column (30 m length, 0.25 mm inner diameter, 0.5 µm film thickness). Each sample was analysed in triplicate and measurements of *n*-alkane standards (C<sub>27</sub>, C<sub>29</sub>, C<sub>33</sub>) with known isotope composition (Arndt Schimmelmann, Indiana) at various concentrations were embedded in-between the three sample batches. The H<sub>3</sub><sup>+</sup> factor was determined before and after each sequence and was stable at 7.57 ± 0.29 (n = 6) during the measurement campaign.

The hemicellulose-derived sugars were extracted hydrolytically (105 °C, 4 h) from aliquots of leaves, O-layers, and A<sub>h</sub>-horizons using 10 ml of 4M trifluoroacetic acid (TFA) following the method described by Zech and Glaser (2009). The extracted monosaccharides were purified via XAD-7 and Dowex 50WX8 resin columns as proposed by Amelung et al. (1996). For quantification, one-fifth of the freeze-dried sugar samples were derivatized using N-methylpyrrolidone (NMP) and heated for 30 min at 75 °C. After cooling, the samples were subjected for the second derivatization using 400 µl bis(trimethylsilyl) trifluoroacetamide (BSTFA) and heated again for 5 min at 75 °C. For compound-specific δ<sup>18</sup>O<sub>sugar</sub> analyses, the remaining four-fifth of the samples were derivatized using the methyl-boronic acid (MBA; 4 mg in 400 µl pyridine) derivatization method and heated for 1 h at 60 °C (Zech and Glaser, 2009).

The compound-specific stable oxygen isotope values were determined using a Trace GC 2000 coupled to a Delta V Advantage IRMS via an <sup>18</sup>O-pyrolysis reactor (GC IsoLink) and a ConFlo IV interface (GC-Py-IRMS, Delta V, Thermo Fisher Scientific, Bremen, Germany). The GC was equipped with a split/splitless injector and an DB-5MS+DG column (60 m length, 0.250 mm inner diameter, 0.25 µm film thickness). Samples were injected in splitless mode and analysed in triplicate. For measurements precision standard blocks of derivatised sugars (arabinose, fucose and xylose) of known isotope composition at various concentrations were embedded in-between the six sample batches.

The measured δ<sup>2</sup>H<sub>*n*-alkane</sub> and δ<sup>18</sup>O<sub>sugar</sub> values were corrected for drift and amount-dependence, according to Zech and Glaser (2009). Out of 62 samples, five samples (four O-layers and one A<sub>h</sub>-horizon below *Erica*) were rejected from further data evaluation and interpretation due to peak areas below detection limit. Similarly, the sugar biomarker fucose was excluded from data evaluation due to too low peak areas. Mean standard error for triplicate measurements of the remaining 57 samples are 0.8‰, 0.9‰, 3.1‰, 2.3‰ for arabinose, xylose, C<sub>29</sub>, and C<sub>31</sub> alkanes, respectively. The standard error for the sugars and *n*-alkanes standards was 2‰ (n = 22) and 5‰ (n = 28), respectively. In the following, δ<sup>2</sup>H<sub>*n*-alkane</sub> values refer to weighted mean values of C<sub>29</sub> and C<sub>31</sub>, and δ<sup>18</sup>O<sub>sugar</sub> values refer to weighted mean values of arabinose and xylose. The

weighted mean for  $\delta^2\text{H}_{n\text{-alkane}}$  and  $\delta^{18}\text{O}_{\text{sugar}}$  values were calculated using the relative amounts of  $\text{C}_{29}$  and  $\text{C}_{31}$  as well as arabinose and xylose, respectively. The  $\delta^2\text{H}_{n\text{-alkane}}$  and  $\delta^{18}\text{O}_{\text{sugar}}$  values are reported in per mil (‰) according to the usual  $\delta$ -notation relative to Vienna Standard Mean Ocean Water (V-SMOW) given in equation 1.

$$\delta = (R_{\text{sample}}/R_{\text{standard}} - 1) \times 10^3 \quad (1)$$

where R refers to the ratio of  $^{18}\text{O}/^{16}\text{O}$  and  $^2\text{H}/^1\text{H}$  for the sample or standard (V-SMOW) materials.

## **2.5 Conceptual framework for interpreting the coupled $\delta^2\text{H}_{n\text{-alkane}}$ - $\delta^{18}\text{O}_{\text{sugar}}$ approach: reconstruction of leaf water, source water, *d*-excess, and relative humidity**

The  $\delta^2\text{H}_{n\text{-alkane}}$  and  $\delta^{18}\text{O}_{\text{sugar}}$  values primarily depend on the isotope composition of precipitation, evaporative enrichment of leaf water, and the biosynthetic fractionation factor (Sessions et al., 1999; Zech et al., 2013b). Each of these factors is again influenced by other climatic parameters. For instance, in high latitudes, the isotope composition of precipitation is mainly temperature-dependent, whereas in the tropics, highly depleted isotope values coincide with major rainy periods, often called the ‘amount effect’ that controls the isotope composition of precipitation (Araguás-Araguás et al., 2000; Craig, 1961; Dansgaard, 1964; Gonfiantini et al., 2001; Rozanski et al., 1993). The isotope composition of precipitation typically plots along the global meteoric water line (GMWL,  $\delta^2\text{H} = 8 \cdot \delta^{18}\text{O} + 10$ ) (Craig, 1961). The isotope enrichment of leaf water due to evapotranspiration depends on relative humidity, temperature and the isotope composition of atmospheric moisture. Due to transpiration, leaf water becomes isotopically enriched compared to source water (precipitation) (Farquhar et al., 2007; Feakins and Sessions, 2010). In a  $\delta^2\text{H}$ - $\delta^{18}\text{O}$  diagram, the leaf water plots along an evaporation line. The isotope composition of leaf water ( $\delta^2\text{H}_{\text{leaf water}}$  and  $\delta^{18}\text{O}_{\text{leaf water}}$ ) can be reconstructed from the isotope composition of biomarkers ( $\delta^2\text{H}_{n\text{-alkane}}$  and  $\delta^{18}\text{O}_{\text{sugar}}$ ) by subtracting biosynthetic fractionation factors (Hepp et al., 2019, 2017; Tuthorn et al., 2015; Zech et al., 2013b). Apart from assuming that the biosynthetic fractionation factors ( $\epsilon_{\text{bio}}$ ) are constant and not significantly variable amongst plants, we assume moreover that both biomarkers (sugars and *n*-alkanes) are primarily leaf-derived. We acknowledge that both assumptions are valid only in approximation. We apply  $\epsilon_{\text{bio}}$  of  $-160\text{‰}$  (Sessions et al., 1999) to reconstruct  $\delta^2\text{H}_{\text{leaf water}}$  (Eq. 2) and  $+27\text{‰}$  (Cernusak et al., 2003; Gessler et al., 2009; Schmidt et al., 2001; Sternberg, 1989) to reconstruct  $\delta^{18}\text{O}_{\text{leaf water}}$  (Eq. 3).

$$\delta^{18}\text{O}_{\text{leaf water}} = (\delta^{18}\text{O}_{\text{sugar}} - \varepsilon^{18}_{\text{bio}})/(1 + \varepsilon^{18}_{\text{bio}}/1000) \quad (2)$$

$$\delta^2\text{H}_{\text{leaf water}} = (\delta^2\text{H}_{n\text{-alkane}} - \varepsilon^2_{\text{bio}})/(1 + \varepsilon^2_{\text{bio}}/1000) \quad (3)$$

Once the isotope composition of leaf water is calculated according to equation 2 and 3, it is possible to reconstruct the isotope composition of source water, *d*-excess and RH according to Eqn. (4), (5), and (6), respectively.

Leaf water becomes isotopically enriched due to evapotranspiration via stomata and will reach isotope steady-state under constant environmental conditions. This process is accompanied by equilibrium and kinetic isotope effects. The isotope composition of  $\delta^2\text{H}_{\text{leaf water}}$  and  $\delta^{18}\text{O}_{\text{leaf water}}$  then depends primarily on RH, the isotope composition of source water and the isotope composition of atmospheric water vapor (Dongmann et al., 1974; Flanagan et al., 1991; Roden and Ehleringer, 1999). Once isotope steady-state is achieved, the isotope enrichment of leaf water can be described using a Craig-Gordon model (Craig and Gordon, 1965) adapted by Gat and Bowser (1991) and later by Zech et al. (2013b). The isotope composition of leaf water at the evaporative site can be calculated using equation 4.

$$\delta_{\text{leaf water}} = \delta_{\text{source water}} + (1-\text{RH}) \varepsilon^* + \Delta\varepsilon \quad (4)$$

where  $\delta_{\text{leaf water}}$  and  $\delta_{\text{source water}}$  are the isotope composition of leaf water and source water, respectively, RH is relative humidity,  $\varepsilon^*$  is equilibrium isotope enrichment  $((1-1/\alpha_{L/V}) \cdot 10^3)$ , and  $\Delta\varepsilon$  is kinetic isotope enrichment [ $\Delta^{18}\varepsilon = C_k^{18} (1-\text{RH})$ ;  $\Delta^2\varepsilon = C_k^2 (1-\text{RH})$ ].  $C_k^{18}$  and  $C_k^2$  are kinetic isotope enrichment constants for  $^{18}\text{O}$  and  $^2\text{H}$ , respectively.

In a two-dimensional  $\delta^2\text{H}$ - $\delta^{18}\text{O}$  diagram, the isotope values of precipitation plot along the GMWL (Craig, 1961; Dansgaard, 1964), whereas the isotope values of leaf water plot along the evaporation line (Tuthorn et al., 2015; Zech et al., 2013b). The distance of the reconstructed leaf water to the GMWL can be described as *d*-excess and serves as a proxy for relative humidity. *d*-excess is a second-order stable isotope parameter measured in meteoric water defined as *d*-excess =  $\delta^2\text{H} - 8*\delta^{18}\text{O}$ . Therefore, *d*-excess of leaf water can be derived using equation 5.

$$d_{\text{leaf water}} = d_{\text{source water}} + (1-\text{RH}) (\varepsilon_2^* - 8*\varepsilon_{18}^* + C_k^2 - 8*\varepsilon_{18}^*) \quad (5)$$

where  $d_{\text{leaf water}}$  and  $d_{\text{source water}}$  are *d*-excess of leaf water and source water, respectively and the equilibrium ( $\varepsilon_2^*$  and  $\varepsilon_{18}^*$ ) and kinetic ( $C_k^2$  and  $C_k^{18}$ ) isotope fractionation of the two isotopes. Equation 5 illustrates that *d*-excess depends primarily on RH. Therefore, RH normalized to the temperature of leaf water can be estimated using equation 6.

$$RH \approx 1 - \frac{\Delta d}{(\varepsilon_2^* - 8 \cdot \varepsilon_{18}^* + C_k^2 - 8 \cdot C_k^{18})} \quad (6)$$

where  $\Delta d$  is the difference between  $d$ -excess of leaf water and  $d$ -excess of source water. Equilibrium isotope fractionation factors ( $\varepsilon_2^*$  and  $\varepsilon_{18}^*$ ) as a function of temperature are calculated according to empirical equations of Horita and Wesolowski (1994). According to Merlivat (1978), the maximum values of kinetic isotope fractionation factors ( $C_k^2$  and  $C_k^{18}$ ) during molecular diffusion of water via a stagnant air for  $^2\text{H}$  and  $^{18}\text{O}$  are 25.1‰ and 28.5‰, respectively. However, we are aware that the kinetic isotope fractionation factors are dependent on aerodynamic conditions (liquid-vapor interface, diffusive, and turbulent layer) characterising a given evaporation process.

The values of  $\delta^2\text{H}_{\text{source water}}$  and  $\delta^{18}\text{O}_{\text{source water}}$  can be estimated when the slope of the evaporation line for leaf water is known. The slope of the evaporation line can be derived from equation 7.

$$S_{\text{LEL}} = \frac{\delta_e^2 - \delta_s^2}{\delta_e^{18} - \delta_s^{18}} \approx \frac{\varepsilon_2^* + C_k^2}{\varepsilon_{18}^* + C_k^{18}} \quad (7)$$

In this equation, we assumed that the isotope composition of source water and atmospheric water vapor reached equilibrium. Thus, the slope of the evaporation line depends on equilibrium ( $\varepsilon_2^*$  and  $\varepsilon_{18}^*$ ) and kinetic ( $C_k^{18}$  and  $C_k^2$ ) isotope fractionation factors of the two isotopes (Gat and Bowser, 1991). In the present study, the slope of the evaporation line ranges between 2.86 to 3.07 ( $\bar{x} = 3 \pm 0.01$ ) for the temperature ranging between 3.2 °C to 12.7 °C. Here in this manuscript,  $\pm$  sign refer to standard error values. Such low slope for evaporating leaf water is in agreement with both field observations and laboratory experiments (Allison et al., 1985; Gat et al., 2007; Walker and Brunel, 1990).

The net isotope difference (also called apparent fractionation,  $\varepsilon_{\text{app}}$ ) between  $\delta^2\text{H}_{n\text{-alkane}}$  and  $\delta^2\text{H}_{\text{prec}}$  as well as  $\delta^{18}\text{O}_{\text{sugar}}$  and  $\delta^{18}\text{O}_{\text{prec}}$  is calculated using equation 8.

$$\varepsilon_{\text{app}} = 1000 \times \left( \frac{\delta_a + 10}{\delta_b + 1000} - 1 \right) \quad (8)$$

where  $a$  is the isotope composition of a biomarker ( $\delta^2\text{H}_{n\text{-alkane}}$  or  $\delta^{18}\text{O}_{\text{sugar}}$ ) and  $b$  is the weighted mean annual isotope composition of precipitation ( $\delta^2\text{H}_{\text{prec}}$  or  $\delta^{18}\text{O}_{\text{prec}}$ ).

### 3. Results and Discussion

#### 3.1 Comparison of $\delta^2\text{H}_{n\text{-alkane}}$ and $\delta^{18}\text{O}_{\text{sugar}}$ results from leaves, O-layers, and $\text{A}_h$ -horizons

The  $\delta^2\text{H}$  values of  $\text{C}_{29}$  and  $\text{C}_{31}$  alkanes as well as the  $\delta^{18}\text{O}$  values of arabinose and xylose correlate highly significant with each other ( $r = 0.9$ ,  $p < 0.0001$  and  $r = 0.8$ ,  $p < 0.0001$ , respectively, data not shown). In the following, we therefore use and refer to  $\delta^2\text{H}_{n\text{-alkane}}$  values for weighted mean values of  $\text{C}_{29}$  and  $\text{C}_{31}$  as well as to  $\delta^{18}\text{O}_{\text{sugar}}$  values for weighted mean values of arabinose and xylose. Weighted mean  $\delta^2\text{H}_{n\text{-alkane}}$  and  $\delta^{18}\text{O}_{\text{sugar}}$  values range from  $-186$  to  $-89\text{‰}$  and from  $+27$  to  $+46\text{‰}$ , respectively (Fig. 4–2). Particularly, the topsoil (O-layer as well as  $\text{A}_h$ -horizon) samples in the Bale Mountains yielded a  $\delta^2\text{H}_{n\text{-alkane}}$  values range between  $-157$  to  $-113\text{‰}$  ( $\bar{x} = -136\text{‰}$ ), which is in good agreement with findings from the highest Eastern African Mt. Kilimanjaro (Hepp et al., 2017; Peterse et al., 2009; Zech et al., 2015).

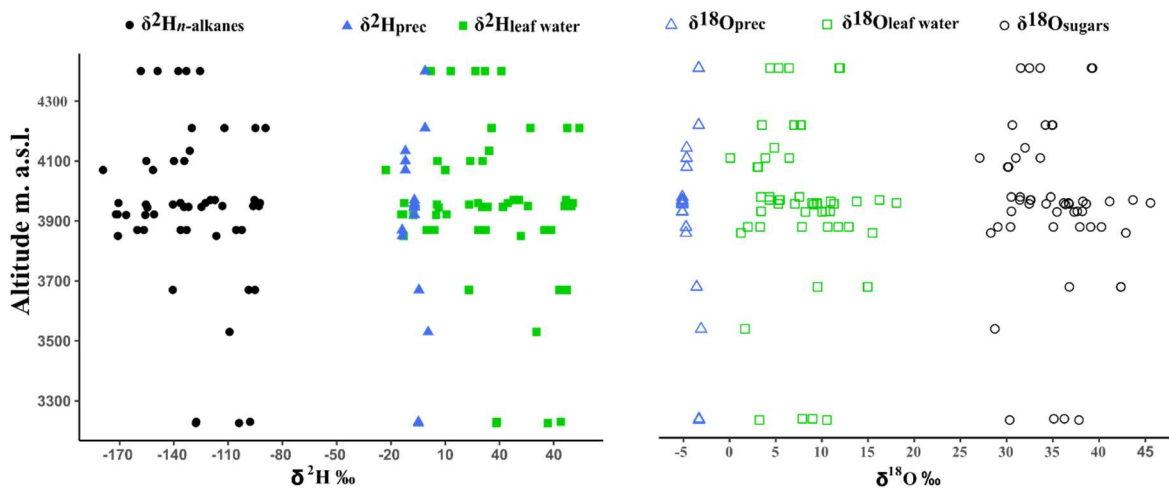


**Fig. 4–2:** Altitudinal  $\delta^2\text{H}$  (left) and  $\delta^{18}\text{O}$  (right) gradients of  $n$ -alkanes (weighted mean of  $\text{C}_{29}$  and  $\text{C}_{31}$ ) and sugar biomarkers (weighted mean of arabinose and xylose), respectively, reconstructed leaf water (squares) and precipitation (triangles).

The  $\delta^2\text{H}_{n\text{-alkane}}$  and  $\delta^{18}\text{O}_{\text{sugar}}$  values of leaves, O-layers, and  $\text{A}_h$ -horizons do not depict statistically significant differences ( $p = 0.7$  and  $p = 0.4$ , respectively) among each other (Fig. 4–3). Hence, our data provide no evidence for degradation effects affecting the isotope composition of the biomarkers. In addition, a contribution of the root and soil microbial-derived  $n$ -alkanes and sugars is not obviously affecting the compound-specific hydrogen and oxygen isotope signals. This is remarkable because our previous chemotaxonomy studies reveal that the characteristic plant biomarker patterns of long-chain  $n$ -alkanes and sugars are strongly

altered in the respective O-layers and A<sub>h</sub>-horizons due to degradation and/or underground input by roots (Lemma et al., 2019b; Mekonnen et al., 2019).

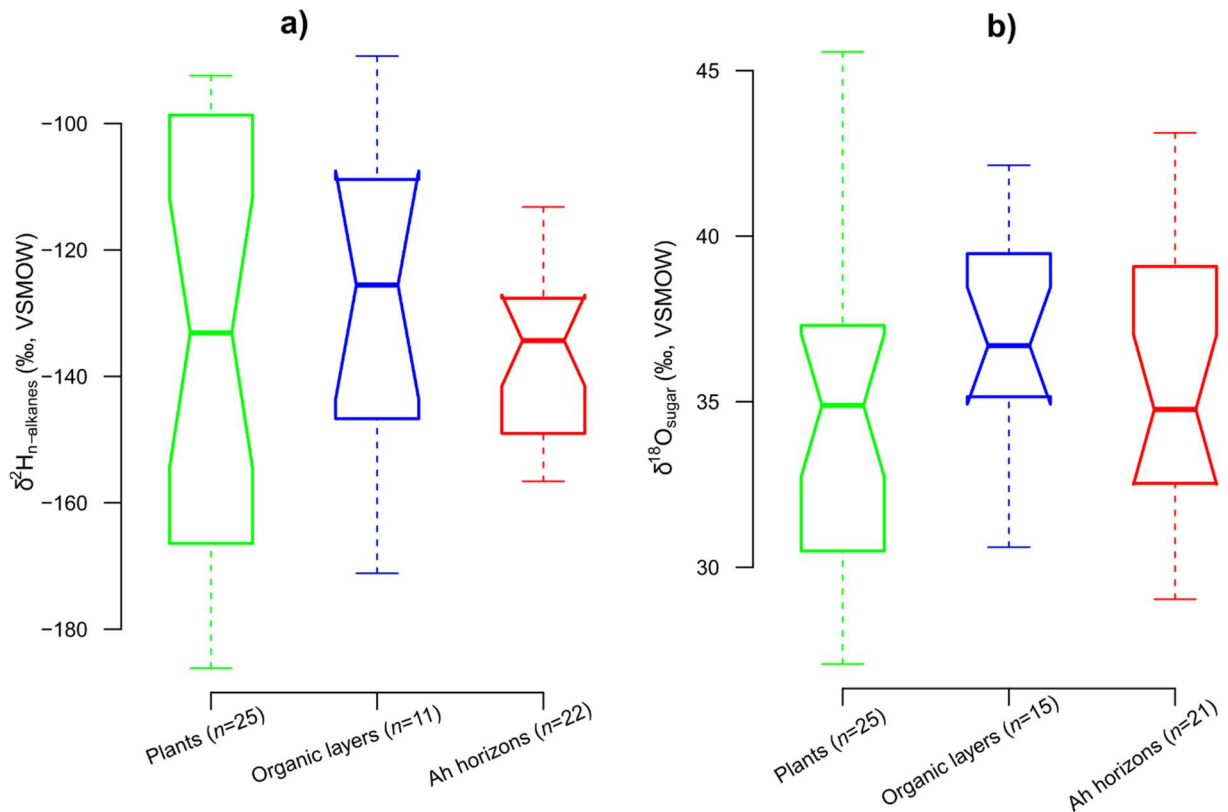


**Fig. 4-3:** Comparison of  $\delta^2\text{H}_{n\text{-alkane}}$  (a) and  $\delta^{18}\text{O}_{\text{sugar}}$  (b) among leaves, O-layers and A<sub>h</sub>- horizons. The notched box plots indicate the median (solid lines between the boxes), interquartile range (IQR) with upper (75%) and lower (25%) quartiles. The notches display the confidence interval around the median within  $\pm 1.57 \cdot \text{IQR} / \sqrt{n}$ .

Concerning  $\delta^{18}\text{O}_{\text{sugar}}$ , Zech et al. (2012b) reported the absence of isotope fractionation during decomposition based on a litter decay study. By contrast, based on the same litter decay sample set, Zech et al. (2011) concluded that the built-up of a microbial *n*-alkane pool can change the  $\delta^2\text{H}_{n\text{-alkane}}$  values of soils compared to litter. The same conclusion was drawn by Tu et al. (2011) based on a  $\delta^{13}\text{C}$  *n*-alkane litter decay study. A possible explanation for this discrepancy could be that  $\delta^2\text{H}_{n\text{-alkane}}$  and  $\delta^{18}\text{O}_{\text{sugar}}$  variability in our dataset are very large within the leaf, O-layer, and A<sub>h</sub>-horizon sub-dataset (Fig. 4-3). Indeed, albeit not significant, the median values of O-layers reveal both the least negative  $\delta^2\text{H}_{n\text{-alkane}}$  and the most positive  $\delta^{18}\text{O}_{\text{sugar}}$ . It is noteworthy that the concentration of *n*-alkanes in roots is much lower than in leaves and the contamination of leaf wax-derived *n*-alkanes in sediment by the roots is negligible (Zech et al., 2013a, 2012a), whereas a partial contribution of especially root-derived sugars to O-layers and A<sub>h</sub>-horizons is very likely. Still, the mean  $\delta^2\text{H}_{n\text{-alkane}}$  and  $\delta^{18}\text{O}_{\text{sugar}}$  values of leaves and A<sub>h</sub>-horizons are almost

identical ( $-134$  versus  $-135\%$  and  $35$  versus  $36\%$ , respectively). Hence, our dataset does not provide evidence for degradation effects and root input affecting  $\delta^2\text{H}_{n\text{-alkane}}$  and  $\delta^{18}\text{O}_{\text{sugar}}$  values of topsoils.

### 3.2 Comparison of $\delta^2\text{H}_{n\text{-alkane}}$ and $\delta^{18}\text{O}_{\text{sugar}}$ results with $\delta^2\text{H}_{\text{prec}}$ or $\delta^{18}\text{O}_{\text{prec}}$ results

The  $\delta^2\text{H}_{n\text{-alkane}}$  values correlate significantly with the weighted mean annual isotope composition of local meteoric water,  $\delta^2\text{H}_{\text{prec}}$  ( $r = 0.3$ ,  $p = 0.04$ ,  $n = 53$ ). However, it does not correlate in a 1:1 relationship ( $\delta^2\text{H}_{\text{prec}} = 0.05 * \delta^2\text{H}_{n\text{-alkane}} - 1.03$ ) and this is the first important indication that  $n$ -alkanes do not directly reflect  $\delta^2\text{H}_{\text{prec}}$ . Instead,  $\delta^2\text{H}_{n\text{-alkane}}$  reflects the isotope signal of local precipitation modified by leaf water enrichment as emphasized by Zech et al. (2015). The isotope composition of precipitation in the Bale Mountains is subjected to altitude, amount, and seasonal effects. The most positive  $\delta^2\text{H}_{\text{prec}}$  and  $\delta^{18}\text{O}_{\text{prec}}$ , as well as the more negative  $\delta^2\text{H}_{\text{prec}}$  and  $\delta^{18}\text{O}_{\text{prec}}$  values, were recorded in the lowermost and highest weather stations of the Bale Mountains, respectively (Lemma et al., 2020). However, the overall significant trend of the altitudinal effect observed in modern precipitation is not reflected in the  $\delta^2\text{H}_{n\text{-alkane}}$  and  $\delta^{18}\text{O}_{\text{sugar}}$  (Fig. 4–2). There is no significant correlation between  $\delta^{18}\text{O}_{\text{sugar}}$  and  $\delta^{18}\text{O}_{\text{prec}}$ . This might indicate that the isotope signal of  $\delta^{18}\text{O}_{\text{prec}}$  is strongly altered prior to the biosynthesis of the sugar biomarkers. Thus, soil water evaporation, leaf water evapo(transpi)ration and seasonality effects are the most likely responsible factors. A recent publication by Strobel et al. (2020) argued that plant-related and/or environmental factors strongly bias the  $\delta^{18}\text{O}_{\text{sugar}}$  signal compared to  $\delta^{18}\text{O}_{\text{prec}}$  and points especially to the significant impact of evapo(transpi)rative soil and leaf water enrichment (Strobel et al., 2020). Similarly, a climate transect study revealed that  $\delta^{18}\text{O}_{\text{hemicellulose}}$  does not reflect  $\delta^{18}\text{O}_{\text{prec}}$  along an Argentinian transect, either (Tuthorn et al., 2014). Overall it can be summarized that our  $\delta^2\text{H}_{n\text{-alkane}}$  and  $\delta^{18}\text{O}_{\text{sugar}}$  values do not directly reflect the isotope composition of precipitation in the Bale Mountains.

The apparent isotope fractionation ( $\epsilon_{\text{app}}$ ) for each investigated plant species (only leaf samples) ranges for hydrogen ( $\epsilon_{\text{app } 2\text{H}}$ ) between  $-180$  to  $-86\%$  and for oxygen ( $\epsilon_{\text{app } 18\text{O}}$ ) between  $+25$  to  $+56\%$ . The  $\epsilon_{\text{app}}$  factors fundamentally depend on three processes (Fig. 4–4, after Strobel et al., 2020). Accordingly, the main processes influencing the imprint of precipitation isotope on biomarkers are soil-water evaporation, leaf-water transpiration, and biosynthetic fractionation. The mean  $\epsilon_{\text{app } 2\text{H}}$  and  $\epsilon_{\text{app } 18\text{O}}$  values of the investigated plant species in the Bale Mountains are  $-128 \pm 6\%$  and  $+40 \pm 2\%$ , respectively. This is in a good agreement and within the range of results reported from a winter rainfall zone transect study in South Africa (Strobel et al., 2020).

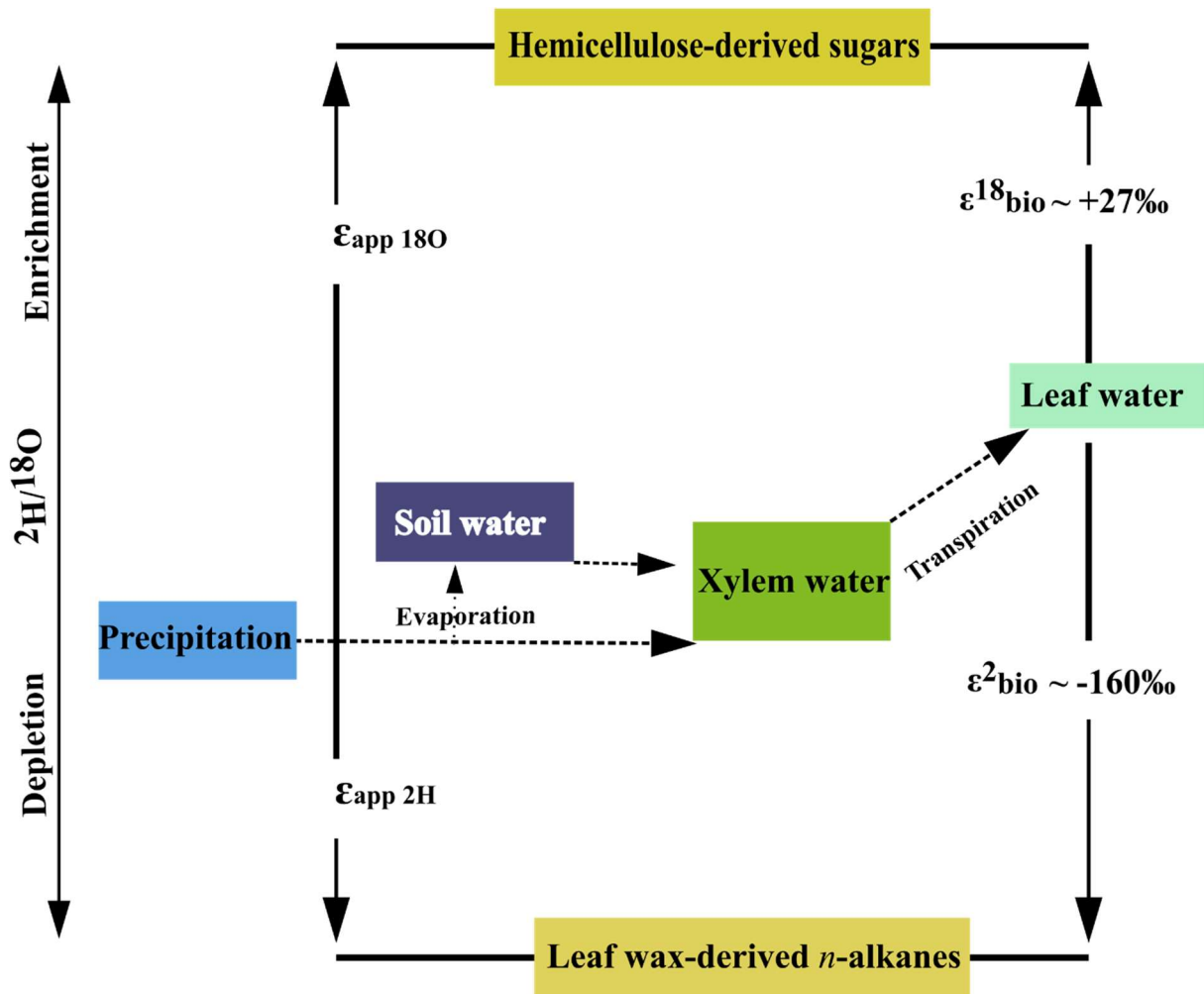


**Fig. 4–4:** Conceptual model demonstrating the hydrogen-isotope and oxygen-isotope relationships, between precipitation, leaf water, and leaf wax-derived *n*-alkanes as well as hemicellulose-derived sugars (after Strobel et al., 2020).  $\epsilon_{\text{app } 2\text{H}}$  = apparent hydrogen-isotope fractionation;  $\epsilon_{\text{app } 18\text{O}}$  = apparent oxygen-isotope fractionation;  $\epsilon^{18}_{\text{bio}}$  = biosynthetic oxygen-isotope fractionation;  $\epsilon^2_{\text{bio}}$  = biosynthetic hydrogen-isotope fractionation.

In the present study, there is no significant correlation between apparent isotope fractionation and mean day time temperature ( $\epsilon_{\text{app } 18\text{O}}$ ,  $r = 0.1$ ,  $p = 0.5$  and  $\epsilon_{\text{app } 2\text{H}}$ ,  $r = 0.3$ ,  $p = 0.1$ ). Thus, the apparent isotope fractionation is not influenced by temperature-related evapo(transpi)rative enrichment. This is in agreement with the results of Strobel et al. (2020) who found that neither  $\epsilon_{\text{app } 2\text{H}}$  nor  $\epsilon_{\text{app } 18\text{O}}$  is significantly dependent on mean annual temperature (MAT).



### 3.3 Interspecies comparison of $\delta^2\text{H}_{n\text{-alkane}}$ and $\delta^{18}\text{O}_{\text{sugar}}$ results from keystone plant species in the Bale Mountains

Combining all leaf, O-layer and A<sub>h</sub>-horizon data, the comparison of the  $\delta^2\text{H}_{n\text{-alkane}}$  values between the plant species under study depicts significant differences (Fig. 4–5a). More specifically, *Erica arborea* and *Erica trimera* yielded the least negative median  $\delta^2\text{H}_{n\text{-alkane}}$  values, whereas *Festuca abyssinica* yielded the most negative median  $\delta^2\text{H}_{n\text{-alkane}}$  value (Fig. 4–5a). Albeit the  $\delta^{18}\text{O}_{\text{sugar}}$  values show no significant difference amongst the dominant plant species (Fig. 4–5b), they reveal the same trends as the  $\delta^2\text{H}_{n\text{-alkane}}$  results. Particularly, *E. arborea* and *E. trimera* depicted the most positive median  $\delta^{18}\text{O}_{\text{sugar}}$  values, whereas *F. abyssinica* depicted the least positive median  $\delta^{18}\text{O}_{\text{sugar}}$  value (Fig. 4–5b). The mean  $\delta^2\text{H}_{n\text{-alkane}}$  and  $\delta^{18}\text{O}_{\text{sugar}}$  values of *E. arborea* and *E. trimera* are  $-114$  and  $-109$ ‰, and  $+37$  and  $+36$ ‰, respectively. These very close mean  $\delta^2\text{H}_{n\text{-alkane}}$  and  $\delta^{18}\text{O}_{\text{sugar}}$  values of the two *Erica* species likely reflect the monophyletic nature (Guo et al., 2014).

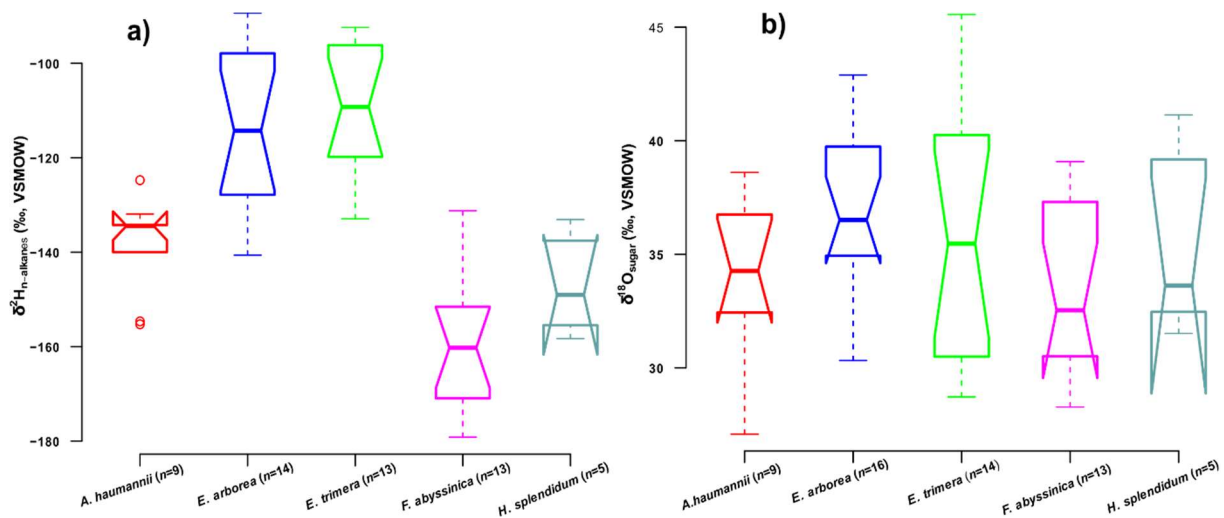


**Fig. 4–5:** Variations of  $\delta^2\text{H}_{n\text{-alkane}}$  (a) and  $\delta^{18}\text{O}_{\text{sugar}}$  (b) between keystone plant species. The notched box plots indicate the median (solid lines between the boxes), interquartile range (IQR) with upper (75%), and lower (25%) quartiles and outliers (empty circle). The notches display the confidence interval around the median within  $\pm 1.57 \cdot \text{IQR} / \sqrt{n}$ .

One might expect that the above described plant-specific differences can be explained with the altitude-dependent different occurrence of the investigated plant species and altitude-dependent  $\delta^2\text{H}_{\text{prec}}$  and  $\delta^{18}\text{O}_{\text{prec}}$  variability. Indeed, the  $\delta^2\text{H}_{\text{prec}}$  and  $\delta^{18}\text{O}_{\text{prec}}$  values in the Bale Mountains exhibit spatial variance along the altitudinal gradient with isotope lapse rates of  $-0.52$ ‰  $\cdot 100 \text{ m}^{-1}$  and  $-0.11$ ‰  $\cdot 100 \text{ m}^{-1}$ , respectively (Lemma et al., 2020). This corresponds roughly to a range of 5 and 1‰ for  $\delta^2\text{H}_{\text{prec}}$  and  $\delta^{18}\text{O}_{\text{prec}}$ , respectively, along the investigated altitudinal

transect (3226 and 4375 m a.s.l.). These ranges are, however, too small to explain the observed large  $\delta^2\text{H}_{n\text{-alkane}}$  and  $\delta^{18}\text{O}_{\text{sugar}}$  variability along the transect (Fig. 4–2). Strikingly, the median  $\delta^2\text{H}_{n\text{-alkane}}$  and  $\delta^{18}\text{O}_{\text{sugar}}$  values of *F. abyssinica* are the lowest compared to the other investigated plant species. This can be attributed to physiological and biochemical differences and the fact that *F. abyssinica* (grass) is a monocot, whereas the other plant species are dicots. The leaves of monocots and dicots differ in structure, location and timing of lipid synthesis (Sachse et al., 2012). The growth of grasses is associated with intercalary meristems. They occur at the base of the grass leaf blade, where leaf water is not fully  $^2\text{H}$ - and  $^{18}\text{O}$ -enriched. Thus, newly synthesized lipids and sugars at the base of grass leaves do not incorporate the full leaf water enrichment signal, which is called  $^2\text{H}_{n\text{-alkane}}$  and  $^{18}\text{O}_{\text{sugar}}$  “signal damping or dampening effect” (Hepp et al., 2020, 2019). On the other hand, the median  $\delta^2\text{H}_{n\text{-alkane}}$  and  $\delta^{18}\text{O}_{\text{sugar}}$  values of *E. arborea* and *E. trimera* are the highest in comparison with other species and show strong leaf water enrichment. The intermediate  $\delta^2\text{H}_{n\text{-alkane}}$  and  $\delta^{18}\text{O}_{\text{sugar}}$  values for *A. haumannii* and *H. splendidum* might be attributed to plant physiological and biochemical differences or microclimatic conditions affecting RH values and thus leaf water enrichment as compared to *Erica* and *F. abyssinica*.

Furthermore, there is a significant difference in  $\epsilon_{\text{app } 2\text{H}}$  between the keystone plant species in the Bale Mountains. Unlike other species, *E. arborea* (−94‰) and *E. trimera* (−92‰) have the least negative and *F. abyssinica* (−161‰) has the most negative  $\epsilon_{\text{app } 2\text{H}}$ . It is known that C3 graminoid (Sachse et al., 2012) and C3 grasses (Gamarra et al., 2016) exhibited the most negative  $\epsilon_{\text{app } 2\text{H}}$  compared to shrubs and trees. Such species-dependent variation of  $\epsilon_{\text{app } 2\text{H}}$  can be attributed to intrinsic factors (e.g., plant physiological, phenological, photosynthesis pathway and biosynthesis-related), plant growth form, place and timing of leaf-wax synthesis, and stomatal nature (Gao et al., 2015; Griepentrog et al., 2019; Liu and Yang, 2008; Sachse et al., 2012; Strobel et al., 2020). Therefore, caution must be given in terms of vegetation change when interpreting  $\delta^2\text{H}_{n\text{-alkane}}$  for paleoclimate reconstruction. There is no significant difference in  $\epsilon_{\text{app } 18\text{O}}$  among keystone plant species in the Bale Mountains and *H. splendidum* shows the least positive  $\epsilon_{\text{app } 18\text{O}}$  value (26‰). This finding might demonstrate that  $\epsilon_{\text{app } 18\text{O}}$  is not strongly sensitive to vegetation type rather climate-related evapo(transpi)rative enrichment. Previous studies of Tuthorn et al. (2014) and Strobel et al. (2020) described  $\delta^{18}\text{O}_{\text{sugar}}$  and  $\epsilon_{\text{app } 18\text{O}}$  are significantly influenced by evapotranspiration and aridity index.

### 3.4 Coupled $\delta^2\text{H}_{n\text{-alkane}}$ and $\delta^{18}\text{O}_{\text{sugar}}$ biomarker results

#### 3.4.1 Reconstructed $\delta^2\text{H}_{\text{leaf water}}$ and $\delta^{18}\text{O}_{\text{leaf water}}$ as well as $\delta^2\text{H}_{\text{source water}}$ and $\delta^{18}\text{O}_{\text{source water}}$

The basic principle of the coupled  $\delta^2\text{H}_{n\text{-alkane}}$  and  $\delta^{18}\text{O}_{\text{sugar}}$  approach is based on the assumption that long-chain *n*-alkanes and pentose sugars are leaf-derived and reflect the isotope composition of leaf water (Hepp et al., 2019, 2017; Tuthorn et al., 2015; Zech et al., 2015, 2013b). The isotope composition of reconstructed leaf water is determined by the isotope composition of local precipitation and evaporative leaf water enrichment. However, soil-water enrichment cannot be excluded but is considered to be negligible. Therefore, the reconstructed  $\delta^2\text{H}_{\text{leaf water}}$  and  $\delta^{18}\text{O}_{\text{leaf water}}$  allow us to reconstruct  $\delta^2\text{H}_{\text{source water}}$  and  $\delta^{18}\text{O}_{\text{source water}}$  as well as *d*-excess and RH. These valuable proxies and additional information can support a better understanding of the paleoclimate history, which cannot be addressed by a single isotope study. The reconstructed  $\delta^2\text{H}_{\text{leaf water}}$  and  $\delta^{18}\text{O}_{\text{leaf water}}$  values range between  $-31$  to  $84\text{‰}$  ( $\bar{x} = 31 \pm 4\text{‰}$ ) and  $0.1$  to  $18\text{‰}$  ( $\bar{x} = 8 \pm 0.6\text{‰}$ ), respectively (Fig. 4–2). Most of the reconstructed leaf water data plot below the GMWL (Fig. 4–6). The reconstructed leaf water data plotting below the GMWL is a typical feature of evaporation loss.

By applying a biosynthetic fractionation factor of  $-160\text{‰}$ , the reconstructed  $\delta^2\text{H}_{\text{leaf water}}$  values highlight that the *n*-alkanes of *F. abyssinica* (Fig. 4–5a) reflect quite accurately and precisely the weighted mean annual  $\delta^2\text{H}_{\text{prec}}$  ( $-2.7 \pm 2\text{‰}$ ) of the Bale Mountains (Lemma et al., 2020). However, it is known that the effect of evaporative leaf water isotope enrichment of grasses is negligible (Helliker and Ehleringer, 2002; McInerney et al., 2011). By contrast, the reconstructed  $\delta^2\text{H}_{\text{leaf water}}$  values of *E. arborea* and *E. trimera* (Fig. 4–5a) do not reflect accurately and precisely the weighted mean annual  $\delta^2\text{H}_{\text{prec}}$  and the reconstructed  $\delta^2\text{H}_{\text{leaf water}}$  is enriched compared to  $\delta^2\text{H}_{\text{prec}}$  by up to  $+55 \pm 5\text{‰}$  (Fig. 4–5a). One well known and widely accepted factor responsible for this finding is leaf water enrichment. For instance, Zech et al. (2015) emphasized that  $\delta^2\text{H}_{n\text{-alkane}}$  data from a climate transect along the southern slopes of Mt. Kilimanjaro do not reflect  $\delta^2\text{H}_{\text{prec}}$  either and explained this with a strongly variable degree of leaf water enrichment along the altitudinal transect. Hence, our datasets clearly indicate that unlike *Erica* (dicots), the reconstructed  $\delta^2\text{H}_{\text{leaf water}}$  of *F. abyssinica* (monocot) does not fully expose to evaporative leaf water enrichment due to signal dampening.

Similarly, considering a biosynthetic fractionation factor of  $+27\text{‰}$  (Cernusak et al., 2003), the reconstructed  $\delta^{18}\text{O}_{\text{leaf water}}$  values of all investigated plant species (Fig. 4–5b) do not reflect the isotope composition of precipitation,  $\delta^{18}\text{O}_{\text{prec}}$  ( $-3.3 \pm 0.4\text{‰}$ ) in the Bale Mountains (Lemma et al., 2020). More specifically, the reconstructed  $\delta^{18}\text{O}_{\text{leaf water}}$  values of *E. arborea* and *E. trimera*

are enriched compared to  $\delta^{18}\text{O}_{\text{prec}}$  by up to  $+9 \pm 1\%$  (Fig. 4–5b). Indeed, yet it is not significant, the reconstructed  $\delta^{18}\text{O}_{\text{leaf water}}$  is also species-dependent. Tree ring research has shown that cellulose does not reflect the full leaf water  $\delta^{18}\text{O}$  enrichment signal (Gessler et al., 2013). Additionally, results from climate chamber experiments indicate that  $\delta^{18}\text{O}_{\text{leaf water}}$  values, reconstructed from sugar biomarker, are enriched compared to plant source water by up to  $+25\%$  (Zech et al., 2014a).

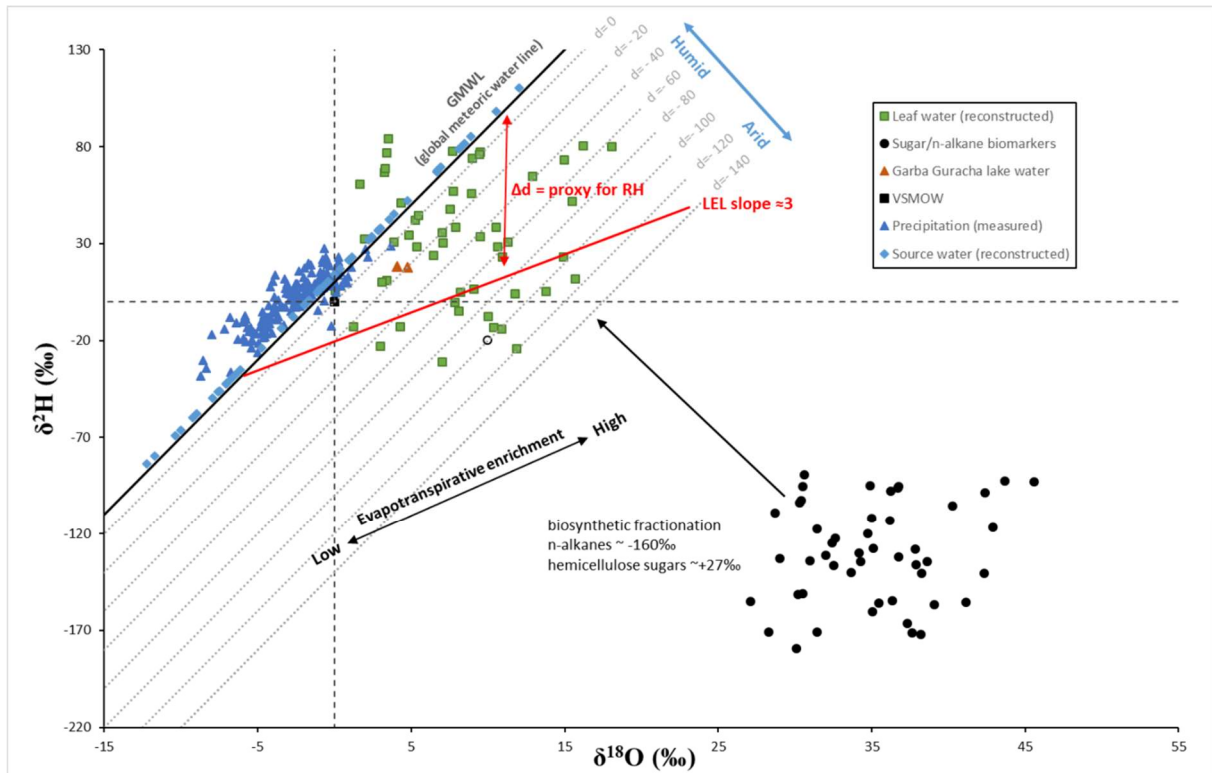


**Fig. 4–6:**  $\delta^{18}\text{O}$  versus  $\delta^2\text{H}$  diagram illustrating the conceptual framework of the coupled (paleo-) hygrometer approach after Zech et al., (2013b). Data are plotted for measured source water/precipitation (blue solid triangle), measured  $\delta^2\text{H}_{n\text{-alkane}}$ , and  $\delta^{18}\text{O}_{\text{sugar}}$  (black solid circle), reconstructed leaf water (green solid rectangle), measured Garba Guracha lake water (brown solid triangle).

Moreover, the coupled  $\delta^2\text{H}_{n\text{-alkane}}$  and  $\delta^{18}\text{O}_{\text{sugar}}$  approach allows us to reconstruct the isotope composition of source water as intersect of the local evaporation line (LEL) with the GMWL (Fig. 4–6). The reconstructed  $\delta^2\text{H}_{\text{source water}}$  and  $\delta^{18}\text{O}_{\text{source water}}$  values range from  $-84$  to  $110\%$  ( $\bar{x} = 8.6 \pm 7\%$ ) and  $-12$  to  $12\%$  ( $\bar{x} = -0.7 \pm 0.8\%$ ) (Fig. 4–7), respectively. Unlike  $\delta^2\text{H}_{\text{prec}}$  and  $\delta^{18}\text{O}_{\text{prec}}$ , the reconstructed  $\delta^2\text{H}_{\text{source water}}$  and  $\delta^{18}\text{O}_{\text{source water}}$  shows a large scattering (Fig. 4–7). The mean reconstructed  $\delta^2\text{H}_{\text{source water}}$  and  $\delta^{18}\text{O}_{\text{source water}}$  values reveal slight isotope enrichment as compared with the modern-day isotope composition of  $\delta^2\text{H}_{\text{prec}}$  ( $-2.7 \pm 2\%$ ) and  $\delta^{18}\text{O}_{\text{prec}}$  ( $-3.3 \pm 0.4\%$ ) in the Bale Mountains, respectively (Lemma et al., 2020). Despite the large

scattering of the reconstructed source water values this finding demonstrates that the coupled  $\delta^2\text{H}_{n\text{-alkane}}\text{-}\delta^{18}\text{O}_{\text{sugar}}$  approach allows to reconstruct the isotope composition of source water quite accurately.

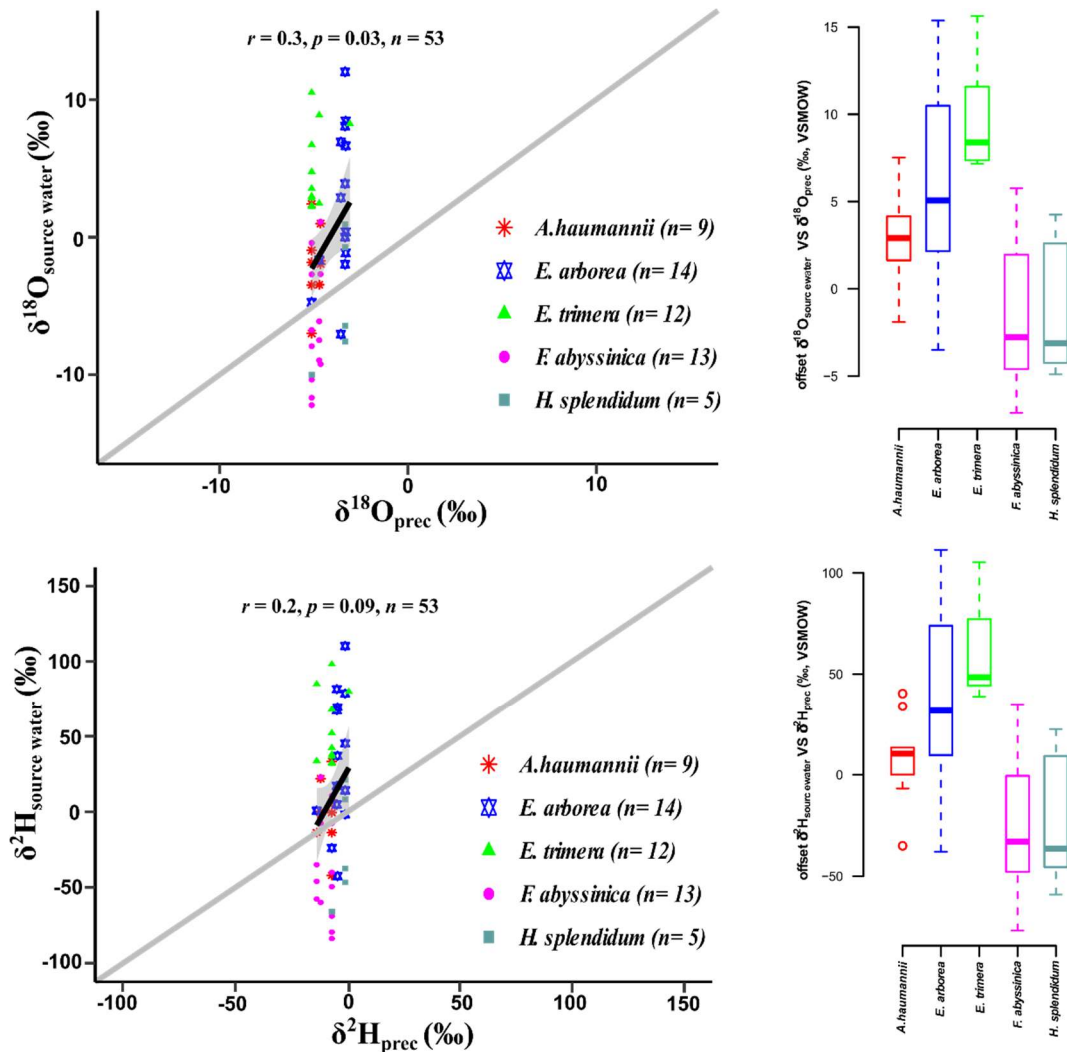


**Fig. 4–7:** The scatter plots to the left show the correlations between  $\delta^{18}\text{O}_{\text{source water}}$  and  $\delta^{18}\text{O}_{\text{prec}}$  as well as  $\delta^2\text{H}_{\text{source water}}$  and  $\delta^2\text{H}_{\text{prec}}$ , respectively. The linear regression lines (black line), correlation coefficients ( $r$ ), 95% confidence intervals (grey area) and significance values ( $p$ ) as well as the 1:1 regression lines (grey lines) are provided for each diagram. The box plots to the right illustrate the offset of  $\delta^{18}\text{O}_{\text{source water}}$  to  $\delta^{18}\text{O}_{\text{prec}}$  and  $\delta^2\text{H}_{\text{source water}}$  to  $\delta^2\text{H}_{\text{prec}}$ , respectively, for keystone plant species. The plots indicate the median (solid line between the boxes), interquartile range (IQR) with upper (75%) and lower (25%) quartiles and outliers (empty circles).

The correlation and offsets between the reconstructed source water and respective  $\delta^{18}\text{O}_{\text{prec}}$  as well as  $\delta^2\text{H}_{\text{prec}}$  are shown in Figure 4-7. The offsets between the reconstructed source water and respective  $\delta^2\text{H}_{\text{prec}}$  and  $\delta^{18}\text{O}_{\text{prec}}$  show a highly significant difference ( $p = 0.001$ ,  $n = 53$ ) among

the investigated plant species (box plots of Fig. 4–7). The median offset of *F. abyssinica* ( $\delta^{18}\text{O} = -3\text{‰}$ ;  $\delta^2\text{H} = -33\text{‰}$ ) and *H. splendidum* ( $\delta^{18}\text{O} = -3\text{‰}$ ;  $\delta^2\text{H} = -36\text{‰}$ ) are very close to each other and *E. trimera* ( $\delta^{18}\text{O} = 8\text{‰}$ ;  $\delta^2\text{H} = 48\text{‰}$ ) exhibits a markedly larger median offset than the other species (Fig. 4–7).

### 3.4.2 Deuterium excess, reconstructed relative humidity and its paleoclimate implication

The distance between the reconstructed leaf water and GMWL can be described as *d*-excess, which is the intercept of the meteoric water line (Dansgaard, 1964), and serves as a proxy for RH (Hepp et al., 2017; 2019). The reconstructed *d*-excess values calculated using equation (5) range between  $-105$  to  $+56\text{‰}$ . The most positive reconstructed *d*-excess values are likely caused by an overestimation of the  $\delta^2\text{H}$  and/or an underestimation of the  $\delta^{18}\text{O}$  values. The most negative reconstructed *d*-excess values are likely caused by an underestimation of the  $\delta^2\text{H}$  and/or an overestimation of the  $\delta^{18}\text{O}$  values. The actual RH ranges between 69 and 82% ( $\bar{x} = 80 \pm 3.4\%$ ) (Fig. 4–8). The reconstructed RH calculated using equation (6) reveals a much wider range of 40 to 121% ( $\bar{x} = 78 \pm 21\%$ ), with eight anomalous values above 100% (Fig. 4–8). These anomalies can be explained by several uncertainties related to  $\Delta d$ ,  $\epsilon^*$ , and  $C_k$  values used in equation (6). The uncertainties of  $\Delta d$  mainly arise from analytical errors associated with the individual  $\delta^2\text{H}_{n\text{-alkane}}$  and  $\delta^{18}\text{O}_{\text{sugar}}$  measurement as well as uncertainties of the  $\epsilon_{\text{bio}}$ . In approximation, the coupled approach of Zech et al. (2013) suggests temperature-independent constant  $\epsilon_{\text{bio}}$  values. However, concerning e.g.  $\delta^{18}\text{O}$ , this value is very likely an underestimation. Slightly higher  $\epsilon_{\text{bio}}$  values for  $^{18}\text{O}$  and  $^2\text{H}$  of  $+2\text{‰}$  and  $+10\text{‰}$  would increase the reconstructed RH by  $+8\%$  and  $6\%$ , respectively (Hepp et al., 2017).

The actual mean annual day time RH measured along the transect is  $80 \pm 3.4\%$ , which is  $+2 \pm 18\%$  higher than the reconstructed mean RH. The reconstructed RH is humidity normalized to leaf temperature. Usually, leaf temperature is higher than the actual ambient temperature (Gates, 1980). Thus, the difference between actual and reconstructed RH might be associated with leaf-air temperature differences (Hepp et al., 2017; Zech et al., 2013b). Additionally, our approach does not consider evaporative enrichment of soil water (Hepp et al., 2015; Tuthorn et al., 2015; Zech et al., 2013b). Moreover, most leaf-derived biomarkers are biosynthesized at an early stage of leaf ontogeny (Gershenson et al., 2000; Tipple et al., 2013) and may not reflect the mean annual isotope composition of precipitation, but rather the isotope composition of precipitation during the growing season. Therefore, the model may not capture the mean annual RH seen during photosynthetically active leaves.

Either the reconstructed  $d$ -excess or RH correlate highly significant and negatively with  $\delta^{18}\text{O}_{\text{leaf water}}$  ( $r = -0.7$ ,  $p < 0.0001$ ,  $n = 53$ ) and positively with  $\delta^2\text{H}_{\text{leaf water}}$  ( $r = 0.6$ ,  $p < 0.0001$ ,  $n = 53$ ). This result might demonstrate that signal changes in  $\delta^{18}\text{O}_{\text{leaf water}}$  due to RH are dissociated from signal changes in  $\delta^{18}\text{O}_{\text{prec}}$ . The negative correlation between the reconstructed RH and  $\delta^{18}\text{O}_{\text{leaf water}}$ , apparent in the present study, is also reported previously by Zech et al. (2013b). Thus, due to evaporation, the lower the reconstructed RH is the higher isotopically enriched leaf water. Moreover, the reconstructed RH values correlate highly significantly and positively with reconstructed  $\delta^2\text{H}_{\text{source water}}$  and  $\delta^{18}\text{O}_{\text{source water}}$  ( $r = 0.9$ ,  $p < 0.0001$ ,  $n = 53$ ). A similar finding was reported by Hepp et al. (2017) applying the coupled  $\delta^2\text{H}_{n\text{-alkane}}$  and  $\delta^{18}\text{O}_{\text{sugar}}$  approach in the Mt. Kilimanjaro region.

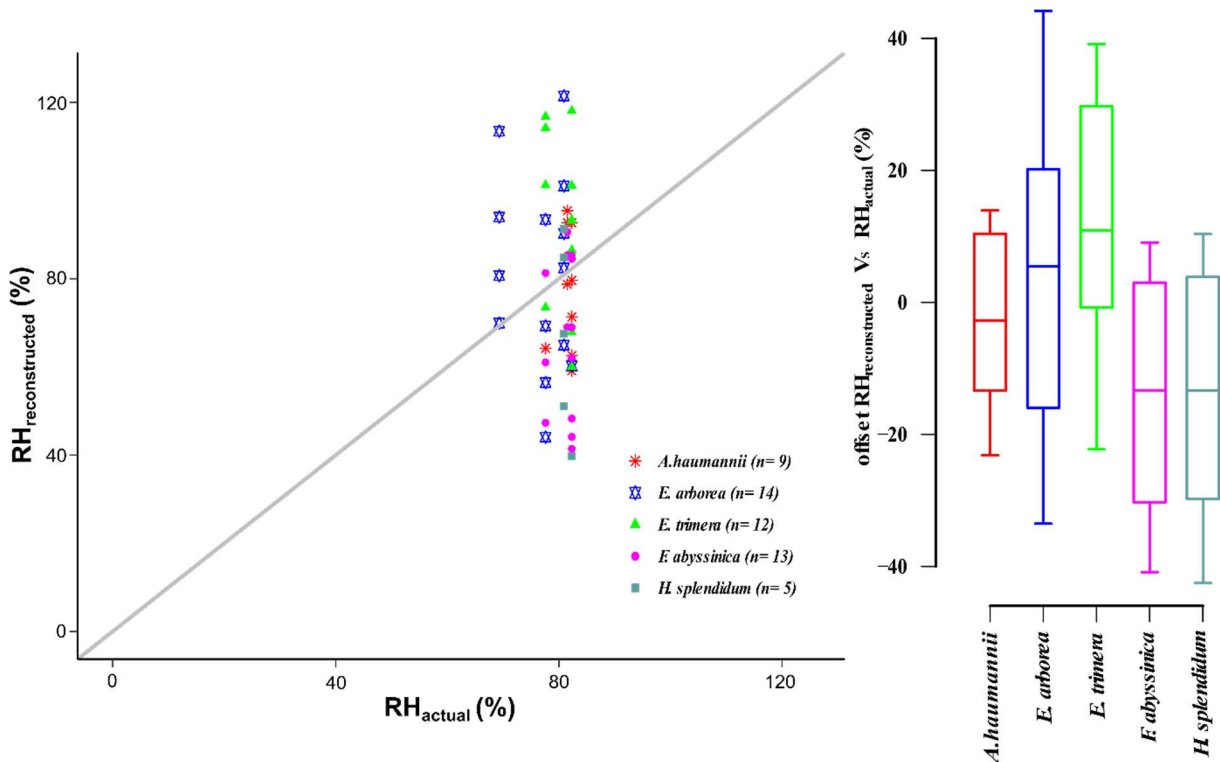


**Fig. 4–8:** The scatter plot to the left shows the correlation between reconstructed RH and actual RH. The linear regression line (black line), correlation coefficient ( $r$ ), 95% confidence interval (grey area), and significance value ( $p$ ) as well as the 1:1 regression line (grey line) are provided. The box plot to the right illustrates the offset of reconstructed RH to actual RH for key stone plant species. The plots indicate the median (solid line between the boxes), interquartile range (IQR) with upper (75%) and lower (25%) quartiles.

## 4. Conclusions

The compound-specific stable hydrogen and oxygen isotope composition of biomarkers (*n*-alkanes and sugars) analysed from leaves, O-layers, and A<sub>h</sub>-horizons along an altitudinal transect in the Bale Mountains were evaluated. There are no systematic  $\delta^2\text{H}_{n\text{-alkane}}$  and  $\delta^{18}\text{O}_{\text{sugar}}$  trends and significant differences between leaves and corresponding O-layers, and A<sub>h</sub>-horizons, respectively. Hence, there is no evidence from our dataset for degradation and underground root input affecting  $\delta^2\text{H}_{n\text{-alkane}}$  and  $\delta^{18}\text{O}_{\text{sugar}}$  values of topsoils.

The keystone plant species in the Bale Mountains are characterized by statistically significant species-dependent  $\delta^2\text{H}_{n\text{-alkane}}$  values and, albeit not significant, also  $\delta^{18}\text{O}_{\text{sugar}}$  values. Substantial species-specific apparent isotope fractionation highlights the importance of investigating apparent as well as biosynthetic isotope fractionation factor of the representative flora at a given geographical region. Thus, vegetation shifts should be considered before applying especially  $\delta^2\text{H}_{n\text{-alkane}}$  records for paleoclimate and -environmental reconstructions.

Additionally, we reconstructed the isotope composition of leaf water and by the use of the coupled  $\delta^2\text{H}$  and  $\delta^{18}\text{O}$  approach, firstly introduced by Zech et al. (2013b), we calculated the *d*-excess and RH. The reconstructed  $\delta^2\text{H}_{\text{leaf water}}$  values of *F. abyssinica* reflect the isotope composition of weighted mean annual  $\delta^2\text{H}_{\text{prec}}$  with a systematic offset of biosynthetic fractionation factor in contrast to *E. arborea* and *E. trimera*. The comparison of isotopically enriched reconstructed  $^2\text{H}_{\text{leaf water}}$  and  $^{18}\text{O}_{\text{leaf water}}$  with weighted mean annual precipitation reveals the effect of evaporative leaf water enrichment prior to biosynthesis. The reconstructed *d*-excess enables us to reconstruct RH. The actual mean annual day time RH measured in the Bale Mountains is  $+2 \pm 18\%$  higher than the reconstructed mean RH. Although several simplified assumptions challenge our interpretation, the coupled  $\delta^2\text{H}_{n\text{-alkane}}\text{-}\delta^{18}\text{O}_{\text{sugar}}$  (paleo-) hygrometer approach holds great potential for deriving additional paleoclimatic information compared to single isotope approaches.

## Acknowledgments

The authors are indebted for the scientific collaboration and technical support obtained from Addis Ababa University, Ethiopian Biodiversity Institute, and Ethiopian Wildlife Conservation Authority. We appreciate Heike Maennicke and Marianne Benesch for laboratory assistance and measurement of compound-specific isotopes, respectively. Furthermore, we are also grateful for the assistance provided by Betelhem Mekonnen and Tobias Bromm during sample



collection and sugar biomarker analyses. Mr. Bruk Lemma greatly appreciates the funding via a Ph.D. fellowship by the Catholic Academic Exchange Services (KAAD).

## Declarations

**Funding:** This research work was funded by the German Research Foundation within the DFG Research Unit ‘The Mountain Exile Hypothesis’ (DFG: ZE 844/10–1, GL 327/18–1,2, ZE 154/70-1,2). We acknowledge the financial support within the funding programme Open Access Publishing by the DFG.

**Conflicts of interest:** The authors have no conflicts of interest to declare that are relevant to the content of this article.

**Availability of data and materials:** Supplementary data are provided and available <https://doi.org/10.5281/zenodo.4072011>

**Code availability:** Not applicable

**Authors Contributions:** Sample collection, Formal analysis and Investigation, Writing – original draft: [Bruk Lemma]; Formal analysis, Writing – review and editing: [Lucas Bittner]; Funding acquisition, Resources, Writing – review and editing, Supervision: [Bruno Glaser]; Writing – review and editing, Supervision: [Seifu Kebede]; Writing – review and editing, Supervision: [Sileshi Nemomissa]; Funding acquisition, Sample collection, Writing – review and editing, Supervision: [Wolfgang Zech]; Funding acquisition, Conceptualization, Methodology, Writing – review and editing, Supervision: [Michael Zech].

## References

- Allison, G.B., Gat, J.R., Leaney, F.W., 1985. The relationship between deuterium and oxygen-18 delta values in leaf water. *Chemical Geology: isotope geoscience section* 58, 145–156.
- Amelung, W., Cheshire, M.V., Guggenberger, G., 1996. Determination of neutral and acidic sugars in soil by capillary gas-liquid chromatography after trifluoroacetic acid hydrolysis. *Soil Biology and Biochemistry* 28, 1631–1639.
- Araguás-Araguás, L., Froehlich, K., Rozanski, K., 2000. Deuterium and oxygen-18 isotope composition of precipitation and atmospheric moisture. *Hydrological processes* 14, 1341–1355.
- Billi, P., 2015. Geomorphological landscapes of Ethiopia, in: *Landscapes and Landforms of Ethiopia*. Springer, pp. 3–32.

- Bittner, L., Bliedtner, M., Grady, D., Gil-Romera, G., Martin-Jones, C., Lemma, B., Mekonnen, B., Lamb, H.F., Yang, H., Glaser, B., 2020. Revisiting afro-alpine Lake Garba Guracha in the Bale Mountains of Ethiopia: rationale, chronology, geochemistry, and paleoenvironmental implications. *Journal of Paleolimnology* 1–22.
- Brittingham, A., Hren, M.T., Hartman, G., 2017. Microbial alteration of the hydrogen and carbon isotopic composition of n-alkanes in sediments. *Organic Geochemistry* 107, 1–8.
- Buggle, B., Zech, M., 2015. New frontiers in the molecular based reconstruction of Quaternary paleovegetation from loess and paleosols. *Quaternary International* 372, 180–187.
- Cernusak, L.A., Wong, S.C., Farquhar, G.D., 2003. Oxygen isotope composition of phloem sap in relation to leaf water in *Ricinus communis*. *Functional Plant Biology* 30, 1059–1070.
- Craig, H., 1961. Isotopic variations in meteoric waters. *Science* 133, 1702–1703.
- Craig, H., Gordon, L.I., 1965. Deuterium and oxygen 18 variations in the ocean and the marine atmosphere.
- Dansgaard, W., 1964. Stable isotopes in precipitation. *Tellus* 16, 436–468.
- Dongmann, G., Nürnberg, H.W., Förstel, H., Wagener, K., 1974. On the enrichment of H<sub>2</sub><sup>18</sup>O in the leaves of transpiring plants. *Radiation and Environmental Biophysics* 11, 41–52.
- Eglinton, G., Hamilton, R.J., 1967. Leaf epicuticular waxes. *Science* 156, 1322–1335.
- Eglinton, T.I., Eglinton, G., 2008. Molecular proxies for paleoclimatology. *Earth and Planetary Science Letters* 275, 1–16.
- Ehleringer, J.R., Phillips, S.L., Schuster, W.S., Sandquist, D.R., 1991. Differential utilization of summer rains by desert plants. *Oecologia* 88, 430–434.
- Ellsworth, P.Z., Williams, D.G., 2007. Hydrogen isotope fractionation during water uptake by woody xerophytes. *Plant and Soil* 291, 93–107.
- Farquhar, G.D., Cernusak, L.A., Barnes, B., 2007. Heavy water fractionation during transpiration. *Plant physiology* 143, 11–18.
- Feakins, S.J., Sessions, A.L., 2010. Controls on the D/H ratios of plant leaf waxes in an arid ecosystem. *Geochimica et Cosmochimica Acta* 74, 2128–2141.
- Flanagan, L.B., Comstock, J.P., Ehleringer, J.R., 1991. Comparison of Modeled and Observed Environmental Influences on the Stable Oxygen and Hydrogen Isotope Composition of Leaf Water in *Phaseolus vulgaris* L. *Plant Physiol.* 96, 588.
- Friis, I., 1986. Zonation of Forest Vegetation on the South Slope of Bale Mountains, South Ethiopia. *Sinet-an Ethiopian Journal of Science* 29–44.

- Gamarra, B., Sachse, D., Kahmen, A., 2016. Effects of leaf water evaporative  $^2\text{H}$ -enrichment and biosynthetic fractionation on leaf wax n-alkane  $\delta^2\text{H}$  values in  $\text{C}_3$  and  $\text{C}_4$  grasses. *Plant, cell & environment* 39, 2390–2403.
- Gao, L., Guimond, J., Thomas, E., Huang, Y., 2015. Major trends in leaf wax abundance,  $\delta^2\text{H}$  and  $\delta^{13}\text{C}$  values along leaf venation in five species of  $\text{C}_3$  plants: physiological and geochemical implications. *Organic Geochemistry* 78, 144–152.
- Gat, J.R., Bowser, C., 1991. The heavy isotope enrichment of water in coupled evaporative systems, in: *Stable Isotope Geochemistry: A Tribute to Samuel Epstein*. The Geochemical Society St. Louis, pp. 159–168.
- Gat, J.R., Yakir, D., Goodfriend, G., Fritz, P., Trumborn, P., Lipp, J., Gev, I., Adar, E., Waisel, Y., 2007. Stable isotope composition of water in desert plants. *Plant and soil* 298, 31–45.
- Gates, D.M., 1980. *Biophysical ecology*. Springer-Verlag New York.
- Gershenzon, J., McConkey, M.E., Croteau, R.B., 2000. Regulation of monoterpene accumulation in leaves of peppermint. *Plant Physiology* 122, 205–214.
- Gessler, A., Brandes, E., Buchmann, N., Helle, G., Rennenberg, H., Barnard, R.L., 2009. Tracing carbon and oxygen isotope signals from newly assimilated sugars in the leaves to the tree-ring archive. *Plant, Cell & Environment* 32, 780–795.
- Gessler, A., Brandes, E., Keitel, C., Boda, S., Kayler, Z.E., Granier, A., Barbour, M., Farquhar, G.D., Treydte, K., 2013. The oxygen isotope enrichment of leaf-exported assimilates—does it always reflect lamina leaf water enrichment? *New Phytologist* 200, 144–157.
- Gil-Romera, G., Adolf, C., Benito, B.M., Bittner, L., Johansson, M.U., Grady, D.A., Lamb, H.F., Lemma, B., Fekadu, M., Glaser, B., 2019. Long-term fire resilience of the Ericaceous Belt, Bale Mountains, Ethiopia. *Biology letters* 15, 20190357.
- Glaser, B., Zech, W., 2005. Reconstruction of climate and landscape changes in a high mountain lake catchment in the Gorkha Himal, Nepal during the Late Glacial and Holocene as deduced from radiocarbon and compound-specific stable isotope analysis of terrestrial, aquatic and microbial biomarkers. *Organic Geochemistry* 36, 1086–1098.
- Gonfiantini, R., Roche, M.-A., Olivry, J.-C., Fontes, J.-C., Zuppi, G.M., 2001. The altitude effect on the isotopic composition of tropical rains. *Chemical Geology* 181, 147–167.
- Griepentrog, M., De Wispelaere, L., Bauters, M., Bodé, S., Hemp, A., Verschuren, D., Boeckx, P., 2019. Influence of plant growth form, habitat and season on leaf-wax n-alkane hydrogen-isotopic signatures in equatorial East Africa. *Geochimica et Cosmochimica Acta* 263, 122–139.

- Guo, N., Gao, J., He, Y., Zhang, Z., Guo, Y., 2014. Variations in leaf epicuticular n-alkanes in some *Broussonetia*, *Ficus* and *Humulus* species. *Biochemical systematics and ecology* 54, 150–156.
- Hedberg, O., 1964. Features of afroalpine plant ecology. Uppsala: Svenska växtgeografiska Sällskapet. *Acta Phytogeographica Suecica*; 49.
- Helliker, B.R., Ehleringer, J.R., 2002. Grass blades as tree rings: environmentally induced changes in the oxygen isotope ratio of cellulose along the length of grass blades. *New Phytologist* 155, 417–424.
- Hepp, J., Schäfer, I.K., Lanny, V., Franke, J., Bliedtner, M., Rozanski, K., Glaser, B., Zech, M., Eglinton, T.I., Zech, R., 2020. Evaluation of bacterial glycerol dialkyl glycerol tetraether and  $^2\text{H}$ - $^{18}\text{O}$  biomarker proxies along a central European topsoil transect. *Biogeosciences* 17, 741–756.
- Hepp, J., Tuthorn, M., Zech, R., Mügler, I., Schlütz, F., Zech, W., Zech, M., 2015. Reconstructing lake evaporation history and the isotopic composition of precipitation by a coupled  $\delta^{18}\text{O}$ - $\delta^2\text{H}$  biomarker approach. *Journal of hydrology* 529, 622–631.
- Hepp, J., Wüthrich, L., Bromm, T., Bliedtner, M., Schäfer, I.K., Glaser, B., Rozanski, K., Sirocko, F., Zech, R., Zech, M., 2019. How dry was the Younger Dryas? Evidence from a coupled  $\delta^2\text{H}$ - $\delta^{18}\text{O}$  biomarker paleohygrometer applied to the Gemündener Maar sediments, Western Eifel, Germany. *Climate of the Past* 15, 713–733.
- Hepp, J., Zech, R., Rozanski, K., Tuthorn, M., Glaser, B., Greule, M., Keppler, F., Huang, Y., Zech, W., Zech, M., 2017. Late Quaternary relative humidity changes from Mt. Kilimanjaro, based on a coupled  $^2\text{H}$ - $^{18}\text{O}$  biomarker paleohygrometer approach. *Quaternary International* 438, 116–130.
- Hillman, J.C., 1988. The Bale Mountains National Park area, southeast Ethiopia, and its management. *Mountain Research and Development* 8, 253–258.
- Hillman, J.C., 1986. Conservation in Bale mountains national park, Ethiopia. *Oryx* 20, 89–94.
- Horita, J., Wesolowski, D.J., 1994. Liquid-vapor fractionation of oxygen and hydrogen isotopes of water from the freezing to the critical temperature. *Geochimica et Cosmochimica Acta* 58, 3425–3437.
- Kidane, Y., Stahlmann, R., Beierkuhnlein, C., 2012. Vegetation dynamics, and land use and land cover change in the Bale Mountains, Ethiopia. *Environmental monitoring and assessment* 184, 7473–7489.

- Ladd, S.N., Sachs, J.P., 2015. Influence of salinity on hydrogen isotope fractionation in *Rhizophora* mangroves from Micronesia. *Geochimica et Cosmochimica Acta* 168, 206–221.
- Lemma, B., Grehl, C., Zech, M., Mekonnen, B., Zech, W., Nemomissa, S., Bekele, T., Glaser, B., 2019a. Phenolic compounds as unambiguous chemical markers for the identification of keystone plant species in the bale mountains, Ethiopia. *Plants* 8, 228.
- Lemma, B., Kebede Gurmessa, S., Nemomissa, S., Otte, I., Glaser, B., Zech, M., 2020. Spatial and temporal  $^2\text{H}$  and  $^{18}\text{O}$  isotope variation of contemporary precipitation in the Bale Mountains, Ethiopia. *Isotopes in Environmental and Health Studies* 1–14.
- Lemma, B., Mekonnen, B., Glaser, B., Zech, W., Nemomissa, S., Bekele, T., Bittner, L., Zech, M., 2019b. Chemotaxonomic patterns of vegetation and soils along altitudinal transects of the Bale Mountains, Ethiopia, and implications for paleovegetation reconstructions—Part II: lignin-derived phenols and leaf-wax-derived n-alkanes. *E&G Quaternary Science Journal* 68, 189–200.
- Liu, W., Yang, H., 2008. Multiple controls for the variability of hydrogen isotopic compositions in higher plant n-alkanes from modern ecosystems. *Global Change Biology* 14, 2166–2177.
- McInerney, F.A., Helliker, B.R., Freeman, K.H., 2011. Hydrogen isotope ratios of leaf wax n-alkanes in grasses are insensitive to transpiration. *Geochimica et Cosmochimica Acta* 75, 541–554.
- Mekonnen, B., Zech, W., Glaser, B., Lemma, B., Bromm, T., Nemomissa, S., Bekele, T., Zech, M., 2019. Chemotaxonomic patterns of vegetation and soils along altitudinal transects of the Bale Mountains, Ethiopia, and implications for paleovegetation reconstructions—Part 1: stable isotopes and sugar biomarkers. *E&G Quaternary Science Journal* 68, 177–188.
- Merlivat, L., 1978. Molecular diffusivities of  $\text{H}_2^{16}\text{O}$ ,  $\text{HD}^{16}\text{O}$ , and  $\text{H}_2^{18}\text{O}$  in gases. *The Journal of Chemical Physics* 69, 2864–2871.
- Miehe, S., Miehe, G., 1994. Ericaceous forests and heathlands in the Bale Mountains of South Ethiopia. Ecology and man's impact. Hamburg: Warnke.
- Osmaston, H.A., Mitchell, W.A., Osmaston, J.N., 2005. Quaternary glaciation of the Bale Mountains, Ethiopia. *Journal of Quaternary Science* 20, 593–606.
- Ossendorf, G., Groos, A.R., Bromm, T., Tekelemariam, M.G., Glaser, B., Lesur, J., Schmidt, J., Akçar, N., Bekele, T., Beldados, A., 2019. Middle Stone Age foragers resided in high elevations of the glaciated Bale Mountains, Ethiopia. *Science* 365, 583–587.

- Peterse, F., van Der Meer, M.T.J., Schouten, S., Jia, G., Ossebaar, J., Blokker, J., Sinninghe Damsté, J.S., 2009. Assessment of soil n-alkane  $\delta D$  and branched tetraether membrane lipid distributions as tools for paleoelevation reconstruction. *Biogeosciences* 6, 2799–2807.
- Roden, J.S., Ehleringer, J.R., 1999. Observations of Hydrogen and Oxygen Isotopes in Leaf Water Confirm the Craig-Gordon Model under Wide-Ranging Environmental Conditions. *Plant Physiol.* 120, 1165.
- Rozanski, K., Araguás-Araguás, L., Gonfiantini, R., 1993. Isotopic patterns in modern global precipitation. *Climate change in continental isotopic records* 78, 1–36.
- Sachse, D., Billault, I., Bowen, G.J., Chikaraishi, Y., Dawson, T.E., Feakins, S.J., Freeman, K.H., Magill, C.R., McInerney, F.A., Van Der Meer, M.T., 2012. Molecular paleohydrology: interpreting the hydrogen-isotopic composition of lipid biomarkers from photosynthesizing organisms. *Annual Review of Earth and Planetary Sciences* 40, 221–249.
- Sachse, D., Radke, J., Gleixner, G., 2004. Hydrogen isotope ratios of recent lacustrine sedimentary n-alkanes record modern climate variability. *Geochimica et Cosmochimica Acta* 68, 4877–4889.
- Schmidt, H.-L., Werner, R.A., Roßmann, A., 2001.  $^{18}O$  pattern and biosynthesis of natural plant products. *Phytochemistry* 58, 9–32.
- Sessions, A.L., Burgoyne, T.W., Schimmelmann, A., Hayes, J.M., 1999. Fractionation of hydrogen isotopes in lipid biosynthesis. *Organic Geochemistry* 30, 1193–1200.
- Sternberg, L. da S.L., 1989. Oxygen and hydrogen isotope ratios in plant cellulose: mechanisms and applications, in: *Stable Isotopes in Ecological Research*. Springer, pp. 124–141.
- Strobel, P., Haberzettl, T., Bliedtner, M., Struck, J., Glaser, B., Zech, M., Zech, R., 2020. The potential of  $\delta^2H_{n\text{-alkanes}}$  and  $\delta^{18}O_{\text{sugar}}$  for paleoclimate reconstruction—A regional calibration study for South Africa. *Science of The Total Environment* 716, 137045.
- Tiercelin, J.-J., Gibert, E., Umer, M., Bonnefille, R., Disnar, J.-R., Lézine, A.-M., Hureau-Mazaudier, D., Travi, Y., Kéravis, D., Lamb, H.F., 2008. High-resolution sedimentary record of the last deglaciation from a high-altitude lake in Ethiopia. *Quaternary Science Reviews* 27, 449–467.
- Tipple, B.J., Berke, M.A., Doman, C.E., Khachatryan, S., Ehleringer, J.R., 2013. Leaf-wax n-alkanes record the plant–water environment at leaf flush. *Proceedings of the National Academy of Sciences* 110, 2659–2664.

- Tu, T.T.N., Egasse, C., Zeller, B., Bardoux, G., Biron, P., Ponge, J.-F., David, B., Derenne, S., 2011. Early degradation of plant alkanes in soils: A litterbag experiment using  $^{13}\text{C}$ -labelled leaves. *Soil Biology and Biochemistry* 43, 2222–2228.
- Tuthorn, M., Zech, M., Ruppenthal, M., Oelmann, Y., Kahmen, A., del Valle, H.F., Wilcke, W., Glaser, B., 2014. Oxygen isotope ratios ( $^{18}\text{O}/^{16}\text{O}$ ) of hemicellulose-derived sugar biomarkers in plants, soils and sediments as paleoclimate proxy II: Insight from a climate transect study. *Geochimica et cosmochimica acta* 126, 624–634.
- Tuthorn, M., Zech, R., Ruppenthal, M., Oelmann, Y., Kahmen, A., del Valle, H.F., Eglinton, T., Rozanski, K., Zech, M., 2015. Coupling  $\delta^2\text{H}$  and  $\delta^{18}\text{O}$  biomarker results yields information on relative humidity and isotopic composition of precipitation—a climate transect validation study. *Biogeosciences* 12, 3913–3924.
- Umer, M., Kebede, S., Osmaston, H., 2004. Quaternary glacial activity on the Ethiopian Mountains, in: *Developments in Quaternary Sciences*. Elsevier, pp. 171–174.
- Umer, M., Lamb, H.F., Bonnefille, R., Lézine, A.-M., Tiercelin, J.-J., Gibert, E., Cazet, J.-P., Watrin, J., 2007. Late pleistocene and holocene vegetation history of the bale mountains, Ethiopia. *Quaternary Science Reviews* 26, 2229–2246.
- Voelker, S.L., Brooks, J.R., Meinzer, F.C., Roden, J., Pazdur, A., Pawelczyk, S., Hartsough, P., Snyder, K., Plavcová, L., Šantrůček, J., 2014. Reconstructing relative humidity from plant  $\delta^{18}\text{O}$  and  $\delta\text{D}$  as deuterium deviations from the global meteoric water line. *Ecological applications* 24, 960–975.
- Walker, C.D., Brunel, J.-P., 1990. Examining evapotranspiration in a semi-arid region using stable isotopes of hydrogen and oxygen. *Journal of Hydrology* 118, 55–75.
- White, J.W., Cook, E.R., Lawrence, J.R., 1985. The DH ratios of sap in trees: Implications for water sources and tree ring DH ratios. *Geochimica et Cosmochimica Acta* 49, 237–246.
- Woldu, Z., Feoli, E., Nigatu, L., 1989. Partitioning an elevation gradient of vegetation from southeastern Ethiopia by probabilistic methods, in: *Numerical Syntaxonomy*. Springer, pp. 189–198.
- Yimer, F., Ledin, S., Abdelkadir, A., 2006. Soil organic carbon and total nitrogen stocks as affected by topographic aspect and vegetation in the Bale Mountains, Ethiopia. *Geoderma* 135, 335–344.
- Zech, M., Buggle, B., Leiber, K., Markovic, S., Glaser, B., Hambach, U., Huwe, B., Stevens, T., Sümege, P., Wiesenberg, G.L., 2009. Reconstructing Quaternary vegetation history in the Carpathian Basin, SE Europe, using n-alkane biomarkers as molecular fossils:

- problems and possible solutions, potential and limitations. *E&G: Quaternary Science Journal* 58, 148–155.
- Zech, M., Glaser, B., 2009. Compound-specific  $\delta^{18}\text{O}$  analyses of neutral sugars in soils using gas chromatography–pyrolysis–isotope ratio mass spectrometry: problems, possible solutions and a first application. *Rapid Communications in Mass Spectrometry: An International Journal Devoted to the Rapid Dissemination of Up-to-the-Minute Research in Mass Spectrometry* 23, 3522–3532.
- Zech, M., Glaser, B., 2008. Improved compound-specific  $\delta^{13}\text{C}$  analysis of n-alkanes for application in palaeoenvironmental studies. *Rapid Communications in Mass Spectrometry: An International Journal Devoted to the Rapid Dissemination of Up-to-the-Minute Research in Mass Spectrometry* 22, 135–142.
- Zech, M., Mayr, C., Tuthorn, M., Leiber-Sauheitl, K., Glaser, B., 2014a. Oxygen isotope ratios ( $^{18}\text{O}/^{16}\text{O}$ ) of hemicellulose-derived sugar biomarkers in plants, soils and sediments as paleoclimate proxy I: Insight from a climate chamber experiment. *Geochimica et Cosmochimica Acta* 126, 614–623.
- Zech, M., Pedentchouk, N., Buggle, B., Leiber, K., Kalbitz, K., Marković, S.B., Glaser, B., 2011. Effect of leaf litter degradation and seasonality on D/H isotope ratios of n-alkane biomarkers. *Geochimica et Cosmochimica Acta* 75, 4917–4928.
- Zech, M., Rass, S., Buggle, B., Löscher, M., Zöller, L., 2013a. Reconstruction of the late Quaternary paleoenvironments of the Nussloch loess paleosol—Response to comments by G. Wiesenberg and M. Gocke. *Quaternary research* 79, 306–307.
- Zech, M., Rass, S., Buggle, B., Löscher, M., Zöller, L., 2012a. Reconstruction of the late Quaternary paleoenvironments of the Nussloch loess paleosol sequence, Germany, using n-alkane biomarkers. *Quaternary Research* 78, 226–235.
- Zech, M., Tuthorn, M., Detsch, F., Rozanski, K., Zech, R., Zöller, L., Zech, W., Glaser, B., 2013b. A 220 ka terrestrial  $\delta^{18}\text{O}$  and deuterium excess biomarker record from an eolian permafrost paleosol sequence, NE-Siberia. *Chemical Geology* 360, 220–230.
- Zech, M., Tuthorn, M., Zech, R., Schlütz, F., Zech, W., Glaser, B., 2014b. A 16-ka  $\delta^{18}\text{O}$  record of lacustrine sugar biomarkers from the High Himalaya reflects Indian Summer Monsoon variability. *Journal of paleolimnology* 51, 241–251.
- Zech, M., Werner, R.A., Juchelka, D., Kalbitz, K., Buggle, B., Glaser, B., 2012b. Absence of oxygen isotope fractionation/exchange of (hemi-) cellulose derived sugars during litter decomposition. *Organic geochemistry* 42, 1470–1475.



Zech, M., Zech, R., Rozanski, K., Gleixner, G., Zech, W., 2015. Do n-alkane biomarkers in soils/sediments reflect the  $\delta^2\text{H}$  isotopic composition of precipitation? A case study from Mt. Kilimanjaro and implications for paleoaltimetry and paleoclimate research. *Isotopes in environmental and health studies* 51, 508–524.

## List of Publications

### I) Peer reviewed journals

- Lemma, B.**, Bittner, L., Glaser, B., Kebede, S., Nemomissa, S., Zech, W., Zech, M.  $\delta^2\text{H}_{n\text{-alkane}}$  and  $\delta^{18}\text{O}_{\text{sugar}}$  biomarker proxies from leaves and topsoils of the Bale Mountains, Ethiopia, and implication for paleoclimate reconstruction. *Biogeochemistry*, BIOG- D- 20-00226. (Submitted)
- Bittner, L., Bliedtner, M., Grady, D., Gil-Romera, G., Martin-Jones, C., **Lemma, B.**, Mekonnen, B., Lamb, H., Yang, H., Glaser, B., Szidat, S., Salazar, G., Rose, N., Opgenoorth, L., Mieke, G., Zech, W., Zech, M. (2020). Revisiting afro-alpine Lake Garba Guracha in the Bale Mountains of Ethiopia: rationale, chronology, geochemistry, and paleoenvironmental implications. *Journal of Paleolimnology* 64, 293-314. <https://doi.org/10.1007/s10933-020-00138-w>
- Lemma, B.**, Kebede, S., Nemomissa, S., Otte, I., Glaser, B., Zech, M. (2020). Spatial and temporal  $^2\text{H}$  and  $^{18}\text{O}$  isotope variation of contemporary precipitation in the Bale Mountains, Ethiopia. *Isotopes in Environmental and Health Studies*, 1–14. <https://doi.org/10.1080/10256016.2020.1717487>
- Lemma, B.**, Mekonnen, B., Glaser, B., Zech, W., Nemomissa, S., Bekele, T., Bittner, L., Zech, M. (2019). Chemotaxonomic patterns of vegetation and soils along altitudinal transects of the Bale Mountains, Ethiopia and implications for paleovegetation reconstructions Part II: Lignin-derived phenols and leaf wax-derived *n*-alkanes. *E&G Quaternary Science Journal*, 68, 189–200. <https://doi.org/10.5194/egqsj-68-189-2019>
- Mekonnen, B., Glaser, B., **Lemma, B.**, Bromm, T., Zech, M., Nemomissa, S., Bekele, T., Zech, W. (2019). Chemotaxonomic patterns of vegetation and soils along altitudinal transects of the Bale Mountains, Ethiopia and implications for paleovegetation reconstructions Part I: Stable isotopes and sugar biomarkers. *E&G Quaternary Science Journal*, 68, 177–188. <https://doi.org/10.5194/egqsj-68-177-2019>
- Lemma, B.**, Grehl C., Zech M., Mekonnen B., Zech W., Nemomissa S., Bekele, T., and Glaser, B. (2019). Phenolic Compounds as Unambiguous Chemical Markers for the Identification of Keystone Plant Species in the Bale Mountains, Ethiopia. *Plants*, 8, 228. <https://doi.org/10.3390/plants8070228>
- Gil-Romera, G., Adolf, C., Benito, B.M., Bittner, L., Johansson, M. U., Grady, D. A., Lamb, H. F., **Lemma, B.**, Fekadu, M., Glaser, B., Mekonnen, B., Callejo, M. S., Zech, M.,

---

Zech, W., Miede, G. (2019). Long-term fire resilience of the Ericaceous Belt, Bale Mountains, Ethiopia. *Biology Letters*, 15 (7): <https://doi.org/10.1098/rsbl.2019.0357>

## II) Conference proceedings

**Lemma, B.**, Kebede, S., Nemomissa, S., Otte, I., Glaser, B., Zech, M. (2019). Spatial and temporal isotopic characterisation ( $^2\text{H}/^1\text{H}$  and  $^{18}\text{O}/^{16}\text{O}$ ) of modern day precipitation in the Bale Mountains, Ethiopia and isotope incorporation into plant biomarkers. 40<sup>th</sup> Annual Meeting of the German Association of Isotope Research. Arbeitsgemeinschaft Stabile Isotope (ASI, October-2019), TU Dresden, Germany (poster presentation).

**Lemma, B.** (2019). Lignin-derived phenols and leaf wax-derived *n*-alkanes in plants and soils along altitudinal transects of the Bale Mountains, Ethiopia as biomarkers for the reconstruction of the paleovegetation. International School on Paleopedology for Young Scholars (1 – 6 August 2019). Novosibirsk, Russia (oral presentation).

**Lemma, B.**, Kebede, S., Nemomissa, S., Otte, I., Glaser, B., Zech, M. (2019). Spatial and temporal isotopic characterisation ( $^2\text{H}/^1\text{H}$  and  $^{18}\text{O}/^{16}\text{O}$ ) of modern day precipitation in the Bale Mountains, Ethiopia. International Symposium on Isotope Hydrology: Advancing the Understanding of Water Cycle Processes. International Atomic Energy Agency (IAEA, May-2019), Vienna, Austria (poster presentation).

**Lemma, B.**, Kebede, S., Nemomissa, S., Otte, I., Glaser, B., Zech, M. (2018). Spatial and temporal isotopic characterisation ( $^2\text{H}/^1\text{H}$  and  $^{18}\text{O}/^{16}\text{O}$ ) of modern day precipitation in the Bale Mountains, Ethiopia. Conference on Hydrogeology and Deep Ground water, Soil, Plants, Atmosphere, Climate, Material Cycles, and Isotope Methods. Arbeitsgemeinschaft Stabile Isotope (ASI, October-2018). TU Munchen, Germany (poster presentation).

## Acknowledgements

Though only my name appears on the cover page of this dissertation, a great many individuals have contributed to its production. I owe my profound gratitude to all those people who have made this Ph.D. thesis possible and because of whom my graduate experience has been one that I will cherish forever.

First and foremost, I offer my sincerest gratitude to my supervisor Prof. Dr. Michael Zech, Technische Universität Dresden, Germany. I have been amazingly fortunate to have an advisor who gave me the freedom to explore on my own and, at the same time, the guidance to recover when my steps wavered. I am grateful for his coaching, hospitality and patience, as well as his golden and motivational words. Furthermore, my deepest gratitude goes to my second supervisor Prof. Dr. Bruno Glaser, Martin-Luther-University, Halle-Wittenberg who provided me the opportunity to join his research team first as a Ph.D. student, and later on as scientific staff. I highly appreciate for offering me a chance to access his laboratory and research facilities. I am indebted to his leadership, scientific support, physical and mental health guidance, and nurturing. My sincere thanks also go to em. Prof. Dr. Wolfgang Zech, who cultivates me scientifically since my master's degree. I am thankful for his encouragement and adorable follow-ups.

I am also pleased to say thank you to Prof. Dr. Sileshi Nemomissa, Prof. Dr. Seifu Kebede, and Assoc. Prof. Dr. Tamrat Bekele for the insightful comments, and engagement in the preparation of the manuscripts. I am obliged to them for holding me to a high research standard, enforcing strict validations for each research result, and teaching me how to conduct research.

Moreover, I would like to thank all members of the Soil Biogeochemistry Department, Martin-Luther-University, Halle-Wittenberg especially Marianne Benesch for the compound-specific stable isotope measurements, but also for her hospitality, care, and memorable trips we had together. Also, Heike Maennicke, Lucas Bittner, Tobias Bromm for unreserved assistance during my laboratory work. Without their precious support it would not be possible to conduct this Ph.D. research work. My special thanks are given to the Department of Plant Biology and Biodiversity Management, Addis Ababa University, Ethiopian Wildlife Authority and Ministry of Water, Irrigation, and Electricity, Ethiopia for their scientific collaboration, allowing us to access the Bale Mountains National Park and access permission to the rainwater, respectively. I am indebted to the Ethiopian Biodiversity Institute for the study leave. Furthermore, I

appreciate the financial support from the Catholic Academic Exchange Service (KAAD) and the German Research Foundation (DFG).

I am very grateful to all members of the central and local project coordinators namely Katinka Thielsen, Mekbib Fekadu, Tiziana Koch, Terefe Endale, Geremew Mebratu, Falk Hänsel, Wege Abebe, Musa Abdi and logistic team Elias Tadesse, and Ermias Getachew, who made our several field campaigns possible.

I would also like to thank my beloved friends, who have supported me throughout the entire process, both by keeping me harmonious and helping me putting pieces together. I will be grateful forever for your love.

Most importantly, none of this would have been possible without the love and patience of my families. My immediate family has been a constant source of love, supporting me morally and spiritually throughout writing this dissertation and strengthen me all those years. I would like to express my heartfelt gratitude to my wife Azeb Bogale, who encouraged me throughout this endeavor. I warmly appreciate the generosity and understanding of my extended family.

## Curriculum Vitae/Lebenslauf



### PERSONAL INFORMATION

Given name: Bruk Lemma  
 Surname: Debebe  
 Data of birth: 07 Oct 1987  
 Birth place: Addis Ababa  
 Sex: Male  
 Nationality: Ethiopian

### CURRENT RESIDENCE

Heinrich-Schütz-Straße 7  
 06120 Halle (Saale), Germany

### Job Related Skills

#### Field research skills

- Weather station installation
- Self-made rain gauge installation
- Lake sediment coring using livingstone and cobra coring machine
- Soil, plant and precipitation sampling
- Mountain Ecology
- Forest Ecology
- Alpine Ecology

#### Laboratory research skill

- Stable isotope analysis ( $^2\text{H}$ ,  $^{18}\text{O}$ .)
- Biomarker analysis (Lignin, Lipid, *n*-alkane, fatty acid, alcohol, and sugar)

#### Experience with measuring machine

- GC-MS
- GC-IRMS
- GC-FID

Skills in evaluating chromatography results using Isodat and GC softwares

### PROFESSIONAL BACKGROUND

#### **Ph.D. Fellow**

Martin-Luther-University Halle-Wittenberg  
 Soil Biogeochemistry  
**Since October 2016**

#### Project: **Paleoclimatology**

**Aim:** Contributing to a semi-quantitative reconstruction of the Late Quaternary paleoclimate history of the Bale Mountains in Ethiopia.

#### **Responsibility**

- Establishing weather stations and rain gauges
- Field research work (lake coring, leaf and soil sampling etc...)
- Identifying suitable biomarkers for planned paleovegetation and paleoclimate studies
- Analyzes of isotopes in precipitation ( $^2\text{H}$  and  $^{18}\text{O}$ )
- Preparing four publications for peer review journals
- Maintenance of weather station and rain gauges

#### **M.Sc. Fellow (Assistant Researcher II)**

Addis Ababa University  
 Plant Biology and Biodiversity Management  
 Addis Ababa, Ethiopia  
**From October 2014 to September 2016**

#### Project: **Paleoecology**

**Aim:** Identifying suitable biomarker for the identification of the paleo-extent of *Erica* shrubs in the Bale Mountains, Ethiopia.

#### **Responsibility**

- Complete 120 ECTS course works
- Field research work (sampling plants, organic and mineral soil)
- Lignin biomarker analyses
- Preparing M.Sc. Thesis

## Digital Skills

---

I have experience in the following software programs and packages:

- ✓ Microsoft office suite
- ✓ R
- ✓ SPSS
- ✓ Origin
- ✓ XLSTATA

## Communication Skills

---

I have excellent interpersonal communication skills with many individuals worldwide.

I develop this skill through my experience as teacher and researcher.

Also, I use social media networks like

- ✓ Skype ([bruk.lemma1](#))
- ✓ Twitter ([@bruklemma](#))
- ✓ Facebook ([bruklemma](#))
- ✓ Instagram ([bruklemma](#))

to share my scientific views for the wider public. So, such activities helped me to strengthen my innate communication skill.

## Leadership Skills

---

- ✓ Student president
- ✓ School director
- ✓ School cluster supervisor
- ✓ Chair of local social union

## Other Skills

---

- ✓ Driving (Class B)
- ✓ Hiking and Climbing high mountains

## PROFESSIONAL BACKGROUND

### Assistant Researcher II

Ethiopian Biodiversity Institute  
Forest and Rangeland Biodiversity Directorate  
Addis Ababa, Ethiopia

**From December 2011 to September 2014**

#### Responsibility

- Regulating Ethiopian Biodiversity
- Controlling bio-piracy
- Researching on the Ethiopian Biodiversity and associated traditional knowledge
- Preparing policy documents on Access and Benefit Sharing (ABS) for the Ethiopian government
- Creating public awareness on sustainable utilization of Biodiversity

#### Educationalist

Addis Ababa city administration bureau of education  
Addis Ababa, Ethiopia

**From July 2007 to November 2011**

#### Responsibility

- Teaching biology and chemistry for grade seven and eight students
- Preparing teaching syllabus
- Conducting class room based research (Action Research)
- Community service
- Student supervision
- School supervision
- Teachers supervision
- Preparing primary school leaving examination
- Organizing question and answer competition among schools
- Ranking the performance of teachers, school directors and schools

**PERSONALITY**

Teamwork

Self collaboration

Communication with colleagues

Social/Cultural outlooks

**Computer skill**

Microsoft Office

Grapher

Statistical software

**Mother tongue: Amharic****Foreign Languages**

English

German

**HOBBIES**

Reading

Sport (athletics and swimming)

**EDUCATIONAL BACKGROUND****Ph.D. student**

Martin-Luther-University Halle-Wittenberg

Soil Biogeochemistry

Since October 2016

**Working title:** Stable isotopes in precipitation and plant biomarkers patterns along transect gradient in the Bale Mountains, Ethiopia.**M.Sc. in Plant Biology and Biodiversity Management**

Addis Ababa University

Plant Biology and Biodiversity Management

Addis Ababa, Ethiopia

From October 2014 to July 2016

**M.Sc. Thesis title:** Reconstruction of vegetation dynamics along altitudinal transects in the Bale Mountains, Ethiopia using CuO-lignin biomarkers.**Final Grade: 4.0 (A<sup>+</sup>) with honour****Thesis Grade: Excellent****B.Sc. in Sport Science**

Kotebe Metropolitan University, Addis Ababa, Ethiopia

From July 2009 to October 2014

**Final Grade: 3.50, Great distinct****B.Sc. in Biology**

Bahir Dar University, Bahir Dar, Ethiopia

From October 2007 to July 2011

**Final Grade: 3.55, Great distinct****Diploma in Biology and Chemistry**

Kotebe Metropolitan University, Addis Ababa, Ethiopia

From September 2004 to July 2007

**Final Grade: 3.79, Very great distinct with honour****OTHER RELEVANT TRAININGS****Certificate in Statistics**

Kassel University

Department of Environmental Chemistry

Witzenhausen,

**Germany**

From 28 March 2019 to 2 April 2019

**Certificate in Handling Hard Forest Seeds**

Royal Botanical Garden, Kew, Millennium Seed Bank Partnership

Ardingly, Haywards Heath, Sussex, London, RH17 6TN

**United Kingdom**

From 19 October 2015 to 30 January 2016

**Certificate in application of Biotechnology and its Regulation**

The Energy and Resource Institute, TERI University

Gwal Pahari, Gurugram, 122 102 New Delhi

**India**

From 9 September 2013 to 28 September 2013



**Eidesstattliche Erklärung / Declaration under Oath**

Ich erkläre an Eides statt, dass ich die Arbeit selbstständig und ohne fremde Hilfe verfasst, keine anderen als die von mir angegebenen Quellen und Hilfsmittel benutzt und die den benutzten Werken wörtlich oder inhaltlich entnommenen Stellen als solche kenntlich gemacht habe.

*I declare under penalty of perjury that this thesis is my own work entirely and has been written without any help from other people. I used only the sources mentioned and included all the citations correctly both in word or content.*

---

Datum

---

Bruk Lemma Debebe

**Erklärung über bestehende Vorstrafen und anhängige Ermittlungsverfahren /  
Declaration concerning Criminal Record and Pending Investigations**

Hiermit erkläre ich, dass ich weder vorbestraft bin noch dass gegen mich Ermittlungsverfahren anhängig sind.

*I hereby declare that I have no criminal record, and there are no preliminary criminal proceedings pending against me.*

---

Datum

---

Bruk Lemma Debebe